ISSN 1300 - 6045
e-ISSN 1309 - 2251

KAFKAS ÜNİVERSİTESİ VETERİNER FAKÜLTESİ DERGİSİ

Journal of the Faculty of Veterinary Medicine, Kafkas University

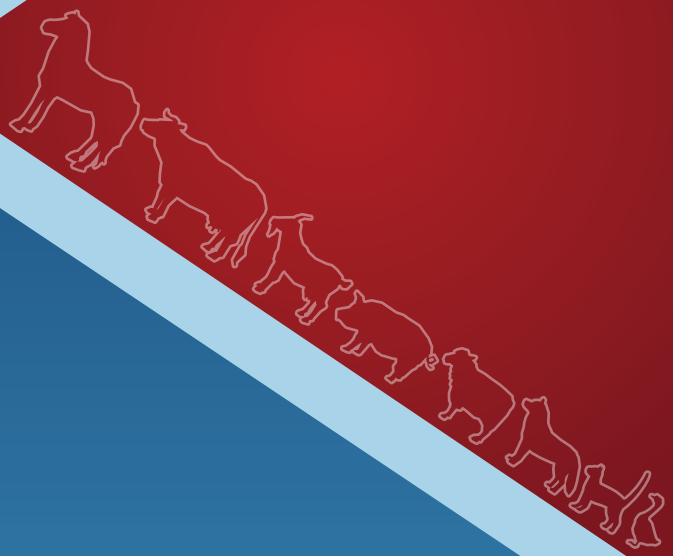

http://vetdergi.kafkas.edu.tr

Online Submission
http://submit.vetdergikafkas.org

Volume: 27
Issue: 6 (November-December)
Year: 2021

ISSN 1300 - 6045
e-ISSN 1309 - 2251

KAFKAS ÜNİVERSİTESİ VETERİNER FAKÜLTESİ DERGİSİ

Journal of the Faculty of Veterinary Medicine, Kafkas University

Published Bi-monthly

Volume: 27
Issue: 6 (November - December)
Year: 2021

ISSN (Print): 1300-6045 **ISSN (Electronic): 1309-2251**

This journal is published bi-monthly, by the Faculty of Veterinary Medicine, University of Kafkas, Kars - Turkey

This journal is indexed and abstracted in:

- Web of Science Core Collection: Science Citation Index Expanded (since 2007)
- Additional Web of Science Indexes: Essential Science Indicators - Zoological Record
- CABI - Veterinary Science Database
- DOAJ
- EBSCO - Academic Search Premier
- Elsevier - SCOPUS
- Elsevier - EMBASE
- Index Copernicus
- SOBİAD Atıf Dizini
- TÜBİTAK/ULAKBİM TR-Dizin
- Türkiye Atıf Dizini

Print

ESER OFSET MATBAACILIK
BOSNAHERSEK CAD. ALTUNALEM YAPI KOOP. ZEMİN KAT - ERZURUM
Tel: +90 442 2334667 E-mail: eserofset25@hotmail.com

Address for Correspondence

Kafkas Üniversitesi Veteriner Fakültesi Dergisi Editörlüğü 36040, Kars - TÜRKİYE
Phone: +90 474 2426807-2426836/5228 Fax: +90 474 2426853 E-mail: vetdergi@kafkas.edu.tr

Electronic Edition http://vetdergikafkas.org **Online Submission** http://submit.vetdergikafkas.org

Editorial Board

The Referees List of This Issue *(in alphabetical order)*

Adnan AYAN	Van Yüzüncü Yıl Üniversitesi Veteriner Fakültesi
Ahmad ALI	University of Veterinary and Animal Sciences, Pakistan
Ahmet AYDOĞAN	Çukurova Üniversitesi Ceyhan Veteriner Fakültesi
Aslı SAKMANOĞLU	Selçuk Üniversitesi Veteriner Fakültesi
Bayazıt MUSAL	Aydın Adnan Menderes Üniversitesi Veteriner Fakültesi
Bengü ERGÜDEN	Gebze Teknik Üniversitesi Mühendislik Fakültesi
Buket BOĞA KURU	Kafkas Üniversitesi Veteriner Fakültesi
Cihan KAÇAR	Kafkas Üniversitesi Veteriner Fakültesi
Durhasan MUNDAN	Harran Üniversitesi Veteriner Fakültesi
Duygu BAKİ ACAR	Afyon Kocatepe Üniversitesi Veteriner Fakültesi
Ece KOLDAŞ ÜRER	Hatay Mustafa Kemal Üniversitesi Veteriner Fakültesi
Elif İlkay ARMUTAK	İstanbul Üniversitesi-Cerrahpaşa Veteriner Fakültesi
Fatih BÜYÜK	Kafkas Üniversitesi Veteriner Fakültesi
Funda YİĞİT	İstanbul Üniversitesi-Cerrahpaşa Veteriner Fakültesi
Gencay Taşkın TAŞÇI	Kafkas Üniversitesi Veteriner Fakültesi
Gülcihan ŞİMŞEK	Fırat Üniversitesi Veteriner Fakültesi
Halit KANCA	Ankara Üniversitesi Veteriner Fakültesi
Hamza AVCIOĞLU	Atatürk Üniversitesi Veteriner Fakültesi
Hasan Hüseyin ORUÇ	Bursa Uludağ Üniversitesi Veteriner Fakültesi
Hatice Esra CANATAN	Ankara Üniversitesi Veteriner Fakültesi
İftar GÜRBÜZ	Burdur Mehmet Akif Ersoy Üniversitesi Veteriner Fakültesi
İrem ERGİN	Ankara Üniversitesi Veteriner Fakültesi
Kamil BEŞOLUK	Selçuk Üniversitesi Veteriner Fakültesi
Mehmet Cemal ADIGÜZEL	Atatürk Üniversitesi Veteriner Fakültesi
Mehmet GÜVENÇ	Hatay Mustafa Kemal Üniversitesi Veteriner Fakültesi
Muammer ELMAS	Selçuk Üniversitesi Veteriner Fakültesi
Murat FINDIK	Ondokuz Mayıs Üniversitesi Veteriner Fakültesi
Mushap KURU	Kafkas Üniversitesi Veteriner Fakültesi
Osman Sabri KESBİÇ	Kastamonu Üniversitesi/Veteriner Fakültesi
Özgür ÇELEBİ	Kafkas Üniversitesi Veteriner Fakültesi
Semine DALGA	Kafkas Üniversitesi Veteriner Fakültesi
Semra KAYA	Kafkas Üniversitesi Veteriner Fakültesi
Serap SAVAŞAN	Aydın Adnan Menderes Üniversitesi Veteriner Fakültesi
Serkan ERAT	Kırıkkale Üniversitesi Veteriner Fakültesi
Sinan KANDIR	Çukurova Üniversitesi Ceyhan Veteriner Fakültesi
Şinasi UMUR	Ondokuz Mayıs Üniversitesi Veteriner Fakültesi
Zülfükar Kadir SARITAŞ	Afyon Kocatepe Üniversitesi Veteriner Fakültesi
Yalçın AKBULUT	Kafkas Üniversitesi Tıp Fakültesi
Yavuz ÖZTÜRKLER	Kafkas Üniversitesi Veteriner Fakültesi

İÇİNDEKİLER (Contents)

Kafkas Universitesi Veteriner Fakultesi Dergisi
ISSN: 1300-6045 e-ISSN: 1309-2251
Journal Home-Page: http://vetdergikafkas.org

Kafkas Univ Vet Fak Derg
27 (6): 675-680, 2021
DOI: 10.9775/kvfd.2021.25993

RESEARCH ARTICLE

A Novel Epithelial and Fibroblastic Cell Isolation and Purification Method Using Primary Culture of Bovine Tongue Tissue

Sukran YILMAZ [1,a (*)]

[1] Ministry of Agriculture and Forestry, Foot and Mouth Disease Institute, Cell Department, TR-06510 Ankara - TURKEY
[a] ORCID: 0000-0002-7945-1124

Article ID: KVFD-2021-25993 Received: 08.05.2021 Accepted: 01.10.2021 Published Online: 04.10.2021

Abstract

Cell lines provide a useful in vitro model to study in different biotechnological fields. The purity of the cell lines plays a pivotal role in research and production activities. This study aims to present a new method to establish pure cell lines by using bovine tongue tissue. For this purpose, the bovine tongue was obtained from the local slaughterhouse. After establishing primary cell culture, the cells were treated with EDTA (0.02%) for 3-5 min at 37°C. Primarily detached fibroblasts were collected into 5 mL EMEM (with 20% FBS), centrifuged and transferred to a new culture flask with EMEM (10% FCS) medium. The remainder cells in the primary flask were incubated for 8 hours with DMEM (10% FCS). Thereafter, the same process was applied with Na_2EDDA (0.01%), and the cells were washed twice with DMEM (with 20% FBS). Reincubation was carried out with decreased FBS concentration (10%) and EGF (10 ng/mL) at 37°C, 5% CO_2 in humidified air conditions. The same processes were repeated after 48 h. Conformational studies of pure cultures were done with immunostaining technique with anti-cytokeratin and anti-vimentin monoclonal antibodies where, after purification, fibroblasts displayed vimentin-positive and epithelial cells cytokeratin-positive. In conclusion, this study successfully demonstrated an easy, effective, and efficient method to generate pure novel cell lines from primary tissue culture or mixed cell cultures.

Keywords: *Primary cell culture, Fibroblast cell, Epithelial cell, Pure culture*

Sığır Dil Dokusu Primer Kültürü Kullanılarak Yeni Bir Epitel ve Fibroblastik Hücre İzolasyonu ve Saflaştırma Yöntemi

Öz

Hücre hatları, farklı biyoteknolojik alanlarda çalışmak için elverişli in vitro modeller olup, saflıkları araştırma ve üretimlerde çok önemli bir rol oynar. Bu çalışmanın amacı, sığır dil dokusunu kullanarak saf hücre hatlarının oluşturulması için yeni bir yöntem oluşturmaktır. Mezbahadan alınan sığır dil dokusundan primer hücre kültürü hazırlandıktan sonra, 37°C'de 3-5 dak EDTA (%0.02) ile muamele edilen hücreler, fibroblastlar yüzeyden ayrılmaya başladığında, %20 FBS içeren 5 mL EMEM ortamında toplandı, santrifüjlendi ve %10 serum içeren EMEM ortamında yeni bir kültür kabına aktarıldı. Eski kültür kabında kalan hücreler 8 saat 5 mL DMEM (%10 FBS'li) ile inkübasyonu takiben, aynı işlem Na_2EDDA (%0.01) ile uygulandıktan sonra hücreler, %20 FBS'li DMEM ile iki kez yıkandı ve bu defa %10 FBS ve 10 ng/ml EGF içeren DMEM ile inkübe edildi. 48 saat sonra aynı işlemler tekrarlandı. Saf kültürlerde sitokeratin ve vimentin için spesifik monoklonal antikorlar kullanılarak doku orijini doğrulaması amacıyla immün boyama protokolü uygulandı. Sonuçlarımız, immünositokimyasal analize göre, saflaştırılmış fibroblast hücrelerinin vimentin pozitif olduğunu ve saflaştırılmış epitel hücrelerinin de sitokeratin pozitif gösterdiğini gösterdi. Sonuç olarak, bu çalışma, primer kültürler ya da karışık hücre kültürlerinden saf yeni hücre hatları oluşturmak için kolay, etkili ve verimli bir yöntem ortaya koymuştur.

Anahtar sözcükler: *Primer hücre kültürü, Fibroblast hücre, Epitelyal hücre, Saf kültür*

INTRODUCTION

Cell cultures are major tools for biotechnological advances from diagnosis to vaccine production. By definition, cell culture is the environment in which cells separated from the tissue by spontaneous migration, mechanical or enzymatic dissociation, and is kept alive, reproduced *in vitro,* and studied away from physicochemical and physiological variables. The first step of culture is called primary culture or primary cell culture [1,2]. However, due to the preparation and cost constraints of primary cultures, cell lines are often used to study biological processes [3,4].

How to cite this article?

Yilmaz S: A novel epithelial and fibroblastic cell isolation and purification method using primary culture of bovine tongue tissue. *Kafkas Univ Vet Fak Derg,* 27 (6): 675-680, 2021.
DOI: 10.9775/kvfd.2021.25993

(*) **Corresponding Author**

Tel: +90 542 641 5112 Fax: +90 312 287 3606
E-mail: sukranyilmaz@gmail.com (Ş. Yılmaz)

Cell lines originating from primary cultures have either a limited lifespan or immortal, capable of continuous proliferation [5]. Although cell lines are a powerful tool, attention should be paid when using them instead of primary cells. They must display and maintain functional characteristics as close as possible to the primary cells. However, animal cell lines are one of the main tools in vaccine production and biotechnological studies, such as generating artificial tissues, gene editing, synthesis of biological compounds and therapeutic proteins. It is a vital experimental process that is easier to control than *in vivo* [6,7]. In this process, maintaining high standards is essential for all scientific studies. Although it is also necessary for the reproducibility, reliability, acceptance, and implementation of the results obtained, most researchers can ignore this issue [4,7,8]. About 32.755 articles of studies with misidentified cell lines are in circulation [9]. Establishing a pure cell line from primary culture provides delicate and proper data to assess scientific research. Many methods have been developed for cell purification from primary culture. Each has advantages and disadvantages that are considered in the goals of the research [10]. Fibroblasts are widely predominant in the mixed culture of epithelial and fibroblastic cells. Intercellular junctions of fibroblasts are weaker than epithelial cells. For this reason, it is easier to remove fibroblastic cells first in primary cultures. Isolation and purification of cells from tissues by maintaining their native characteristics are substantial. Otherwise, they may hamper our understanding of their physiological, biological, growth, and differentiation characteristics [11]. Therefore, the advantages of working with well purified, identified, and contamination-free cell lines are indisputable. For this purpose, the purification step of the novel cell lines to be created from the primary cultures and confirmation of the histological origin are of great importance.

Epithelial and mesenchymal (connective) tissues constitute the two main classes of vertebrate tissues. The epithelial tissues of ectodermal or endodermal origin containing small amounts of intercellular substances. The mesenchymal tissues are mesodermal origin and have significant amounts of extracellular proteins [12]. Cell metabolism or cell membrane protein expression is highly critical during the purification process [13]. Immunocytochemistry (ICC), which is used to verify the cell cultures' tissue origins, is one of the methods performed using monoclonal antibodies specific to the relevant tissue intermediate filament. Intermediate filaments, cytoskeletal elements, differ from tissue to tissue. While the intermediate filaments of epithelial cells are generally composed of specific cytokeratin combinations, fibroblast cells consist of several intermediate filaments, mainly vimentin and collagen type 1 [14].

This study aimed to generate an easy, effective, and efficient method to develop pure novel cell lines from primary culture or mixed cell cultures using bovine tongue tissue.

Material and Methods

Establishment of Primary Cell Culture

Bovine tongue tissue was obtained from the local slaughterhouse. After washing with cold phosphate-buffered saline (PBS) and sterilization with 70% ethanol, the tongue was transported to the laboratory in ice-cold PBS supplemented with antibiotics. The upper layer of tissue was chopped with scissors into small fragments after removing the *stratum corneum* layer under sterile conditions [15,16]. Then, tissue fragments were digested in an enzyme solution containing collagenase I (0.4 mg/mL, Sigma, USA) and dispase (1.2 mg/mL, Sigma USA) for 45 min at 37°C. After 2 times centrifugation, the resulting pellet was collected and dispersed in DMEM/F-12 medium (Hyclone, USA) supplemented with 10% fetal bovine serum (FBS) (Biowest, France), 5 µg/mL insulin (Sigma, USA), 10 ng/mL epidermal growth factor (Sigma, USA), 100 nM/mL transferrin (Sigma, USA), 100 U/mL penicillin (Sigma, USA), 100 µg/mL streptomycin (Sigma, USA), and 2.5 µg/mL amphotericin-B (Sigma, USA) [17-20]. The cell density was determined using the trypan blue dye exclusion (0.4%, Sigma, USA) method [21]. The cells were transferred into T75 cell culture flasks at $1x10^6$ cells/mL and allowed to incubate (37°C, 5% CO_2). The culture was examined every 48 h with an inverted phase-contrast microscope, and the growth medium was changed. On the first, third and fifth days of the culture, proliferation was checked with an inverted phase-contrast microscope and monitored by micrography (Olympus IX71, Japan).

Purification of Epithelial and Fibroblastic Cells

In primary culture, fibroblastic cells usually predominant and mixed with epithelial or surrounded the epithelial islets. Herein, a combined protocol was created by utilizing some parts of the techniques used in different studies to obtain the purity of two different cell groups. When the culture was 70% confluent cell layer, the conventional detaching procedure with trypsin (0.25%) was applied after washing with Ca^{+2}-Mg^{+2} free PBS [13,21]. The next step was EDTA (ethylenediaminetetraacetic acid, 0.02%) addition and incubation (3-5 min at 37°C) [22]. Fibroblasts were collected in 5 mL EMEM (Eagle's minimum essential medium, Multicell-Wisent, Canada) with 20% FBS, centrifuged (800 rpm, 5 min) and transferred to a new culture flask in EMEM with 10% serum. The residual cells in the primary culture flask were washed twice with DMEM (with 20% FBS) and cultivated with 5 mL DMEM (with 10% FBS) in 5% CO_2 atmosphere at 37°C for 8 h. Following incubation, the same process was applied with Na_2EDDA (disodiumethylenediamine-N,N'-diacetic acid, 0.01%) to complete the removal of the fibroblasts. Then, the cells were washed twice with DMEM containing 20% FBS, reincubated with decreased FBS concentration (10%) and epithelial growth factor (EGF) (10 ng/mL) at 37°C humidified conditions [19,23-25]. The same processes were

repeated after 48 h, and the separation and purification of fibroblast and epithelial cells from primary cell culture were completed.

Immunophenotyping

Immunostaining was conducted based on the general immunocytochemistry procedures. For this purpose, ab M3515 and ab M0821 (Dako, USA) were used after 1/50 dilution and ab M0725 (Dako, USA) were used after 1/100 dilution as primary antibodies. As secondary antibodies for cytokeratin, goat anti-mouse IgG FITC (fluorescent isocyanate) (Dako, USA) and for vimentin, goat anti-mouse IgG TRITC (tetramethylrhodamine-isothiocyanate) (Southern Biotech, USA) were used after 1/100 dilution. Hep-2 (human larynx epidermoid cells) cell line was originally derived from an epidermoid carcinoma of the larynx, but it contains HeLa marker chromosomes and were derived via HeLa contamination [26]. Hep-2 cells positive for cytokeratin were used as the positive control group for purified epithelial cells. It was obtained from HÜKÜK (Cell Culture Collection, HÜKÜK, Ankara). MRC-5 cell line established from normal human fetal lung tissue positive for vimentin was used as a positive control group for purified fibroblast cells [27]. It was obtained from ATCC (American Type Culture Collection, Rockville, MD). MRC-5 cells and Hep-2 cells were maintained in Dulbecco's minimal essential medium (DMEM) supplemented with 10% FBS.

Purified epithelial cells, fibroblasts, and the control group cells were separately inoculated to an 8-well chamber slide at 200 cells/well (Lab-Tek II, Thermo Fisher Scientific) left incubation for 24 h in 37°C, 5% CO_2. After the incubation period, the cells were fixed with 400 µL 4% paraformaldehyde for 15 min at 37°C, left in 400 µL permeabilization solution [(0.1 M Tris-Cl (pH 7.4) + 50 mM EDTA (pH 8) + 0.5% TritonX-100)] for 15 min at room temperature to allow antibodies to penetrate cellular membranes. Following PBS washing, the cells were treated with a blocking buffer for 2 h to prevent nonspecific interaction of antibodies in different cellular compartments. Primary antibodies (M3515, M0821, M0725, Dako, USA) were diluted according to the manufacturer's recommendation, applied to the cells and incubated at room temperature for 2 h. After PBS washing, secondary antibodies were applied and incubated at room temperature for 90 min [28]. Following incubation, the cells were stained with DAPI [2-(4-amidinophenyl)-1H-indole-6-carboxamidine] and were evaluated under fluorescence microscope (Olympus IX71, Japan).

Results

Primary Cell Culture

Primary cell culture was established by disaggregation of the tongue tissue using a combined enzymatic and mechanical method. In order to dominate the culture in general and to show cell morphologies in the inverted phase-contrast microscope images of the primary culture, the magnification of images was taken as 100x and 200x. Epithelial-like cell foci formation was observed on the 1st and 3rd days following the attachment of the cells to the culture surface *(Fig. 1-A,B)*. On day 5, proliferation of dispersed fibroblast-like cell populations and epithelial-like cell islets was observed *(Fig. 1-C)*.

Purification and Subcultivation

Purification of the fibroblastic and epithelial cell populations was based on the 0.02% EDTA and 0.01% Na_2EDDA treatment of the primary culture. The culture was monitored at the 5th passage level by microphotography for morphological

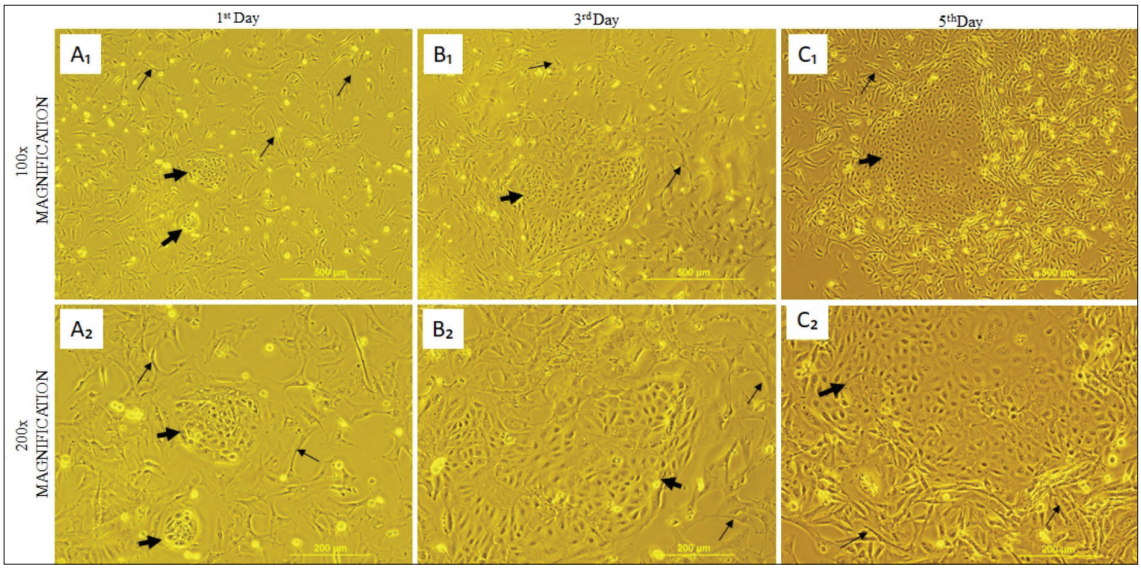

Fig 1. Phase contrast microscope images of the primary culture on day 1, day 3 and day 5. *Thin arrows* indicate fibroblast cells, and *bold arrows* indicate epithelial cell foci (magnification 100X for A_1, B_1, C_1 and magnification 200X for A_2, B_2,C_2)

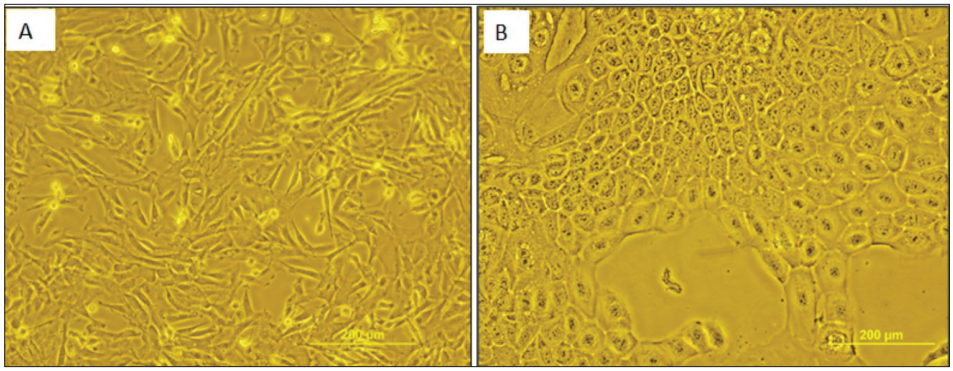

Fig 2. Phase contrast microscope images from passage 5 of purified cells. (A) Fibroblast cell line presents fibroblast-specific elongation and spindle morphology, (B) epithelial cell line presents regular polygonal and islet-shaped proliferative morphology specific to epithelial cells (magnification 200X)

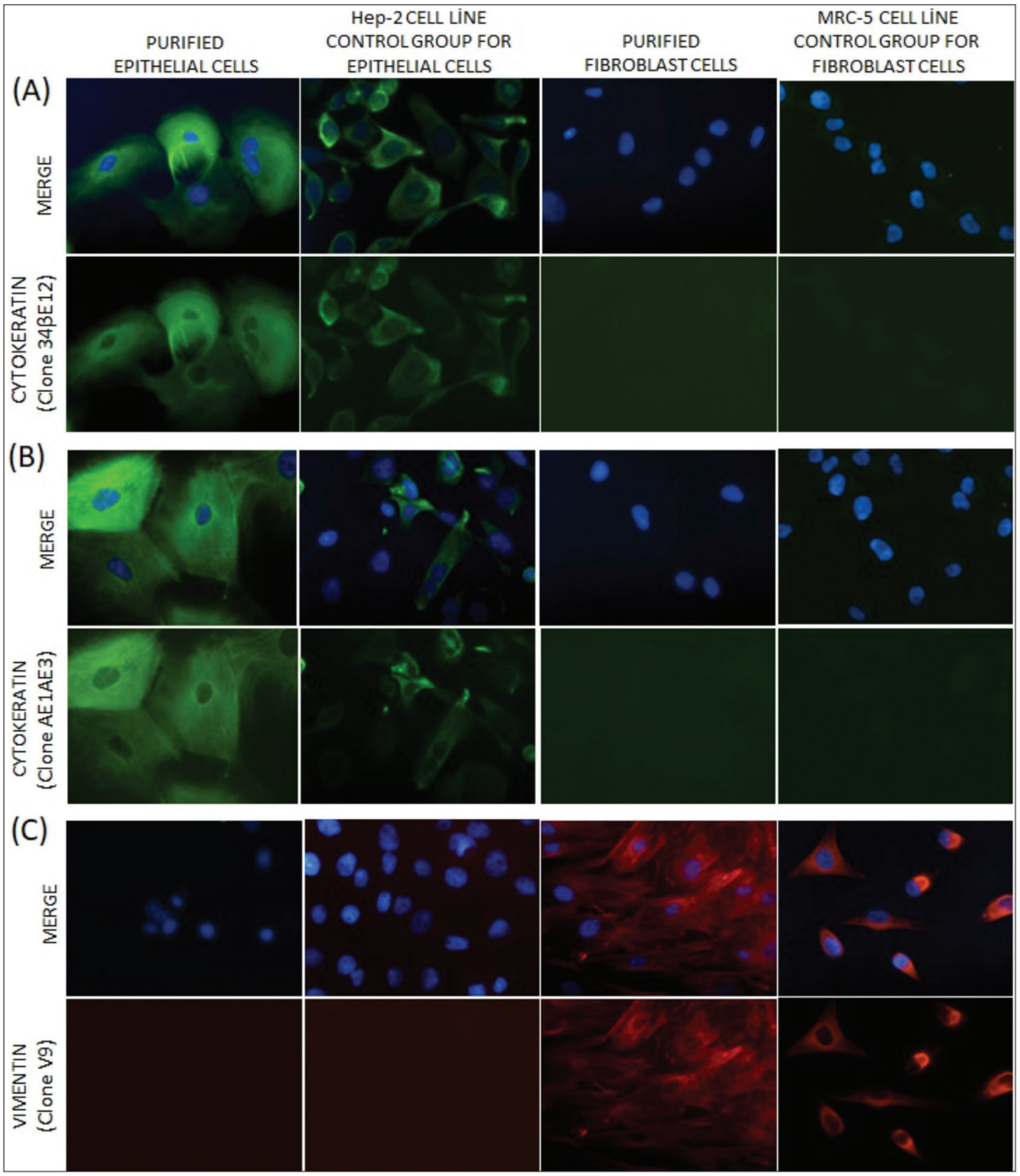

Fig 3. Intermediate filament protein expression of purified epithelial and fibroblast cells. **A, B:** Purified epithelial cells and positive control cells were positive for different cytokeratin expressions, while negative for vimentin expression. **C-** Purified fibroblastic cells and positive control cells were positive for vimentin expression, while negative for cytokeratin expression (magnification 400X)

inspection. While fibroblasts performed scattered, elongated, spindle-shaped and uniform appearance *(Fig. 2-A)*, epithelial cells were standing out with their polygonal shape and islets in different sizes *(Fig. 2-B)*.

Immunophenotyping

After purification, all of the cells were stained with specific markers to examine their epithelial and fibroblastic characters; for cytokeratin and vimentin expression. The purified epithelial cells expressed strong cytokeratin *(Fig. 3-A,B)* and negative for vimentin *(Fig. 3-C);* on the contrary, purified fibroblasts expressed strong vimentin *(Fig. 3-C)* and negative for cytokeratin *(Fig. 3-A,B)* as expected.

Discussion

Today, scientific studies with living systems pose several ethical problems. For this reason, studies on cell culture techniques have been used in the creation of tiny copies of the living environment. Development of the new methods with advancing technology in this field, day by day cell culture areas is becoming more prevalent. The cell lines purified from primary cultures play a pivotal role in producing biotechnological products, cell-based diagnosis and treatments. Fibroblasts can grow faster and differentiate at a higher rate *in vitro*. Because of these properties, fibroblast contamination or dominance is common in primary cultures [23,29]. In this study, two different purified cell populations, epithelial and fibroblast cells, were formed from primary or mixed cell cultures using a novel purification method. In the preparation of primary culture from the bovine tongue, collagenase and dispase enzymes were used together to isolate fibroblasts and epithelial cells from tissue and healthily separate them. Although dispase, a neutral protease, is an effective agent to separate the epidermis from the dermis and is a gentle agent that preserves cellular membrane integrity, sometimes it may be insufficient to separate epithelial cells from the tissue alone. Therefore, it has been used together with the collagenase I [30,31]. In the secondary culture, serum concentration, a mitotic stimulant for fibroblasts, decreased to 5% in the medium and partially reduced the dense fibroblast cell population. Thus, a preliminary preparation was made to remove fibroblasts from the culture in the next step [17]. More robust binding properties than fibroblasts characterize epithelial cells. Keratinocytes compose muscular cell-cell adhesions in a calcium-rich environment. They need extracellular calcium for the formation of adhesive bonds and desmosomes. Different methods, such as enzymatic and chelation, can separate or remove fibroblasts from cultures.

Na_2EDDA is a chelate that binds calcium ions and enables epithelial cells to stay in cell culture flask by strengthening their connections [22]. Singer et al.[32] used the 1B10 monoclonal antibody, which they produced against human thymic fibroblasts, to remove them in culture and recognize fibroblasts with different origins (skin, thymus, synovia) without discrimination. Although this method is complex and relatively expensive, they have shown that the fibroblasts in the culture are eliminated through the complement-mediated cytotoxic effect of the 1B10 monoclonal antibody following 0.02% EDTA treatment in mixed cultures. Drewa et al.[24]. removed fibroblasts from keratinocyte culture using long-term Na_2EDDA treatment. Fibroblasts in keratinocyte cultures produced in DMEM/F12 medium containing autologous serum and some additional additives for epidermal grafting were treated with 0.01% Na_2EDDA until removing in another successful but also time-consuming study, fetal bovine epithelial primary cell culture was treated with 0.01% Na_2EDDA for 2-3 min, then incubated in 2% serum media for 6, 12 and 24 h and again treated with 0.01% Na_2EDDA. These procedures were repeated until the complete removal of the fibroblasts [25].

In this study, primarily, Pal and Grover's method, treatment the culture with antibiotic in Hanks' balanced salt solution, which is a practical and economical method to remove fibroblasts, was used [23]. Still, the fibroblasts could not be eradicated completely. Then, Jeon and Hwang's purification method was applied, the cells were purified, but it was observed that epithelial cells lost their membrane integrity in the 0.05% Na_2EDDA solution used in the first step and granulations were appeared in the cells following subculture [19]. After these experiences, a protocol that combines the different stages of the methods mentioned earlier has been developed. According to this protocol, the serum concentration in secondary culture was reduced to 5%. The dominance of fibroblasts was limited, followed by short trypsinization (0.25%), which saves time in the long-term Na_2EDDA method of Drewa et al.[24]. At the last stage, fibroblasts and epithelial cells were purified by treatment with 0.02% EDTA and Na_2EDDA (0.01%), which binds calcium ions. In the microscopic examination, it was observed that their viability and morphology were healthy. Tissue origins of purified cells were confirmed by using immunostaining. It was observed that epithelial cells expressed cytokeratin and fibroblast cells expressed vimentin.

In conclusion, this study demonstrates an economical, effective, and easy method that can be applied to remove fibroblasts from the environment in primary or mixed cultures and create different cell lines by purifying epithelial and fibroblastic cells.

Funding Support

There is no specific grant funding source.

Conflict of Interest

The author declare that have no conflict of interest.

Availability of Data and Materials

Datasets analyzed during the current study are available in the author on reasonable request.

Acknowledgements

The author sincerely acknowledges the Foot and Mouth Disease Institute for providing the facilities for this work. I would also like to S. İsmet Deliloğlu Gürhan, D.V.M. PhD (Emeritus Professor, Ege University, İzmir, Turkey) for providing critical review of the manuscript

References

1. Hayflick L, Moorhead PS: The serial cultivation of human diploid cell strains. *Exp Cell Res*, 25, 585-621, 1961. DOI: 10.1016/0014-4827(61)90192-6

2. Jedrzejczak-Silicka M: History of cell culture. **In,** Gowder SJT (Ed): New Insights into Cell Culture Technology, 1-29. *IntechOpen*, Janeza Trdine 9, 51000 Rijeka, Croatia 2017. DOI: 10.5772/66905

3. Fukai K, Morioka K, Yamada M, Nishi T, Yoshida K, Kitano R, Yamazoe R, Kanno T: Comparative performance of fetal goat tongue cell line ZZ-R 127 and fetal porcine kidney cell line LFBK-αvβ6 for *Foot-and-mouth disease virus* isolation. *J Vet Diagn Investig,* 27, 516-521, 2015. DOI: 10.1177/1040638715584156

4. Pamies, D, Bal-Price A, Chesné C , Coecke S , Dinnyes A, Eskes C, Grillari R, Gstraunthaler G, Hartung T, Jennings P, Leist M, Martin U, Passier R, Schwamborn JC, Stacey GN, Ellinger-Ziegelbauer H, Daneshian M: Advanced Good Cell Culture Practice for human primary, stem cell-derived and organoid models as well as microphysiological systems. *Altex,* 35 (3): 353-378, 2018. DOI: 10.14573/altex.1710081

5. Geraghty RJ, Capes-Davis A, Davis JM, Downward J, Freshney RI, Knezevic I, Lovell-Badge R, Masters JR, Meredith J, Stacey GN, Thraves P, Vias M: Guidelines for the use of cell lines in biomedical research. *Br J Cancer*, 111 (6): 1021-1046, 2014. DOI: 10.1038/bjc.2014.166

6. Masters JRW: Human cancer cell lines: Fact and fantasy. *Nat Rev Mol Cell Biol*, 1, 233-236, 2000. DOI: 10.1038/35043102

7. Coecke S, Balls M, Bowe G, Davis J, Gstraunthaler G, Hartung T, Hay R, Merten OW, Price A, Schechtman L, Stacey G, Stokes W: Guidance on good cell culture practice: A report of the second ECVAM task force on good cell culture practice. *Altern Lab Anim*, 33, 261-287, 2005. DOI: 10.1177/026119290503300313

8. Kaplan J, Hukku B: Cell line characterization and authentication. *Methods Cell Biol,* 57, 203-216, 1998. DOI: 10.1016/s0091-679x(08)61579-4

9. Horbach SPJM, Halffman W: The ghosts of HeLa: How cell line misidentification contaminates the scientific literature. *Plos One*, 12 (10): e0186281, 2017. DOI: 10.1371/journal.pone.0186281

10. Patil R, Kale A, Mane D, Patil D: Isolation, culture and characterization of primary cell lines of human buccal mucosal fibroblasts: A combination of explant enzamytic technique. *J Oral Maxillofac Pathol*, 24 (1): 68-75, 2020. DOI: 10.4103/jomfp.JOMFP_282_19

11. Ulrich AB, Pour PM: Cell Lines. Brenner's Encyclopedia of Genetics, 481-482. Elsevier, 2001. DOI: 10.1016/B978-0-12-374984-0.00212-6

12. Bragulla HH, Homberger DG: Structure and functions of keratin proteins in simple, stratified, keratinized and cornified epithelia. *J Anat*, 214, 516-559, 2009. DOI: 10.1111/j.1469-7580.2009.01066.x

13. Tauchi H, Imashiro C, Kuribara T, Fujii G, Kurashina Y, Totani K, Takemura K: Effective and intact cell detachment from a clinically ubiquitous culture flask by combining ultrasonic wave exposure and diluted trypsin. *Biotechnol Bioprocess Eng*, 24, 536-543, 2019. DOI: 10.1007/s12257-018-0491-2

14. Burry RW: Immunocytochemistry, 1-6: Springer, New York, 2010. DOI: 10.1007/978-1-4419-1304-3

15. Henrot P, Laurent P, Levionnois E, Leleu D, Pain C, Truchetet ME, Cario M: A method for ısolating and culturing skin cells: Application to endothelial cells, fibroblasts, keratinocytes, and melanocytes from punch biopsies in systemic sclerosis skin. *Front Immunol,* 11:566607, 2020. DOI: 10.3389/fimmu.2020.566607

16. Yi X, Chen F, Liu F, Peng Q, Li Y, Li S, Du J, Gao Y, Wang Y: Comparative separation methods and biological characteristics of human placental and umbilical cord mesenchymal stem cells in serum-free culture conditions. *Stem Cell Res Ther,* 11:183 2020. DOI: 10.1186/s13287-020-01690-y

17. Kaushik RS, Begg AA, Wilson HL, Aich P, Abrahamsen MS, Potter A, Babiuk LA, Griebel P: Establishment of fetal bovine intestinal epithelial cell cultures susceptible to bovine rotavirus infection. *J Virol Methods*, 148, 182-196, 2008. DOI: 10.1016/j.jviromet.2007.11.006

18. Desmarets LM, Theuns S, Olyslaegers DA, Dedeurwaerder A, Vermeulen BL, Roukaerts ID, Nauwynck HJ: Establishment of feline intestinal epithelial cell cultures for the propagation and study of feline enteric coronaviruses. *Vet Res*, 44 (1): 71, 2013. DOI: 10.1186/1297-9716-44-71

19. Jeon KL, Hwang KK: Establishment of canine kidney cell line for canine distemper virus replication. *J Biomed Res*, 16, 6-12, 2015. DOI: 10.12729/jbr.2015.16.1.006

20. Zhang Y, An J, Liu M, Li N, Wang W, Yao H, Li N, Yang X, Sun Y, Xu N, Wu L: Efficient isolation, culture, purification, and stem cell expression profiles of primary tumor cells derived from uterine cervical squamous cell carcinoma. *Am J Reprod Immunol*, 84 (2): e13251, 2020. DOI: 10.1111/aji.13251

21. Freshney RI: Culture of Animal Cells: A Manual of Basic Technique and Specialized Applications. 6th ed., 196-335, John Wiley & Sons Inc, Hoboken, New Jersey, 2010. DOI: 10.1002/9780470649367

22. Singer KH, Scearce RM, Tuck DT, Whichar LP, Dennin SM, Haynes BF: Removal of fibroblasts from human epithelial cell cultures with use of a complement fixing monoclonal antibody reactive with human fibroblasts and monocytes/macrophages. *J Invest Dermatol*, 92 (2): 166-170, 1989. DOI: 10.1111/1523-1747.ep12276685

23. Pal K, Grover PL: A simple method for the removal of contaminating fibroblasts from cultures of rat mammary epithelial cells. *Cell Biol Int Rep*, 7 (10): 779-783, 1983.

24. Drewa T, Szmytkowska K, Wlodarczyk Z, Sir I, Kierzenkowska-Mila C: Does the presence of unwanted dermal fibroblasts limit the usefullness of autologous epidermal keratinocyte grafts? *Transplant Proc*, 38 (9): 3088-3091, 2006. DOI: 10.1016/j.transproceed.2006.08.103

25. Jeon K, Hwang K: Establishing bovine epithelial cells by removing fibroblast during primary culture. *Lab Anim Res*, 25 (3): 251-256, 2009.

26. Gorphe PA: Comprehensive review of Hep-2 cell line in translational research for laryngeal cancer. *Am J Cancer Res*, 9 (4): 644-649, 2019.

27. Jacobs JP, Jones CM, Baılle JP: Characteristics of a human diploid cell designated MRC-5. *Nature*, 227,168-170, 1970. DOI: 10.1038/227168a0

28. Bocksteins E, Shepherd AJ, Mohapatra DP, Snyders DJ: Immuno-staining of voltage-gated ıon channels in cell lines and neurons - Key concepts and potential pitfalls. in applications of immunocytochemistry. **In,** Dehghani H (Ed): Applications of Immunocytochemistry, 3-28, *InTech*, Janeza Trdine 9, 51000 Rijeka, Croatia, 2012. DOI: 10.5772/34817

29. Kisselbach L, Merges M, Bossie A, Boyd A: CD90 Expression on human primary cells and elimination of contaminating fibroblasts from cell cultures. *Cytotechnology*, 59 (1): 31-44, 2009. DOI: 10.1007/s10616-009-9190-3

30. Mirbolooki MR, Bozorgmanesh H, Foster C, Kuhtrieber W, Lakey JRT: Cell Isolation from Tissue. **In,** Comprehensive Biotechnology 2nd ed., Vol. 1, 591-598, Elsevier, 2011.

31. Li F, Adase CA, Zhang L: Isolation and culture of primary mouse keratinocytes from neonatal and adult mouse skin. *J Vis Exp*, 125:56027. 2017. DOI: 10.3791/56027

32. Brückner RB, Janshoff A: Importance of integrity of cell-cell junctions for the mechanics of confluent MDCK II cells, *Sci Rep*, 8:14117, 2018. DOI: 10.1038/s41598-018-32421-2

Kafkas Universitesi Veteriner Fakultesi Dergisi
ISSN: 1300-6045 e-ISSN: 1309-2251
Journal Home-Page: http://vetdergikafkas.org

Kafkas Univ Vet Fak Derg
27 (6): 681-690, 2021
DOI: 10.9775/kvfd.2021.26080

RESEARCH ARTICLE

Mechanism of miR-665 Regulating Luteal Function Via Targeting HPGDS

Yan-yan SHAO [1,a,#] Lin FU [2,b,#] Meng-ting ZHU [1,c] Ying NAN [1,d] Heng YANG [3,4,e (*)] Zong-sheng ZHAO [1,f (*)]

[1] College of Animal Science and Technology, Shihezi University, Shihezi 832000, Xinjiang, CHINA
[2] Research Institute of Herbivorous Livestock, Chongqing Academy of Animal Sciences, Chongqing, CHINA
[3] College of Veterinary Medicine, Southwest University, Chongqing, CHINA
[4] Immunology Research Center, Medical Research Institute, Southwest University, Chongqing, CHINA
ORCIDs: [a] 0000-0002-7564-6776; [b] 0000-0002-2724-2566; [c] 0000-0002-1153-6914; [d] 0000-0002-8674-112 X; [e] 0000-0002-2072-0713
[f] 0000-0002-0953-5365

Article ID: KVFD-2021-26080 Received: 30.05.2021 Accepted: 27.11.2021 Published Online: 28.11.2021

Abstract

Given few reports on the interaction of miRNA-665/target gene pair, we aimed to construct a dual luciferase reporter gene vector for 3′-untranslated region (3′-UTR) of the haematopoietic prostaglandin D synthase (HPGDS) gene and elucidate the underlying molecular mechanism of miR-665 regulation of HPGDS. Bioinformatics software was used to predict miR-665 targeting of 3′-UTR region of HPGDS gene. The reliability of the synthetic psiCHECK-HPGDS-w/m-3′-UTR was determined using double luciferase digestion method. Then, miR-665 mimic/negative control was separately co-transfected with sheep luteal cells, and then, luciferase activity and HPGDS expression were detected. Results showed that 3′-UTR wild-type (psiCHECK2-HPGDS-w-3′UTR) and mutant (psiCHECK2-HPGDS-m-3′UTR) expression vectors for HPGDS were successfully constructed, and dual luciferase reporter gene assay showed that the expression of relative luciferase activity was inhibited in the w-3′-UTR group, with 52% decrease compared to the blank/negative control group, and the difference was statistically significant ($P<0.05$). Whereas in luteal cells, compared to the blank/negative control group, RT-PCR and western blot assays showed lower HPGDS expression levels when miR-665 overexpression in miR-665-mimic group. Meanwhile, our result also showed that P4 concentration significantly increased using ELISA test in above group. In brief, our data verified that 3′-UTR wild-type dual luciferase reporter gene vector of HPGDS was successfully constructed, and miR-665 could target the gene by acting on the 3′-UTR region of HPGDS to regulate the ovine luteal cell function, providing a strong support to study the function and molecular mechanism of miR-665 in targeting HPGDS, especially in the ovarian-luteal tissue of sheep.

Keywords: *3′-UTR, miRNA, Target gene, Luteal cells, Sheep*

MiR-665'nin HPGDS Hedefli Luteal Fonksiyon Düzenleme Mekanizması

Öz

MiRNA-665/hedef gen çiftinin etkileşimi hakkında az sayıdaki rapor göz önüne alındığında, hematopoietik prostaglandin D sentaz (HPGDS) geninin 3′-kodlanmayan bölgesi (3′-UTR) için bir çift lusiferaz raportör gen vektörünün oluşturulması ve HPGDS'nin miR-665 regülasyonunun moleküler mekanizmasının aydınlatılması amaçlandı. HPGDS geninin 3′-UTR bölgesini hedefleyen miR-665'nin saptanması için biyoinformatik yazılım kullanıldı. Sentetik psiCHECK-HPGDS-w/m-3′-UTR'nin güvenilirliği, dual lusiferaz sindirim yöntemi ile belirlendi. Daha sonra miR-665 mimik/negatif kontrolün, koyun luteal hücreleri ile ayrı ayrı ko-transfeksiyonu yapıldı ve ardından lusiferaz aktivitesi ve HPGDS ekspresyonu tespit edildi. Sonuçlar, HPGDS için 3′-UTR yabanıl tip (psiCHECK2-HPGDS-w-3′UTR) ve mutant (psiCHECK2-HPGDS-m-3′UTR) ekspresyon vektörlerinin başarıyla oluşturulduğunu ve dual lusiferaz raportör gen analizi, relatif lusiferaz aktivite ekspresyonunun, blank/negatif kontrol grubuna kıyasla %52'lik bir düşüşle w-3′-UTR grubunda inhibe edildiğini ve farkın istatistiksel olarak anlamlı olduğunu gösterdi ($P<0.05$). Luteal hücrelerde, blank/negatif kontrol grubu ile karşılaştırıldığında, RT-PCR ve western blot deneyleri, miR-665-mimik grubunda miR-665'in aşırı ekspresyonunda HPGDS'nin daha düşük oranda eksprese olduğunu gösterdi. Ayrıca, sonuçlarımız yukarıda bahsedilen grupta ELISA testi kullanılarak P4 konsantrasyonunun önemli ölçüde arttığını gösterdi. Özetle, verilerimiz özellikle koyunların yumurtalık luteal dokusunda HPGDS'yi hedeflemede miR-665'nin işlevini ve moleküler mekanizmasını incelemek için güçlü destek sağlayarak, HPGDS'nin 3′-UTR yabanıl tip dual lusiferaz raportör gen vektörünün başarıyla oluşturulduğunu ve miR-665'in, koyun luteal hücre fonksiyonunu düzenlemede HPGDS'nin 3′-UTR bölgesi üzerinde hareket ederek geni hedefleyebildiğini doğruladı.

Anahtar sözcükler: *3′-UTR, MiRNA, Hedef gen, Luteal hücre, Koyun*

How to cite this article?

Shao YY, Fu L, Zhu MT, Nan Y, Yang H, Zhao ZS: Mechanism of miR-665 regulating luteal function via targeting HPGDS. *Kafkas Univ Vet Fak Derg,* 27 (6): 681-690, 2021.
DOI: 10.9775/kvfd.2021.26080

(*) Corresponding Author

Tel: +86 13627697651; +86 1356 5735767
E-mail: yh20183007@swu.edu.cn (H. Yang); zhaozongsh@shzu.edu.cn (Z. Zhao)

Introduction

Haematopoietic prostaglandin D synthase (HPGDS) belongs to the GST superfamily and the sigma family [1]. HPGDS contains GST C-terminal structural domain and GST N-terminal structural domain. HPGDS is a cytosolic enzyme that heterodimerises PGH_2 and is able to selectively and efficiently heterodimerise PGH_2 to PGD_2 [2], whereas other GST isoenzymes non-selectively catalyse the conversion of PGH_2 to PGD_2, PGE_2, and $PGF_{2\alpha}$ [3,4]. HPGDS is widely expressed in mast cells, macrophages, Th2 cells, and other leukocytes, and it is believed that it can promote PGD_2 synthesis and play an important regulatory role in most inflammatory responses [5,6]. Moreover, HPGDS can exist as a homodimer in living organisms and is highly expressed in the adipose tissue, placenta, ovary, and corpus luteum [7,8]. This also suggests that HPGDS may be actively involved in lipid synthesis and metabolism as well as in reproductive regulation (e.g., follicular development and luteal maintenance and degeneration) in animals.

MicroRNAs (miRNAs) are endogenous non-coding RNAs with regulatory functions in eukaryotic organisms, whose mature bodies recognise target mRNAs through base complementary pairing and direct silencing complexes to degrade target genes or block mRNA transcription depending on the degree of complementarity [8-10]. Accumulating evidence suggests that miRNA mediated post-transcriptional modification of genes can regulate many pathophysiological processes, such as inflammation, angiogenesis, fibrotic repair, apoptosis, and uterine adhesion [11]. miR-665 is a newly identified miRNA, which is closely associated with the functions of the reproductive system in females, playing a regulatory role in follicular-luteal transition [12]. This study aims to investigate the changes in miR-665 expression in luteal tissue after follicle-luteal transition in females and conduct experimental validation and correlation analyses using the bioinformatics target gene prediction results of our group, that is, the existence of target binding sites between miRNA-665 and HPGDS, to lay a solid foundation for an in-depth investigation of miR-665 role in luteal tissue and its targeted regulation of HPGDS in the molecular regulation mechanism of luteal cells.

Material and Methods

Primary Cell Culture and Identification

Mid-term luteal tissue of 20 healthy Kazakh nulliparous ewes was obtained from Shihezi Slaughterhouse in Xinjiang, China in September 2020, and brought back to the laboratory with fat and connective tissue removed. The tissue was cut into 1-mm^3 pieces, and the shredded luteal tissue was digested using collagenase II (Gibco, USA) at 37°C for 1 h. The resulting cell precipitate was then inoculated in DMEM/F12 medium containing 10% foetal bovine serum and cultured at 37°C in a 5% CO_2 incubator. Purified ewe luteal cells were obtained after 3-4 passages of the culture. Synaptophysin (SYP) (Bioss, China) immunocytochemical staining was used to identify ewe luteal cells.

MicroRNA-665 Target Gene Prediction

Target scan *(http://www.targetscan.org/)* and RNA hybrid *(http://bibiserv.techfak.uni-bielefeld.de/)* target gene software were used simultaneously to predict the target gene of miR-665, namely HPGDS, and to obtain more plausible miR-665 and HPGDS-3′ sequence pairing sites through screening and analysis.

Construction and Characterisation of Wild-Type and Mutant psiCHECK-HPGDS-w/m-3′-UTR Vectors

Our laboratory provided the vector psiCHECK-2 (Promega, USA) and sent it to Shanghai Bioengineering Co., Ltd. for direct synthesis of psiCHECK-HPGDS-w/m-3′-UTR, which contains Luc marker gene expression (the Appendix for information on the wild-type and mutant HPGDS sequences *(Table 1)*. To verify the reliability of the synthesised w/m-3¢-UTR vector, the target fragments were inserted into XhoI and NotI sites for enzymatic cleavage in the following system: w/m-3′-UTR vector (500 ng/μL) 4 μL, 10×H buffer 2 μL, XhoI 1 μL, NotI 1 μL, ddH_2O 12 μL, in a constant temperature water bath at 37°C for 1 h, followed by addition of 1.5% agarose gel for double digestion. Then,

Table 1. Wild-type HPGDS-3'UTR and Mutant-type HPGDS-3'UTR sequences

Wild-type HPGDS-3'UTR Sequences
TCACCAGAGTCTAGCAATAGCAAGATACTTGACCAGAAACACAGATTTGGCTGGAAAAACAGAACTTGAACAATGTCAAGTGGATG CAATTGTGGACACACTGGATGATTTCATGTCTCGTTTTCCTTGGGCAGAGAAAAGACAAGATATAAAAAATCAGATATTTAAGGAGC TACTTACCTGTGATGCACCTCCTCTTCTGCAAAGTTTGGACACATACTTAGGGGAAAACGAGTGGTTTATTGGTGACTCTGTAACTTG GGCAGACTTCTACTGGGAAATTTGCAGTACCACACTTTTGGTCTTTAAACCTGATTTGTTGGACATCCACCCCAGGCTGGTGACATT ACGGAAGAAAGTCCAAAGCATCCCTGCCATCGCTGACTGGATACTGCGAAGGCCCCAGACCAAACTCTAG
Mutant-type HPGDS-3'UTR Sequences
TCACCAGAGTCTAGCAATAGCAAGATACTTGACCAGAAACACAGATTTGGCTGGAAAAACAGAACTTGAACAATGTCAAGTGGATG CAATTGTGGACACACTGGATGATTTCATGTCTCGTTTTCCTTGGGCAGAGAAAAGACAAGATATAAAAAATCAGATATTTAAGGAGC TACTTACCTGTGATGCACCTCCTCTTCTGCAAAGTTTGGACACATACTTAGGGGAAAACGAGTGGTTTATTGGTGACTCTGTAACTTc GtCAGACTTgTcCaGtGAAATTTGCAGTACCACACTTTTGGTCTTTAAACCTGATTTGTTGGACATCCACCCCAGGCTGGTGACATTAC GGAAGAAAGTCCAAAGCATCCCTGCCATCGCTGACTGGATACTGCGAAGGCCCCAGACCAAACTCTAG

w/m-3′-UTR was transformed into DH5α receptor cells for expansion and plasmid extraction. The concentration and purity of the plasmids were determined using NanoDrop 2000 (Thermo, USA), and the qualified plasmids were used for the later transfection assays.

Cell Grouping and Transfection

Luteinising cells were inoculated in 12-well plates with 2×10^6 cells/well and incubated overnight. When the cell density reached 70%-80%, five groups were made, namely, blank control group (adding equal volume of blank liposome mixture, abbreviated BC), test group 1 (psiCHECK-HPGDS-w-3′UTR + miR-665 mimic, abbreviated w-3′-UTR), negative control group 1 (psiCHECK-HPGDS-w-3′UTR + miR-665 negative control, abbreviated w-NC), test group 2 (psiCHECK-HPGDS-m-3′UTR + miR-665 mimic, abbreviated m-3′-UTR), and negative control group 2 (psiCHECK-HPGDS-m-3′UTR + miR-665 negative control, abbreviated m-NC). Each group of 3 wells was replicated and transiently transfected with luteinising cells by lipofectamine 3000 (Invitrogen, USA), incubated at 37°C for 6 h, and then, the cell culture medium was changed. After 48 h of incubation, the wells were washed 3 times with PBS and 1 mL of total RNA lysate was added to each well and agitated on a shaker for sufficient lysis. The total RNA was extracted by centrifuging supernatant lysate and their concentration was measured, and then, it was stored at -80°C until further analysis.

Dual Luciferase Reporter Gene Activity Assay

After 48 h of transfection, the instructions of the manufacturer of the dual luciferase reporter gene assay kit (Beyotime, China) were followed, and finally, the fluorescence values were read, and the relative fluorescence activity was calculated using Synergy H4 multifunctional enzyme marker (BioTek, USA).

Changes in HPGDS and miR-665 Expression were Evaluated Using qRT-PCR

When the density of the luteinising cells in the culture dish reached 70%-80%, miR-665-mimic/negative control transfection test was continued and three groups were set up, namely, blank control group, miR-665-mimic group, and negative control group. After 48 h, total RNA and miRNA were extracted from each group and were subjected to reverse transcription using reverse transcription kit at 42°C for 15 min and 85°C for 5 min, and then stored at -20°C. The ploidy changes of the target genes were calculated using the $2^{-\Delta\Delta CT}$ method according to SYBR Mixture kit (TaKaRa, Japan) instructions. All primers are shown in *Table 2*. Three parallel sets were set up for each test group. The test was repeated thrice and the results were recorded.

Changes in HPGDS Expression were Evaluated Using Western Blot

Luteinising cells from each group transfected for 48 h were collected and total protein was extracted from each group using RIPA strong cell lysate. Protein from cells was extracted using RIPA lysis buffer, and the protein concentrations was detected using the BCA protein quantification kit (Abcam, Britain). 30 μg protein samples were performed SDS-PAGE, and transferred to PVDF membranes (Millipore, USA) after 1.5 h. 5% skimmed milk was used to block for 30 min at room temperature. The membranes were incubated with the primary antibodies overnight at 4°C (Rabbit anti-Bcl-2 (ab196495; 1:500), rabbit anti-caspase3 (ab90437; 1:1,000) and rabbit anti-β-actin (ab8227; 1:1,000), Abcam, Britain). After washing with PBS three times, the membranes were incubated with goat anti-rabbit immunoglobulin G (IgG) at room temperature for 2 h. Protein bands were visualized using an Electrochemiluminescence (ECL) chemiluminescence kit (WBULS0500; EMD Millipore, USA) and the bands intensity was quantified with Quantity One software.

Table 2. *All primers for miR-665 and HPGDS*

Name	Primers
miR-665	ACCAGTAGGCCGAGGCC
U6	CAAGGATGACACGCAAATTCG
HPGDS	F: ATGCCTAACTACAAACTGCTT
	R: CTAGAGTTTTGTCTGTGGCCT
β-actin	F: CAGCAGATGTGGATCAGCAAGCAG
	R: TTGTCAAGAAAAAGGGTGTAACGCA

Detection of Progesterone Concentration in Culture Medium Using ELISA

All culture medium from each group transfected for 48 h were collected, and then these samples were centrifuged and their upper part liquid were absorbed to detected using Sheep P_4 ELISA Kit according to the manufacturer's instruction. Three parallel sets were set up for each test group. The test was repeated thrice and the results were recorded.

Statistical Analysis

Data were presented in figures. Bar graph with y-axis indicating mean and error bar as standard deviation in *Fig. 5, 6* and *7*. Student's t-test or One-way ANOVA followed by Tukey's test was used to analyse the statistical differences among groups (normally distributed and the group variances are homogenous) based on SPSS 20.0 software (SPSS, Inc., Chicago, IL, USA). $P<0.05$ was regarded as a statistically significant difference.

Results

Culture and Identification of Corpus Luteal Cells

The corpus luteal cells isolated by collagenase II digestion were in a single dispersed state, and the cell bodies were transparent, round or polygonal cells with a relatively

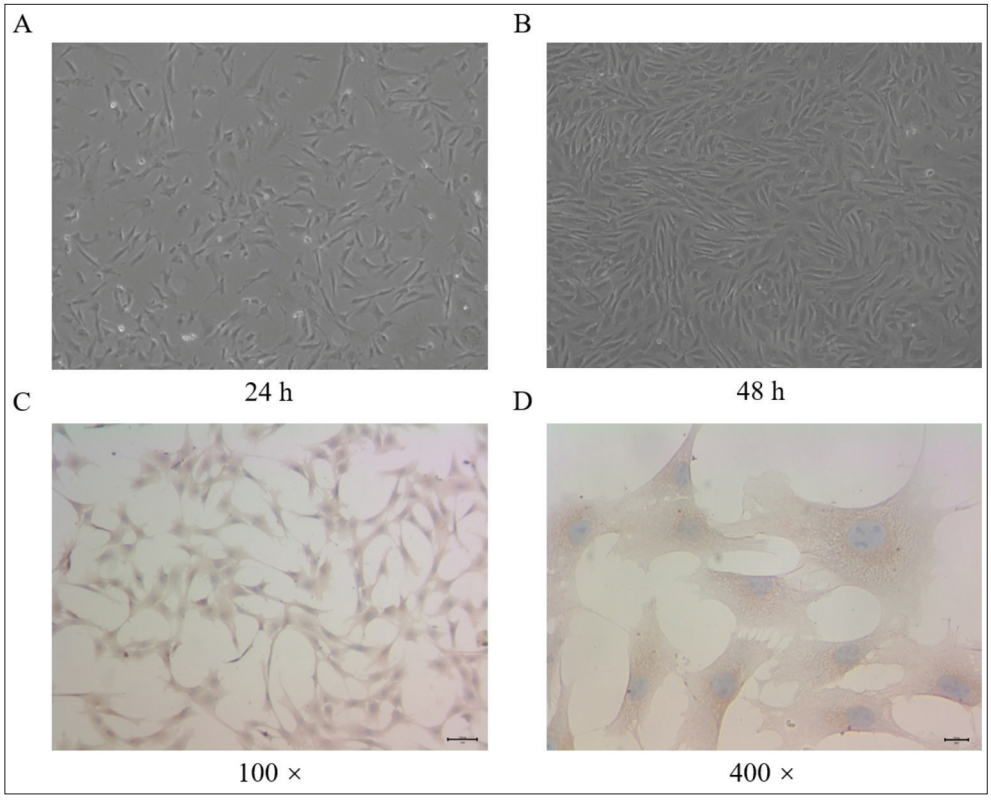

Fig 1. Primary luteal cells were cultured *in vitro* and its specific marker, the expressions of SYP protein was identified with immunohistochemistry. A and B were cultured for 24 and 48 h *in vitro,* respectively. C and D were cultured for 48 h, SYP protein was detected by immunocytochemistry

small volume. After 24 h of culture, the corpus luteal cells began to adhere to the wall, showing an irregular shape with a tendency to extend outward, and connections between adjacent cells began to be established *(Fig. 1-A)*. After culturing for 48 h, the cells entered the logarithmic growth phase, and the cells were completely attached to the wall, showing a fusiform or irregular shape *(Fig. 1-B)*. Mammalian corpus luteum belongs to the diffuse neuroendocrine system, and SYP is a more comprehensive neuroendocrine marker. The positive rate of corpus luteal cells identified by SYP cell immunohistochemistry was over 90% *(Fig. 1-C,D)*, indicating that the isolated cells were sheep corpus luteal cells.

Target Genes of miR-665 were Predicted Using Targetscan and miRDB Software

The predictions from the two databases were amalgamated and potential binding sites between miR-665 and HPGDS were found to exist. The plausible target sites for HPGDS were obtained using the Targetscan software prediction, as shown in *Fig. 2*. Meanwhile, these sites (GGGC and CUACUGG) were mutated to CGUC and GUCCAGU in 3′-UTR mutant vector *(Fig. 2)*.

Identification of the Dual Luciferase Reporter Plasmid psiCHECK-HPGDS-w/m-3′-UTR

To verify the reliability of synthesising psiCHECK-HPGDS-w/m-3′-UTR vector, the target fragments were inserted into XhoI and NotI sites for enzymatic cleavage, and the results here indicated that the target gene HPGDS had been inserted into psiCHECK successfully, as shown in *Fig. 3*. And then, the constructed psiCHECK-HPGDS-w/m-3′-UTR vectors were sent to Bioengineering (Shanghai) Co. for sequence determination, the sequencing results demonstrated that the sequence bases were correct *(Fig. 4-A,B)*, which could be used subsequently for large-scale extraction of plasmids from the constructed vectors and further transfection experiments using the endotoxin-free plasmid bulk extraction kit.

Dual Luciferase Reporter Test

Luciferase reporter assays were performed, and total cellular RNA was extracted for qRT-PCR analysis. The results showed that transfection with miR-665 significantly reduced the relative fluorescence activity ratio (abbreviated Rluc/Luc) of luteal cells transfected with psiCHECK2-HPGDS-w-3′UTR compared to that of w-NC/m-NC group ($P<0.01$), whereas there was no significant change in Rluc/Luc of luteal cells transfected with psiCHECK2-HPGDS-m-3′UTR ($P>0.05$) *(Fig. 5)*.

miR-665 Negatively Regulates HPGDS Expression in Luteal Cells

After miR-665 mimic/negative control transfection of luteal cells, total RNA, miRNA, and protein were extracted after

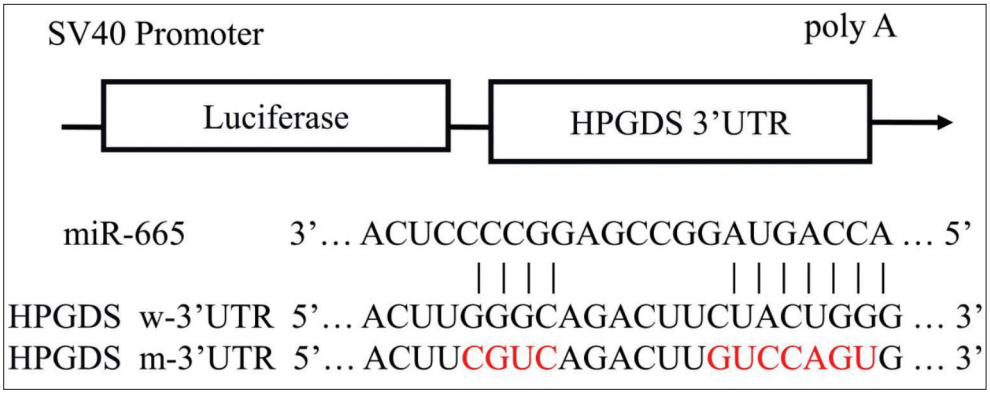

Fig 2. Schematic diagram of target binding site between miR-665 and HPGDS (in red font for mutation sites)

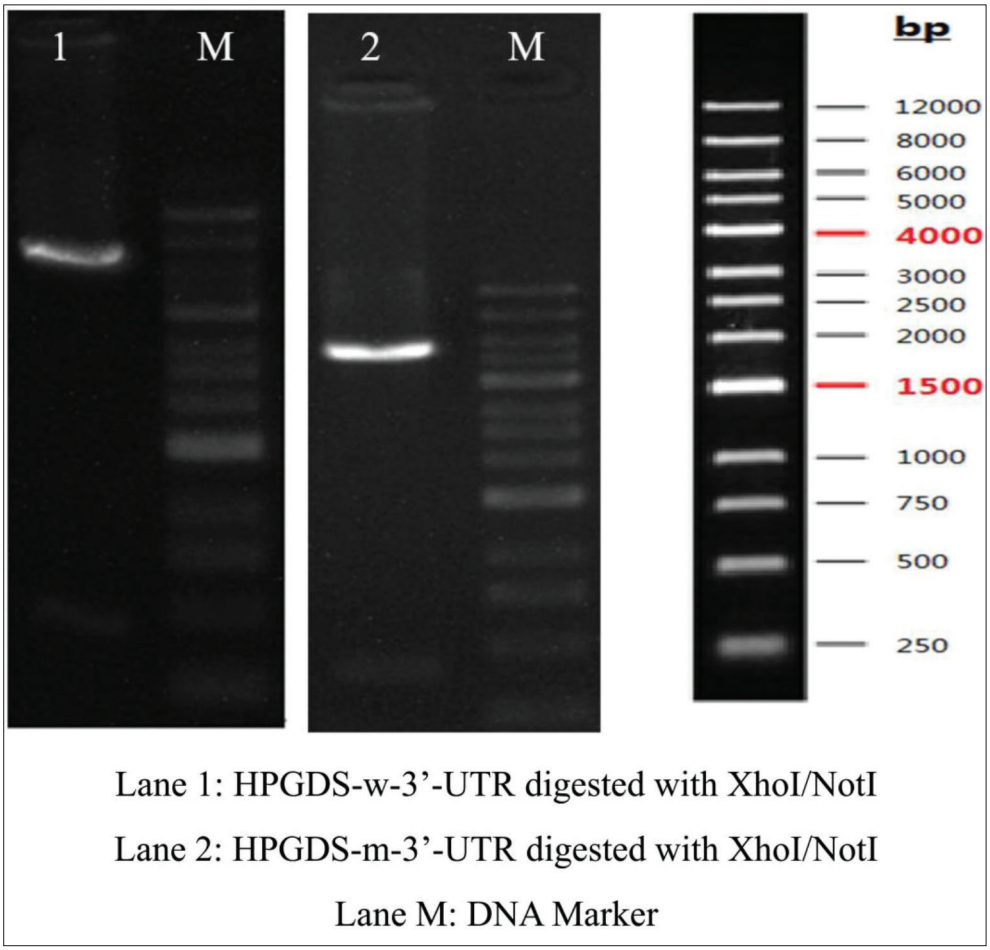

Fig 3. Expression vector psiCHECK-HPGDS-w/m-3'UTR was correctly constructed, identified with double-enzyme digestion

48 h of culture and the changes in HPGDS expression were detected using qRT-PCR and western blot. The results revealed that miR-665 mimic caused miR-665 overexpression, when compared with the miR-655 expression in the blank control and negative control groups *(Fig. 6-A)* ($P<0.001$). However, at the mRNA level, the results showed that HPGDS expression was significantly inhibited in luteal cells ($P<0.01$) *(Fig. 6-B)*; moreover, the results of western blotting showed a significant decrease in HPGDS protein levels ($P<0.01$) *(Fig. 6-C,D)*.

Progesterone Concentration Test

Cell cultures from the different treatment groups in the previous section were collected and their P_4 concentrations were measured separately using ELISA method, as shown in *Fig. 7*. The results showed that P_4 concentration

A

HPGDS-3'UTR	TCACCAGAGTCTAGCAATAGCAAGATACTTGACCAGAAACACAGATTTGGCTGGAAAAAC
Sequencing	CTCGAGTCACCAGAGTCTAGCAATAGCAAGATACTTGACCAGAAACACAGATTTGGCTGGAAAAAC
HPGDS-3'UTR	AGAACTTGAACAATGTCAAGTGGATGCAATTGTGGACACACTGGATGATTTCATGTCTCGTTTTCCT
Sequencing	AGAACTTGAACAATGTCAAGTGGATGCAATTGTGGACACACTGGATGATTTCATGTCTCGTTTTCCT
HPGDS-3'UTR	TGGGCAGAGAAAAGACAAGATATAAAAAATCAGATATTTAAGGAGCTACTTACCTGTGATGCACCT
Sequencing	TGGGCAGAGAAAAGACAAGATATAAAAAATCAGATATTTAAGGAGCTACTTACCTGTGATGCACCT
HPGDS-3'UTR	CCTCTTCTGCAAAGTTTGGACACATACTTAGGGGAAAACGAGTGGTTTATTGGTGACTCTGTAACTT
Sequencing	CCTCTTCTGCAAAGTTTGGACACATACTTAGGGGAAAACGAGTGGTTTATTGGTGACTCTGTAACTT
HPGDS-3'UTR	GGGCAGACTTCTACTGGGAAATTTGCAGTACCACACTTTTGGTCTTTAAACCTGATTTGTTGGACAT
Sequencing	GGGCAGACTTCTACTGGGAAATTTGCAGTACCACACTTTTGGTCTTTAAACCTGATTTGTTGGACAT
HPGDS-3'UTR	CCACCCCAGGCTGGTGACATTACGGAAGAAAGTCCAAAGCATCCCTGCCATCGCTGACTGGATACT
Sequencing	CCACCCCAGGCTGGTGACATTACGGAAGAAAGTCCAAAGCATCCCTGCCATCGCTGACTGGATACT
HPGDS-3'UTR	GCGAAGGCCCCAGACCAAACTCTAG
Sequencing	GCGAAGGCCCCAGACCAAACTCTAGGCGGCCGC

B

HPGDS-3'UTR-mut	TCACCAGAGTCTAGCAATAGCAAGATACTTGACCAGAAACACAGATTTGGCTGGAAAAAC
Sequencing	CTCGAGTCACCAGAGTCTAGCAATAGCAAGATACTTGACCAGAAACACAGATTTGGCTGGAAAAAC
HPGDS-3'UTR-mut	AGAACTTGAACAATGTCAAGTGGATGCAATTGTGGACACACTGGATGATTTCATGTCTCGTTTTCCT
Sequencing	AGAACTTGAACAATGTCAAGTGGATGCAATTGTGGACACACTGGATGATTTCATGTCTCGTTTTCCT
HPGDS-3'UTR-mut	TGGGCAGAGAAAAGACAAGATATAAAAAATCAGATATTTAAGGAGCTACTTACCTGTGATGCACCTCC
Sequencing	TGGGCAGAGAAAAGACAAGATATAAAAAATCAGATATTTAAGGAGCTACTTACCTGTGATGCACCTCC
HPGDS-3'UTR-mut	TCTTCTGCAAAGTTTGGACACATACTTAGGGGAAAACGAGTGGTTTATTGGTGACTCTGTAACTTCGTC
Sequencing	TCTTCTGCAAAGTTTGGACACATACTTAGGGGAAAACGAGTGGTTTATTGGTGACTCTGTAACTTCGTC
HPGDS-3'UTR-mut	AGACTTCTCCaGTGAAATTTGCAGTACCACACTTTTGGTCTTTAAACCTGATTTGTTGGACATCCACCCC
Sequencing	AGACTTGTCCaGTGAAATTTGCAGTACCACACTTTTGGTCTTTAAACCTGATTTGTTGGACATCCACCCC
HPGDS-3'UTR-mut	AGGCTGGTGACATTACGGAAGAAAGTCCAAAGCATCCCTGCCATCGCTGACTGGATACTGCGAAGGC
Sequencing	AGGCTGGTGACATTACGGAAGAAAGTCCAAAGCATCCCTGCCATCGCTGACTGGATACTGCGAAGGC
HPGDS-3'UTR-mut	CCCAGACCAAACTCTAG
Sequencing	CCCAGACCAAACTCTAGGCGGCCGC

Fig 4. psiCHECK-HPGDS-w/m-3'UTR vector synthesis and sequencing sequences. A was psiCHECK-HPGDS-3'UTR vector synthesis and sequencing sequence; B was psiCHECK-HPGDS-3'UTR-mut vector synthesis and sequencing sequences. The sequence for cloning is shown in grey and the predicted binding site is shown in green

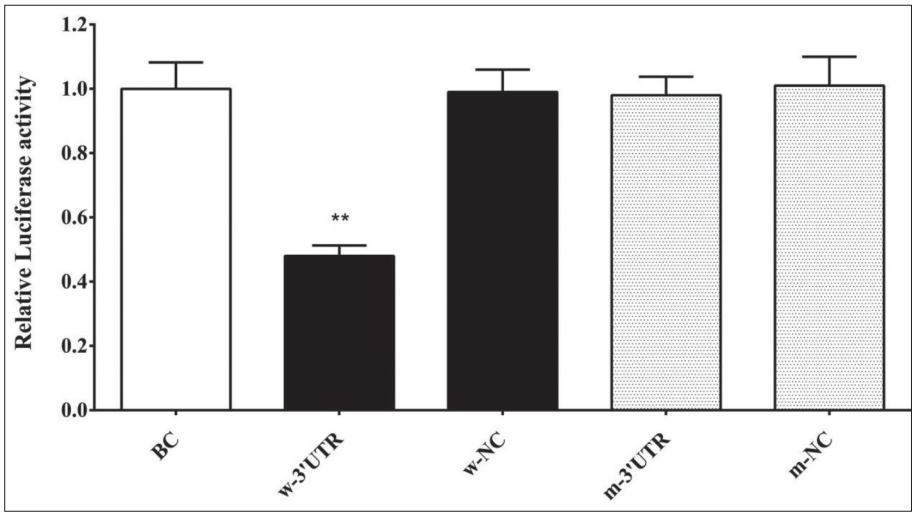

Fig 5. Analysis of dual relative luciferase activity of psi-CHECK2-HPGDS-w/m-3'UTR in luteal cells. Compared with BC and w-NC groups, Rluc/Luc of the w-3'UTR, ** P<0.01; Compared with BC and m-NC groups, *Rluc*/Luc of the m-3'UTR, not significant. P>0.05

significantly increased in the transfected miR-665 group compared to the blank control group (P<0.01), while P_4 concentration in the luteal cells transfected with negative control did not change significantly (P>0.05) *(Fig. 7)*.

Discussion

miRNA mimic is a new technique and method of gene silencing that imitates the high expression levels of endo-

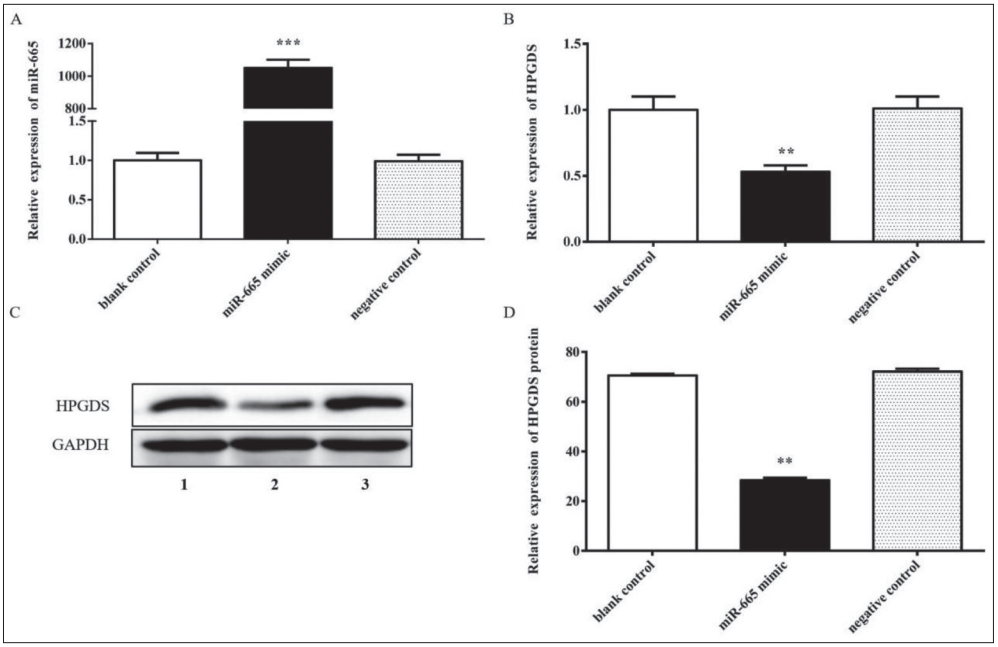

Fig 6. Expression of miR-665, HPGDS mRNA and protein in miR-665 mimic transfected luteal cells. A shows miR-665 expression, B and C represent HPGDS mRNA and protein expression and D indicates its protein expression using Image J software. Note: Compared with blank control and negative groups, expression of miR-665 in the w-3'UTR group, *** P<0.001; expression of HPGDS mRNA and protein in the w-3'UTR group, ** P<0.01. Each group was replicated three times

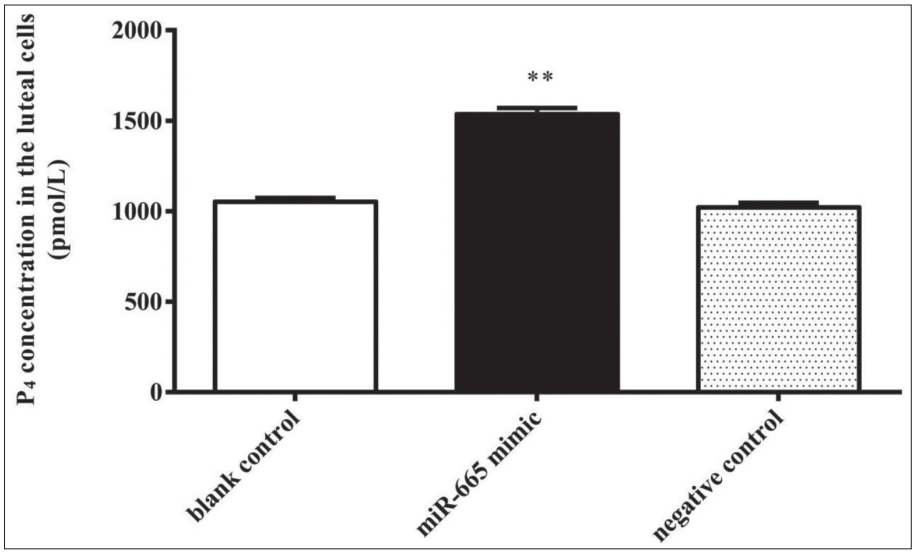

Fig 7. P_4 concentrations in miR-665 mimic transfected luteal cells. Compared with blank control and negative groups, P_4 concentrations in the w-3'UTR group, ** P<0.01

genous, mature miRNAs in cells to enhance their regulatory role. This method can generate unnatural double-stranded miRNA-like RNA fragments [13]. Such RNA fragments are designed to carry a motif at their 5'-end, which is partially complementary to the selected sequence in the unique 3'-UTR of the target gene. Once introduced into the cell, the mimic and its endogenous miRNA bind specifically to their target gene, causing a post-transcriptional repressive effect on that gene. miR-mimic approaches are "miRNA-targeting" and "miRNA-gain-of-function" strategies, mainly used as an exogenous tool to study gene function by targeting mRNAs in mammalian cells through miRNA-like actions [14]. For experiments, the cells are simply transfected with a transfection reagent package and ready for the next step, eliminating the need for cumbersome vector construction and the fear of viral infection.

Dual luciferase reporter gene detection system is designed for RNA interference, especially when using miRNA mimic for miRNA function study. It has become a convenient,

fast, and efficient method of detecting miRNA target sites for validation and is widely used in laboratory and clinical settings [15,16]. PsiCEHCK™-2 vector used in this pilot study included two luciferases, namely *Renilla* and firefly luciferase, which were used to detect and validate the target genes of miRNAs. The vector can be expressed in plant and animal cells with high efficiency. In this vector, the downstream polyclonal site of *Renilla* luciferase is after its stop codon, so that the target fragment to be detected can be inserted. Moreover, as no fusion protein is expressed, there is no concern regarding code shift mutations. *Renilla* luciferase and target fragment are expressed in a fused manner. After co-staining with RNAi vector and binding to the target site, the fusion product of *Renilla* luciferase and the target fragment were cleaved and degraded, thus attenuating *Renilla* luciferase signal [17-19].

In the present preliminary study, miR-665 was utilised to co-transfect luteinising cells with wild-type recombinant vector psiCHECK-HPGDS-w-3'UTR and mutant psiCHECK-HPGDS-m-3'UTR, respectively. A comparative analysis based on w-3'-UTR group (psiCHECK-HPGDS-w-3'UTR + miR-665 mimic) and the BC group revealed that the activity of *Renilla* luciferase significantly changed. In other words, the relative activity of Rluc/Fluc reduced by about 52% in the w-3'-UTR group (HPGDS) compared to that in the BC group, which indicated that HPGDS was the true target gene of miR-665. It has been recently shown that miR-665 is significantly upregulated in the inflamed mucosa of mice suffering from colitis and can participate in regulating inflammatory response process in animals [20,21]. Another study demonstrated that miR-665 not only inhibits cell proliferation but also participates in regulating apoptosis [20]; moreover, Engelsvold et al.[22] reported that miR-665 was also found to induce neovascularisation and promote the repair of cardiac function after myocardial ischaemia. In addition, one report showed that miRNA-665 could regulate cell proliferation and apoptosis through the Bcl-2 and Akt signalling pathways [23,24]. However, little has been reported about the function of miR-665 in the regulation of reproduction in females, especially the expression profile in the luteal tissue. Therefore, a dual-luciferase reporter approach was used to study miR-665 expression patterns and its regulatory functions in the luteal tissue of females, which is the first report of its kind. Based on this, our data also established that HPGDS was a bona fide target gene of miR-665. This gene was initially identified in rat spleen [25] and later in other tissues [26]. HPGDS is the only vertebrate sigma-like member of the GST superfamily and is widely distributed in antigen-presenting cells, Th2 lymphocytes, mast cells, and megakaryocytes [27]. It has been shown that in mouse models of asthma and allergic disease, HPGDS has significant pro-inflammatory effects, modulating many hallmark features, including eosinophilia, airway hyperresponsiveness, mucus production, and Th2 cytokine levels [28,29]. However, it has been demonstrated that HPGDS also exhibits significant anti-inflammatory effects in HPGDS knockout mouse assay [30]. This phenomenon is most likely related to the type of receptor in its downstream mechanism. HPGDS is a key synthase of the D member of the prostaglandin family, which catalyses the conversion of PGH_2 to PGD_2 and plays a role in the production of prostaglandin-like substances in target cells. Some studies have shown that HPGDS mRNA is highly expressed in female reproductive organs such as the fallopian tubes and the uterus [31], and the study conducted by Kanaoka et al.[2] indicated that HPGDS plays a key role in the regulation of inflammation in the fallopian tubes. Interestingly, Dozier et al.[4] found increased mRNA expression of HPGDS in the cultures of luteinised granulosa cells collected from rats after treatment with human chorionic gonadotropin, suggesting that HPGDS, like PGFS (synthase of PGF) or PGES (synthase of PGE), probably also plays an important regulatory role in the formation, maintenance, and degeneration of the corpus luteum, especially in the early stages of luteal formation [32]. Thus, the ovary is considered a potential site of action for HPGDS-catalysed synthesis of PGD_2, where HPGDS maintains the *in vivo* dynamic balance of the function and morphology of the female reproductive organs. This was further verified by Farhat et al.[8] who found that HPGDS-catalysed synthesis of PGD_2 could activate the expression of steroidogenic Cyp11A1 and StAR genes and subsequently promoted the secretion of progesterone, thereby playing a regulatory role in follicle growth by inhibiting the proliferation of granulosa cells. Based on the above results and analysis, we inferred that miR-665 and its target gene HPGDS probably also play important roles in the formation, maintenance, and degeneration of the corpus luteum in females, such as the proliferation and apoptosis of luteal cells involved in the formation and degeneration of the corpus luteum, which was in accordance with the functional mechanism of miR-665 reported so far. Furthermore, the target gene HPGDS and its synthesiser PGD_2 are members of the PGs family (which is recognised as a key factor involved in the regulation of luteal structure and function), suggesting that miR-665 is likely to be involved in the regulation of luteal function by targeting this PGs family members (HPGDS/PGD_2), which is also demonstrated in the present study, as shown by the increase in progesterone concentration after miR-665 transfection.

In conclusion, dual-luciferase reporter vector pisCHECK2-HPGDS-w/m-3'UTR was synthesised artificially for the first time, in this study, and the vector was verified to be successfully constructed using double digestion assay and sequencing. Moreover, after the upregulation of miR-665 expression, it was demonstrated that miR-665 could target the gene by acting on the 3'-UTR region of HPGDS to regulate the ovine luteal cell function, which provides a new perspective and material for studying the role of miRNAs in regulating the reproductive function in females, especially in the ovarian-luteal tissue of sheep.

Availability of Data and Materials

The datasets during and/or analyzed during the current study available from the corresponding authors (H. Yang and Z. Zhao) on reasonable request.

Ethical Statement

This study was approved by the Shihezi University Animal Experiments Local Ethics Committee (Approval no: 2020108).

Acknowledgement

The authors are grateful to the laboratory colleagues for providing expertise and advice necessary to conduct this study.

Financial Support

This work was supported by National Natural Science Foundation of China (31802065) and Natural Science Foundation Project of CQ (cstc2020jcyj-msxmX0427).

Conflict of Interest

The authors declared that there is no conflict of interest.

Author Contributions

Y.S., L.F., H.Y. and Z.Z. conceived and designed the experiment and analyzed and interpreted the data. Y.S. wrote the manuscript. Y.S., L.F., H.Y. and Z.Z. collected samples and data. Z.T., Y.N. participated in RNA extraction and analysis. All authors have read and agreed to the published version of the manuscript.

References

1. Asada K, Shimamoto S, Oonoki T, Maruno T, Kobayashi Y, Aritake K, Urade Y, Hidaka Y: Molecular recognition mechanism of hematopoietic prostaglandin D synthase with its cofactor and substrate. *Biophys J,* 112 (3): 494a, 2017. DOI: 10.1016/j.bpj.2016.11.2675

2. Kanaoka Y, Ago H, Inagaki E, Nanayama T, Miyano M, Kikuno R, Fujii Y, Eguchi N, Toh H, Urade Y, Hayaishi O: Cloning and crystal structure of hematopoietic prostaglandin D synthase. *Cell,* 90 (6): 1085-1095, 1997. DOI: 10.1016/S0092-8674(02)09631-9

3. Yamamoto K, Tsubota T, Uno T, Tsujita Y, Yokota S, Sezutsu H, Mita K: A defective prostaglandin E synthase could affect egg formation in the silkworm *Bombyx mori*. *Biochem Biophys Res Commun,* 521 (2): 347-352, 2020. DOI: 10.1016/j.bbrc.2019.10.121

4. Dozier BL, Watanabe K, Duffy DM: Two pathways for prostaglandin F2α synthesis by the primate periovulatory follicle. *Reproduction,* 136 (1): 53-63, 2008. DOI: 10.1530/REP-07-0514

5. Arima M, Fukuda T: Prostaglandin D_2 and T_H2 inflammation in the pathogenesis of bronchial asthma. *Korean J Intern Med,* 26 (1): 8-18, 2011. DOI: 10.3904/kjim.2011.26.1.8

6. Xue L, Salimi M, Panse I, Mjösberg JM, McKenzie ANJ, Spits H, Klenerman P, Ogg G: Prostaglandin D_2 activates group 2 innate lymphoid cells through chemoattractant receptor-homologous molecule expressed on T_H2 cells. *J Allergy Clin Immunol,* 133 (4): 1184-1194, 2014. DOI: 10.1016/j.jaci.2013.10.056

7. Borel V, Gallot D, Marceau G, Sapin V, Blanchon L: Placental implications of peroxisome proliferator-activated receptors in gestation and parturition. *PPAR Res,* 2008:758562, 2008. DOI: 10.1155/2008/758562

8. Farhat A, Philibert P, Sultan C, Poulat F, Boizet-Bonhoure B: Hematopoietic-prostaglandin D_2 synthase through PGD_2 production is involved in the adult ovarian physiology. *J Ovarian Res,* 4:3, 2011. DOI: 10.1186/1757-2215-4-3

9. Qi R, Han X, Wang J, Qiu X, Wang Q, Yang F: MicroRNA-489-3p promotes adipogenesis by targeting the Postn gene in 3T3-L1 preadipocytes. *Life Sci,* 278:119620, 2021. DOI: 10.1016/J.LFS.2021.119620

10. Lytle JR, Yario TA, Steitz JA: Target mRNAs are repressed as efficiently by microRNA-binding sites in the 5'UTR as in the 3'UTR. *PNAS,* 104 (23): 9667-9672, 2007. DOI: 10.1073/pnas.0703820104

11. Liu X, Duan H, Zhang HH, Gan L, Xu Q: Integrated data set of microRNAs and mRNAs involved in severe intrauterine adhesion. *Reprod Sci,* 23 (10): 1340-1307, 2016. DOI: 10.1177/1933719116638177

12. Baddela VS, Onteru SK, Singh D: A syntenic locus on buffalo chromosome 20: Novel genomic hotspot for miRNAs involved in follicular-luteal transition. *Funct Integr Genomics,* 17 (2-3): 321-334, 2017. DOI: 10.1007/s10142-016-0535-7

13. Bernardo BC, Charchar FJ, Lin RC, McMullen JR: A microRNA guide for clinicians and basic scientists: Background and experimental techniques. *Heart Lung Circ,* 21 (3): 131-142, 2012. DOI: 10.1016/j.hlc.2011.11.002

14. Younger ST, Corey DR: Transcriptional gene silencing in mammalian cells by miRNA mimics that target gene promoters. *Nucleic Acids Res,* 39 (13): 5682-5691, 2011. DOI: 10.1093/nar/gkr155

15. Ling X, Li F: Silencing of antiapoptotic survivin gene by multiple approaches of RNA interference technology. *Biotechniques,* 36 (3): 450-460, 2004. DOI: 10.2144/04363RR01

16. Du G, Yonekubo J, Zeng Y, Osisami M, Frohman MA: Design of expression vectors for RNA interference based on miRNAs and RNA splicing. *FEBS J,* 273 (23): 5421-5427, 2006. DOI: 10.1111/j.1742-4658.2006.05534.x

17. Fuchs A, Riegler S, Ayatollahi Z, Cavallari N, Giono LE, Nimeth BA, Mutanwad KV, Schweighofer A, Lucyshyn D, Barta A, Petrillo E, Kalyna M: Targeting alternative splicing by RNAi: From the differential impact on splice variants to triggering artificial pre-mRNA splicing. *Nucleic Acids Res,* 49 (2): 1133-1151, 2021. DOI: 10.1093/NAR/GKAA1260

18. Bhaumik S, Lewis XZ, Gambhir S: Optical imaging of *Renilla* luciferase, synthetic *Renilla* luciferase, and firefly luciferase reporter gene expression in living mice. *J Biomed Opt,* 9 (3): 578-586, 2004. DOI: 10.1117/1.1647546

19. Shifera AS, Hardin JA: Factors modulating expression of Renilla luciferase from control plasmids used in luciferase reporter gene assays. *Anal Biochem,* 396 (2): 167-172, 2010. DOI: 10.1016/j.ab.2009.09.043

20. Li M, Zhang S, Qiu Y, He Y, Chen B, Mao R, Cui Y, Zeng Z, Chen M: Upregulation of miR-665 promotes apoptosis and colitis in inflammatory bowel disease by repressing the endoplasmic reticulum stress components XBP1 and ORMDL3. *Cell Death Dis,* 8 (3):e2699, 2017. DOI: 10.1038/cddis.2017.76

21. Moein S, Vagharitabari M, Qujeq D, Majidinia M, Nabavi SM, Yousefi B: MiRNAs and inflammatory bowel disease: An interesting new story. *J Cell Physiol,* 234 (4): 3277-3293, 2019. DOI: 10.1002/jcp.27173

22. Engelsvold DH, Utheim TP, Olstad OK, Gonzalez P, Eidet JR, Lyberg T, Trøseid AMS, Dartt DA, Raeder S: MiRNA and mRNA expression profiling identifies members of the miR-200 family as potential regulators of epithelial-mesenchymal transition in pterygium. *Exp Eye Res,* 115, 189-198, 2013. DOI: 10.1016/j.exer.2013.07.003

23. Hu J, Ni G, Mao L, Xue X, Zhang J, Wu W, Zhang S, Zhao H, Ding L, Wang L: LINC00565 promotes proliferation and inhibits apoptosis of gastric cancer by targeting miR-665/AKT3 axis. *Onco Targets Ther,* 12, 7865-7875, 2019. DOI: 10.2147/OTT.S189471

24. Yu J, Yang W, Wang W, Wang Z, Pu Y, Chen H, Wang F, Qian J: Involvement of miR-665 in protection effect of dexmedetomidine against oxidative stress injury in myocardial cells via CB2 and CK1. *Biomed Pharmacother,* 115:108894, 2019. DOI: 10.1016/j.biopha.2019.108894

25. Kanaoka Y, Urade Y: Hematopoietic prostaglandin D synthase.

Prostaglandins Leukot Essent Fatty Acids, 69, 163-167, 2003. DOI: 10.1016/S0952-3278(03)00077-2

26. Mohri I, Eguchi N, Suzuki K, Urade Y, Taniike M: Hematopoietic prostaglandin D synthase is expressed in microglia in the developing postnatal mouse brain. *Glia,* 42 (3): 263-274, 2003. DOI: 10.1002/glia.10183

27. Fujitani Y, Kanaoka Y, Aritake K, Uodome N, Okazaki-Hatake K, Urade Y: Pronounced eosinophilic lung inflammation and Th2 cytokine release in human lipocalin-type prostaglandin D synthase transgenic mice. *J Immunol,* 168 (1): 443-449, 2002. DOI: 10.4049/jimmunol.168.1.443

28. Lee J, Kim HS: The role of autophagy in eosinophilic airway inflammation. *Immune Netw,* 19 (1):e5, 2019. DOI: 10.4110/in.2019.19.e5

29. Brightling CE, Brusselle G, Altman P: The impact of the prostaglandin D_2 receptor 2 and its downstream effects on the pathophysiology of asthma. *Allergy,* 75 (4): 761-768, 2020. DOI: 10.1111/all.14001

30. Rajakariar R, Hilliard M, Lawrence T, Trivedi S, Colville-Nash P, Bellingan G, Fitzgerald D, Yaqoob MM, Gilroy DW: Hematopoietic prostaglandin D_2 synthase controls the onset and resolution of acute inflammation through PGD_2 and 15-deoxy$\Delta^{12\text{-}14}$ PGJ_2. *PNAS,* 104 (52): 20979-20984, 2007. DOI: 10.1073/pnas.0707394104

31. Saito S, Tsuda H, Michimata T: Prostaglandin D_2 and reproduction. *Am J Reprod Immunol,* 47 (5): 295-302, 2002. DOI: 10.1034/j.1600-0897.2002.01113.x

32. Zelinski-Wooten MB, Stouffer RL: Intraluteal infusions of prostaglandins of the E, D, I, and A series prevent PGF2α-induced, but not spontaneous, luteal regression in rhesus monkeys. *Biol Reprod,* 43, 507-516, 1990. DOI: 10.1095/biolreprod43.3.507

Kafkas Universitesi Veteriner Fakultesi Dergisi
ISSN: 1300-6045 e-ISSN: 1309-2251
Journal Home-Page: http://vetdergikafkas.org

Kafkas Univ Vet Fak Derg
27 (6): 691-698, 2021
DOI: 10.9775/kvfd.2021.26084

RESEARCH ARTICLE

The Effect of Using Zeolite (Clinoptilolite) as a Litter on Some Milk Yield and Welfare Parameters in Tent-Type Sheep Shelters

Mücahit KAHRAMAN [1,a (*)] Aydın DAŞ [1,b] Gülşah GÜNGÖREN [1,c]
Besime DOĞAN DAŞ [2,d] Akın YİĞİN [3,e] Mustafa Ünal BOYRAZ [4,f]

[1] Harran University, Faculty of Veterinary Medicine, Animal Husbandry Department, TR-63250 Şanlıurfa - TURKEY
[2] Harran University, Faculty of Veterinary Medicine, Animal Nutrition and Nutritional Diseases Department, TR-63250 Şanlıurfa - TURKEY
[3] Harran University, Faculty of Veterinary Medicine, Genetic Department, TR-63250 Şanlıurfa - TURKEY
[4] Harran University, Faculty of Veterinary Medicine, Histology Department, TR-63250 Şanlıurfa - TURKEY
ORCIDs: [a] 0000-0002-7757-2483; [b] 0000-0003-0371-5434; [c] 0000-0002-0360-7735; [d] 0000-0003-2163-2632; [e] 0000-0001-9758-1697
[f] 0000-0002-5455-0353

Article ID: KVFD-2021-26084 Received: 31.05.2021 Accepted: 09.11.2021 Published Online: 13.11.2021

Abstract

This research was conducted to determine the effect of using zeolite used as a litter in tent-type sheep shelters on milk yield, milk quality, and animal welfare parameters. A total of 34 İvesi sheep in the control (n=17) and zeolite (n=17) groups were used as animal material in the study. Milk yield, milk quality, and blood parameters were monitored for 30 days period from the beginning of the study. In-shelter climatic conditions were recorded daily. The average milk yield in the control and zeolite groups were 1137.18 and 1168.94 g on the 2nd control (P>0.05); 536.83 and 790.88 g (P<0.05) on the 3rd control (P<0.05) respectively. In terms of somatic cell count, the zeolite group got a lower value on the 2nd and 3rd control of the study (P<0.05). According to the findings obtained from the research, other milk quality parameters were not affected by zeolite. Ammonia and humidity rates in the shelter are lower in the zeolite group (P<0.05). On the 3rd control of the study, significant differences were found between the groups in terms of BUN, urea, LDL, and TAC values (P<0.05). According to the our results, it may be stated that using zeolite as a litter contributes positively to the improvement of milk yield and animal welfare in the tent-type shelter environment.

Keywords: *Milk quality, Milk yield, Sheep, Welfare, Zeolite*

Çadır Tipi Koyun Barınaklarında Altlık Olarak Zeolit (Klinoptilolit) Kullanılmasının Bazı Süt Verimi ve Refah Parametreleri Üzerine Etkisi

Öz

Bu araştırma çadır tipi koyun barınaklarında altlık olarak kullanılan zeolitin, süt verimi, süt kalitesi ve hayvan refahı parametreleri üzerine etkisini belirlemek amacıyla yapılmıştır. Araştırmada hayvan materyali olarak kontrol (n=17) ve zeolit (n=17) gruplarında toplam 34 baş İvesi koyun kullanılmıştır. Süt verimi, süt kalitesi ve kan parametreleri araştırma başlangıcından itibaren 30 günlük periyodlarla takip edilmiştir. Barınak içi iklimsel koşullar günlük olarak kayıt edilmiştir. Kontrol ve zeolit grubunda ortalama süt verimi sırasıyla 2. kontrolde 1137.18 ve 1168.94 g (P>0.05); 3. kontrolde sırasıyla 536.83 ve 790.88 g (P<0.05) olarak tespit edilmiştir. Somatik hücre sayısı bakımdan zeolit grubu araştırmanın 2. ve 3. kontrolünde daha düşük değer almıştır (P<0.05). Araştırmadan elde edilen bulgulara göre diğer süt kalite parametreleri üzerinde zeolitin etkisi olmamıştır. Barınak içi amonyak ve nem oranı zeolit grubunda daha düşük tespit edilmiştir (P<0.05). Biyokimyasal parametreler bakımından araştırmanın 3. kontrolünde gruplar arasında BUN, üre, LDL ve TAC değeri bakımından önemli farklar saptanmıştır (P<0.05). Elde edilen sonuçlara göre, koyun yetiştiriciliğinde çadır tipi barınaklarda altlık olarak zeolit kullanılmasının, süt verimi ve hayvan refahının iyileştirilmesine olumlu katkı sağladığı ifade edilebilir.

Anahtar sözcükler: *Koyun, Refah, Süt kalitesi, Süt verimi, Zeolit*

INTRODUCTION

Sheep husbandry is practiced in different climatic and geographical conditions. Ewes are reared under different environmental conditions depending on the purpose of breeding and farming business model [1]. The nomadic pastoralist system of sheep husbandry is practiced in regions with expanses of land, where different climates

How to cite this article?

Kahraman M, Daş A, Güngören G, Doğan Daş B, Yiğin A, Boyraz MÜ: The effect of using zeolite (clinoptilolite) as a litter on some milk yield and welfare parameters in tent-type sheep shelters. *Kafkas Univ Vet Fak Derg,* 27 (6): 691-698, 2021.
DOI: 10.9775/kvfd.2021.26084

(*) **Corresponding Author**

Tel: +90 414 318 3918 Cellular phone: +90 543 508 9122 Fax: +90 414 318 3922
E-mail: mucahitkahraman@harran.edu.tr (M. Kahraman)

and pastures are suitable for housing and feeding animals in different seasons. In this type of sheep husbandry, sheep are transported from one region to another according to the climatic and pasture conditions. Livestock should be protected from extreme environmental factors in areas with large differences between temperatures during the day and those at night. Therefore, tent-type portable shelters are often used in nomadic sheep husbandry [2]. In addition, such shelters are generally preferred by farmers because of their low cost. However, adverse ground and ventilation conditions in shelters may affect animal health and welfare along with product quality [3].

The production performance of farm animals is affected by various factors. To obtain high-yield performance, animals with high genetic potential should be used and optimal care, feeding, and housing conditions should be provided [4]. Scientific studies and field applications have demonstrated that improving housing conditions increase the yield in animal husbandry [5].

Zeolites find application in many sectors and are widely used in geology, chemistry, physics, agriculture, animal husbandry, and medicine for scientific and commercial purposes. The most important feature of zeolite minerals is that they keep liquid and gas molecules away from the environment by trapping them in the spaces within their structure. They are used in eliminating the unpleasant odor of fertilizers in agriculture and animal husbandry [6] and in pH regulation of acidic volcanic soils [7]. Clinoptilolite is the most abundant natural zeolite in the world and has optimal properties. It is widely used as a feed additive in organic livestock breeding due to its nonfibrous mineral structure; a composition that is free of harmful elements; and high quality [8]. Although there is a limited number of studies on the effect of zeolites on ruminant barn odor, ruminant litter quality, and environmental humidity, it has been reported that zeolites improve litter quality and ensure dry feces in poultry, reduce the ammonia ratio, and ensure clean air in the poultry house [6,9].

In this study, the effects of application of zeolite on the ground on animal welfare, milk yield, milk quality, and serum biochemical parameters were investigated in tent-type shelters, which are widely used in rural areas with subtropical climates of Turkey.

Material and Methods

Ethical Statement

This study was approved by the Harran University Animal Experiments Local Ethics Committee (Approval no: 2018/08-01-07), Şanlıurfa, Turkey

Animals and Feedings

The animals used as research material were selected from a herd (approximately 500 heads) whose oestrus was synchronized. Thirty-four İvesi sheeps on the 80±10th days (mean ± SD) of milk production of first lactation and multiparous were selected for this research. Their body weights were an average 54.16±6.65 kg. The ewes were fed in the pen during the lambing period. During the pasture period, the animals were not taken out of the pen until the hoarfrost rises from the pasture in the morning, and they were kept in the tent-shelter at night. The sheep were kept in pasture for 14 h and 10 h in tent. They were fed with concentrate feed (18% CP, 2600 kcal/kg ME) and wheat hay in the evening after returning from pasture.

Experimental Design

The ewes divided into two similar groups according to the age, avarege daily milk yield and milk composition at the beginning of the experiment. Within the scope of the research, a tent-type shelter used in the nomadic pastoralist system was designed. The tent was divided into two parts, and 36 m^2 of floor space was prepared for each group. The tent is placed in such a way that both groups are exposed to the same amount of daylight at the same time. Each group is provided with ventilation with a 2 m^2 window area.

The granular form of clinoptilolite was obtained from a commercial enterprise, and it was applied to the litter homogeneously over the entire natural soil ground (2.7 kg/m^2 on average each time) in the shelters of only one of the two experimental groups every 15 days (days 0, 15, 30 and 45). Throughout the experiment, a total of 389 kg clinoptilolite was used for the zeolite group [6,7].

Ammonia, Temperature and Humidity Measurements

Since the beginning of the study period, the ammonia level in the tent was measured by using a gas measuring device (Industrial Scientific) once a day in the morning before taking the sheep to the pasture. Humidity ratios and temperature were measured daily with a TESTO-branded humidity and temperature measuring device. Measurement data were recorded after the readings stabilized.

Milking Data Collection

The births on the sheep farm started in February. Ewes were selected on the days when the births increased and care was taken to keep the date of lactation onset close to each other. Milking controls were started when the firstborn lamb was 15 days old. On control days, the lambs were separated from their mothers at 06:00 pm on the previous day and left until after milking the next test day. The morning and evening milk yields in the control milking were summed and the milk yields on the control day were calculated. Control milkings were done in 15 days from the beginning of lactation to the peak of lactation. From the data obtained on the control days, the daily

milk yields of each sheep on days 15, 30, 45, 60, 75 were determined. Milk yield was calculated according to the Trapez II method [10]. According to the data obtained, two homogeneous groups were formed. After the beginning of the research, milking controls were made in 30 days periods. Average daily milk yields were determined with control milking performed at the beginning (80th day of lactation-1st Control), 110th day of lactation (2nd Control), and 140th day of lactation (3rd Control) of the study. The ewes were milked using a machine twice a day, at 06:00 am and 06:00 pm. The amount of milk was determined by using a balance with a sensitivity of 1 g. The vacuum pressure, pulsation rate, and pulsation ratio of the milking machines were set to 40 kPa, 120, and 60:40, respectively [11]. Routine practices regarding milking hygiene were performed before and after machinery milking.

Sampling and Laboratory Analyses

Blood samples were collected from the jugular vein on control days to determine the biochemical parameters examined within the scope of the study. Samples were centrifuged at 3500 rpm for 10 min, and then the serum was separated into microcentrifuge tubes and delivered under cold chain conditions to the analysis laboratory (Yasamlab, Adana/Turkey). For analyses of the status of oxidative stress and antioxidant levels, blood samples collected in ethylenediaminetetraacetic acid-coated tubes on control days were centrifuged at 3000 rpm for 10 min, and plasma was stored at -80ºC until the time of analysis. Total oxidative stress (TOS) and total antioxidant capacity (TAC) were determined according to the commercial kit (Rel assay, Turkey) protocol, and subsequently, the oxidative stress index (OSI) was calculated [TOS/(TACx10)] according to the protocol specified in the kit.

One hundred and two milk samples collected during morning milking on the control days were used to determine the milk quality parameters. Dry matter, fat, lactose, and protein ratios and somatic cell count (SCC) in milk were determined with a combined milk analyzer (Bentley); color properties with a portable color meter (Lovibond); and pH value with a portable pH meter (Mettler Toledo) [12,13].

Statistical Analysis

Descriptive statistical values related to the parameters examined in the research groups were given as the mean ± standard error of mean (SEM). The groups were by the normal distribution according to the Shapiro-Wilk test. After observing the normal distribution in the data, the comparison of the control and zeolite groups was analyzed by using independent sample T-Test. SPSS (SPSS Version 18.0®, Chicago, IL, USA) program was used for all statistical analyses. The differences between the groups in terms of the parameters examined were considered significant at the P<0.05 level.

Results

Meteorological data of the study period are presented in *Table 1*. As expected, the highest and lowest temperatures were measured in July and May, respectively.

Table 1. *Research period climatic conditions*

Mounth	Temperature (ºC)			Rainfall (mm) Mean
	Mean	Maximum	Minimum	
May	22.1	28.6	15.2	26.7
June	28.0	34.6	20.4	4.4
July	31.9	38.7	24.2	2.0

Milk yields and milk quality parameters obtained in the study are presented in *Table 2*. The groups had similar milk yields at the beginning of the study. The difference became significant on the 3rd control; milk yields of the control and zeolite groups were 0.54 kg and 0.79 kg, respectively (P<0.05). The difference between the groups in terms of SCC became apparent on the 2nd control of the study and continued to increase on the 3rd control (P<0.05). There were no significant differences between the groups in terms of fat, protein, lactose, dry matter ratio, freezing point, pH and color (L*, a*, b*) properties (P>0.05).

The climatic parameters in the shelter determined during the study are presented in *Table 3*. The differences between the groups in terms of ammonia levels and humidity ratios were found to be significant (P<0.05).

Blood biochemical parameters of the ewes used in the study are shown in *Table 4*. Significant differences were detected between the groups in terms of blood urea nitrogen (BUN), urea, low density lipoprotein (LDL), and TAC levels on the 3rd control (P<0.05). There were no significant differences in other biochemical parameters (P>0.05).

Discussion

In the present study, the effects of using zeolite-litter supplementation in shelters in nomadic sheep husbandry, which is widely practiced in the Middle East, were experimentally established. The care and feeding conditions of the animals were also established in accordance with this system. The study was initiated after the lambs were weaned. In this way, we ensured that the lambs received a sufficient amount of milk from their mothers and that the environmental conditions suitable for nomadic sheep husbandry were provided. In addition, the study was initiated after the peak period of lactation, and thus the chances of the increase in yield being attributed to lactation physiology were eliminated [14].

To obtain an optimum yield from sheep, the optimum ambient temperature of the shelters should be set within

Table 2. *Milk yield and milk quality traits*

Traits	Groups	1st Control	2nd Control	3rd Control
Daily Milk (g)	Control	1321.59±69.25	1137.18±100.18	536.35±83.26[b]
	Zeolite	1338.29±72.29	1168.94±91.83	790.88±89.23[a]
Fat (%)	Control	6.33±0.09	6.80±0.31	7.54±0.22
	Zeolite	6.35±0.12	6.80±0.27	7.06±0.28
Protein (%)	Control	4.91±0.12	5.61±0.10	5.58±0.16
	Zeolite	5.05±0.11	5.66±0.13	5.38±0.18
Lactose (%)	Control	5.27±0.05	4.60±0.09	4.17±0.14
	Zeolite	5.13±0.05	4.66±0.15	4.38±0.13
Dry Matter (%)	Control	17.89±0.19	18.18±0.40	18.26±0.33
	Zeolite	17.93±0.19	18.40±0.38	17.93±0.42
Freezing Point (°C)	Control	0.58±0.00	0.57±0.01	0.57±0.00
	Zeolite	0.58±0.00	0.57±0.00	0.58±0.00
SCC (x10³cell/mL)	Control	133.13±40.68	154.38±39.51[a]	227.88±61.53[a]
	Zeolite	110.81±33.38	63.12±12.60[b]	51.69±11.33[b]
pH	Control	6.54±0.02	6.02±0.07	5.92±0.04
	Zeolite	6.57±0.02	5.94±0.06	5.82±0.05
L*	Control	70.85±0.71	73.55±0.37	73.00±0.41
	Zeolite	71.39±0.48	74.33±0.24	72.91±0.46
a*	Control	-6.66±0.14	-5.76±0.11	-5.69±0.11
	Zeolite	-6.57±0.10	-5.79±0.15	-5.68±0.09
b*	Control	6.46±0.25	7.05±0.26	7.71±0.33
	Zeolite	7.02±0.17	6.89±0.22	7.64±0.26

[a,b] Values within a row with different superscripts differ significantly at P<0.05; X±SEM: Mean±Standart error of mean

Table 3. *The climatic parameters in the shelter*

Groups	NH_3 (ppm)	Temperature (°C)	Humidity (%)
Control	21.03±0.79[a]	20.88±0.28	68.87±0.76[a]
Zeolite	15.55±0.56[b]	20.99±0.41	65.88±1.07[b]

[a,b] Values within a row with different superscripts differ significantly at P<0.05; X ±SEM: Mean ± Standart error of mean

the range of 6°C-14°C for sheep, 12°C-14°C for lambs, and 14°C-16°C for butchery muttons [15]. In contrast, the thickness and quality of fleece on sheep can adapt to lower temperatures depending on air flow. Considering the average temperature in Şanlıurfa during the study period, the environmental temperature was found to be higher in our study compared to that reported [15] in the literature *(Table 1)*. This was predicted by the investigators before commencing the study. Therefore, to reduce the effect of this stress factor, the study was commenced after the ewes in the farm were sheared.

In the present study, the difference detected between the groups in lactation milk yield on the 3rd control was found to be significant *(Table 2)*. No study has been found in the literature in which zeolite (clinoptilolite) was used as litter material in sheep or goat shelters. It may be observed that the milk yield of the zeolite group on the 3rd control (corresponding to the last days of lactation in the study) was higher than that of the control group. It is believed that this finding will be favorable in warranting further studies in terms of increasing the milk yield of sheep throughout the entire lactation period.

Previous studies on clinoptilolite in the past generally evaluated this substance as a feed additive [16,17]. Among these studies, the only study evaluating lactation milk yield was conducted on dairy goats by Katsoulos et al.[17]. In that study, they reported that adding zeolite to feed did not result in a difference in lactation milk yield between experimental and control groups. Although the yield obtained in their study was similar to the average lactation milk yield (0-60 days) observed in the present study, a difference of approximately 100 g between the two groups was striking. High milk yield requires plenty of fresh air with suitable quality because insufficient

Table 4. *Blood biochemical parameters in sheep*

Traits	Groups	1st Control	2nd Control	3rd Control
Blood Urea Nitrogen (BUN) (mg/dL)	Control	18.85±1.47	20.32±0.58	14.81±0.96[a]
	Zeolite	16.32±1.06	18.30±1.14	10.66±0.53[b]
Urea (mg/dL)	Control	40.29±3.14	43.50±1.25	31.71±2.04[a]
	Zeolite	34.93±2.27	39.13±2.46	22.82±1.13[b]
Creatinine (mg/dL)	Control	0.56±0.04	0.54±0.02	0.74±0.03
	Zeolite	0.52±0.02	0.50±0.02	0.66±0.02
Creatine Kinase (IU/L)	Control	309.65±46.25	198.30±16.18	120.53±6.20
	Zeolite	273.29±15.90	163.88±7.51	130.18±8.70
Triglyceride (mg/dL)	Control	15.06±1.19	17.30±2.31	17.24±1.53
	Zeolite	14.64±1.17	19.88±2.73	15.18±1.21
Cholesterol (mg/dL)	Control	66.65±3.51	61.70±3.02	62.65±2.68
	Zeolite	66.86±2.98	61.00±3.02	59.35±1.68
High Density Lipoprotein (mg/dL)	Control	43.29±2.10	41.10±1.68	34.06±1.70
	Zeolite	46.50±2.17	40.13±1.54	35.29±0.84
Low Density Lipoprotein (mg/dL)	Control	20.53±2.31	17.00±1.91	25.24±1.38[a]
	Zeolite	17.43±1.27	16.88±2.07	21.00±1.29[b]
Aspartate Transaminase (U/L)	Control	115.71±2.10	120.10±4.63	108.29±3.50
	Zeolite	112.57±4.00	115.13±5.27	111.00±4.65
Alanine Amino Transferase (U/L)	Control	22.24±1.57	25.00±1.94	21.82±1.23
	Zeolite	22.64±1.99	23.00±1.88	23.47±1.61
Gamma Glutamyl Transferase (U/L)	Control	70.59±2.97	51.90±3.55	57.12±2.15
	Zeolite	66.79±3.99	63.00±3.17	56.24±2.98
Total Bilirubin (mg/dL)	Control	0.13±0.01	0.15±0.02	0.12±0.01
	Zeolite	0.15±0.01	0.13±0.01	0.11±0.01
Total Protein (g/dL)	Control	7.51±0.09	7.48±0.20	7.19±0.15
	Zeolite	7.58±0.14	7.64±0.11	6.98±0.12
Albumine (g/dL)	Control	3.13±0.07	3.36±0.07	3.10±0.06
	Zeolite	3.18±0.07	3.54±0.13	3.03±0.07
C-Reactive Protein (mg/dL)	Control	0.0031±0.00	0.0150±0.00	0.0147±0.00
	Zeolite	0.0049±0.00	0.0125±0.00	0.0124±0.00
Lactate Dehydrogenase (U/L)	Control	585.29±16.95	570.70±17.12	516.88±20.43
	Zeolite	610.50±17.61	578.63±30.96	532.76±17.55
Total Antioxidant Capacity	Control	1.00±0.03	1.09±0.01	1.15±0.02[a]
	Zeolite	0.97±0.03	1.05±0.03	1.06±0.02[b]
Total Oxidative Status	Control	8.98±0.49	11.19±0.77	7.65±0.67
	Zeolite	9.10±0.50	12.42±1.05	6.55±0.41
Oxidative Stress Index	Control	0.91±0.05	1.03±0.07	0.67±0.06
	Zeolite	0.95±0.05	1.19±0.10	0.62±0.04

[a,b] Values within a row with different superscripts differ significantly at P<0.05; X ± SEM: Mean ± Standart error of mean

oxygen slows down the metabolism, which affects milk production. Insufficient ventilation air exchange inside the barn causes increased air humidity as well as the concentration of harmful gases produced as a result of the decomposition of animal waste. High air humidity can have a negative impact on animal welfare and lead to the growth of pathogenic bacteria [18,19]. The interior surface area of clinoptilolite is 300 m^2/g, which accounts for its high absorptive capacity [20]. Zeolites are incorporated into the litter to reduce ammonia and moisture levels, thanks to their ability to adsorb ions and water [20]. Due to these properties, zeolite can improve environmental conditions, production performance, and hygiene of farm animals.

Varying results have been reported with respect to SCC in the milk of healthy sheep [21,22]. In the present study, significant differences were found between the two groups in terms of SCC *(Table 2)*. Similar results have been reported in studies where clinoptilolite was added to the feed in dairy goats [17], and it has been reported that zeolite enhanced milk hygiene. Furthermore, there are similar studies showing that zeolite reduces SCC in cattle [23]. When the results obtained were compared with other studies conducted in sheep regardless of the zeolite litter, they were determined to be similar to the values reported by Yağcı and Kaymaz [24] in normal milk samples and lower than the values reported by Leitner et al.[21]. In dairy ewes, mastitis has a significant effect on reducing milk yield and quality, resulting in greater economic losses than those reported for dairy cattle [25]. SCC in milk is positively correlated with the pathogens causing mastitis and severity of infection [26]. Clinoptilolites are minerals that have a variety of characteristics, including water absorption, ion adsorption, and cation exchange capacity [20]. Litter chemical modifiers are substances that improve the physical, chemical, and microbiological integrity of the litter [20]. It has been reported that natural clinoptilolite is able to selectively adsorb bacteria and bind certain toxins [27]. Loch et al.[28] confirmed that zeolite added to the litter directly affects the survival of microorganisms by reducing pH and water activity. Because of these properties, zeolite may reduce the somatic cell count in dairy animals by reducing the contamination from the litter in the mammary tissue. Increased SCC poses a risk for subclinical mastitis in flocks especially during the last days of lactation [13,21,24]. In our study, although the increase in SCC continued in the control group, it decreased in the zeolite group as lactation progressed, which was evaluated as a factor that eliminated the risk of subclinical mastitis. The difference in milk yield detected in the zeolite group also supports this finding. In the present study, there was no difference between the groups in terms of the parameters determining milk composition and quality *(Table 2)*. These data were consistent with the results of other studies in which different feed additives were used [29-31].

Climatic conditions in the shelter greatly affect the stress levels of animals in warm areas [32]. Poor housing conditions are regarded as an important reason for the decrease in livestock production and animal welfare [3]. Excessive heat and relative humidity in the shelters as a result of sheep breeding can be harmful to animal health. Relative humidity in the shelter should not exceed 80% unless required [15]. High relative humidity decreases the quality as well as quantity of fleece and affects the health of sheep [33]. The values found in the study for the control and zeolite groups *(Table 3)* were consistent with the findings of studies by Alkan [34] and Mutaf and Sönmez [35]. Intensive animal farming, which is currently practiced, has a negative impact on the environment due to the spread of various gases and unpleasant odors. Ammonia build-up in the shelter environment irritates the respiratory mucosa, leading to cough and decreased lung capacity [36]. In the present study, the ammonia level in the shelter decreased significantly, especially in the zeolite group *(Table 3)*. A study conducted on cattle reported that adding zeolite to the litter in sloping shelters with straw litter could be a promising way to reduce carbon dioxide, nitrous oxide, and ammonia emissions [37]. The present study concluded that a decrease in the level of ammonia in the shelter environment due to zeolites will contribute to the practice of sheep husbandry.

Biochemical analyses are often used to assess the physiological condition of animals [38]. In our study, quantitative changes in biochemical parameters were monitored to ascertain whether the sheep were in normal physiological condition. Urea and BUN levels generally indicate kidney health. The ammonia released during protein digestion is converted into urea and excreted by the kidneys. BUN and urea levels increase in renal failure, hypovolemia, dehydration, bleeding, shock, and high protein diet intake, whereas they decrease in liver diseases, fasting, and low protein intake [39]. Urea, BUN, and creatinine levels were consistent with the reference values reported by Nisbet et al.[40], Şimşek et al.[41], Toprak et al.[42], and Comba et al.[43]. Although serum levels of muscle enzymes including those of creatine phosphokinase (CPK or CK), aldolase, and lactic dehydrogenase (LDH) are used to diagnose muscle disorders, CK level is the most commonly used indicator in practice. CK values obtained in the study were consistent with those reported by Comba et al.[43]. Measurement of parameters such as triglyceride, cholesterol, high-density lipoprotein, and LDL levels is referred to as lipid profile tests [44,45]. These tests are critical in cardiovascular diseases. Triglyceride values found in the study were consistent with those reported by Udum et al.[44], whereas they were lower than the values reported by Kurt et al.[45]. Fatty liver is a problem frequently associated with intensive animal farming. This may be one of the reasons for decreased blood cholesterol levels. In the literature, it has also been reported that zeolite added to feed adsorbs bile acid salts on the surface of the digestive tract, leading to a decrease in serum cholesterol level [46]. The present study did not find any differences in cholesterol levels between the groups. This may be due to the fact that zeolite was not given to animals as feed, but was only used as litter material. Serum cholesterol values found in this study were similar to those reported by Nisbet et al.[40], Kurt et al.[45], and Şimşek et al.[41]. Serum or plasma concentrations of different oxidants and antioxidants can be measured separately by direct or indirect methods. However, there are advantages and disadvantages of measuring each parameter separately. These measurements do not provide a general cumulative measurement of oxidative and antioxidant status. Individual measurements require time consuming, costly, and complex techniques. Therefore, we used measurements of TAC, TOS, and OSI in this

study, which are more economical [47]. TAC and TOS values obtained in the present study were similar to those reported by Mis et al.[48], whereas there was a difference in terms of OSI values. This may be due to the difference in the methods used to calculate OSI values or having used a different breed of sheep in the present study. Blood parameters differed between animal species, as well as by the race, age, and sex of animals, regions where they were bred, and their diets [40].

In the present study, it was observed that the use of zeolite litter in tent-type sheep shelters decreased the ammonia level in the shelter environment and improved milk yield and SCC. It was determined that mixing zeolite with litter material did not have a negative effect on milk quality parameters, blood biochemistry, and oxidative markers of sheep. According to the results of the present study, it is recommended to use zeolite litter in the shelter environment to increase milk yield and improve animal welfare.

Availability of Data and Materials

The datasets during and/or analyzed during the current study available from the corresponding author on reasonable request.

Acknowledgements

The authors would like to thank Assoc. Prof. Dr. İsmail KOYUNCU and Prof. Dr. Ömür KOÇAK for providing their expertise and support.

Funding Support

This study was financially supported by HUBAK with project numbers 19046 (y. 2021).

Conflict of Interest

The authors declared that there is no conflict of interest.

Author Contributions

MK and AD planned, designed the research, analyzed all data and drafted manuscript, GG, BDD, AY and MÜB provided and help in the research. All authors discussed the results and contributed to the final manuscript.

References

1. Haile A, Getachew T, Mirkena T, Duguma G, Gizaw S, Wurzinger M, Soelkner J, Mwai O, Dessie T, Abebe A, Abate Z, Jembere T, Rekik M, Lobo RNB, Mwacharo JM, Terfa ZG, Kassie GT, Mueller JP, Rischkowsky B: Community-based sheep breeding programs generated substantial genetic gains and socioeconomic benefits. *Animal*, 14 (7): 1362-1370, 2020. DOI: 10.1017/S1751731120000269

2. Ansari-Renani HR: An investigation of organic sheep and goat production by nomad pastoralists in southern Iran. *Pastoralism*, 6 (8): 1-9, 2016. DOI: 10.1186/s13570-016-0056-y

3. Grandin T: Welfare problems in cattle, pigs, and sheep that persist even though scientific research clearly shows how to prevent them. *Animals*, 8 (7): 124, 2018. DOI: 10.3390/ani8070124

4. Polsky L, von Keyserlingk MAG: Invited review: Effects of heat stress on dairy cattle welfare. *J Dairy Sci*, 100 (11): 8645-8657, 2017. DOI: 10.3168/jds.2017-12651

5. Fernandes JN, Hemsworth PH, Coleman GJ, Tilbrook AJ: Costs and benefits of improving farm animal welfare. *Agriculture*, 11 (2): 104, 2021. DOI: 10.3390/agriculture11020104

6. Aksoy G, Avcı M, Biricik HS, Kaplan O, Yertürk M: Şanlıurfa doğal barınak besiciliğinde zeolit mineralinin hayvan refahı üzerine etkisi. *Harran Univ Vet Fak Derg*, 7 (2): 200-206, 2018. DOI: 10.31196/huvfd.508984

7. Schneider AF, De Almeida DS, Yuri FM, Zimmermann OF, Gerber MW, Gewehr CE: Natural zeolites in diet or litter of broilers, *Br Poult Sci,* 57 (2): 257-263, 2016. DOI: 10.1080/00071668.2016.1150962

8. Eroglu N, Emekci M, Athanassiou CG: Applications of natural zeolites on agriculture and food production. *J Sci Food Agric*, 97 (11): 3487-3499**,** 2017. DOI: 10.1002/jsfa.8312

9. Kale O, Durmuş İ: The comparison of effects of supplementation of zeolite and Yucca Schidigera powder to diet on liver enzymes (AST, ALT, GGT) in sheep. *TURJAF*, 8 (9): 1923-1927, 2020. DOI: 10.24925/turjaf.v8i9.1923-1927.3527

10. Ünal N, Akçapınar H, Atasoy F, Yakan A, Uğurlu M: Milk yield and milking traits measured with different methods in Bafra sheep. *Rev Med Vet,* 159 (10): 494-501, 2008.

11. Romero G, Peris C, Fthenakis GC, Diaz JR: Effects of machine milking on udder health in dairy ewes. *Small Ruminant Res*, 188 (2020): 106096. DOI: 10.1016/j.smallrumres.2020.106096

12. Priolo A, Lanza M, Barbagallo D, Finocchiaro L, Biondi L: Can the reflectance spectrum be used to trace grass feeding in ewe milk? *Small Ruminant Res,* 48, 103-107, 2003. DOI: 10.1016/s0921-4488(03)00006-3

13. Kahraman M, Yüceer-Özkul B: Akkaraman, Bafra ve Bafra x Akkaraman F1 koyunlarda süt verimi ve bazı süt kalitesi özellikleri. *Eurasian J Vet Sci,* 36 (2): 86-95, 2020. DOI: 10.15312/EurasianJVetSci.2020.264

14. Gorewit RC: Lactation biology and methods of increasing efficiency. Designing Foods: Animal Product Options in the Marketplace, 208-233. The National Academies Press, Washington DC, USA, 1988.

15. Damm T: Stallbau. Landwirtscahftsverlag GmbH, Münster-Hiltrup. 139-141, Frankfurt, Germany, 1997.

16. Ništiar F, Mojžiš J, Kovac G, Seidel H, Racz O: Influence of intoxication with organophosphates on rumen bacteria and rumen protozoa and protective effect of clinoptilolite-rich zeolite on bacterial and protozoan concentration in rumen. *Folia Microbiol*, 45 (6): 567-571, 2000. DOI: 10.1007/BF02818728

17. Katsoulos PD, Zarogiannis S, Roubies N, Christodoulopoulos G: Effect of long-term dietary supplementation with clinoptilolite on performance and selected serum biochemical values in dairy goats. *Am J Vet Res*, 70 (3): 346-352, 2009. DOI: 10.2460/ajvr.70.3.346

18. Herbut P, Angrecka S, Nawalany G: Influence of wind on air movement in a free stall barn during the summer period. *Ann Anim Sci,* 13 (1): 109-119, 2013. DOI: 10.2478/v10220-012-0063-x

19. Herbut P, Angrecka S: Ammonia concentrations in a free-stall dairy barn. *Ann Anim Sci,* 14 (1): 153-166, 2014. DOI:10.2478/aoas-2013-0065

20. Schneider AF, Zimmermann OF, Gewehr CE: Zeolites in poultry and swine production. *Cienc Rural,* 47 (8): e20160344, 2017. DOI: 10.1590/0103-8478cr20160344

21. Leitner G, Chaffer M, Caraso Y, Ezra E, Kababea D, Winkler M, Glickman A, Saran A: Udder infection and milk somatic cell count, NAGase activity and milk composition-fat, protein and lactose-in Israeli-Assaf and Awassi sheep. *Small Ruminant Res*, 49, 157-164, 2003. DOI: 10.1016/s0921-4488(03)00079-8

22. Pengov A: The role of coagulase-negative *Staphylococcus* spp. and associated somatic cell counts in the ovine mammary gland. *J Dairy Sci,* 84 (3): 572-574, 2001. DOI: 10.3168/jds.S0022-0302(01)74509-2

23. Ural DA: Efficacy of clinoptilolite supplementation on milk yield

and somatic cell count. *Rev MVZ Cordoba*, 19 (3): 4242-4248, 2014. DOI: 10.21897/rmvz.86

24. Pir Yağcı İ, Kaymaz M: Koyunlarda klinik, mikrobiyolojik ve biyokimyasal metotlar ile subklinik mastitislerin saptanması. *Ankara Univ Vet Fak Derg*, 53 (1): 31-35, 2006.

25. Watson DJ, Buswell JF: Modern aspects of sheep mastitis. *Br Vet J*, 140 (6): 529-534, 1984. DOI: 10.1016/0007-1935(84)90003-4

26. Leitner G, Chaffer M, Zamir S, Mor T, Glickman A, Winkler M, Weisblit L, Saran A: Udder disease etiology, milk somatic cell counts and NAGase activity in Israeli Assaf sheep throughout lactation. *Small Ruminant Res*, 39 (2): 107-112, 2001. DOI: 10.1016/s0921-4488(00)00190-5

27. Wang LC, Zhang TT, Wen C, Jiang ZY, Wang T, Zhou YM: Protective effects of zinc-bearing clinoptilolite on broilers challenged with *Salmonella pullorum*. *Poult Sci*, 91 (8): 1838-1845, 2012. DOI: 10.3382/ps.2012-02284

28. Loch FC, Oliveira MC D, Silva DD, Gonçalves BN, Faria BFD, Menezes JFS: Quality of poultry litter submitted to different treatments in five consecutive flocks. *R Bras Zootec*, 40, 1025-1030, 2011. DOI: 10.1590/S1516-35982011000500013

29. Migliorati L, Abeni F, Cattaneo MP, Tornielli C, Pirlo G: Effects of adsorbents in dairy cow diet on milk quality and cheese-making properties. *Ital J Anim Sci*, 6 (1): 460-462, 2007. DOI: 10.4081/ijas.2007.1s.460

30. Ristevski M, Toholj B, Cincović M, Trojačanec P, Starič J, Smolec O: Milk production, body condition score and metabolic parameters at the peak of lactation as risk factors for chronic lameness in dairy cows. *Kafkas Univ Vet Fak Derg,* 23 (5): 721-727, 2017. DOI: 10.9775/kvfd.2017.17593

31. Đuričić D, Benić M, Maćešić N, Valpotić H, Turk R, Dobranić V, Cvetnić L, Gračner D, Vince S, Grizelj J, Starič J, Lojkić M, Samardžija M: Dietary zeolite clinoptilolite supplementation influences chemical composition of milk and udder health in dairy cows. *Vet Stanica*, 48 (4): 257-265, 2017.

32. Pinto S, Hoffmann G, Ammon C, Amon B, Heuwieser W, Halachmi I, Banhazi T, Amon T: Influence of barn climate, body postures and milk yield on the respiration rate of dairy cows. *Ann Anim Sci*, 19 (2): 469-481, 2019. DOI: 10.2478/aoas-2019-0006

33. Balaban A, Şen E: Tarımsal Yapılar. 244, Ziraat Fakültesi, Ankara Üniversitesi, 1988.

34. Alkan Z: Ağıl planlama tekniği üzerinde bir araştırma. **In,** *1. Hayvancılık Çayır Mera ve Yem Bitkileri Teknik Kongresi*, 14-17 Ocak, Erzurum, Türkiye, 1975.

35. Mutaf S, Sönmez R: Hayvan barınaklarında iklimsel çevre ve denetimi. 280, Ziraat Fakültesi, Ege Üniversitesi, 1984.

36. Milic D, Tofant A, Vucemilo M, Venglovsky J, Ondrasovicova O: The performance of natural zeolite as a feed additive in reducing aerial ammonia and slurry ammonium ion concentration in the pig farm nursery. *Folia Vet*, 49, 23-25, 2005.

37. Shah GA, Shah GM, Rashid MI, Sadiq M, Khan F, Mahmood I, Hassan Z, Anwar A, Luqman M, Tarar ZH, Groot JCJ, Lantinga EA: Additives used with straw bedding can mitigate ammonia and greenhouse gaseous emissions from solid cattle manure in sloping-floor housing system. *Preprints*, 2020. DOI: 10.20944/preprints202001.0297.v1

38. Tian W, Wu T, Zhao R, Xu J, He Y, Wang H: Responses of milk production of dairy cows to jugular infusions of a mixture of essential amino acids with or without exclusion leucine or arginine. *Anim Nutr*, 3 (3): 271-275, 2017. DOI: 10.1016/j.aninu.2017.05.003

39. Saad EA, El-Gayar HA, El-Demerdash RS, Radwan KH: Frankincense administration antagonizes adenine-induced chronic renal failure in rats. *Pharmacogn Mag,* 14 (58): 634-640, 2018. DOI: 10.4103/pm.pm_271_18

40. Nisbet C, Yarım GF, Çiftçi G: Sağlıklı Karayaka ırkı koyunlara ait bazı serum biyokimyasal değerleri. *Ankara Univ Vet Fak Derg*, 53 (1): 57-59, 2006. DOI: 10.1501/Vetfak_0000000063

41. Şimşek Ö, Karaşahin T, Güner B, Dursun Ş: Hasak ve Hasmer melez koyun ırklarına ait bazı hematolojik ve biyokimyasal parametreler. *Ataturk Univ Vet Bil Derg*, 10 (1): 27-32, 2015. DOI: 10.17094/avbd.51112

42. Toprak NN, Yılmaz A, Öztürk E, Yigit O, Cedden F: Effect of micronized zeolite addition to lamb concentrate feeds on growth performance and some blood chemistry and metabolites. *S Afr J Anim Sci*, 46 (3): 313-320, 2016. DOI: 10.4314/sajas.v46i3.11

43. Comba B, Mert H, Comba A, Mis L, Mert N: The some hematological and biochemical parameters ın Karakul and Norduz sheep. *Van Vet J*, 28 (3): 137-140, 2017.

44. Udum D, Üstüner H, Belenli D, Uzabacı E: Kıvırcık ırkı koyunlara ait bazı biyokimyasal değerlerin belirlenmesi üzerine bir araştırma. *Uludag Univ J Fac Vet Med*, 32 (2): 7-10, 2013. DOI: 10.30782/uluvfd.163479

45. Kurt D, Yokuş B, Çakır DÜ, Denli O: Investigation levels of certain serum biochemistry components and minerals of pasturing Akkaraman sheep in Adiyaman province. *Dicle Univ Vet Fak Derg*, 1 (2): 34-37, 2008.

46. Prvulović D, Jovanović-Galović A, Stanić B, Popović M, Grubor-Lajšić G: Effects of a clinoptilolite supplement in pig diets on performance and serum parameters. *Czech J Anim Sci*, 52 (6): 159-166, 2007. DOI: 10.17221/2317-CJAS

47. Harma M, Harma M, Erel O: Measurement of the total antioxidant response in preeclampsia with a novel automated method. *Eur J Obstet Gynecol Reprod Biol*, 118 (1): 47-51, 2005. DOI: 10.1016/j.ejogrb.2004.04.012

48. Mis L, Mert H, Comba A, Comba B, Doğan Söğütlü İ, Irak K, Mert N: Some mineral substance, oxidative stress and total antioxidant levels in Norduz and Morkaraman sheep. *Van Vet J*, 29 (3): 131-134, 2018.

Kafkas Universitesi Veteriner Fakultesi Dergisi
ISSN: 1300-6045 e-ISSN: 1309-2251
Journal Home-Page: http://vetdergikafkas.org

Kafkas Univ Vet Fak Derg
27 (6): 699-706, 2021
DOI: 10.9775/kvfd.2021.26135

RESEARCH ARTICLE

Protective and Therapeutic Effect of Quercetin in Hepatotoxicity Induced by Sepsis in Rats

Mevlüt DOĞUKAN [1,a (*)] Murat BIÇAKCIOĞLU [2,b] Mehmet DURAN [1,c]
Zümrüt DOĞAN [3,d] Bilge AYDIN TÜRK [4,f] Öznur ULUDAĞ [1,e]

[1] Anesthesiology and Reanimation Department, Adiyaman University Faculty of Medicine, TR-02100 Adiyaman - TURKEY
[2] Anesthesiology and Reanimation Department, Balıkesir University Faculty of Medicine, TR-10010 Balıkesir - TURKEY
[3] Anatomy Department, Adiyaman University Faculty of Medicine, TR-02100 Adiyaman - TURKEY
[4] Pathology Department, Adiyaman University Faculty of Medicine, TR-02100 Adiyaman - TURKEY
ORCIDs: [a] 0000-0002-4890-758X; [b] 0000-0001-9101-6857; [c] 0000-0001-7568-3537; [d] 0000-0001-7131-2317; [e] 0000-0003-1592-1040
[f] 0000-0002-6017-5836

Article ID: KVFD-2021-26135 Received: 12.06.2021 Accepted: 10.11.2021 Published Online: 16.11.2021

Abstract

Septicemia caused by Gram-negative bacteria is an infection associated with liver dysfunction. Quercetin is a natural flavonoid found in vegetables and fruits and has anti-inflammatory, antioxidant, cytoprotective and antiallergic properties. This research aims to investigate the effects of quercetin on the liver against tissue damage due to sepsis-induced oxidative stress. Thirty-two male rats were used in the study. The animals were randomly divided into 5 groups. Quercetin was dissolved in 20 mg/kg of olive oil daily for 15 days and given through oral gavage. The cecal-ligation sepsis model was applied to the group 3 and group 4. In histopathological evaluation; inflammation involving moderate neutrophils and lymphocytes was observed in most portal areas in the group where sepsis was created (Group 3). In the sepsis group administered quercetin (Group 4) only a few portal areas had a milder inflammation with fewer neutrophils than the sepsis group. There was a significant difference between group 3, 4, and all other groups in ALT and AST values. A significant difference was observed between group 3, 4 and other groups in terms of tissue MDA, GSH levels. It was concluded that quercetin, a powerful antioxidant, can reduce liver damage caused by sepsis and has the potential to be used to help treat sepsis.

Keywords: *Quercetin, Sepsis, Hepatotoxicity, Rat*

Sıçanlarda Sepsisin Neden Olduğu Hepatotoksisitede Kuersetin'in Koruyucu ve Terapötik Etkisi

Öz

Gram negatif bakterilerin yol açtığı septisemi, karaciğer fonksiyon bozukluğu ile ilişkili bir enfeksiyondur. Kuersetin, sebzeler ve meyvelerde bulunan doğal bir flavonoid olup antienflamatuar, antioksidan, sitoprotektif ve antialerjik etkilidir. Bu araştırmanın amacı sepsis kaynaklı oksidatif stress sonucu olaşan doku hasarına karşı kuersetinin karaciğer üzerine etkilerini araştırmaktır. Çalışmada 32 erkek sıçan kullanıldı. Hayvanlar randomize olarak 5 gruba ayrıldı. Kursetin, 15 gün boyunca, günlük 20 mg/kg zeytinyağı içerisinde çözülerek oral gavaj ile verildi. Çekal ligasyonlu sepsis modeli grup 3 ve 4'e uygulandı. Histopatolojik değerlendirmede sepsis oluşturulan grupta (Grup 3) portal alanların çoğunda orta derecede nötrofilleri ve lenfositleri içeren inflamasyon izlendi. Kuarsetin uygulanan sepsis grubunda (Grup 4) sadece birkaç portal alanda sepsis grubuna göre daha az nötrofil içeren daha hafif bir inflamasyon mevcuttu. ALT ve AST değerlerinde grup 3, 4 ile diğer tüm gruplar arasında anlamlı farklılık vardı. Doku MDA, GSH Düzeyleri açısından grup 3, 4 ile diğer gruplar arasında anlamlı olarak farklılık gözlendi. Güçlü bir antioksidan olan kuersetinin sepsisin neden olduğu karaciğer hasarını azaltabileceği ve sepsis tedavisine yardımcı olarak kullanılma potansiyeline sahip olacağı sonucuna varıldı.

Anahtar sözcükler: *Kuersetin, Sepsis, Hepatotoksisite, Rat*

INTRODUCTION

Sepsis is a serious health problem that progresses with a deep systemic inflammatory response to infection and requires intensive care treatment [1]. Because of high mortality and morbidity rates, clinicians have difficulty in coping with patients with sepsis. Severe septic shock, tissue damage, multi-organ dysfunction, and death are common in sepsis [1,2].

How to cite this article?

Doğukan M, Bıçakçıoğlu M, Duran M, Doğan Z, Aydın Türk B, Uludağ Ö: Protective and therapeutic effect of quercetin in hepatotoxicity induced by sepsis in rats. *Kafkas Univ Vet Fak Derg,* 27 (6): 699-706, 2021.
DOI: 10.9775/kvfd.2021.26135

(*) **Corresponding Author**

Tel: +90 416 2231690 Cellular phone: +90 505 253 6441 Fax: +90 416 223 1693
E-mail: drmevlud@hotmail.com (M. Doğukan)

Septicemia caused by Gram-negative bacteria is a dangerous infection associated with the frequency of liver dysfunction. Severe and acute hepatotoxicity is probably due to the intense release of endotoxin into the systemic circulation after the death of bacteria. The direct toxic effect of endotoxin is probably due to the increased production of reactive oxygen intermediates such as oxygen-peroxides and nitric oxide [2,3]. Quercetin is a natural flavonoid found in vegetables and fruits. It is known to have anti-inflammatory, antioxidant, free radical scavenging, cytoprotective, and antiallergic action [4]. Liver damage caused by sepsis is a common pathology in the clinic and its treatment is of absolute importance to the physician and patient. Although Wichterman et al.[5] described the sepsis model with using cecal ligation in rats in 1980, it has also been applied to mice and sheep. It is frequently preferred because of creation a clinical picture similar to the sepsis model in humans. We also used this model in our study. For this reason, we aimed to use quercetin, which has a high antioxidant capacity, as a preservative and treatment against tissue damage due to oxidative stress caused by sepsis.

Material and Methods

Ethical Approval

The study protocol was approved by the Local Ethics Committee for Animal Experiments of Adiyaman University, Turkey (Approval no: ADYU-HADYEK: 2019-045)

Animal Sampling

In the study, thirty-two male Spraque Dawley rats, weighing about 280-300 g were used. The animals were randomly divided into 5 groups *(Table 1)*. Rats were housed in a room with a controlled heating (22±2°C) and lighting (12 h dark/light), and fed a diet of feed and water *ad libitum*.

The rats were randomly divided into five groups. The groups were as follows:

Group 1 (Control): Intragastric saline was administered in doses of 1.5 mL (n=6).

Group 2 (Sham Surgery): A surgical incision was made and 1.5 mL of olive oil was given in an intragastric way (since quercetin dissolves in oil, n=6).

Group 3 (Sepsis): The sepsis model was created using the cecal ligation and drilling method.

Group 4 (Sepsis and Quercetin): Quercetin was intragastrically administered at a dose of 20 mg/kg from 15 days before the surgical procedure until the end of the experiment and a sepsis model was created simultaneously with Group 3 (n=7).

Group 5 (Quercetin): Quercetin was intragastrically administered at a dose of 20 mg/kg from 15 days before the surgical procedure until the end of the experiment (n=5).

Table 1. *Blood Parameters of the study groups*

Parameters	Group (n)	Mean±SD	P
ALT (U/L)	Group 1 (6) Group 2 (6) Group 3 (7) Group 4 (7) Group 5 (5)	41.83±15.14 42.83±11.44 **149±97.82** **86.43±21.61** 44±13.51	**.001**
AST (U/L)	Group 1 (6) Group 2 (6) Group 3 (7) Group 4 (7) Group 5 (5)	121.67±19.77 170.33±27.95 **740.43±299.51** **672.57±196.83** 107±20.99	**.001**
LDH (U/L)	Group 1 (6) Group 2 (6) Group 3 (7) Group 4 (7) Group 5 (5)	712.67±100.28 1525.5±495.39 **1963.29±1203.18** **2243.29±424.01** 768.6±197.35	**.001**
GGT (U/L)	Group 1 (6) Group 2 (6) Group 3 (7) Group 4 (7) Group 5 (5)	8.17±4.88 6±1.1 8.14±4.95 5.14±1.21 6.4±1.14	.38
CRP (mg/dL)	Group 1 (6) Group 2 (6) Group 3 (7) Group 4 (7) Group 5 (5)	0.15±0.07 0.13±0.03 0.15±0.06 0.18±0.07 0.13±0.03	.45

No statistically significantdifference between the Group 3 and Group 4 (P>0.05)

Quercetin Application: Quercetin (quercetin dihydrate, 97%, CAS: 6151-25-3; Alfa Aesar, Germany) was dissolved in 20 mg/kg of olive oil daily and given with oral gavage for 15 days [6].

The Cecal Ligation and Drilling Method: Ketamine HCl 70 mg/kg (Ketalar; Eczacıbaşı, İstanbul, Turkey) and xylazine HCl 20 mg/kg (Rompun 2%; Bayer Türk İlaç Ltd. Şti.) were intraperitoneally administered to all rats to be operated on the 16th day of the study under aseptic conditions under the supervision of a veterinarian. The cecum was exposed and connected distally through the ileocecal valve. It was drilled twice with an 18G needle from the antimesenteric edge. The skin, muscle, and peritoneum were closed by suture, the animal was given subcutaneous fluid supplements according to its weight [7]. One day after the sepsis procedure, 70 mg/kg of ketamine hydrochloride and 20 mg/kg of xylazine hydrochloride were administered to rats under aseptic conditions, and blood and tissue samples were taken. All animals were sacrificed under anesthesia at the end of the study.

Blood Analysis

Blood samples were drawn at the end of the procedure. They were transferred to EDTA tubes and centrifuged at 3000 rpm for 5 min. The plasma was then kept in the freezer (-20°C). Blood urea nitrogen (BUN), creatinine, alanine

aminotransferase (ALT), aspartate aminotransferase (AST), lactate dehydrogenase (LDH), and c-reactive protein (CRP) were analyzed [8].

Preparation of Tissue Homogenates

After the liver tissue was washed with physiological saline solution at +4°C, divided into small sections in accordance with cold chain principles, then put in Eppendorf tubes and stored at -80°C until assayed. Tissue homogenates for malondialdehyde (MDA) in tissue samples were prepared in a cold environment using a homogenizer in 0.15 M KCl (10%, w/v) [9].

Biochemical Evaluation

Analysis of malondialdehyde (MDA) level; Tissue MDA concentration as a lipid peroxidation marker was analyzed according to the thiobarbituric acid reaction (TBARS) method defined by Beuge and Aust [10]. Liver tissue was centrifuged after being homogenized in 10% trichloroacetic acid. After mixing the superficial liquid part with 0.67% thiobutyric acid in equal volume, it was cooled and centrifuged after being incubated in boiling water for 15 min at 90°C. Tissue MDA concentrations were measured under 532 nm absorbance and expressed as nmol/g tissue.

Analysis of glutathione peroxidase (GSH) level; It was determined according to the method described by Ellman [11]. The glutathione in the analysis tube reacted with 5.5′-ditiyobis 2-nitrobenzoic acid and gave yellow-greenish color, and the light intensity of this color was measured in 410 nm wavelength by a spectrophotometer and the amount of reduced glutathione was determined.

Histopathological Procedure

The extracted liver tissue was fixed in 10% formaldehyde for histopathological examinations. The fixed tissues were subjected to a routine histological tissue follow-up procedure. The tissues followed up were turned into paraffin blocks. Sections with a thickness of 5 µm were taken from the blocks for histopathological examination. The resulting sections were stained with hematoxylane-Eozin (HE). The stained sections were histologically evaluated under an Olympus BX53 microscope (Olympus Corporation, 2014, Hamburg). The evaluation took into account necrosis in the liver, fibrosis, inflammatory cell infiltration in portal areas, dilatation in sinusoids, and congestion in vascular structures [12].

Statistical Analysis

Statistical analysis was performed with SPSS 15.0 for Windows (SPSS Inc.). The one-sample Kolmogorov-Smirnov test was used to determine whether the data were distributed normally. Groups were compared using the One-way ANOVA or the Kruskal Wallis H test whichever one is appropriate. As a result of these analyses, the groups which were found significant were compared using Tukey's multiple range test or pairwise Mann Whitney U test (Bonferroni correction was applied for which p-values <0.005 (i.e., and 0.05/10 comparisons)). The results were reported as mean±SD or median (min-max). A p-value <0.05 was considered statistically significant.

Results

ALT, AST, GGT, LDH, and CRP Values

While there was a significant difference between Group 3 and Group 4, and all other groups in ALT and AST values, there was no statistically significant difference between Group 3 and Group 4. While the increase in LDH values in Groups 2, 3, and 4 was statistically significantly different from other groups, there was no significant difference among these three groups. When GGT and CRP values were compared between the groups, no intergroup differences were observed. All blood values, intergroup comparison, and P values are presented in *Table 1*.

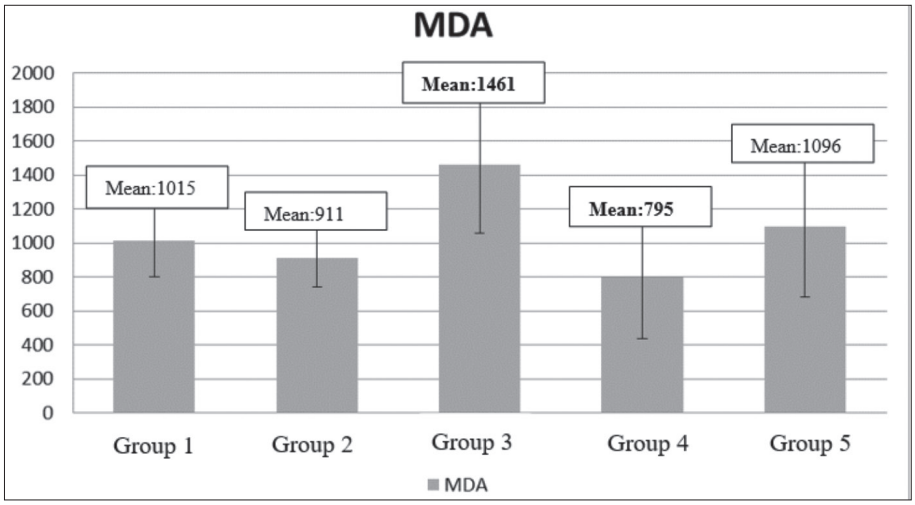

Fig 1. The graphic of MDA levels

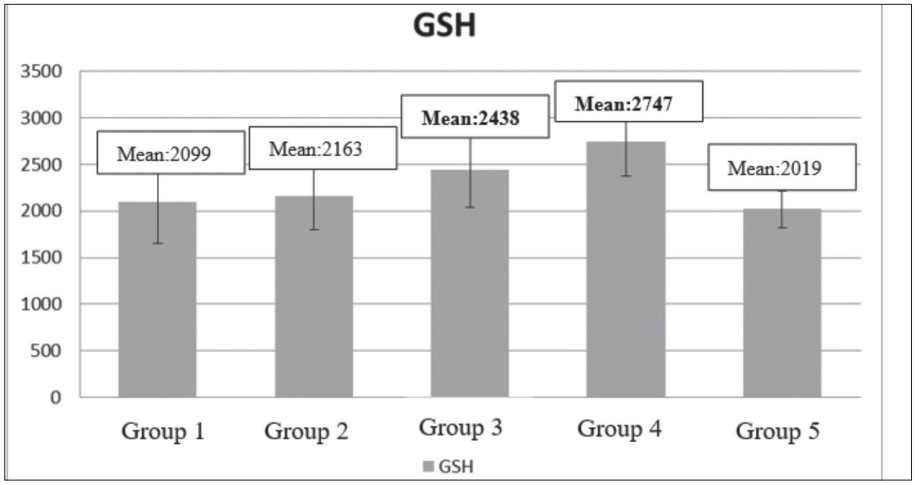

Fig 2. The graphic of GSH Levels

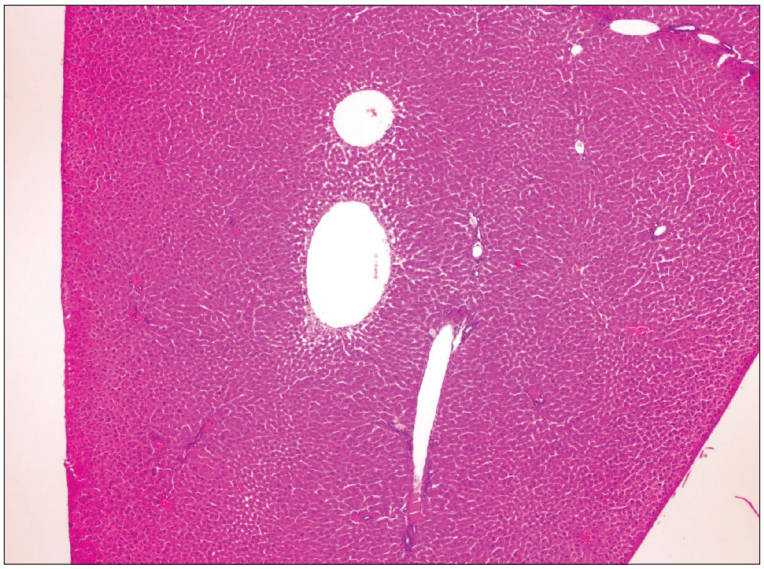

Fig 3. Sham group (Group 2) central veins are dilated, portal fields have normal appearance (HE X100)

Tissue MDA and, GSH Levels

While the MDA values were not statistically significant among Group 1, 2, and 5, there was a significant difference between Group 3 and 4 and between the Group 3, 4, and other Groups (P=0.011) *(Fig. 1)*.

While GSH values were not statistically significant between the Group 1, 2, and 5, there was a significant difference between the Group 3 and 4 and between the Group 3, 4, and other Groups (P=0.012) *(Fig. 2)*.

Histopathological Findings

In terms of the histopathological findings, no structural changes, fibrosis or necrosis were observed in the liver in any of the groups. No abnormal histopathological changes were found in the Control (Group 1) and Sham (Group 2) groups *(Fig. 3)*. In the group where sepsis was created (Group 3), inflammation involving moderate neutrophils and lymphocytes was observed slightly in most of the portal areas *(Fig. 4)*. There was a slight expansion of sinusoids. Dilatation and congestion were observed in central veins, and slight expansion in some portal areas *(Fig. 5)*. In the sepsis group which was administered quercetin (Group 4); only a few portal areas had a milder inflammation with fewer neutrophils than that of in the sepsis group. Dilatation and congestion were observed in the central veins. There was a slight expansion of sinusoids *(Fig. 6)*. In the quercetin group, sinusoids had a pronounced dilated appearance. Milder lymphocytic infiltration was present in the portal areas and no neutrophils were observed. Dilatation was present in the veins in the portal areas *(Fig. 7)*.

Discussion

Sepsis is a disease with an uncontrolled inflammatory response. It rapidly progresses and has a high mortality rate [13]. More than 19 million people worldwide are affected by sepsis every year. Half of the patients who survive and are discharged after sepsis recover, one-third die within a year, and one-sixth have serious permanent damage [14]. The liver has a key role during sepsis. Bacterial clearanceis necessary for the regulation of immune defenses during

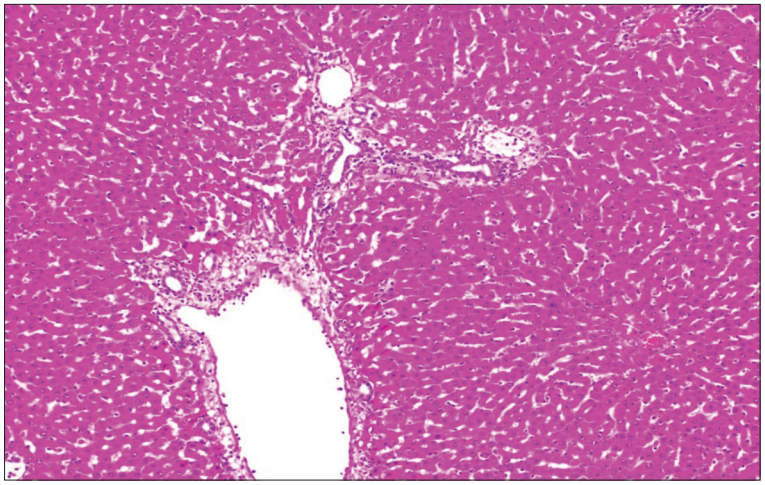

Fig 4. Chronic active inflammation and dilated vascular structure in the portal area of the sepsis group (Group 3) (HE X100)

Fig 5. Neutrophil presence in the portal area of the sepsis group (Group 3) (HE X200)

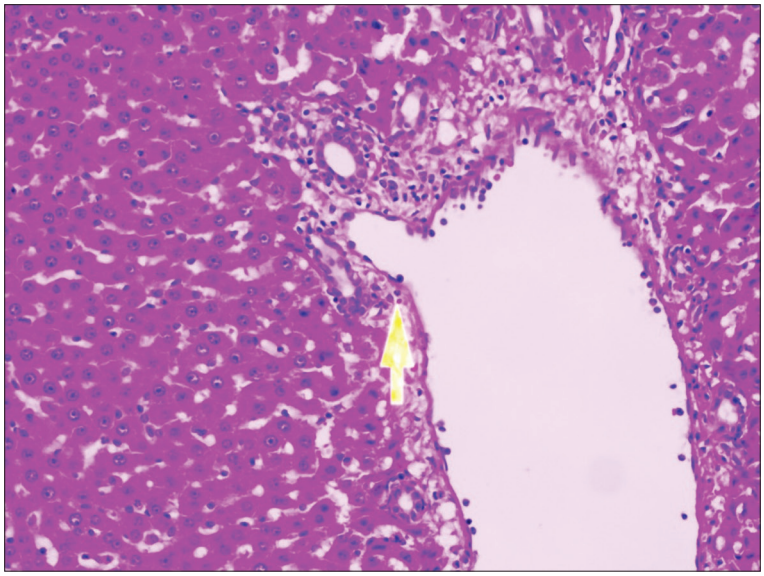

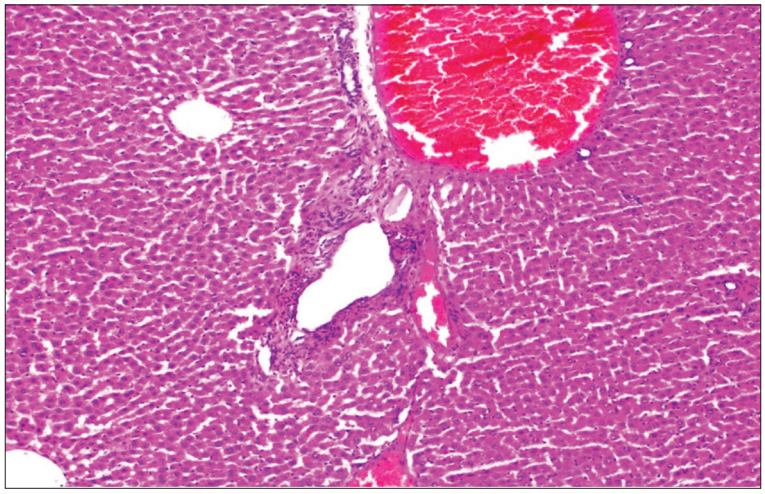

Fig 6. Mild inflammation and dilated congested vascular structure in the portal area of the quercetin-sepsis group (Group 4) (HE X100)

systemic infections through mechanisms such as the production of acute-phase protein/cytokines and metabolic adaptation to inflammation. The liver is also a target for sepsis-related damage in critical patients, including hypoxic hepatitis due to ischemia and shock, cholestasis due to altered bile metabolism, hepatocellular damage due to drug toxicity or excessive inflammation, as well as different pathologies such as secondary sclerosing cholangitis. Therefore, hepatic dysfunction can significantly adversely affect the prognosis of sepsis [15]. Treatments

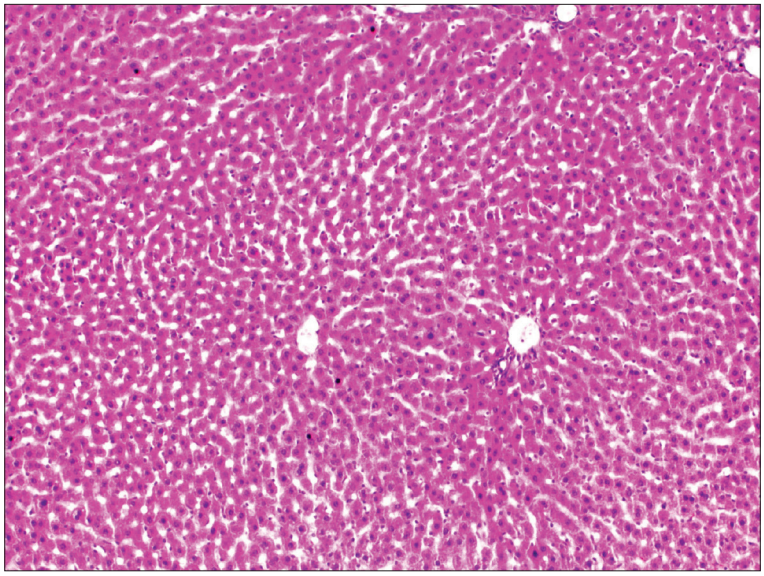

Fig 7. Normal liver structure in the quercetin group (Group 5), portal area and central vein (HE X 100)

for sepsis focus on macro circulatory failures, such as decreased artery mean pressure and heart rate. However, increasing evidence suggests that impaired oxygen consumption of the cell can play an important role in the pathogenesis of sepsis. Therefore, it has given rise to the idea that treatments aimed at providing redox hemostasis can be useful in the management of sepsis [16]. No study existing that shows the clear efficacy of Vitamin C, as an antioxidant especially in sepsis [17]. Quercetin is a flavonoid with strong antioxidant activity. It is abundant in fruits and vegetables such as cabbage, onions, red grapes, apples, and broccoli in nature, as well as tea and red wine. It has been shown to prevent various diseases such as osteoporosis, some cancers, and lung and cardiovascular diseases [18]. Quercetin has been shown to have protective effects against LPS-induced tissue damage and septic shock by improving inflammatory response in animal models [19].

In our study, we examined the effects of quercetin at a dose of 20 mg/kg for 15 days on liver damage caused by sepsis. A significant increase took place in ALT, AST, and LDH values of the sepsis-generated groups. Although these values were lower in the sepsis group (Group 4) administered quercetin, the difference was not statistically significant. ALT and AST values are commonly used to detect liver damage [20]. Wei et al.[21] found that ALT and AST values are significantly lower in the group administered quercetin in their study, in which they demonstrated the protective effect of quercetin against liver damage caused by triptolide. Ma et al.[22] showed that quercetin prevented liver damage caused by CCl_4. The study examined the efficacy of quercetin at a dose of 40 and 80 mg/kg/day through oral gavage. They recorded decreases in ALT and AST values in both doses, more pronounced at the dose of 80 mg/kg/day. Peng et al.[23] intraperitoneally administered quercetin at doses of 25 mg/kg/day, 50 mg/kg/day, and 100 mg/kg/day for 6 days against lipopolysaccharide/D-galactosamine induced liver damage and found that it was protective in a dose-dependent manner. In the study, they observed that ALT and AST values decreased as the dose of quercetin increased. In their study, Yousef et al.[24] reported that quercetin could improve this condition by lowering the increased ALT, AST, and LDH values in liver damage. Although we observed a decrease in ALT and AST values thanks to quercetin in our study, we did not find this decrease significant. This was either related to the number of subjects or the dose of quercetin we used.

We observed that histological changes were milder in the quercetin-sepsis group (Group 4) than in the sepsis group (Group 3). The heaviest histological changes were observed in the sepsis group (Group 3). In their study where experimental cirrhosis was created with carbon tetrachloride in rats, Pavanato et al.[25] found quercetin was effective against liver damage and said that it positively prevented histological changes. Wei et al.[21] reported liver damage and necrosis due to triptolide by quercetin. Kanter administered quercetin at a dose of 15mg/kg/day for 4 weeks to rats on which bile duct ligation was performed and reported the protective effect of quercetin against cholestatic liver damage [26]. Histologically, he followed up the bile duct proliferation and fibrosis, mononuclear cell infiltration, neutrophil infiltration, dilatation changes in portal areas and observed that quercetin reduced these histological changes, and associated this result with the potential antioxidant effect of quercetin.

In our study, we found tissue MDA values significantly higher in the sepsis group (Group 3) than in all other groups. The quercetin-administered sepsis group had the highest GSH values, which was statistically significant. On the other hand, this group (Group4) had the lowest MDA value. This suggested two outcomes. The first was oxidative damage caused by sepsis, and the second was that this oxidative damage was effectively prevented by quercetin. Quercetin also inhibits macrophage-induced early

and late proinflammational cytokines in infection and is predicted to play a role in the pathogenesis of sepsis of mitochondrial dysfunction through oxidative stress [19,27,28]. As reported by Chang et al.[19] quercetin significantly reduced the TNF-α and IL-1β levels in macrophages and inhibited the phosphorylations of KB kinase (IKKs), Akt and c-Jun N-terminal kinase (JNK) inhibitors, induced by LPS. Quercetin causes a significant reduction in the phosphorylation and degradation of the κBα (IκBα) inhibitor, as well as a significant reduction in the nuclear level of nuclear factor-B (NF-κB). However, these effects are observed in the acute application of quercetin, but not observed in the chronic application. Kukongviriyapan et al.[29] showed the beneficial effect of quercetin on the mitigation of oxidative stress and vascular dysfunction against endotoxin-induced shock in mice.

Although it seems possible that quercetin, a powerful antioxidant, can reduce liver damage caused by sepsis, it is obvious that it alone is not enough to treat sepsis. But it has the potential to be an adjuvant therapy for sepsis.

Availability of Data and Materials

The datasets during and/or analyzed during the current study available from the corresponding author on reasonable request.

Funding Support

There is no funding source.

Conflict of Interest

The authors report no conflicts of interest. The authors alone are responsible for the content and writing of paper.

Author Contributions

MD, MB and MD the present study, conducted this experiment, and wrote this manuscript. ZD and MB collected and analyzed data. ZD and ÖU made laboratory measurements. BAT applied the histopathological examination of the study. All authors contributed to the critical revision of the manuscript and have read and approved the final version.

References

1. Gerin F, Sener U, Erman H, Yilmaz A, Aydin B, Armutcu F, Gurel A: The effects of quercetin on acute lung injury and biomarkers of inflammation and oxidative stress in the rat model of sepsis. *Inflammation,* 39, 700-705, 2016. DOI: 10.1007/s10753-015-0296-9

2. Huang R, Zhong T, Wu H: Quercetin protects against lipopolysaccharide-induced acute lung injury in rats through suppression of inflammation and oxidative stress. *Arch Med Sci,* 11 (2): 427-432, 2015. DOI: 10.5114/aoms.2015.50975

3. Çenesiz S: The role of oxidant and antioxidant parameters in the infectious diseases: A systematic literature review. *Kafkas Univ Vet Fak Derg,* 26 (6): 849-858, 2020. DOI: 10.9775/kvfd.2020.24618

4. Xu D, Hu MJ, Wang YQ, Cui YL: Antioxidant activities of quercetin and its complexes for medicinal application. *Molecules*, 24 (6): 1123, 2019. DOI: 10.3390/molecules24061123

5. Wichterman KA, Baue AE, Chaudry IH: Sepsis and septic shock-a review of laboratory models and a proposal. *J Surg Res,* 29, 189-201, 1980. DOI: 10.1016/0022-4804(80)90037-2

6. Dogan Z, Cetin A, Elibol E, Vardi N, Turkoz Y: Effects of ciprofloxacin and quercetin on fetal brain development: A biochemical and histopathological study. *J Matern Fetal Neonatal Med,* 32, 1783-1791, 2019. DOI: 10.1080/14767058.2017.1418222

7. Uchiyama M, Mihara M: Determination of malonaldehyde precursor in tissue by thiobarbituric acid test. *Anal Biochem,* 86, 271-278, 1978. DOI: 10.1016/0003-2697(78)90342-1

8. Kumru S, Godekmerdan A, Kutlu S, Ozcan Z: Correlation of maternal serum high-sensitive C-reactive protein levels with biochemical and clinical parameters in preeclampsia. *Eur J Obstet Gynecol Reprod Biol,* 124 (2): 164-167, 2006. DOI: 10.1016/j.ejogrb.2005.05.007

9. Uraz S, Tahan V, Aygun C, Eren F, Unluguzel G, Yuksel M, Senturk O, Avsar E, Haklar G, Celikel C, Hulagu S, Tozun N: Role of ursodeoxycholic acid in prevention of methotrexate-induced liver toxicity. *Dig Dis Sci*, 53, 1071-1077, 2008. DOI: 10.1007/s10620-007-9949-3

10. Buege JA, Aust SD: Microsomal lipid peroxidation. *Methods Enzymol,* 52, 302-310, 1978. DOI: 10.1016/s0076-6879(78)52032-6

11. Elman GL: Tissue sulphydryl groups. *Arch Biochem Biophys,* 82 (1): 70-77, 1959. DOI: 10.1016/0003-9861(59)90090-6

12. Yener Z, Celik I, Ilhan F, Bal R: Effects of Urtica dioica L. seed on lipid peroxidation, antioxidants and liver pathology in aflatoxin-induced tissue injury in rats. *Food Chem Toxicol*, 47 (2): 418-424. 2009. DOI: 10.1016/j.fct.2008.11.031

13. Wang Z, Chen V, Li Y, Zhang S, Lou H, Lu X, Fan X: Reduning injection and its effective constituent luteoloside protect against sepsis partly via inhibition of HMGB1/TLR4/NF-κB/MAPKs signaling pathways. *J Ethnopharmacol,* 270, 113783, 2021. DOI: 10.1016/j.jep.2021.113783

14. Prescott HC, Angus DC: Enhancing recovery from sepsis: A review. *JAMA,* 319 (1): 62-75, 2018. DOI: 10.1001/jama.2017.17687

15. Strnad P, Tacke F, Koch A, Trautwein C: Liver-guardian, modifier and target of sepsis. *Nat Rev Gastroenterol Hepatol*, 14 (1): 55-66, 2017. DOI: 10.1038/nrgastro.2016.168

16. Mantzarlis K, Tsolaki V, Zakynthinos E: Role of oxidative stress and mitochondrial dysfunction in sepsis and potential therapies. *Oxid Med Cell Longev*, 2017, 5985209, 2017. DOI: 10.1155/2017/5985209

17. Kuhn SO, Meissner K, Mayes LM, Bartels K: Vitamin C in sepsis. *Curr Opin Anaesthesiol,* 31 (1): 55-60, 2018. DOI: 10.1097/ACO.0000000000000549

18. Marunaka Y, Marunaka R, Sun H, Yamamoto T, Kanamura N, Inui T, Taruno A: Actions of quercetin, a polyphenol, on blood pressure. *Molecules,* 22 (2): 209, 2017. DOI: 10.3390/molecules22020209

19. Chang YC, Tsai MH, Sheu WHH, Hsieh SC, Chiang AN: The therapeutic potential and mechanisms of action of quercetin in relation to lipopolysaccharide-induced sepsis in vitro and in vivo. *PLoS One*, 8 (11): e80744, 2013. DOI: 10.1371/journal.pone.0080744

20. Morovvati H, Armand N: Assessment of changes in serum concentrations of liver function (ALT, ALP, AST, LDH, GGT) after the intake of Narcissus Bulbs. *J Fasa Univ Med Sci*, 9, 1736-1742, 2019.

21. Wei CB, Tao K, Jiang R, Zhou LD, Zang OH, Yuan CS: Quercetin protects mouse liver against triptolide-induced hepatic injury by restoring Th17/Treg balance through Tim-3 and TLR4-MyD88-NF-κB pathway. *Int Immunopharmacol,* 53, 73-82, 2017. DOI: 10.1016/j.intimp.2017.09.026

22. Ma JQ, Li Z, Xie WR, Liu CM, Liu SS: Quercetin protects mouse liver against CCl_4-induced inflammation by the TLR2/4 and MAPK/NF-κB pathway. *Int Immunopharmacol*, 28 (1): 531-539, 2015. DOI: 10.1016/j.intimp.2015.06.036

23. Peng Z, Gong X, Yang Y, Huang L, Zhang Q, Zhang P, Wan R, Zhang B: Hepatoprotective effect of quercetin against LPS/D-GalN induced acute liver injury in mice by inhibiting the IKK/NF-κB and MAPK signal

pathways. *Int Immunopharmacol*, 52, 281-289, 2017. DOI: 10.1016/j.intimp.2017.09.022

24. Yousef MI, Omar SAM, El-Guendi MI, Abdelmegid LA: Potential protective effects of quercetin and curcumin on paracetamol-induced histological changes, oxidative stress, impaired liver and kidney functions and haematotoxicity in rat. *Food Chem Toxicol*, 48 (11): 3246-3261, 2010. DOI: 10.1016/j.fct.2010.08.034

25. Pavanato A, Tuñón MJ, Sánchez-Campos S, Marroni CA, Llesuy S, González-Gallego J, Marroni N: Effects of quercetin on liver damage in rats with carbon tetrachloride-induced cirrhosis. *Dig Dis Sci*, 48, 824-829, 2003. DOI: 10.1023/a:1022869716643

26. Kanter M: Protective effect of quercetin on liver damage induced by biliary obstruction in rats. *J Mol Histol,* 41 (6): 395-402, 2010. DOI: 10.1007/s10735-010-9301-7

27. Prauchner CA: Oxidative stress in sepsis: Pathophysiological implications justifying antioxidant co-therapy. *Burns*, 43 (3): 471-485, 2017. DOI: 10.1016/j.burns.2016.09.023

28. Nagar H, Piao S, Kim CS: Role of mitochondrial oxidative stress in sepsis. *Acute Crit Care,* 33 (2): 65-72, 2018. DOI: 10.4266/acc.2018.00157

29. Kukongviriyapan U, Sompamit K, Pannangpetch P, Kukongviriyapan V, Donpunha W: Preventive and therapeutic effects of quercetin on lipopolysaccharide-induced oxidative stress and vascular dysfunction in mice. *Can J Physiol Pharmacol*, 90 (10): 1345-1353, 2012. DOI: 10.1139/y2012-101

Kafkas Universitesi Veteriner Fakultesi Dergisi
ISSN: 1300-6045 e-ISSN: 1309-2251
Journal Home-Page: http://vetdergikafkas.org

Kafkas Univ Vet Fak Derg
27 (6): 707-715, 2021
DOI: 10.9775/kvfd.2021.26148

RESEARCH ARTICLE

Development of a Multiplex PCR Assay for the Simultaneous Detection of *Echinococcus* spp. in Wild Canids in the Qinghai-Tibet Plateau Area of China

Xueyong ZHANG [1,2,a] Yingna JIAN [1,2,b] Yong FU [1,c] Hong DUO [1,d (*)] Zhihong GUO [1,e (*)]

[1] Qinghai Academy of Animal Sciences and Veterinary Medicine, Qinghai University, Xining Qinghai, 810016, P.R. CHINA
[2] Institute of Traditional Chinese Veterinary Medicine, College of Veterinary Medicine, Gansu Agricultural University, Lanzhou Gansu, 730070, P.R. CHINA
ORCIDs: [a] 0000-0001-5076-9211; [b] 0000-0002-5696-2546; [c] 0000-0003-3354-9107; [d] 0000-0002-3013-9818; [e] 0000-0001-6308-6612

Article ID: KVFD-2021-26148 Received: 16.06.2021 Accepted: 19.10.2021 Published Online: 19.10.2021

Abstract

Infections of *Echinococcus granulosus sensu stricto, E. multilocularis* and *E. shiquicus* are usually prevalent or coendemic in wild canids in the Qinghai-Tibet Plateau area (QTPA) of China. Thus, an efficient method for the detection of infected hosts and the identification of *Echinococcus* species is needed. The present work aims to establish a multiplex PCR (mPCR) method that can simultaneously detect the three main *Echinococcus* species mentioned above, and provide technical support for the diagnosis, prevention and control of *Echinococcus* infection. Three pairs of specific primers were designed for this mPCR based on the *Echinococcus* mitochondrial genes in GenBank, and these primers were validated by specificity and sensitivity experiments and applied for simulated coinfection samples detection and filed samples. This mPCR method was able to successfully identify both simplex and mixed target *Echinococcus* spp. and generate expected amplicons of different sizes for each species. The sensitivity of this mPCR method was tested with serially diluted gene recombinant plasmid, and the results showed a detection threshold of less than 10^3 for both species. The specificity, which was assessed against 10 other parasites, was found to be 100%. The assay was also used on 15 simulated clinical samples, and the results confirmed the high reliability of the method, indicating that the mPCR method established in this study can be used to analyze clinical samples from the QTPA. This mPCR method has potential application in rapid detection, diagnosis and broad-scale screening and is expected to become a key technology for clinical detection and environmental monitoring.

Keywords: *Echinococcus granulosus, Echinococcus multilocularis, Echinococcus shiquicus, Multiplex PCR, Wild canids, China*

Çin'in Qinghai-Tibet Platosu Bölgesindeki Yabani Köpekgillerde *Echinococcus* spp.'nin Eşzamanlı Saptanması İçin Multipleks PCR Yönteminin Geliştirilmesi

Öz

Echinococcus granulosus sensu stricto, E. multilocularis ve *E. shiquicus* enfeksiyonları, Çin'in Qinghai-Tibet Platosu bölgesindeki (QTPA) yabani köpekgillerde genellikle yaygın ve koendemik seyretmektedir. Bu nedenle, enfekte konakçıların tespiti ve *Echinococcus* türlerinin tanımlanması için etkili bir teşhis yöntemine ihtiyaç vardır. Bu çalışmada, bahsedilen bu üç temel *Echinococcus* türünün aynı anda tespit edilmesi ve *Echinococcus* enfeksiyonlarının teşhisi, önlenmesi ve kontrolü için teknik destek sağlayan bir multipleks PCR (mPCR) yönteminin geliştirilmesi amaçlandı. mPCR için, *Echinococcus*'un GenBank'ta mevcut olan mitokondriyal genlerine bağlı olarak üç çift spesifik primer tasarlandı ve bu primerlerin özgüllük ve duyarlılıkları doğrulanarak temsili koenfeksiyon örneklerinin tespiti ve saha örnekleri için kullanıldı. mPCR yöntemi, hem bireysel hem de karma hedef *Echinococcus*'ları başarıyla tanımladı ve her tür için farklı boyutlarda beklenen amplikonlar oluşturdu. mPCR yönteminin duyarlılığı, seyreltilmiş gen rekombinant plazmidi ile test edildi ve her iki grup için 10^3'ten daha düşük bir saptama eşik değeri gösterdi. Diğer 10 parazite karşı değerlendirilerek, yöntemin spesifitesi %100 saptandı. mPCR yöntemi ayrıca temsili 15 klinik örnekte test edildi ve geliştirilen bu yönteminin QTPA'da klinik örneklerin analizinde kullanılabilecek yüksek güvenilirliğe sahip olduğu doğrulandı. Geliştirilen bu mPCR yönteminin, hızlı tespit, teşhis ve geniş ölçekli tarama çalışmalarında potansiyelinin olduğu saptanmıştır ve böylelikle klinik tespit ve çevresel izleme için kilit bir teknoloji olması beklenmektedir.

Anahtar sözcükler: *Echinococcus granulosus, Echinococcus multilocularis, Echinococcus shiquicus, Multipleks PCR, Çin*

How to cite this article?

Zhang X, Jian Y, Fu Y, Duo H, Guo Z: Development of a multiplex PCR assay for the simultaneous detection of *Echinococcus* spp. in wild canids in the Qinghai-Tibet Plateau area of China. *Kafkas Univ Vet Fak Derg,* 27 (6): 707-715, 2021.
DOI: 10.9775/kvfd.2021.26148

(*) Corresponding Author

Tel: +86-971-5226221
E-mail: 1984990033@qhu.edu.cn (G. Zhihong) 1995990036@qhu.edu.cn (D. Hong)

Introduction

Echinococcosis is a zoonotic disease caused by metacestodes (larval stage) of *Echinococcus* spp., which include one or more of nine species recognized in the most recent taxonomic revision of the genus *Echinococcus* [1,2]. Echinococcosis is currently a neglected zoonotic disease worldwide, resulting in great public health concerns and economic losses globally [3]. There are two *Echinococcus* spp. that seriously threaten human health, namely, *Echinococcus granulosus sensu stricto* (genotypes G1-G3) and *E. multilocularis*, which cause cystic echinococcosis (CE) and alveolar echinococcosis (AE), respectively. *E. canadensis* (G6) infections also result in CE, but *E. shiquicus*, which is the sister species of *E. multilocularis*, has not been reported to cause human echinococcosis thus far. To date, *E. multilocularis*, *E. granulosus s.s.*, *E. shiquicus* and *E. canadensis* (G6) have been reported in China, and *E. granulosus s.s.*, *E. multilocularis* and *E. shiquicus* are mainly prevalent in the QTPA [4-6]. It is estimated that cystic and alveolar echinococcosis results in the loss of 1.000.000 and 600.000 disability-adjusted life years (DALYs) each year, respectively [7,8]. In China, there are 368 endemic counties distributed in nine provinces/autonomous regions with an estimated 166.000 cases nationally [9]. Obviously, the world's highest prevalence of echinococcosis is in China; moreover, the QTPA is located in western China, has the highest prevalence of echinococcosis in the country [9]. Echinococcosis is a very serious public health problem in the QTPA, and it causes a great threat to human health and livestock economic development.

The life cycle of *Echinococcus* parasites is complex and involves two hosts: definitive hosts and intermediate hosts [5]. *E. granulosus s.s.* is generally transmitted between canids (dogs) and livestock (yak, cattle and sheep) [10-12], while *E. multilocularis* and *E. shiquicus* are mainly transmitted between canids (dogs and foxes) and small mammals (voles and pikas) [13-15]. At present, imaging examinations, immunological methods, histological detection, and microscopic observation are the main methods widely used in clinical and surgical procedures and in survey work. However, it is difficult to morphologically distinguish the adults and eggs of some *Echinococcus* tapeworms, such as *E. multilocularis* and *E. shiquicus*. With the development of molecular biology technology, many molecular identification methods have been established using parasite total DNA as target genes [16,17]. These methods can be used to distinguish the species of the *Echinococcus* tapeworms and eggs found in the fecal samples of the definitive host. However, it is also difficult to accurately identify species in the unobvious hydatid tissue samples from different intermediate hosts. Thus PCR-based molecular detection has been used for the differential diagnosis of echinococcosis.

To date, many known PCR-related approaches targeting parasite total DNA have been designed and developed to identify different stages of the *Echinococcus* life cycle in different hosts, and some of these methods are used for the identification/discrimination of single species with singular amplification [18,19]. PCR-RFLP or LAMP for species discrimination and nested-PCR, which consists of two PCR steps with higher sensitivity, are slow, laborious and costly methods, and these methods cannot meet the needs of rapid diagnosis and large-scale detection. Several mPCR methods have been developed for identifying *Echinococcus* species [18-21].

The mPCR method can simultaneously detect different target pathogens species by using multiple specific primers in one tube, which is fast; reagent-, material- and labor-saving; and cost- effective. In addition, this method can also distinguish pathogens from mixed infections with accuracy and efficiency at the same time. The mPCR method is also very suitable for large-scale multi-sample epidemiological investigations in epidemic areas, such as studies of echinococcosis in the QTPA.

In this study, we describe the development and evaluation of a simultaneous mPCR method for the detection of single and mixed infections of three *Echinococcus* species that are prevalent in the QTPA, to quickly and accurately detect and identify the *Echinococcus* species in intermediate hosts or fecal samples of definitive hosts. This study was performed to provide technology for the epidemiological investigation of *Echinococcus* spp. and to promote the effective treatment and control of echinococcosis.

Material and Methods

Parasites

The total DNA of *E. multilocularis* (Em), *E. granulosus s.s.* (Eg), *E. shiquicus* (Es), *Taenia multiceps* (Tm), *Taenia saginata* (Ts), *Taenia asiatica* (Ta), *Dipylidium caninum* (Dc), *Taenia hydatigena* (Th), *Toxocara canis* (Tc) and *Fasciola hepatica* (Fh) are stored in the zoonotic disease laboratory of the Institute of Veterinary Medicine, Qinghai Academy of Animal Sciences and Veterinary Medicine.

Primer Design

The complete sequence of the mitochondrial genomes of *E. granulosus s.s.*, *E. multilocularis* and *E. shiquicus* were compared using MEGA 5.05 software [22]. Genes with less similarity among the three species of *Echinococcus* spp. were selected as target genes, and then, the partial sequences of the selected target genes with high similarity were selected to design primers by using Primer Premier 3.0 [23]. The primers are listed in *Table 1* and synthesized by Genewiz Suzhou Biological Technology Co., Ltd. (Suzhou, China). The target genes included the NADH dehydrogenase 1 (*nad*1) gene from *E. granulosus s.s.*, the NADH dehydrogenase 5 (*nad*5) gene from *E. multilocularis*, and the NADH dehydrogenase 4 (*nad*4) gene from *E.*

Table 1. *Primer sequences used for Echinococcus spp. mPCR amplification and the expected amplicon sizes*

***Echinococcus* Species**	**Gene**	**Primer Sequence (5′→3′)**	**Product (bp)**
Echinococcus granulosus	*nad*1	*nad*1F: TTGTGTTATTAATGGCTTTGG	545
		*nad*1R: TAATAAATTAAACACTAACACCAACA	
Echinococcus multilocularis	*nad*5	*nad*5F: AGTTATTTGTCAATTTTTAGCTTT	193
		*nad*5R: ACAAAACAACGTAACCATTAAG	
Echinococcus shiquicus	*nad*4	*nad*4F: GGTTAGAGTGGGCTATAGA	354
		*nad*4R: CAACCAAAAAACTCATAAC	

shiquicus. These genes were highly conserved in these *Echinococcus* spp. *(Table 1)*.

Standard Plasmid Preparation

Three *Echinococcus* spp. recombinant plasmids were reconstructed and used as the positive controls in this study. Briefly, species-specific gene fragments were first amplified with a simplex PCR primer *(Table 1)*, and simplex PCR amplification was performed in a total of 50.0 µL, including 2.0 µL each of the forward and reverse primers (10 µmol.L), 2.0 µL of DNA template (5 ng.µL), 25.0 µL of ExTaq PCR Premix (TaKaRa, Dalian, China), and 19.0 µL of PCR grade water. The following PCR program was used: predenaturation at 98°C for 1 min, denaturation at 98°C for 10 s, annealing at 50°C for 30 s, and extension at 72°C for 40 s, for a total of 35 cycles. At end of the cycle, extension was continued at 72°C for 10 min, with a final hold at 4°C. The amplified PCR products (6.0 µL) were analyzed using agarose gel (10 g.L) containing GelStain (0.6 mg.mL) (Beijing Transgen Biotech Co. Ltd, Beijing, China) and were observed under UV light. After detection, all remaining products were purified in accordance with the EasyPure PCR Purification Kit instructions (Beijing Transgen Biotech Co. Ltd, Beijing, China). After purification, the expected PCR fragments were cloned into the pMD-19T vector (TaKaRa, Dalian, China) to obtain the recombinant plasmids. Then, the recombinant plasmids were transformed into *E. coli* DH5α competent cells (TaKaRa, Dalian, China), which were then coated onto Luria-Bertani (LB) solid plate medium containing the antibiotic ampicillin, IPTG and X-gal, and incubated at 37°C overnight. After blue-white screening, a single white colony on the transformation plate was picked, inoculated into liquid LB medium containing the antibiotic ampicillin, and cultured with constant shaking at 37°C for approximately 15 h. After PCR amplification and identification of the bacterial liquids, the positive recombinant plasmids were extracted using EasyPure Plasmid MiniPrep Kit (TransGen, Beijing China) from bacterial liquids, then the plasmids were sent to Genewiz Suzhou Biological Technology Co., Ltd. for sequencing. The identified recombinant plasmids were named pMD19-Eg, pMD19-Em and pMD19-Es. The concentration of the recombinant plasmids was determined by NanoDrop-1000 (Thermo Fisher NanoDrop,USA), and then, the plasmid copy number was calculated.

Simplex and mPCR

The mPCR primer sets, *nad*1F/R, *nad*5F/R and *nad*4F/R were individually validated to determine their specificity. Each simplex PCR condition and program was performed as described above. After completion of PCR amplification, 10 µL of PCR product was electrophoresed on a 1.5% agarose gel containing 0.6 mg.mL GelStain (TransGen, Beijing China) in Tris–acetate-EDTA (TAE) buffer at 120 V for 35 min, and the gel was visualized under UV light.

Optimized mPCR was performed in a final volume of 35 µL containing 24.6 µL ExTaq PCR Premix (TaKaRa, Dalian, China), (0.4-1.2) µL each of the forward *(nad*1/4/5F) and reverse *(nad*1/4/5R) (10 µmol/L) primers, 3.0 µL of DNA plasmids, and 2.0 µL of dNTP (10 mmol/L (each)). The reaction conditions included an initial denaturation step at 98°C for 1 min, followed by 35 cycles of denaturation at 98°C for 10 s, primer annealing at varied temperature (47.1°C-59.1°C) for 40 s, and extension at 72°C for 40 s. A final extension at 72°C for 10 min was performed. Then, 10 µL of the PCR product was analyzed by gel electrophoresis on a 1.5% agarose gel, as described above. For multiplex primer concentration optimization, 9 sets of different primer concentrations were tested. For annealing temperature optimization, 8 gradients were used to identify the optimal reaction conditions for mPCR. The optimal primer concentrations and annealing temperatures for mPCR were determined based on obvious target bands, few primer dimers, and no nonspecific amplified bands.

Specificity of Simplex and mPCR

The specificity of simplex and mPCR was tested using other common canine parasites (including *T. multiceps*, *T. saginata*, *T. asiatica*, *D. caninum*, *T. hydatigena*, *T. canis* and *F. hepatica*). The total DNA of non targeted parasites was used as a template for mPCR amplification. The amplified products were detected by agarose gel electrophoresis to evaluate and verify the specificity of the mPCR method constructed in this study.

Sensitivity of mPCR

To determine the detection limit of the mPCR, the pMD19-Eg, pMD19-Em and pMD19-Es plasmids were used to create ten individual series of 10-fold dilutions from 1×10^9

copies/μL to 1×10^0 copies/μL. In addition, these three species of mixed plasmids were also diluted by 10-fold gradient dilutions to evaluate the sensitivity of the mPCR assays in amplifying genes from samples containing mixed plasmid DNA templates. The mPCR was performed using the optimized conditions described above.

Simulated Coinfection Samples and Field Samples Detection

Fecal samples from dogs that had been verified as positive or negative by simplex PCR were used as positive or negative samples [20]. Total DNA of *Echinococcus* spp. mixed with negative dog feces was used to create clinical samples to evaluate and verify the practicability of the mPCR method established in this study. The field samples (35 fox fecal samples) were collected in Yushu county and were tested to evaluate the capability of the mPCR method. All the positive PCR products were directly sequenced by Genewiz Suzhou Biological Technology Co., Ltd. (Suzhou, China).

Results

Primer Design and Simplex PCR Amplification

The results of comparing the sequences of the forward and reverse primers are shown in *Fig. 1*, and the primer sequences and expected amplicon sizes are shown in *Table 1*. There are multiple different sites in the primer sequences among the *Echinococcus* spp. Based on observing the gel electrophoresis results with the gel imaging system, the three pairs of specific primers for the three species of *Echinococcus* spp. could amplify the corresponding target genes, and the sizes of the bands were consistent with the expected sizes. The expected sizes of the products for *E. granulosus s.s.*, *E. multilocularis* and *E. shiquicus* were 545 bp *(Fig. 2)*, 193 bp *(Fig. 2)* and 354 bp *(Fig. 2)*, respectively.

Identification of Recombinant Plasmids

The expected PCR products were purified by gel extraction and then cloned into the pMD-19T vector. The three recombinant plasmids were constructed correctly, which was confirmed by bacterial liquid PCR and sequencing identification *(Fig. 3)*, and the plasmids were named pMD19-Eg, pMD19-Em and pMD19-Es.

Establishment and Optimization of the mPCR Method

The volume of the multiple PCR primers (0.4-1.2 μL) and the annealing temperature (47.1-59.1°C) were optimized. Avoidance of the amplification of nonspecific bands was achieved, and amplification efficiency (bright or weak of bands) of the target bands and reduced primer dimer formation were observed. When the primer ratios for the three target genes were adjusted to optimize the concentration ratio to 1:1:1, the PCR amplification efficiency was high and there were no nonspecific bands produced, so 0.9 μL each of the forward primers and reverse primers of the three genes was used *(Fig. 4)*. The target gene plasmids of the three *Echinococcus* spp. were

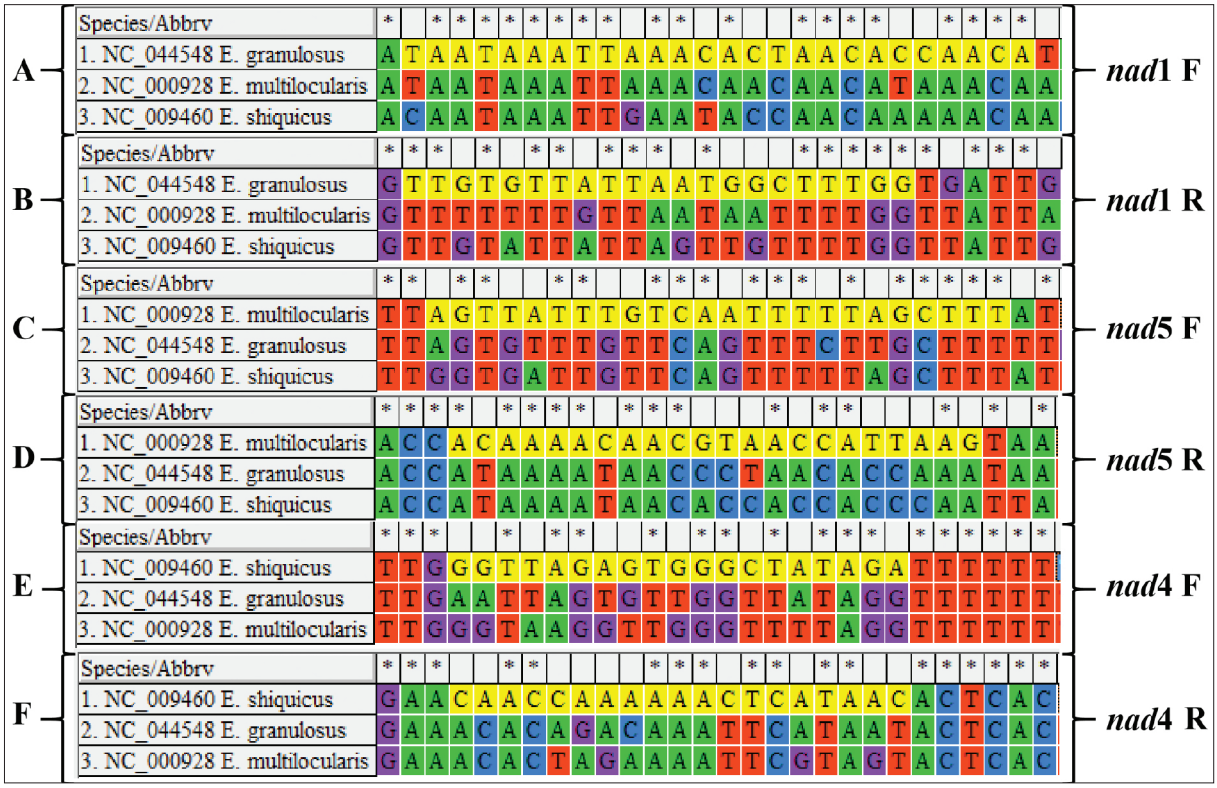

Fig 1. Sequence analysis of primers based on *Echinococcus* spp. mitochondrial target genes

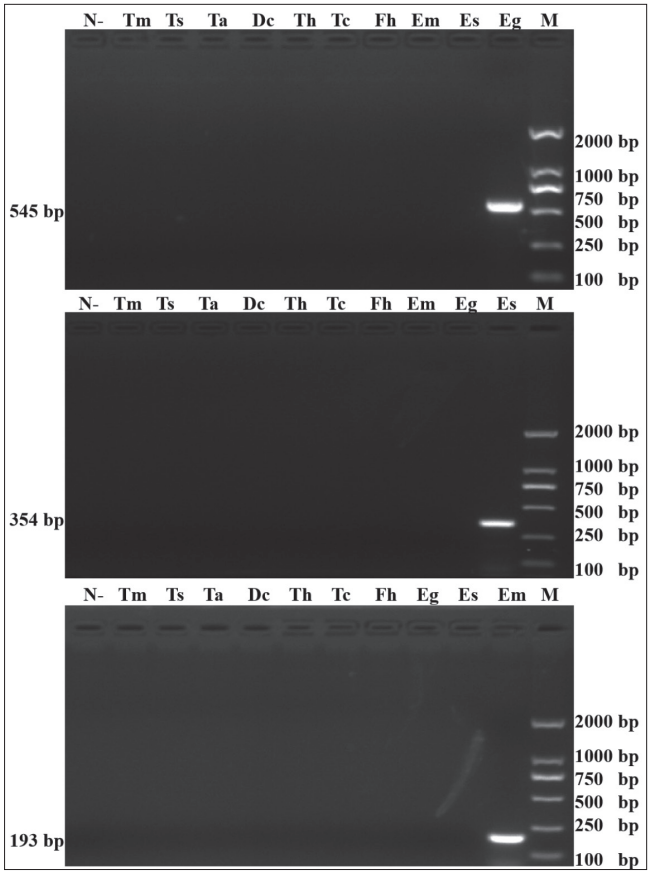

Fig 2. Simplex PCR amplification results based on *Echinococcus* spp. mitochondrial target genes. Eg: *E. granulosus s.s.*; Em: *E. multilocularis*; Es: *E. shiquicus*; Tm: *T. multiceps*; Ts: *T. saginata*; Ta: *T. asiatica*; Dc: *D. caninum*; Th: *T. hydatigena*; Tc: *T. canis*; and Fh: *F. hepatica*

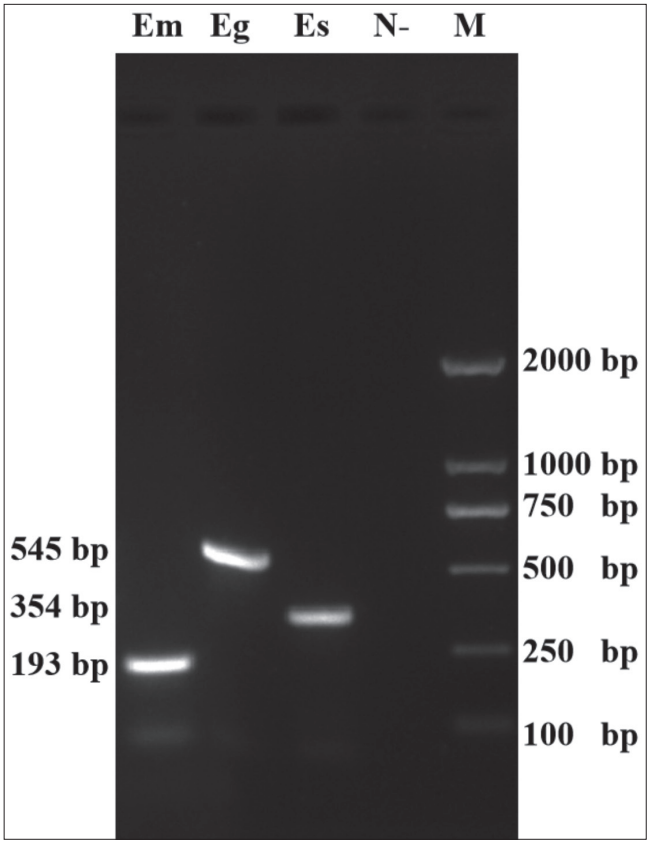

Fig 3. PCR results of the identification of the constructed plasmids of mitochondrial target genes in *Echinococcus* spp.

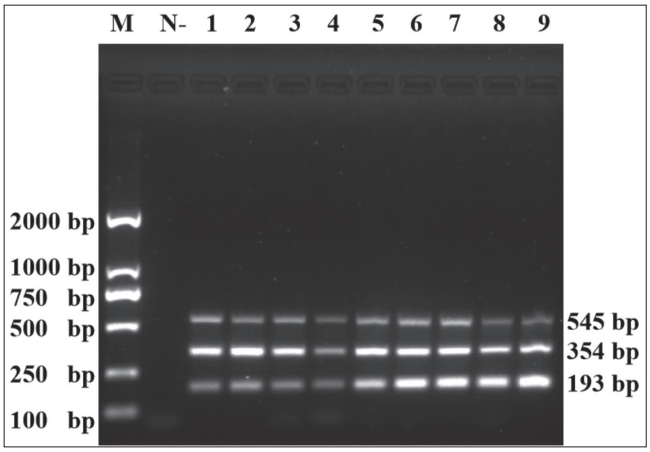

Fig 4. The results of optimization of the concentration of primers specific for *Echinococcus* spp. mitochondrial target genes. N-: Negative control, 1: 0.4 μL, 2: 0.5 μL, 3: 0.6 μL, 4: 0.7 μL, 5: 0.8 μL, 6: 0.9 μL, 7: 1.0 μL, 8: 1.1 μL, and 9: 1.2 μL; *(primer concentration: 10 μmol.L)

mixed in equal amounts as templates, and then, the annealing temperature of multiple PCR was optimized by a temperature gradient at the annealing step. The results showed that when the annealing temperature was 50°C, the amplification efficiency of the multiple PCR was the best *(Fig. 5)*. The final mPCR system included a volume of 55.0 μL. The forward and reverse primers of the three genes totalled 0.9 μL each, the templates were used at volumes of 2.0 μL each, 2×Ex Taq PCR Premix was used at a volume of 39.6 μL, and dNTP (10 mmol/L (each)) was used at a volume of 4.0 μL. The optimal reaction conditions were as follows: predenaturation at 98°C for 1 min; denaturation at 98°C for 10 s, annealing at 50°C for 50 s, and extension at 72°C for 50 s, for a total of 35 cycles; and 72°C for further extension for 10 min.

Multiple PCR Specificity Results

The total DNA of the three target parasites *(E. multilocularis*, *E. granulosus s.s.* and *E. shiquicus)* and the nontarget parasites *(T. multiceps*, *T. saginata*, *T. asiatica*, *D. caninum*, *T. hydatigena*, *T. canis* and *F. hepatica)* were used as templates. In the 55.0 μL system, only three target parasite DNA were amplified by 3 pairs of specific primers. When the three target parasite genomes were present, three corresponding target bands could be amplified *(Fig. 6*: Eg 545 bp + Em 193 bp + Es 354 bp). When only two target parasite DNA exist, only two corresponding bands could be amplified *(Fig. 6*: Eg 545 bp + Em 193 bp, Eg 545 bp+Es 354 bp, Em 193 bp+Es 354 bp). When only one target parasite DNA exist, only one corresponding target band could be amplified *(Fig. 6*: Eg 545 bp, Em 193 bp, and Es 354 bp). When nontarget parasite DNA was present, no target

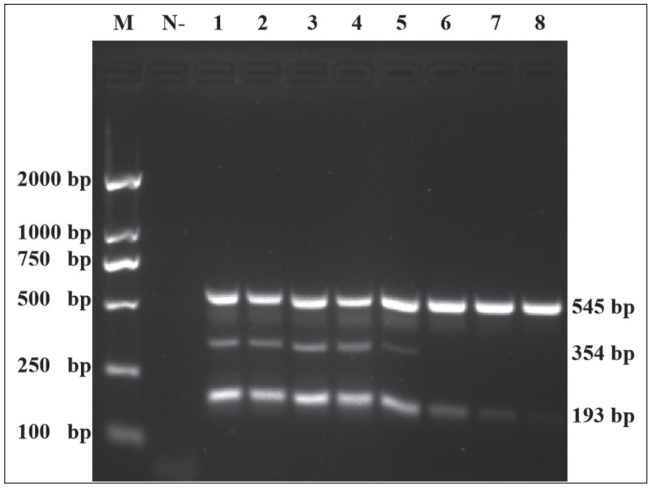

Fig 5. The results of optimization of the annealing temperature for *Echinococcus* spp. mitochondrial target genes. 1: 47.1°C, 2: 47.7°C, 3: 49.2°C, 4: 51.6°C, 5: 54.6°C, 6: 56.9°C, 7: 58.4°C, and 8: 59.1°C

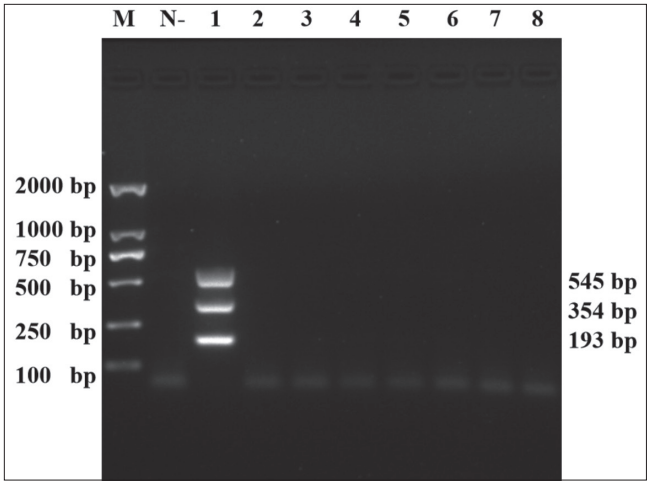

Fig 7. The results of the mPCR method for *Echinococcus* spp. species-specific detection. 1: Eg+Es+Em, 2: Tm, 3: Ts, 4: Ta, 5: Dc, 6: Th, 7: Tc, and 8: Fh

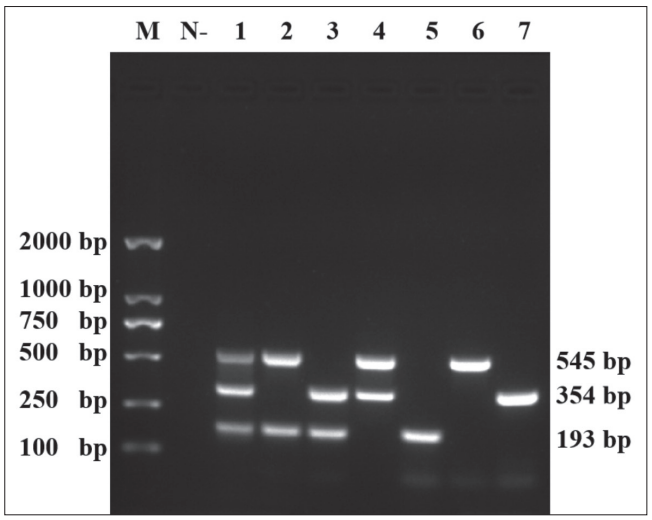

Fig 6. The results of the mPCR method for *Echinococcus* spp. intraspecies-specific detection. N-: Negative control, 1: Eg+Es+Em, 2: Eg+Em, 3: Es+Em, 4: Eg+Es, 5: Em, 6: Eg, and 7: Es

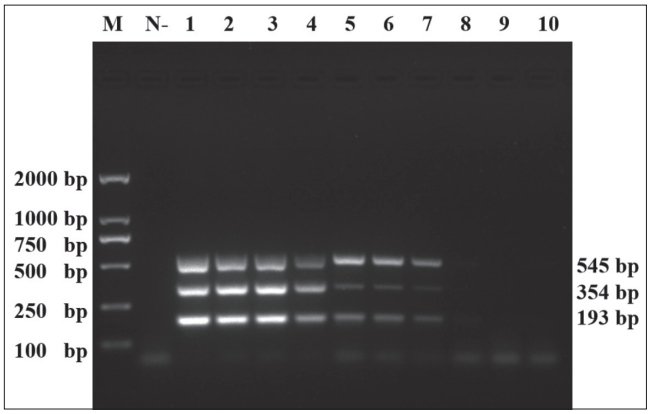

Fig 8. The sensitivity results of the mPCR method for *Echinococcus* spp. N-: Negative control, and 1-10: 1×10^{9} ~ 1×10^{0} copies.μL

fragments were amplified, and the result was negative *(Fig. 7)*. The same results were obtained, when the experiment was repeated 3 times, which indicated that the multiplex established a PCR method with good specificity and reproducibility.

Multiple PCR Sensitivity Results

The three *Echinococcus* spp. target gene plasmids pMD19-Eg, pMD19-Em and pMD19-Es, were diluted to produce 10 gradient dilutions between 1×10^{0}~1×10^{9} copies/μL. Each gradient dilution of the three target gene plasmids was mixed in equal amounts to prepare the DNA templates. The sensitivity of the established multiple PCR was analyzed. As shown in *Fig. 8*, when the three DNA templates were mixed, the detection limit of each parasite was 1 $\times10^{3}$copies/μL.

Simulated Clinical Samples and Field Samples Detection

As shown in *Fig. 9*, we simulated triplex, duplex and simplex infections of different combinations of *Echinococcus* spp. at the same concentration. In total, 15 simulated clinical samples were examined using the developed multiple PCR method and simplex PCR with the same primers. The result showed that 11 samples were *Echinococcus* spp.-positive, including 1 triple positive sample with Eg + Em + Es, 4 double positive samples with Eg + Em (2), Eg + Es (1) and Em + Es (1), 6 simplex positive samples with Eg (2), Em (2) and Es (2), and 4 negative samples. The results of the multiple PCR method were consistent with those of the simplex PCR method. For the field samples, 35 fox fecal samples were also detected using the triplex/simplex PCR methods. Only one fox fecal samples was detected as *E. multilocularis* by both methods. All the PCR products were directly sequenced in both directions, and the sequence analysis results confirmed the species of *Echinococcus* again. It was indicated that the mPCR method established in this study can be used for clinical samples detection.

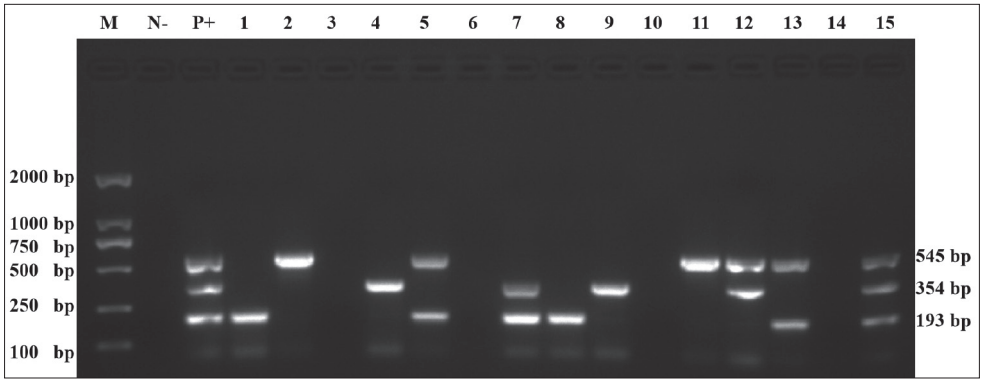

Fig 9. The results of the mPCR method for detecting simulated clinical samples. N-: Negative control, P+: Positive control, 1: Em, 2: Eg, 3: Negative, 4: Es, 5: Eg+Em, 6: Negative, 7: Es+ Em, 8: Em, 9: Eg, 10: Negative, 11: Eg, 12: Eg+Es, 13: Eg+Em, 14: Negative, and 15: Eg+Es+Em

Discussion

Echinococcosis has been one of the great public health threats in northwest China, especially, in the QTPA. This area is now the most severe pandemic region for CE in humans and livestock, which is caused mainly by *E. granulosus s.s.*, and AE in humans and small wild mammals, which is caused by *E. multilocularis* [24-26]. *E. canadensis* also causes CE in humans and livestock, but *E. shiquicus* has not been validated to infect humans and cause echinococcosis in endemic areas [27,28]. It is reported that few cases of *E. canadensis* are found in the QTPA, indicating a low prevalence of this species in this area [27]. *E. granulosus s.s.*, *E. multilocularis* and *E. shiquicus* are mainly prevalent in intermediate hosts or fecal samples of definitive hosts in the QTPA [25]. The pathogenic factors causing the spread of echinococcosis in this area are quite complicated [29,30]. In fact, double infections with different species of *Echinococcus* in animal hosts have been reported [31]. Because of the close relationship between dogs and humans, humans are very susceptible to infection. In the QTPA of China, an increasingly large number of human AE and CE cases originating from infected dogs occur, causing a heavy burden on public health and veterinary services [20]. Therefore, it is necessary to develop an accurate, rapid and effective method for the simultaneous detection and identification of different life stages of the three *Echinococcus* spp. Moreover, the method will be beneficial for the monitoring, management, diagnosis and prevention of echinococcosis. It is essential to develop such a needed method for clinical and epidemiological investigations.

The mPCR is a method that can detect multiple target species by using multiple pairs of primers in a simplex reaction tube. Since this method was first described in 1988, it has been successfully applied for the identification of pathogenic bacteria, viruses, fungi and parasites [32,33]. Primer design is the key factor for the successful establishment of an mPCR method. As is known, the conventional primer design of simplex PCR is very simple. The design of mPCR primers is more complicated and difficult, because it is not a simple combination of several simplex PCR primers. When multiple pairs of primers are mixed in one reaction tube, the primers may be randomly paired in the mixture to form a new reaction system, making the process much more complicated than a simplex reaction. The design of mPCR primers needs to overcome many difficulties, including low sensitivity and specificity, different annealing temperatures of different primers, and easy formation of primer dimers [32,34]. At present, there are no software programs or methods to predict the performance of the multiple primers; thus, there are only empirical experiments and trial-and-error approaches.

Methods for recovering eggs and morphological identification are usually used in traditional tapeworm epidemiological surveys. However, it is impossible to morphologically identify the eggs of *Echinococcus*, which has prompted the development of several molecular detection methods [17,35]. When the mPCR method is used to determine the pathogens in the host, the advantages of the mPCR method become obvious.

An mPCR method for detecting and distinguishing *E. multilocularis*, *E. granulosus s.s.* and *E. shiquicus* was successfully developed in this study. This method can pair well with simplex or mixed target template DNA to amplify and produce the expected specific amplicons, which are highly consistent with their target *Echinococcus* species. There was a high degree of species specificity in testing the cross-reactivity of the assay, and there were no amplicons from any other worms or negative samples (no DNA). The multiple reactions of the primer sets (three pairs of primers) worked well on all tested templates in simplex reaction tubes, and for the three tested *Echinococcus* tapeworms, specific amplicons of the expected length were produced.

In the recent taxonomic revision, *Echinococcus* spp. was divided into nine species, including *E. felidis*, *E. equinus*, *E. oligarthra*, *E. vogeli*, *E. ortleppi*, *E. canadensis*, *E. granulosus s.s.*, *E. multilocularis* and *E. shiquicus* [2]. DNA samples from the first five species of *Echinococcus* are not available because they are not found anywhere in China. Nevertheless, to minimize the possibility of nonspecific amplicons from these closely related species, the target sequences of the first six species were compared with the primer targeted sequences of the three target species, and the

results showed that there are 4-10 base pair differences between these species. Only one sequence (R) had only 2 base pair differences, and the L sequence had only 5 base pair differences (in *E. equinus)*. This result is the same as that observed in research by Liu, in which there were 6-11 base pair differences between these species, and due to such large differences, it is extremely unlikely that any amplicons would be generated from these 5 species in the mPCR detection method [20]. Therefore, due to its high species specificity, it is extremely unlikely that any amplicons would be produced from these species during mPCR.

Previous studies have shown that compared with simplex PCR, mPCR has lower sensitivity [16,36]. The designed method proved to be similarly sensitive in this study, with detection thresholds as low as 0.2 -1 pg for *E. multilocularis*, *E. granulosus s.s.* and *E. shiquicus* (plasmid conversions). The detection limit is lower than the detection limit of 0.32-1.6 pg *(E. granulosus* s. s. and *E. multilocularis)* [37] and is the same as the detection limit of mPCR reported by Liu [20] (0.1-5 ng and 10-20 pg, respectively). According to the report, each parasite egg contains approximately 8 pg of nuclear DNA [38], and it is reported that at least 15 eggs can produce a positive result [21]. Thus, when the detection method is used to detect *Echinococcus* spp. in canid feces, its sensitivity may not be good enough, especially in mixed infections. To avoid false-negative results caused by low-level infections, it is recommended to expand the detection volume to accurately detect the infection of parasitic pathogens. Due to the lack of such mixed-infection samples, none of the fecal materials showed coinfection phenomenon, but the results of the plasmid DNA fully proved that the detection method developed in this research can effectively detect double and/or triple mixed infections of the target species.

For all cyst samples previously confirmed by gene sequencing, genotyping can be successfully confirmed by mPCR. In addition, no amplicons were observed in any of the samples of fox feces and dog feces that have been identified, which indicates that host DNA does not interfere with this method. Actually, due to there were only two human echinococcosis cases infected with *E. canadensis* in China, compared with the other three *Echinococcus* tapeworms involved in the method, *E. canadensis* is almost not prevalent in the QTPA, so *E. canadensis* is not the main detection target of the detection method. If necessary, the method can be further improved by adding a pair of specific primers for *E. canadensis*, for the establishment of a four-fold PCR detection method for the ecological and biological research of *Echinococcus* species.

The established mPCR method that could simultaneously, quickly and accurately determine *E. granulosus s.s.*, *E. multilocularis* and *E. shiquicus* in this study. It has high potential for application and may greatly assist in the diagnosis of canine-derived stool samples on the QTPA. In addition, due to its reliability and accuracy, the method can be used as a useful tool for evaluation, supplementing the results of serological testing and further improving the accuracy of animal-derived stool samples. This method has potential application in rapid detection and broad-scale screening, and it is expected to become a useful technology for clinical diagnosis and environmental samples monitoring.

Availability of Data and Materials

The datasets during and/or analyzed during the current study available from the corresponding author on reasonable request.

Funding

This study was supported by the National Natural Science Foundation of China (No. 31860700), the Basic Scientific Independent Research Project of Qinghai Academy of Animal Science and Veterinary Medicine (MKY-2019-10), the State Key Laboratory of Veterinary Etiological Biology, Lanzhou Veterinary Research Institute, Chinese Academy of Agricultural Sciences (SKLVEB2020KFKT004) and the Applied Basic Research of Qinghai Province (2021-ZJ-724).

Acknowledgment

The authors thank all of the veterinarians for aiding in sample collection.

Conflict of Interest

The authors declare no conflict of interest.

Author Contributions

X. ZHANG and Y. JIAN designed and performed experiments, analyzed results, wrote and reviewed the manuscript. Y. FU, Z. GUO and H. DUO provided advice, reviewed and edited the manuscript.

References

1. Deplazes P, Rinaldi L, Alvarez Rojas CA, Torgerson PR, Harandi MF, Romig T, Antolova D, Schurer JM, Lahmar S, Cringoli G, Magambo J, Thompson RC, Jenkins EJ: Global distribution of alveolar and cystic Echinococcosis. *Adv Parasitol*, 95, 315-493, 2017. DOI: 10.1016/bs.apar.2016.11.001

2. Nakao M, Lavikainen A, Yanagida T, Ito A: Phylogenetic systematics of the genus *Echinococcus* (Cestoda: Taeniidae). *Int J Parasitol*, 43 (12-13): 1017-1029, 2013. DOI: 10.1016/j.ijpara.2013.06.002

3. Kern P, Menezes da Silva A, Akhan O, Mullhaupt B, Vizcaychipi KA, Budke C, Vuitton DA: The Echinococcoses: Diagnosis, clinical management and burden of disease. *Adv Parasitol*, 96, 259-369, 2017. DOI: 10.1016/bs.apar.2016.09.006

4. Boufana B, Qiu J, Chen X, Budke CM, Campos-Ponce M, Craig PS: First report of *Echinococcus shiquicus* in dogs from eastern Qinghai-Tibet plateau region, China. *Acta Trop*, 127 (1): 21-24, 2013. DOI: 10.1016/j.actatropica.2013.02.019

5. Z Wang, Wang X, Liu X: Echinococcosis in China: A review of the epidemiology of *Echinococcus* spp. *Ecohealth*, 5 (2): 115-126, 2008. DOI: 10.1007/s10393-008-0174-0

6. Zhang LH, Chai JJ, Jiao W, Osman Y, McManus DP: Mitochondrial genomic markers confirm the presence of the camel strain (G6 genotype) of *Echinococcus granulosus* in north-western China. *Parasitology*, 116, 29-33, 1998. DOI: 10.1017/s0031182097001881

7. Budke CM, Deplazes P, Torgerson PR: Global socioeconomic impact of cystic echinococcosis. *Emerg Infect Dis*, 12 (2): 296-303, 2006. DOI: 10.3201/eid1202.050499

8. Torgerson PR, Keller K, Magnotta M, Ragland N: The global burden of alveolar echinococcosis. *PLoS Negl Trop Dis*, 4 (6): e722, 2010. DOI: 10.1371/journal.pntd.0000722

9. Wu WP, Wang H, Wang Q, Zhou XN, Wang LY, Zheng CJ, Cao JP, Xiao N, Wang N, Zhu YY, Niu YL, Xue CZ, Zeng XM, Fang Q, Han S, Yu Q, Yang SJ, Fu Qing, Bai XF, Tian T, Li JJ, Zhang MY, Wu WT, Zhang SS, Hou YY, Feng Y, Ma X, Li B, Li FK, Guo WD, Yang YM, Wu XL, Jin XL, Zhang HW, Yu SC: A nationwide sampling survey on echinococcosis in China during 2012-2016. *Chin J Parasitol Parasit Dis*, 36, 1-14, 2018.

10. Deplazes P, Alther P, Tanner I, Thompson RC, Eckert J: *Echinococcus multilocularis* coproantigen detection by enzyme-linked immunosorbent assay in fox, dog, and cat populations. *J Parasitol*, 85 (1): 115-121, 1999. DOI: 10.2307/3285713

11. Sobrino R, Gonzalez LM, Vicente J, Fernandez de Luco D, Garate T, Gortazar C: *Echinococcus granulosus* (Cestoda, Taeniidae) in the Iberian wolf. *Parasitol Res*, 99 (6): 753-756, 2006. DOI: 10.1007/s00436-006-0229-5

12. Li X, Jiang S, Wang X, Hui W, Jia B: iTRAQ-based comparative proteomic analysis in different developmental stages of *Echinococcus granulosus*. *Parasite*, 28:15, 2021. DOI: 10.1051/parasite/2021012

13. Guislain MH, Raoul F, Poulle ML, Giraudoux P: Fox faeces and vole distribution on a local range: Ecological data in a parasitological perspective for *Echinococcus multilocularis*. *Parasite*, 14 (4): 299-308, 2007. DOI: 10.1051/parasite/2007144299

14. Hajialilo E, Harandi MF, Sharbatkhori M, Mirhendi H, Rostami S: Genetic characterization of *Echinococcus granulosus* in camels, cattle and sheep from the south-east of Iran indicates the presence of the G3 genotype. *J Helminthol*, 86 (3): 263-270, 2012. DOI: 10.1017/S0022149X11000320

15. Zhu GQ, Yan HB, Li L, Ohiolei JA, Wu YT, Li WH, Zhang NZ, Fu BQ, Jia WZ: First report on the phylogenetic relationship, genetic variation of *Echinococcus shiquicus* isolates in Tibet Autonomous Region, China. *Parasit Vectors*, 13 (1): 590, 2020. DOI: 10.1186/s13071-020-04456-w

16. Boufana B, Umhang G, Qiu J, Chen X, Lahmar S, Boue F, Jenkins D, Craig P: Development of three PCR assays for the differentiation between *Echinococcus shiquicus*, *E. granulosus* (G1 genotype), and *E. multilocularis* DNA in the co-endemic region of Qinghai-Tibet plateau, China. *Am J Trop Med Hyg*, 88 (4): 795-802, 2013. DOI: 10.4269/ajtmh.12-0331

17. Mathis A, Deplazes P: Copro-DNA tests for diagnosis of animal taeniid cestodes. *Parasitol Int*, 55, S87-S90, 2006. DOI: 10.1016/j.parint.2005.11.012

18. Roelfsema JH, Nozari N, Pinelli E, Kortbeek LM: Novel PCRs for differential diagnosis of cestodes. *Exp Parasitol*, 161, 20-26, 2016. DOI: 10.1016/j.exppara.2015.12.010

19. Trachsel D, Deplazes P, Mathis A: Identification of taeniid eggs in the faeces from carnivores based on multiplex PCR using targets in mitochondrial DNA. *Parasitology*, 134 (6): 911-920, 2007. DOI: 10.1017/S0031182007002235

20. Liu CN, Lou ZZ, Li L, Yan HB, Blair D, Lei MT, Cai JZ, Fan YL, Li JQ, Fu BQ, Yang YR, McManus DP, Jia WZ: Discrimination between *E. granulosus sensu stricto*, *E. multilocularis* and *E. shiquicus* Using a Multiplex PCR Assay. *PLoS Negl Trop Dis*, 9 (9): e0004084, 2015. DOI: 10.1371/journal.pntd.0004084

21. Shang JY, Zhang GJ, Liao S, Huang Y, Yu WJ, He W, Yang GY, Li TY, Chen XW, Zhong B, Wang Q, Wang Q, Li RR, Wang H: A multiplex PCR for differential detection of *Echinococcus granulosus sensu stricto*, *Echinococcus multilocularis* and *Echinococcus canadensis* in China. *Infect Dis Poverty*, 8:68, 2019. DOI: 10.1186/s40249-019-0580-2

22. Tamura K, Peterson D, Peterson N, Stecher G, Nei M, Kumar S: MEGA5: Molecular evolutionary genetics analysis using maximum likelihood, evolutionary distance, and maximum parsimony methods. *Mol Biol Evol*, 28 (10): 2731-2739, 2011. DOI: 10.1093/molbev/msr121

23. Untergasser A, Cutcutache I, Koressaar T, Ye J, Faircloth BC, Remm M, Rozen SG: Primer3-new capabilities and interfaces. *Nucleic Acids Res*, 40 (15): e115, 2012. DOI: 10.1093/nar/gks596

24. Shang J, Zhang G, Yu W, He W, Wang Q, Zhong B, Wang Q, Liao S, Li R, Chen F, Huang Y: Molecular characterization of human echinococcosis in Sichuan, Western China. *Acta Trop*, 190, 45-51, 2019. DOI: 10.1016/j.actatropica.2018.09.019

25. Ma J, Wang H, Lin G, Zhao F, Li C, Zhang T, Ma X, Zhang Y, Hou Z, Cai H, Liu P, Wang Y: Surveillance of *Echinococcus* isolates from Qinghai, China. *Vet Parasitol*, 207 (1-2): 44-48, 2015. DOI: 10.1016/j.vetpar.2014.11.012

26. Li T, Ito A, Nakaya K, Qiu J, Nakao M, Zhen R, Xiao N, Chen X, Giraudoux P, Craig PS: Species identification of human echinococcosis using histopathology and genotyping in northwestern China. *Trans R Soc Trop Med Hyg*, 102 (6): 585-590, 2008. DOI: 10.1016/j.trstmh.2008.02.019

27. Wu Y, Li L, Zhu G, Li W, Zhang N, Li S, Yao G, Tian W, Fu B, Yin H, Zhu X, Yan H, Jia W: Mitochondrial genome data confirm that yaks can serve as the intermediate host of *Echinococcus canadensis* (G10) on the Tibetan Plateau. *Parasit Vectors*, 11 (1): 166, 2018. DOI: 10.1186/s13071-018-2684-0

28. Xiao N, Qiu J, Nakao M, Li T, Yang W, Chen X, Schantz PM, Craig PS, Ito A: *Echinococcus shiquicus*, a new species from the Qinghai-Tibet plateau region of China: Discovery and epidemiological implications. *Parasitol Int*, 55, S233-S236, 2006. DOI: 10.1016/j.parint.2005.11.035

29. Wang Q, Zhao S, A J, Guo Y, Yang J, Naveed A, Gao W: Co-occurrence of cystic and alveolar echinococcosis in the liver: A Case Report. *Iran J Parasitol*, 16 (1): 168-172, 2021. DOI: 10.18502/ijpa.v16i1.5539

30. Xu X, Gao C, Ye H, Wang Z, Wang Z, Zhou Y, Wang H, Zhang B, Pang M, Zhou H, Pan S, Zhao M, Fan H: Diagnosis and treatment of a case of hepatic mixed echinococcosis infection combined with distant organ metastasis. *J Int Med Res*, 48 (2): 1-9, 2020. DOI: 10.1177/0300060519851651

31. Xiao N, Nakao M, Qiu J, Budke CM, Giraudoux P, Craig PS, Ito A: Dual infection of animal hosts with different *Echinococcus* species in the eastern Qinghai-Tibet plateau region of China. *Am J Trop Med Hyg*, 75 (2): 292-294, 2006. DOI: 10.4269/ajtmh.2006.75.292

32. Elnifro EM, Ashshi AM, Cooper RJ, Klapper PE: Multiplex PCR: optimization and application in diagnostic virology. *Clin Microbiol Rev*, 13 (4): 559-570, 2000. DOI: 10.1128/cmr.13.4.559-570.2000

33. Henegariu O, Heerema NA, Dlouhy SR, Vance GH, Vogt PH: Multiplex PCR: Critical parameters and step-by-step protocol. *Biotechniques*, 23 (3): 504-511, 1997. DOI: 10.2144/97233rr01

34. Wieland HA, Hamilton BS, Krist B: Hammerhead ribozymes that selectively cleave the NPY Y1, Y4, and Y5 receptor full-length RNA. *Antisense Nucleic Acid Drug Dev*, 8 (5): 435-440, 1998. DOI: 10.1089/oli.1.1998.8.435

35. Deplazes P, Dinkel A, Mathis A: Molecular tools for studies on the transmission biology of *Echinococcus multilocularis*. *Parasitology*, 127, S53-S61, 2003. DOI: 10.1017/s0031182003003500

36. Bharathi MJ, Murugan N, Rameshkumar G, Ramakrishnan R, Venugopal Reddy YC, Shivkumar C, Ramesh S: Comparative evaluation of uniplex, nested, semi-nested, multiplex and nested multiplex PCR methods in the identification of microbial etiology of clinically suspected infectious endophthalmitis. *Curr Eye Res*, 38 (5): 550-562, 2013. DOI: 10.3109/02713683.2013.772205

37. Chen F, Liu L, He Q, Huang Y, Wang W, Zhou G, Yu W, He W, Wang Q, Zhang G, Liao S, Li R, Yang L, Yao R, Wang Q, Zhong B: A multiplex PCR for the identification of *Echinococcus multilocularis*, *E. granulosus sensu stricto* and *E. canadensis* that infect human. *Parasitology*, 146 (12): 1595-1601, 2019. DOI: 10.1017/S0031182019000921

38. Gottstein B, Mowatt MR: Sequencing and characterization of an *Echinococcus multilocularis* DNA probe and its use in the polymerase chain reaction. *Mol Biochem Parasitol*, 44 (2): 183-193, 1991. DOI: 10.1016/0166-6851(91)90004-P

Kafkas Universitesi Veteriner Fakultesi Dergisi
ISSN: 1300-6045 e-ISSN: 1309-2251
Journal Home-Page: http://vetdergikafkas.org

Kafkas Univ Vet Fak Derg
27 (6): 717-723, 2021
DOI: 10.9775/kvfd.2021.26163

RESEARCH ARTICLE

Exposure to Aqueous-Alcoholic Extract of Parsley Leaves *(Petroselinum crispum)* in Lead-Treated Rats Alleviate Liver Damage

Fatemeh BASTAMPOOR [1,a] Seyed Ebrahim HOSSEINI [2,b (*)] Mehrdad SHARIATI [3,c] Mokhtar MOKHTARI [4,d]

[1] Department of Biology, Kazerun Branch, Islamic Azad University, Kazerun, IRAN
[2] Department of Biology, Faculty of Sciences, Zand Institute of Higher Education, Shiraz, IRAN
[3] Department of Biology, Kazerun Branch, Islamic Azad University, Kazerun, IRAN
[4] Department of Biology, Kazerun Branchh, Islamic Azad University, Kazerun, IRAN
ORCIDs: [a] 0000-0002-4366-817X; [b] 0000-0003-0548-0114; [c] 0000-0001-7360-0208; [d] 0000-0002-9051-6590

Article ID: KVFD-2021-26163 Received: 21.06.2021 Accepted: 05.10.2021 Published Online: 06.10.2021

Abstract

Lead (Pb) poisoning and the induced potential of the lesion is a global concern with harmful effects on multiple body systems, particularly the liver system. In this study, we have investigated the efficacy of aqueous-alcoholic extract of parsley leaves (PAE), which is a component of flavonoids that could play an important role in the antioxidant property, in preventing liver Pb-damages. For this, sixty adult male rats were randomly divided into six groups in a factorial arrangement: control; receiving oral gavage for 21 days with 2 mL water; 500 ppm Pb; 100 and 200 mg/kg PAE in combination form with Pb, and 200 mg/kg PAE. Liver enzymes and oxidative stress indexes were computed for liver stress, in blood serum. Apoptosis levels were assessed in the evaluation of liver gene expression. Data indicated that Pb reduced liver weight and feed intake. The results showed that Pb significantly increased the liver enzymes contents in the blood serum in the comparison vehicle group. Furthermore, the MDA contents of the Pb group rats were significantly more than that of the vehicle group. Likewise, T-AOC and the activities of CAT and SOD were significantly reduced. Meanwhile, Pb administration induced liver apoptosis-related genes by upregulating Bax and TNF-α genes and downregulating the Bcl-2 gene of animals. At the same time, administration of PAE significantly improved liver oxidative and apoptosis changes. Thus, this study provides a novel mechanistic approach concerning Pb-induced toxicity, due to PAE antioxidant activity.

Keywords: *Lead, Stress, Liver, Apoptosis, Parsley leaves*

Kurşun Toksikasyonu Oluşturulan Ratlarda Maydanoz Yapraklarının *(Petroselinum crispum)* Sulu-Alkollü Ekstraktı Karaciğer Hasarını Hafifletir

Öz

Kurşun (Pb) zehirlenmesi ve indüklenen lezyonun potansiyeli, başta karaciğer olmak üzere vücudun diğer birçok sistemi üzerine zararlı etkileri olan küresel bir endişedir. Bu çalışmada, antioksidan özelliğinde önemli bir rol oynayabilecek flavonoidlerin bir bileşenini içeren maydanoz yapraklarının (PAE) sulu-alkollü ekstraktının, kurşun tarafından indüklenen karaciğer hasarını önlemedeki etkinliğini araştırdık. Bunun için altmış yetişkin erkek rat, faktöriyel bir düzenle; kontrol grubu; 2 mL su ile 21 gün boyunca oral gavaj yapılan sham grubu; 500 ppm kurşun uygulanan grup; kurşun ile kombine halde 100 mg/kg ve 200 mg/kg PAE uygulanan gruplar ve 200 mg/kg PAE uygulanan grup olmak üzere rastgele altı gruba ayrıldı. Kan serumlarında karaciğer stresi için karaciğer enzimleri ve oksidatif stres indeksleri hesaplandı. Karaciğer gen ekspresyonunun değerlendirilmesinde apoptoz seviyeleri ölçüldü. Veriler, kurşun uygulamasının karaciğer ağırlığını ve yem alımını azalttığını gösterdi. Kontrol grubu ile karşılaştırıldığında kurşun uygulanan grubun kan serumundaki karaciğer enzimlerinin içeriğinin önemli ölçüde arttığı saptandı. Ayrıca, kurşun uygulanan gruba ait ratların MDA içerikleri, kontrol grubundan önemli ölçüde daha fazlaydı. Benzer şekilde, T-AOC ve CAT ve SOD aktiviteleri önemli ölçüde azalmıştı. Aynı zamanda, kurşun uygulaması, ratlarda Bax ve TNF-α gen ekspresyonlarını artırıp Bcl-2 gen ekspresyonunu azaltarak karaciğer apoptozisi ile ilgili genleri indükledi. Bununla beraber, PAE uygulaması, karaciğerin oksidatif ve apoptozis değişikliklerini önemli ölçüde iyileştirdi. Bu nedenle, PAE'nın antioksidan aktivitesiyle bu çalışma, kurşun kaynaklı toksisitede yeni bir mekanistik yaklaşım sağlamaktadır.

Anahtar sözcükler: *Kurşun, Stres, Karaciğer, Apoptozis, Maydanoz yaprağı*

How to cite this article?

Bastampoor F, Hosseini SE, Shariati M, Mokhtari M: Exposure to aqueous-alcoholic extract of parsley leaves *(Petroselinum crispum)* in lead-treated rats alleviate liver damage. *Kafkas Univ Vet Fak Derg,* 27 (6): 717-723, 2021.
DOI: 10.9775/kvfd.2021.26163

(*) Corresponding Author

Tel: +98 713 6392346; Fax: +98 713 6392346
E-mail: ebrahim.hossini@yahoo.com (S.E. Rahimi)

Introduction

Millions of people are exposed to environmental contaminants via drinking water, which contaminates soil, air, as well as fish, and other sea organisms living in contaminated waters. Human activities, particularly mining of metallic ores, is an important reason of environmental contamination. Lead (molecular formula: Pb, molecular weight: 207 g/mol) is a one of the most important common environmental contaminants that is widely distributed all around the world. It is also known as the most abundant heavy metals in the Earth's crust [1]. In new reports of WHO, as of August 19, 2019, there is no level of exposure to Pb that is known to be without harmful effects. Thus, its cumulative toxicant that affects multiple body systems, particularly liver organs.

The liver performs many physiological processes essential for good health. These include macronutrient metabolism, immune system support, blood volume regulation, endocrine control of growth signaling pathways, and the breakdown of xenobiotic compounds, including many current drugs [2,3]. Some reports have pointed out that the Pb causes varying degrees of toxicities in liver system of organisms such as humans [4-7], poultry animals [8,9], and carp [10].

There is an increasing interest in this topic (medicinal herbs), due to the overall indicators of health decrease in industrialized countries, but there is still much to know concerning the effect of environmental pollutants on the liver system. In folk medicine, *Petroselinum crispum*, parsley, is used to treat a wide variety of conditions [11]. It is thought that the health promoting effect (antibacterial and antioxidant activity) of parsley may be due to its phenolic compounds [12]. Further, Kamal et al.[13] reported that the parsley showed a significant decrease in the blood serum activity of liver enzymes. This result indicated that parsley had able to regenerate liver system after liver cell damage in diabetes mellitus as it contains flavonoids, particularly the quercetin. In a study by Soliman et al.[14], performed on rats, dexametasone exposure increased oxidative stress indices, while parsley extracts succeeded to modulate these observed abnormalities as indicated by the reduction of glucose, cholesterol, liver thiobarbituric acid, liver enzymes and the pronounced improvement of the investigated biochemical and antioxidant parameters. Since studies on the rat model and including Pb and liver quality data are lacking, the present study was designed to investigate the effect of antioxidant content of parsley leaves on the recovery of liver damages in Pb toxicity in a rat model.

Material and Methods

Chemicals and Ethics

Unless otherwise indicated, all reagents were obtained from Merck (Darmstadt, Germany). The kits to evaluate liver enzymes aspartate aminotransferase (AST), alanine aminotransferase (ALT), and alkaline phosphatase (ALK), and various oxidative stress indices including malondialdehyde (MDA), superoxide dismutase (SOD), catalase (CAT), and total antioxidant capacity (T-AOC) were purchased from Nanjing Jiancheng Bioengineering Institute (China). The Animal Care and Use Committee of the Islamic Azad University (Shiraz, Iran) approved all experimental procedures of the study that were performed according to international guidelines (Permit Number: 99-02-18-44385).

Animals

Healthy adult male Wistar rats (210±25 g; 8-week-old) were purchased from the Pasteur Research Center (Karaj, Iran). Rats were kept in an air-conditioned room under 12 h light:dark cycle under standard environmental conditions (22±1°C, 52±5% humidity) with free access to tap water and commercial dry pellet diet. Rats were housed in polypropylene cages lined with pine wood husk, changed every day.

Method for Used Aqueous-Alcoholic Parsley Leaves Extraction

The method used for extraction of parsley leaves in this experiment was performed as previously described by Ozsoy-Sacan et al.[15]. Briefly, the air-dried leaves were extracted by adding sufficient ethanol in percolator device for 24 h. The extract was then filtered, and the filtrates were evaporated, using a rotary evaporator under reduced pressure to dryness. The extract was dissolved in distilled water before the administration to normal and Pb-induced animals.

Experimental Design

Sixty adult rats were divided into six groups in a factorial arrangement: control (no treatment); receiving oral gavage for 21 days with 2 mL water; 500 ppm Pb administrated as lead acetate; 100 and 200 mg/kg aqueous-alcoholic extract of parsley leaves (PAE) [16] in combination form with Pb, and 200 mg/kg PAE. One day after the last treatment, blood samples were processed for liver enzymes and oxidative stress parameters and liver tissue samples were processed for apoptosis-related genes expression. Body weight and feed consumption per animal were recorded weekly. Measurements were obtained in the fasting state.

Liver Enzymes Assay

Blood was obtained via the tail vein for the assay of AST, ALT, and ALK. The serum was separated by centrifugation (4000 rpm for 10 min), kept at -20°C and assessed by radioimmunoassay (MonobindInc kit), as recommended by the manufacturer.

Determination of Oxidative Stress Indices

The method used to detect the oxidative stress indices

levels in this experiment was performed as previously described by Jiang et al.[17]. Briefly, the levels of MDA, the enzymatic activities of SOD, and reduced CAT were measured by commercial kits, as recommended by the manufacturer. Absorbance of the supernatant was calculated at 532, 550 and 405 nm, respectively.

Firstly, 0.006 g 2,2-diphenyl-1-picryhydrazyl (DPPH) was mixed in 15 µL methanol/water solution (1:9; 380 µL (100 mM) pH 7.4 + 20 µL Sample + 400 µL DPPH). The mixture was maintained at 20°C for 30 min and the absorption rate was measured at 530 nm.

The following protocols were used to prepare the blank (1) and the method of calculating the absorption of samples:

(1): 380 µL methanol + 400 µL DPPH + 20 µL phosphate buffer

(2): Activity [% of DPPH reduction] = [(A−Ax)/A] × 100%

A = DPPH + methanol

Ax = DPPH + sample

Quantitative Real-time PCR

Total RNA was isolated from livers weighing 25-30 mg using Trizol reagent (Life Technologies, Carlsbad, CA, USA). The 2% agarose gel electrophoresis was used to assess the integrity of total RNA and the A260/280 ratio was in the range of 1.8-2.0 evaluated by NanoDrop 2000 (Thermo Fisher Scientific, Waltham, MA, USA). RNA was reverse transcribed using a PrimeScript™ RT Master Mix kit. QRT-PCR was carried out using the QuantStudio 7 Flex QRT-PCR system (Stratagene, USA) and SYBR® Premix Ex Taq™ II kit. Specific primers were designed by Invitrogen, USA *(Table 1)*. β-actin (reference gene) was used in order to normalize the expression level of target genes. Duplicated Ct values were measured for each sample, and the comparative Ct method was used to determine the relative expression level of the target genes.

Statistical Analysis

Statistical analysis was performed using SPSS 13.0 software. The results were expressed as the means and standard deviations (mean±SD) and performed with one-way analysis of variance (ANOVA) followed by Dunnett's new multiple range test and values of $P<0.05$ were considered as statistically significant.

Results

Information about the phenolic compounds identified in parsley leaves are presented in *Table 2*.

Effects of orally administrated of Pb and PAE (single and combined) on the body and liver weights, liver enzymes and oxidative stress indexes of rats are presented in *Table 3* and *Fig. 1, 2*, and *3*, respectively.

The *Table 3* shows body and liver (average) weights in each group (mean±SD). Significant difference was not observed ($P>0.05$) for the body weight between the treatment groups. Feed intake and liver weight was significantly lower in the Pb diet group comparing to the other groups ($P<0.05$). Compared with Pb-treated rats, the administration of PAE significantly ($P<0.05$) increased feed intake and liver weight.

Results presented in *Fig. 1* showed significant increase in the liver enzymes (AST, ALT, and ALK) in Pb-treated animals. Administration of PAE (especially 200 mg/kg) in Pb given animals caused significant ($P<0.01$) recovery in the liver enzymes production similar to controls, however not attaining the same level in the controls.

Considering the control group, Pb-given animals exhibited significantly higher blood serum of the MDA contents. Results regarding to the oxidative stress indices showed significant ($P<0.05$) changes in contents in rats diet supplemented with Pb (with oral gavge) as compared to control at the end of the experiment. Concurrently, all these changes were recovered by PAE as a candidate therapy *(Fig. 2*, $P<0.05$).

Data of mRNA expression levels of apoptosis markers gene such as Bax and TNF-α and Bcl-2 were examined by QRT-PCR *(Fig. 3)*. mRNA expression levels of apoptosis markers genes (Bax and TNF-α) were significantly up-regulated in

Table 1. *Primers used for QRT-PCR, sequence, and product size*

Target Gene	PCR Fragment Length (bp)	Sequences (5'-3')
BAX	111	Forward: AGGCGAATTGGCGATGAACTGG
		Reverse: AAACATGTCAGCTGCCACACGG
BCL-2	126	Forward: TGGCTCTGCCATTCCTGTACG
		Reverse: GCTGCTTGCCTGTTAGTTCGC
TNF-α	238	Forward:AGGCAATAGGTTTTGAGGGCCAT
		Reverse: CATCAAGGATACCCCTCACACTC
β-actin	233	Forward: AGACTTCGAGCAGGAGATGG
		Reverse: GCACTGTGTTGGCATAGAGG

Primer sets designed using free online software Primer3Plus (v. 0.4.0) http://primer3plus.cgi

Table 2. *Phenolic compounds of parsley (Petroselinum crispum) in the aqueous-alcoholic extracts of the tested parsley leaves*					
Compounds	**Retention Times (min)**	**Percentage (%)**	**Compounds**	**Retention Times (min)**	**Percentage (%)**
Sabinene	7.79	0.211	Trans-chrysanthenyl acetate	18.88	0.422
Limonene	9.98	2.530	Carvone	19.89	4.716
Cis-b-ocimene	10.23	46.390	Unknown	20.34	9.744
d-Ocimene	10.54	6.406	Bicyclogermacrene	32.78	0.915
Dihydrotagetone	11.10	1.408	Hexadecanoic acid	53.29	3.238
Trans-ß-ocimene	15.33	6.938	Eicosane	57.61	0.915
Trans-tagetone	15.95	2.393	Methyl linoleate	59.68	6.192
Verbenone	18.54	0.563	Stearic acid	60.28	0.492
Total					93.385

Table 3. *Effects of dietary lead (Pb) and aqueous-alcoholic extract of parsley leaves (PAE) on body and liver weights (g) and feed intake (g) of rats (means±S.D.; n=10)*			
Group	**Body**	**Liver**	**Feed Intake**
Control	265±18.04	11.59±0.92 ^{a}	2.98±0.67 ^{a}
Sham	264±18.26	11.23±0.8 ^{ab}	2.88±0.53 ^{ab}
Pb	245±23.8	8.59±1.32 ^{f}	1.87±0.32 ^{f}
Pb+PAE 100	254.28±14.2	10.22±0.79 ^{abcde}	2.17±0.12 ^{abcd}
Pb+PAE 200	257±20.01	10.99±0.81 ^{abcd}	2.13±0.56 ^{abcde}
PAE 200	260±16.25	11.01±0.72 ^{abc}	2.24±0.42 ^{abc}
Superscripts (a-f) show significant differences in each column (P<0.05)			

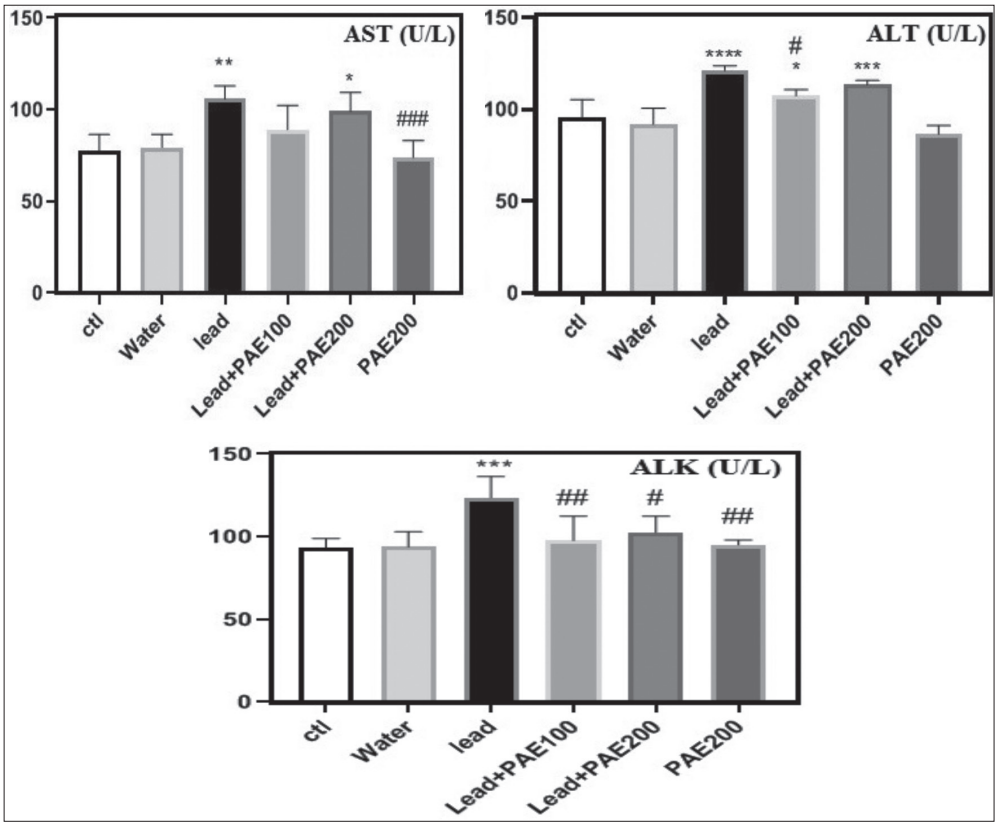

Fig 1. Effects of dietary lead and aqueous-alcoholic extract of parsley leaves (PAE) on liver enzymes level of rats. Aspartate amino transferase (AST); alanine amino transferase (ALT); alkaline phosphatase (ALK). Graphs show means±S.D. of 10 rats; Symbols indicate that treatments differ P<0.05 within each groups

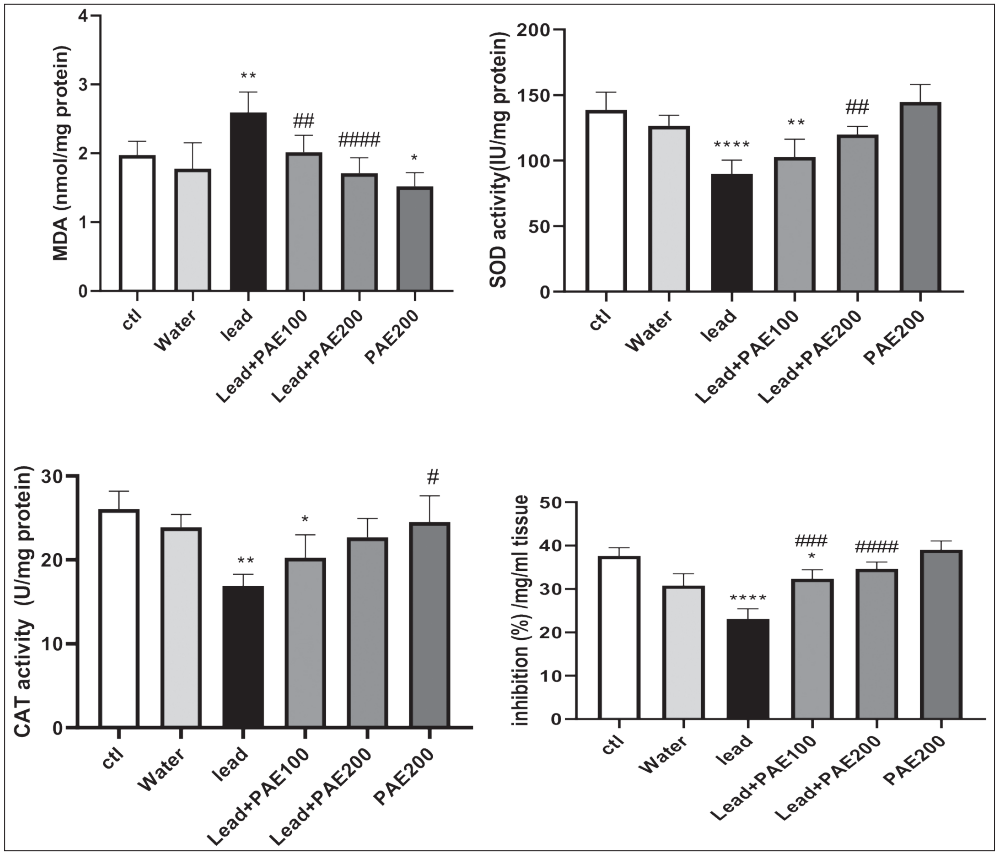

Fig 2. Effects of dietary lead and aqueous-alcoholic extract of parsley leaves (PAE) on oxidative stress indexes of rats. Malon-dialdehyde (MDA), superoxide dismutase (SOD), catalase (CAT), total antioxidant capacity or inhibition. Graphs show means ± S.D. of 10 rats; Symbols indicate that treatments differ P<0.05 within each groups

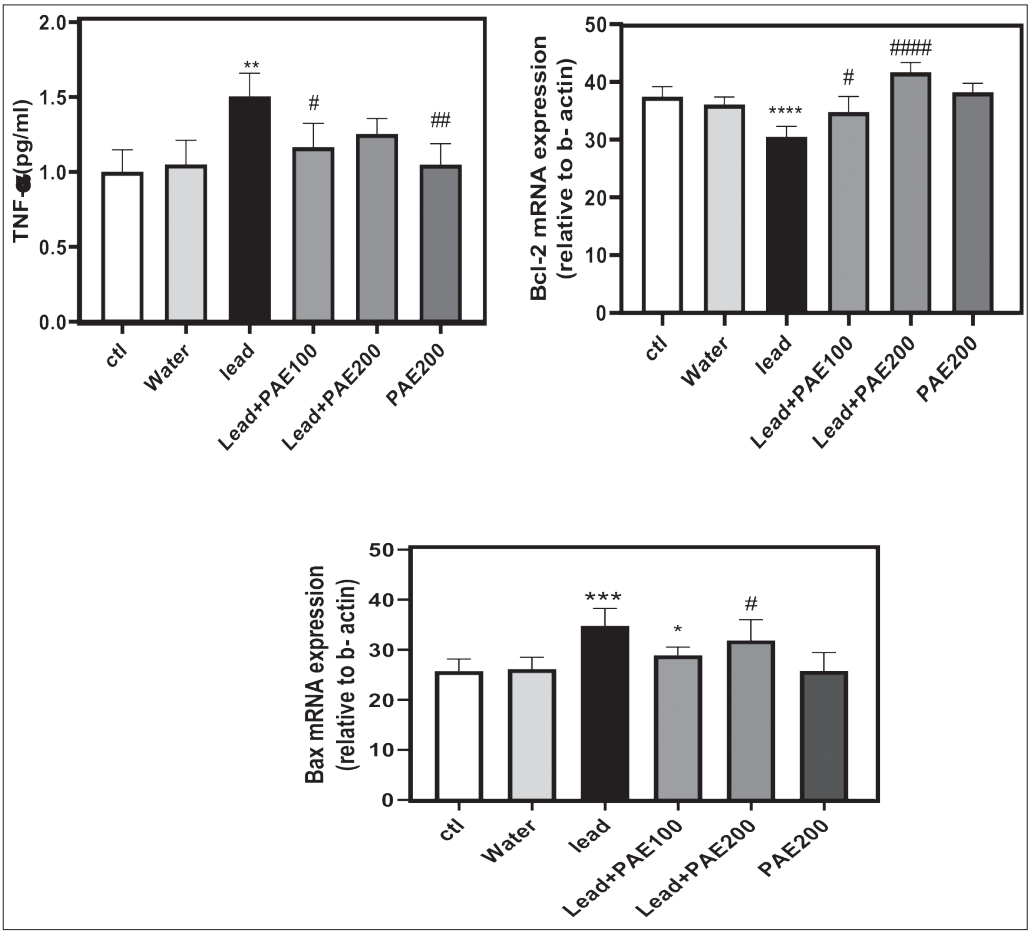

Fig 3. Effects of dietary lead and aqueous-alcoholic extract of parsley leaves (PAE) on liver apoptosis-related genes of rats. Graphs show means±S.D. of 10 rats; Symbols indicate that treatments differ P<0.05 within each groups

Pb exposed groups compared to control group (P<0.05). However, Bcl-2 was down-regulated by Pb administration. Meanwhile, exposure to PAE in this study, led to a significant decrease in apoptosis related genes (P<0.05). All these changes proportionally were abolished by treatment with PAE (especially 200 mg/kg).

Discussion

In the era of rising environmental contaminant, scientists need to be more aware of the detrimental effects of these agents on multiple body systems, particularly liver system. Nowadays, many environmental pollutants affect the liver system, and common therapeutic methods often results in unsatisfactory results for management of disorders of the liver, including liver disease, hepatitis, cirrhosis and liver cancer.

Supplementing medicinal herbs in animal model for the promotion of health is an increasingly more common management tool. Likewise, this experiment reported the potential beneficial health effect of PAE on Pb-induced liver dysfunction in rats and explored the possible mechanisms.

In the present study, the difference in feed intake, liver weight, liver enzymes, oxidative biomarkers and apoptosis-related genes between control and treated Pb animals is likely attributed to differences in daily content of diet with oral gavage of Pb and PAE. In Pb given groups feed intake was reduced, thus during the study maybe the animals compensate their need to energy through lipolysis. It can be concluded that Pb increases lipolysis through increasing the production of free radicals *(Fig. 2)* and formation of reactive oxygen species and decreasing feed intake *(Table 3)*. Our study proved that Pb promotes the excessive generation of free radicals, which could disrupt the balance between oxidant and antioxidant enzyme systems in liver tissues. Thus, the activities of antioxidant enzymes fail to inhibit the excessive generation of lipid peroxide, especially MDA contents (the end product of lipid peroxidation). In Pb-given groups, liver damage is associated with enhanced MDA levels. And, most of the recent literature have reported that excess of reactive oxygen species (ROS) will break homeostasis, such as the increase of MDA content, the reduction of oxidative damages, and the ability to resist OH% and inhibition of many anti-oxidative enzyme activities [18,19]. The low levels of MDA in PAE groups might be responsible for the withdrawal of the inhibitory effect of Pb toxicity on liver antioxidant system as well as the diminution in free radical generation. All these changes in oxidative stress indices proportionally were abolished by PAE as a candidate therapy.

Organism's exposure to environmental pollutants are usually analyzed through the evaluation of blood. Results of blood analysis show that a significant increase in liver enzymes and the amount of oxidative stress indices reported post Pb exposure, partly due to increased oxidative stress. This phenomenon is in line with the earlier reports in humans [5-7], poultry [8,9], and carp [10] models, which have been reported that change in liver status may be due to tissue-specific toxicity of Pb on it.

Concretely, the liver health including liver enzymes and the amount of oxidative stress indices improved in rats with PAE administration. However, results of blood analysis show that the recovery with medicinal herbs therapy (100 or 200 mg/kg PAE; 21 days continuously) to stimulate liver function is rapid. This rapid improvement could be associated with antioxidant activity of PAE by preventing lipid peroxidation and hepatic cells from oxidative damage by scavenging of free radicals. In agreement with the results of current study, previous studies have reported that PAE demonstrates a significant hepatoprotective effect since significantly cause lower levels of blood glucose, ALT and ALK in diabetic rats [20], and reduction of cholesterol, liver thiobarbituric acid, and the pronounced improvement of the investigated biochemical and anti-oxidant parameters [14], due to its flavones components [12]. Further understanding of natural antioxidant drugs and their effects on the liver system could help improving health treatments in patients.

By analyzing the expression level of several genes related to cell apoptosis (Bax and TNF-α) and survival (Bcl-2) apoptosis was shown to occur as a possible side effect of Pb use. Our data proved that Pb as an extracellular stimuli, could cause apoptosis-mediated pathway in the liver system of rat model, which might ultimately act either as a death safeguard effects. Pb administered in male rat generates an inflammatory-oxidative microenvironment that induces apoptosis of liver tissue by activation of Bax, and TNF-α increases together with Bax/Bcl-2 imbalance. The results of mRNA expression levels of apoptosis markers exhibited that Pb could induce mitochondrial impairment in liver cells or tissues of rat model, which maybe one of the potential mechanisms of Pb hepatic toxicity. Thus, study on apoptosis maker expressions in the liver tissues of laboratory animal may be advantageous to understand whether Pb induce apoptosis response against hepatic toxicity. Collectively, our findings indicated that PAE exposure could change expression of genes related to cell apoptosis. Our results exhibited a marked up-regulation of the expressions of Bcl-2. Overexpression of Bcl-2 increases cell viability and prevents apoptosis in adverse tissue circumstances [21].

Taken together, these results demonstrated that PAE exerted a vital protective effect on liver dysfunction in a rat model, which could be attributed to its direct protective effect on damaged liver via dual inhibiting oxidative changes and regulating the expressions of apoptosis-related genes.

Availability of Data and Materials

This manuscript contains original data and it is not under editorial consideration elsewhere. We have adhered to the ethical guidelines of your journal.

Acknowledgments

The authors would like to acknowledge Prof. Dr. Ali Olfati (A.Olfati65@Gmail.Com; ORCID: 0000-0003-0620-4138) for all efforts to improve the written language of the paper.

Funding Support

None declared.

Competing Interests

None.

Authors' Contributions

All authors have accepted responsibility for the entire content of this manuscript and approved its submission.

References

1. Tong S, von Schirnding YE, Prapamontol T: Environmental lead exposure: A public health problem of global dimensions. *Bull World Health Organ,* 78 (9): 1068-1077, 2000.

2. Trefts E, Gannon M, Wasserman DH: The liver. *Curr Biol,* 27 (21): R1147-R1151, 2017. DOI: 10.1016/j.cub.2017.09.019

3. Olfati A, Tvrda E: Riboflavin recovery of spermatogenic dysfunction via a dual inhibition of oxidative changes and regulation of the PINK1-mediated pathway in arsenic-injured rat model. *Physiol Res*, 70, 591-603, 2021. DOI: 10.33549/physiolres.934658

4. Olfati A, Moghaddam G, Baradaran B: FSH and estradiol benzoate administration recover spermatogenesis and sexual hormone levels in a busulfan-injured rat model. *Comp Clin Pathol,* 29, 53-59, 2020. DOI: 10.1007/s00580-019-03029-3

5. Kasperczyk A, Dziwisz M, Ostałowska A, Swietochowska E, Birkner E: Function of the liver and bile ducts in humans exposed to lead. *Hum Exp Toxicol*, 32 (8): 787-796, 2013. DOI: 10.1177/0960327112468177

6. Liang Y, Yi X, Dang Z, Wang Q, Luo H, Tang J: Heavy metals contamination and health risk assessment in the vicinity of a tailing pond in Guangdong, China. *Int J Environ Res Public Health,* 14:1557, 2017. DOI: 10.3390/ijerph14121557

7. Nakhaee S, Amirabadizadeh A, Brent J, Mehrpour O: Impact of chronic lead exposure on liver and kidney function and haematologic parameters. *Basic Clin Pharmacol Toxicol,* 124 (5): 621-628, 2019. DOI: 10.1111/bcpt.13179

8. Suleman M, Khan AA, Hussain Z, Zia MA, Roomi S, Rashid F, Iqbal A, Ishaq R: Effect of lead acetate administered orally at different dosage levels in broiler chicks. *Afr J Environ Sci Technol,* 5 (12): 1017-1026, 2011. DOI: 10.5897/AJEST10.278

9. Ashrafizadeh M, Rafiei H, Ahmadi Z: Histological changes in the liver and biochemical parameters of chickens treated with lead acetate II. *Iranian J Toxicol,* 12 (6): 1-5, 2018.

10. Baghshani H, Shahsavani D: Effects of lead acetate exposure on metabolic enzyme activities in selected tissues of common carp *(Cyprinus carpio). Comp Clin Pathol,* 22, 903-907, 2013. DOI: 10.1007/s00580-012-1497-3

11. Yanardag R, Bolkent S, Tabako-Oguz A, Ozsoy-Sacan O: Effects of *Petroselinum crispum* extract on pancreatic B cells and blood glucose of streptozocin-induced diabetic rats. *Biol Pharm Bulletin,* 26, 1206-1210, 2003.

12. Petrolini FVB, Lucarini R, de Souza MGM, Pires RH, Cunha WR, Martins CHG: Evaluation of the antibacterial potential of Petroselinum crispum and Rosmarinus officinalis against bacteria that cause urinary tract infections. *Braz J Microbiol,* 44, 829-834, 2013. DOI: 10.1590/S1517-83822013005000061

13. Kamal T, Abd-Elhady M, Sadek K, Shukry M: Effect of parsley *(Petroselium crispum)* on carbon tetrachloride-induced acute hepatotoxicity in rats. *Res J Pharm Biol Chem Sci,* 5, 1524-1534, 2014.

14. Soliman HA, El-Desouky MA, Hozayen WG, Ahmed RR, Khaliefa AK: Hepatoprotective effects of parsley, basil, and chicory aqueous extracts against dexamethasone-induced in experimental rats. *J Intercult Ethnopharmacol,* 5 (1): 65-71, 2016. DOI: 10.5455/jice.20160124113555

15. Ozsoy-Sacan O, Yanardag R, Orak H, Ozgey Y, Yarat A, Tunali T: Effects of parsley (Petroselinum crispum) extract versus glibornuride on the liver of streptozotocin-induced diabetic rats. *J Ethnopharmacol,* 104 (1-2): 175-181, 2006. DOI: 10.1016/j.jep.2005.08.069

16. Azab AE, Abushofa FA, Abdul Rahman HMA: Nephroprotective effect of aqueous extract of parsley against nephrotoxicity induced by carbon tetrachloride in the male rats. *J Biotechnol Bioeng*, 3 (4): 16-26, 2019.

17. Jiang YP, Yang JM, Ye RJ, Liu N, Zhang WJ, Ma L, Zheng P, Niu JG, Liu P, Yu JQ: Protective effects of betaine on diabetic induced disruption of the male mice blood-testis barrier by regulating oxidative stress-mediated p38 MAPK pathways. *Biomed Pharmacother,* 120:109474, 2019. DOI: 10.1016/j.biopha.2019.109474

18. Reddy UA, Prabhakar PV, Mahboob M: Biomarkers of oxidative stress for *in vivo* assessment of toxicological effects of iron oxide nanoparticles. *Saudi J Biol Sci,* 24, 1172-1180, 2017. DOI: 10.1016/j.sjbs.2015.09.029

19. Sun X, Li J, Zhao H, Wang Y, Liu J, Shao Y, Xue Y, Xing M: Synergistic effect of copper and arsenic upon oxidative stress, inflammation and autophagy alterations in brain tissues of *Gallus gallus*. *J Inorg Biochem,* 178, 54-62, 2018. DOI: 10.1016/j.jinorgbio.2017.10.006

20. Bolkent S, Yanardag R, Ozsoy-Sacan O, Karabulut-Bulan O: Effects of parsley *(Petroselinum crispum)* on the liver of diabetic rats: A morphological and biochemical study. *Phytother Res,* 18 (12): 996-999, 2004.

21. Toruner M, Fernandez-Sapico M, Sha JJ, Pham L, Urrutia R, Egan LJ: Antianoikis effect of nuclear factor-κB through upregulated expression of osteoprotegerin, Bcl-2 and IAP-1. *J Biol Chem,* 281, 8686-8696, 2006.

Kafkas Universitesi Veterinar Fakultesi Dergisi
ISSN: 1300-6045 e-ISSN: 1309-2251
Journal Home-Page: http://vetdergikafkas.org

Kafkas Univ Vet Fak Derg
27 (6): 725-731, 2021
DOI: 10.9775/kvfd.2021.26194

RESEARCH ARTICLE

Annual and Seasonal Variations of Testicular and Pituitary-Thyroid Axis Activities in Bucks Native to Sahara Desert

Nadia CHERGUI [1,2,3,a (*)] Nouria BOUKENAOUI-FERROUK [1,2,3,b] Salima CHARALLAH-CHERIF [2,3,c]
Farida KHAMMAR [2,3,d] Zaina AMIRAT [2,3,e] Pierre MORMEDE [4,f]

[1] Saad DAHLAB University Blida 1, Institute of Veterinary Sciences, Blida, ALGERIA
[2] Houari BOUMEDIENE University of Sciences and Technology, Faculty of Biology, Laboratory of Research on Arid Lands, Bab Ezzouar, Algiers, ALGERIA
[3] Benyoucef BENKHEDDA University of Algiers 1, Department of Biology, ALGERIA
[4] University of Toulouse, INRAE, ENVT, GenPhySE, F-31326, Castanet Tolosan, FRANCE
ORCIDs: [a] 0000-0001-8705-4199; [b] 0000-0002-8688-4614; c 0000-0002-4519-3163; [d] 0000-0001-7499-1431; [e] 0000-0002-2710-6679
[f] 0000-0003-0345-1432

Article ID: KVFD-2021-26194 Received: 24.06.2021 Accepted: 07.11.2021 Published Online: 10.11.2021

Abstract

This study was conducted to assess comparative annual and seasonal patterns described in morphometric parameters, sexual and thyroid activities in indigenous bucks native to Sahara Desert. Seven adult bucks were used to establish seasonal patterns of body weight, testicular volume, plasma testosterone concentration measured by radioimmunoassay and pituitary-thyroid axis activity estimated by plasma concentrations of TSH, FT3 and FT4 measured by enzyme-linked fluorescent assay. The results showed monthly and seasonal variations characterized by a minimum in January for body weight, from December to February for testicular volume, followed by plasma testosterone concentration in March; they progressively increased to their respective maxima reached in July, August and September when ambient temperature and photoperiod were the highest. In October, there was a rapid fall in testosterone levels, preceding that of body weight and testicular volume ($P<0.001$). Plasma TSH showed no significant variations, while the monthly rhythms of FT4 and particularly FT3 ($P<0.001$) were inverted to the sexual cycle, since the highest values occurred in winter (January) and the lowest in summer (July). These results suggest morphometric and hormonal interrelations in this indigenous seasonal breeder goat in order to survive and reproduce in its natural arid environment.

Keywords: *Buck, Sahara Desert, Seasonal variations, Testicular activity, Thyroid activity*

Sahra Çölü'ne Özgü Antilopların Testis ve Hipofiz-Tiroid Aksı Aktivitelerinin Yıllık ve Mevsimsel Değişimleri

Öz

Bu çalışma, Sahra Çölü'ne özgü yerli antilopların morfometrik parametreler, seksüel ve tiroid aktivitelerinin tanımlanan karşılaştırmalı yıllık ve mevsimsel modellerinin araştırılması için yapılmıştır. Vücut ağırlığı, testis hacmi, radyoimmünoassay ile ölçülen plazma testosteron konsantrasyonu ve TSH, FT3 ve FT4 plazma konsantrasyonlarının enzim işaretli floresan yöntemiyle ölçülmesiyle belirlenen hipofiz-tiroid eksen aktivitesinin mevsimsel modellerini belirlemek için yedi adet yetişkin antilop kullanıldı. Sonuçlar, vücut ağırlığının Ocak ayında, testis hacminin Aralık ile Şubat ayları arasında ve plazma testosteron konsantrasyonunun Mart ayında minimum seviyelerde yer alarak aylık ve mevsimsel varyasyonlar sergilediğini; çevre sıcaklığının ve fotoperiyodun en yüksek olduğu Temmuz, Ağustos ve Eylül aylarında bu değerlerin maksimum seviyelere aşamalı olarak yükseldiğini gösterdi. Ekim ayında, vücut ağırlığı ve testis hacminden önce testosteron seviyelerinde hızlı bir düşüş saptandı ($P<0.001$). Plazma TSH miktarı önemli bir değişiklik göstermezken, FT4 ve özellikle de FT3'ün ($P<0.001$) aylık ritimleri, en yüksek konsantrasyonlarının kışın (Ocak) ve en düşük konsantrasyonlarının yazın (Temmuz) saptanması nedeniyle seksüel siklusun tersine döndü. Bu sonuçlar, bu yerli mevsimlik damızlık antilopların doğal kurak ortamlarında hayatta kalma ve üremeleri için morfometrik ve hormonal ilişkiler sergilediğini göstermektedir.

Anahtar sözcükler: *Antilop, Sahra Çölü, Mevsimsel değişim, Testiküler aktivite, Tiroid aktivitesi*

How to cite this article?

Chergui N, Boukenaoui-Ferrouk N, Charallah-Cherif S, Khammar F, Amirat Z, Mormede P: Annual and seasonal variations of testicular and pituitary-thyroid axis activities in bucks native to Sahara Desert. *Kafkas Univ Vet Fak Derg,* 27 (6): 725-731, 2021.
DOI: 10.9775/kvfd.2021.26194

(*) Corresponding Author

Tel: +213 540 664 029
E-mail: n_chergui@univ-blida.dz (N. Chergui)

Introduction

The goat is one of the most adaptable livestock species distributed worldwide across a large variety of climatic and geographical areas [1]. In Algeria, most of them are raised mainly in the arid and semi-arid regions. Their adaptation to periodic environmental changes results in the appearance of biological rhythms, particularly reflected by breed differences in the time of maximum body weight (BW), testis volume, testicular and thyroid activities [2].

The photoperiod has been suggested as the main factor influencing the seasonal reproduction. The length of the day is transduced by the pineal gland into a chemical message via its rhythmic secretion of melatonin, which regulates the hypothalamic-pituitary-gonadal function [3]. Furthermore, the reproduction is a costly process in terms of energetics for the male which may reflect competition for access to females, aggressive behavioral, territorial defense, and paternal behavior [4].

The central mechanisms regulating reproduction and energy balance by environmental factors are tightly linked. Indeed, several investigations have targeted the interrelationships between reproduction and hypothalamic-pituitary-thyroid axis, in relation with the annual cycle [5,6]. These studies showed that the thyroid hormone (TH) are required for seasonal transition from breeding to non-breeding state [5], and for metabolic adjustments in response to heat stress [6]. Understanding the physiological mechanisms involved in this regulation is an important issue to breeding optimization. Males with better sexual behavior under high temperature conditions can be selected for the development of breeds adapted to arid climate [2].

By using scientific methods, the production of this indigenous ruminant will be increased in the future in order to improve the nutrition of Saharan populations and the preservation of this local well adapted species. So, the purpose of this work is to characterize annual and seasonal patterns in (1) BW, (2) sexual activity as estimated by testicular biometry and plasma concentration of testosterone and (3) pituitary-thyroid axis activity, measured by thyroid stimulating hormone (TSH) and TH plasma concentrations in bucks reared in their natural biotope, under arid climate conditions.

Material and Methods

Ethical Approval

The methodology protocols of the present study followed the ethical concepts in animal experimentation, recommended by FELASA and approved by the Algerian Ministry of Higher Education and Scientific Research (Executive Decree 10-90 supplementing the Algerian government decree 04-82) and the AASEA (45/DGLPAG/DVA.SDA.14).

Site of Study and Meteorological Data

The study was carried out at Béni Abbès research station located in the Algerian Sahara Desert (30°07′ N, 2°10′ W, elevation 495 m, South West of Algeria), characterized by cold and humid winter, and hot and dry summer *(Table 1; Fig. 1)*. The temperature-humidity index (THI) was calculated using the formula of Mader et al.[7]:

$$THI = 0.8 \times AT + [(RH \div 100) \times (AT - 14.4)] + 46.4$$

AT: Ambient temperature (°C), RH: Relative humidity (%).

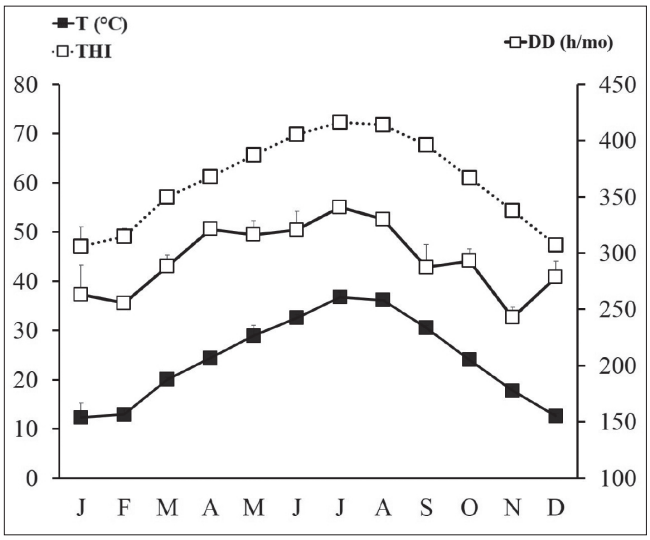

Fig 1. Annual variations of temperature, temperature-humidity index and daylight duration from the Béni-Abbès region (30°07′ N, 2°10′ W, elevation 495 m, South West of Algeria) during the experimental period (mean±sem). **T:** Temperature; **THI:** Temperature-humidity index; **DD:** Daylight duration; **mo:** month. Data were obtained from the Algerian meteorological center

Table 1. *Meteorological seasonal data (minimum - maximum values) from the Béni-Abbès region (30°07′ N, 2°10′ W, elevation 495 m, South West of Algeria) during the experimental period*

Seasons	Ambient Temperature (°C)	Relative Humidity (%)	Temperature Humidity Index	Daylight Duration (h/month)	Precipitation (mm/month)
Winter	4-19	26-63	47-64	186-314	0-42
Spring	20-33	15-37	63-80	305-378	0-27
Summer	20-41	12-31	67-87	304-365	0-6
Autumn	12-31	22-47	55-79	230-322	0-5

Animals

Seven bucks (3-4 years old; BW: 30-48 kg) were used in this study, which was conducted over 2 consecutive years. The animals were clinically healthy and have typical libido characteristics, they were reared under open shelter, undergoing the influence of all natural variations of climatic factors. Bucks were fed forage and a mixture of oats and barley (about 1 kg per buck) once daily (4:30 p.m.) with ad libitum access to water and mineral salt licks.

Morphometric Parameters

The BW and testicular morphometric parameters were measured twice a month during two consecutive years. The large and small diameters for the left and right testes were measured with a sensitive caliper in order to calculate the testicular volume according to a mathematical model (TVM) [8]:

$$TVM\ (cm^3) = 4/3 \times \pi \times ab^2$$

where a and b represent respectively half of the large and small diameters.

The testicular volume was also estimated with a volumetric technique by water immersion [9]; the animal being in a standing position, the two testes were immersed in a calibrated 2-liters beaker filled with lukewarm water; the testicular volume is given by the water displacement (TVW in mL).

Blood Sampling

Blood samples (5 mL) were collected at 9:00 a.m. every 15 days during two consecutive years, by jugular vein puncture in heparinized vacutainer tubes (lithium heparinate, Venoject Terumo; Leuven, Belgium) and kept on ice before centrifugation at 4000 x g for 10 min at 4°C. Plasma samples were separated rapidly and stored at -20°C for further analyses.

Testosterone Assay

Testosterone assay was performed by radioimmunoassay (RIA), after extraction of steroids with a mixture of ethyl acetate - cyclohexane (v/v), using a specific antibody raised in rabbit by immunization with carboxymethyl-oxime of testosterone coupled to bovine serum albumin [10]. The specificity of this method was estimated by measuring the cross-reactivity of the antibody with dihydroxytestosterone (47%), androstenedione (16%) and less than 0.5% with other steroids; the sensitivity was 0.02 ng/mL and the intra- and inter-assay coefficients of variation were 5.1 and 9.3%, respectively.

TSH and Thyroid Hormones Assays

Plasma TSH, FT3 and FT4 concentrations were determined by Enzyme Linked Fluorescent Assay (ELFA) (VIDAS Vitek ImmunoDiagnostic Assay System, Biomérieux, Lyon, France). The principle of the assay associates the immuno-enzymatic method with a final fluorescence detection step, using mouse monoclonal immunoglobulins anti-TSH (Ref: 30 441, TSH3) and sheep antibody for anti-FT3 (Ref: 30 402, FT3) and anti-FT4 (Ref: 30 459, FT4N), labelled with alkaline phosphatase. The assay sensitivity was 0.005 µIU/mL for TSH, ≤0.7 pmol/L for FT3 and = 1.11 pmol/L for FT4. No interference was seen for TSH antibody with other hormones (<0.01% with FSH, LH and hCG). For FT4 antibody no interference observed up to the concentration of 12.51 µg/L for L-triiodothyronine and 2.28 µg/L for D-thyroxine. The cross reactivity of FT3 antibody was of 0.2% with L-thyroxin. The intra- and inter-assay coefficients of variation were respectively 2.44 and 4.30% for TSH, 4.83 and 5.28% for FT3 and 5.40 and 8.49% for FT4 (kit values).

Statistical Analysis

Data are expressed as the means±sem. The bimonthly values were grouped by month and then by seasons (the two years combined) determined conventionally as follows: winter from December 21st to March 20th, spring from March 21st to June 20th, summer from June 21st to September 20th and autumn from September 21st to 20th December. Statistical evaluation of differences was done by analysis of variance (ANOVA), using IBM SPSS Statistics 25 (Copyright IBM and its licensors 1989, 2017), including months or seasons as fixed factors and animals as random factors. Normality and homogeneity of variance were respectively investigated by Shapiro-Wilk and Levene's test. The difference between the variables was calculated post hoc using the Tukey test. Correlations were calculated between the months and seasons by means of Pearson's correlation coefficient (r). A probability level of $P<0.05$ was used for significance.

Results

Evolution of Monthly Patterns

Body Weight

The monthly BW values *(Fig. 2)* were the lowest in January, increased progressively till April (+16.4% vs January, $P<0.01$) and the maximum body mass was reached in July (+22.6% vs January, $P<0.001$). It was followed by a progressive decrease until December (-16.3% vs July, $P<0.01$), leading to highly significant annual variations.

Testicular Volume

The monthly variations of testicular volume paralleled that of BW *(Table 2; Fig. 2)*, whether evaluated by measuring testicular diameters mathematically TVM ($r=0.823$, $P<0.01$) or by water immersion TVW ($r=0.908$, $P<0.01$). The TVM showed a sensitive increase in May (+22.5% vs January, $P<0.01$), and the maximum was reached in August (+39.3% vs January, $P<0.001$). In September, TVM fell significantly

(-31.4% vs August, P<0.001) and progressively until the minimum occurring in December (-36.2% vs August, P<0.001). The TVW showed the same pattern as that of the TVM *(Fig. 2)*. However, the values always remained at a significantly higher level than TVM, characterized by a minimum in February and a maximum in July (+38.0% vs February, P<0.001). The correlation coefficient *(Table 2)* shows a highly significant positive relationship between the two methods of measure (r=0.805, P<0.01).

Plasma Testosterone Concentration

The pattern of monthly values of plasma testosterone concentration *(Fig. 3)* showed annual variations (P<0.01) with a minimum level in March, a gradually increase until June (+447% vs March, P<0.01) and a peak reached in September (+601% vs March, P<0.001); then a gradual decrease from October (-61.3% vs September, P<0.01) until December (-76.3% vs September, P<0.001). The correlation coefficient *(Table 3)* shows a significant positive relationship (P<0.05) with BW (r=0.616) and TVW (r=0.637).

Plasma TSH and Thyroid Hormones Concentrations

Plasma concentration of TSH showed no significant variations *(Fig. 3)*. FT3 and FT4 showed similar patterns of evolution through the year (P<0.001), with maximum values in January, followed by a progressive decrease from February (-12.6% for FT3 and -10,7.0% for FT4) until April (-48.4% for FT3 and -23.7% For FT4 vs January, P<0.001); the decrease becomes significant in May vs January (-45.2% for FT3 (P<0.001) and -18.8% for FT4 (P<0.01)). A gradual increase appears from November (+82.3% for FT3 and +38.9% for FT4 vs October) until December (+149% for FT3 vs October and +40.9% for FT4 vs October). A significant increase was observed only in December for FT3 (+107% vs July, P<0.001).

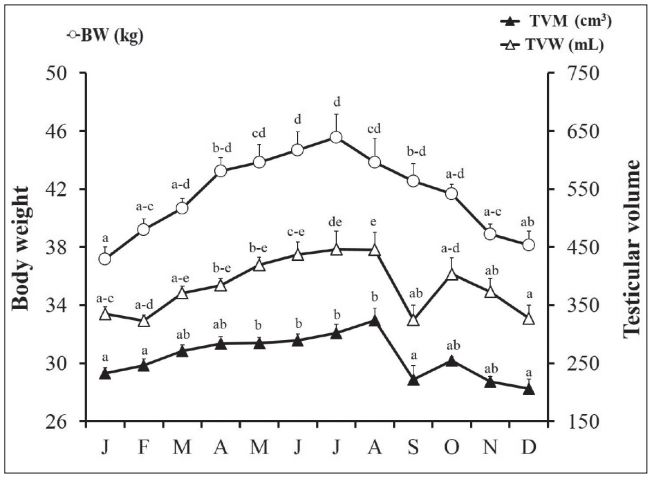

Fig 2. Annual variations in body weight and testicular volume in the buck reared under arid environment (mean±sem, n = 7). Measurements taken twice a month during two consecutive years were grouped by month for each buck. **BW:** Body weight; **TVM:** Testicular volume by measure according to a mathematical model; **TVW:** Testicular volume by immersion in water. Different superscripts indicate significant differences between months (P<0.05)

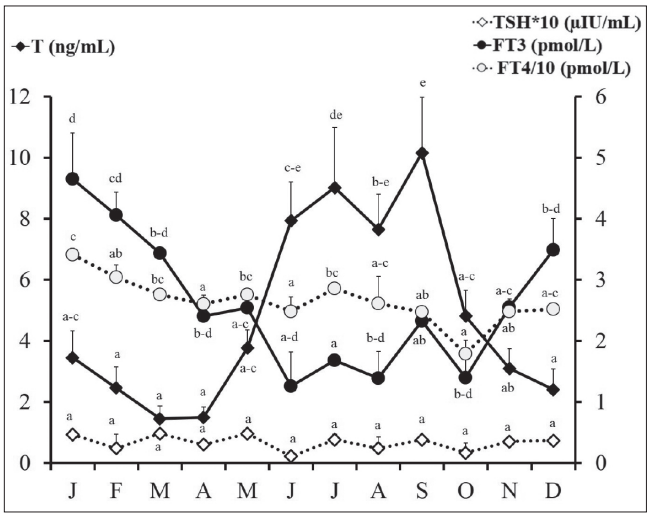

Fig 3. Annual variations of plasma testosterone, TSH and thyroid hormones (FT3 and FT4) concentrations in the buck reared under arid environment (mean±sem, n = 7). Levels measured twice a month during two consecutive years and grouped by month. **T:** Testosterone; **TSH:** Thyroid stimulating hormone (mean values multiplied by 10); **FT3:** Free triiodothyronine; **FT4:** Free thyroxine (mean values divided by 10). Different superscripts indicate significant differences between months (P<0.05)

Table 2. *Coefficients of correlation between mean monthly body weight, testicular and thyroid activities in the buck reared under arid environment (n=7)*

Parameter	BW	TVM	TVW	T	TSH	FT3	FT4
BW	1						
TVM	0.823**	1					
TVW	0.908**	0.805**	1				
T	0.616*	0.336	0.637*	1			
TSH	-0.327	-0.328	-0.119	-0.030	1		
FT3	-0.600*	-0.184	-0.624*	-0.578*	-0.216	1	
FT4	-0.357	-0.175	-0.140	-0.024	0.868**	0.022	1

Data were obtained from the Algerian meteorological center
BW: *Body weight;* ***TVM or TVW:*** *Testicular volume;* ***T:*** *Testosterone;* ***TSH:*** *Thyroid stimulating hormone;* ***FT3:*** *Free triiodothyronine;* ***FT4:*** *Free thyroxine. Correlations were calculated between the months by means of Pearson's correlation coefficient; * indicates statistical significance at P<0.05; ** indicates statistical significance at P<0.01*

Table 3. *Coefficients of correlation between mean seasonal body weight, testicular and thyroid activities in the buck reared under arid environment (n=7)*

Parameter	BW	TVM	TVW	T	TSH	FT3	FT4
BW	1						
TVM	0.925	1					
TVW	0.992**	0.879	1				
T	0.764	0.665	0.813	1			
TSH	-0.580	-0.376	-0.571	-0.046	1		
FT3	-0.769	-0.516	-0.842	-0.886	0.395	1	
FT4	-0.368	-0.098	-0.384	0.079	0.954*	0.351	1

BW: *Body weight;* ***TVM or TVW:*** *Testicular volume;* ***T:*** *Testosterone;* ***TSH:*** *Thyroid stimulating hormone;* ***FT3:*** *Free triiodothyronine;* ***FT4:*** *Free thyroxine. Correlations were calculated between the seasons by means of Pearson's correlation coefficient; * indicates statistical significance at P<0.05; ** indicates statistical significance at P<0.01*

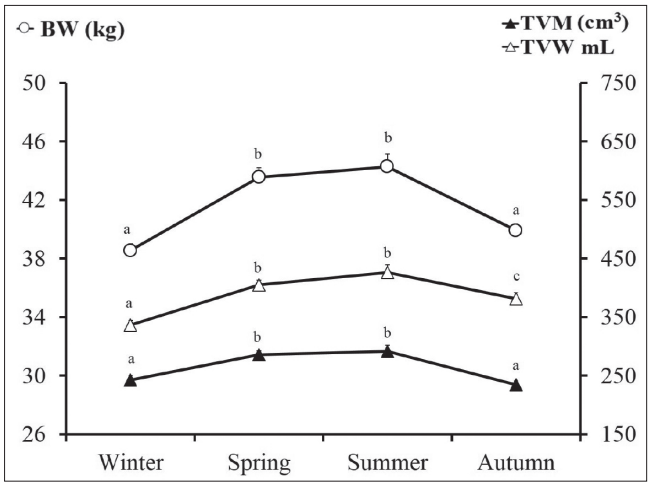

Fig 4. Comparative seasonal profiles of body weight and testicular volume (TVM and TVW) in the buck reared under arid environment (mean±sem, n = 7). **BW:** Body weight; **TVM:** Testicular volume by measure according to a mathematical model; **TVW:** Testicular volume by immersion in water. Data grouped by season including all experimental years. Different superscripts indicate significant differences between seasons (P<0.05)

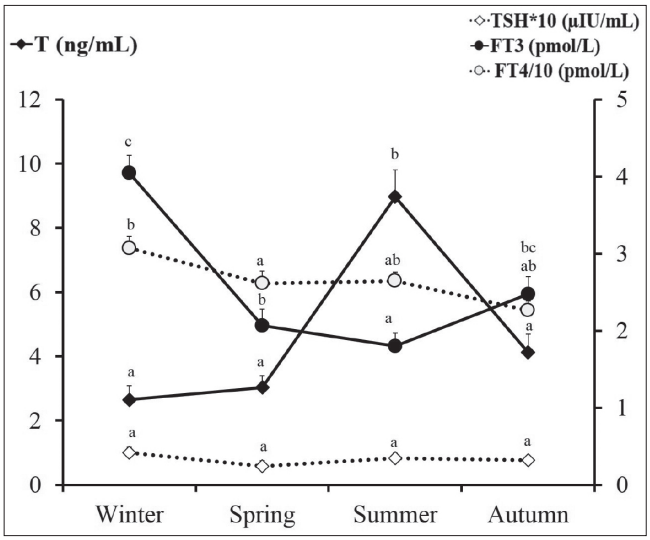

Fig 5. Comparative seasonal profiles of plasma concentration of testosterone, TSH and thyroid hormones (FT3 and FT4) in the buck reared under arid environment (mean±sem, n = 7). **T:** Testosterone; **TSH:** Thyroid stimulating hormone (as mean values multiplied by 10); **FT3:** Free triiodothyronine; **FT4:** Free thyroxine (as mean values divided by 10). Data grouped by season including all experimental years. Different superscripts indicate significant differences between seasons (P<0.05)

Evolution of Seasonal Patterns

When grouping values by season, the patterns exhibited important seasonal variations but the differences were indeed attenuated. The lowest values of the BW *(Fig. 4)* being observed in autumn-winter and the highest in spring-summer (+14.9% winter vs summer, P<0.001). The seasonal difference (summer vs winter) for testicular volume were +19.9% (P<0.001) for TVM and 26.7 for TVW (P<0.001) *(Fig. 4)*. A significant positive correlation *(Table 3)* was observed with the TVW and BW (r=0.992, P<0.01).

The seasonal pattern of plasma testosterone *(Fig. 5)* showed a gradual increase from a minimum in winter to a maximum in summer (+239%, P<0.001). These variations were positively correlated *(Table 3)* with those of morphometric parameters as BW (r=0.764), TVM (r=0.665) and TVW (r=0.813). The plasma thyroid hormones *(Fig. 5)* showed also significant seasonal variations, particularly for FT3 (P<0.001), characterized by highest values in winter and the minimum was occurred in summer (-55.5% vs winter, P<0.001). The pattern of FT4, showed a significant diminution in spring (-13.8% vs winter, P<0.05) which paralleled that of TSH (r=0.954, P<0.05) *(Table 3)*.

Compared Patterns Between Testicular and Thyroid Activities

The monthly *(Table 2; Fig. 3)* and the seasonal *(Table 3; Fig. 5)* variations of testicular and thyroid activities revealed a reversed evolution between the concentrations of testosterone and TH, particularly that of FT3. The two annual cycles were significantly opposite, the Pearson correlation coefficient was r=-0.578 (P<0.05). The FT3 showed also negative correlation with that of BW (r=-0.600, P<0.05) and testicular volume (r=-0.624, P<0.05) *(Table 2)*.

Discussion

In this study, we found that Desert bucks, living in their natural arid environment, show important annual and seasonal variations in their BW, which paralleled those of the reproductive activity, as measured by the testicular volume and plasma testosterone concentration. These variations were reported in several ungulate species living in the same conditions of arid and semi-arid areas of Algeria, especially in rams [11] and camel [12]. The appearance of the seasonal rhythm of BW, although the bucks received the same diet, is probably related to the physiological state and the reproductive performance, regardless of feeding level, as reported by Zarazaga et al.[13]. Indeed, the BW gain was observed when the males are sexually inactive, corresponding to the seasonal anestrous of the females [14,15], which appears mainly in winter. In other hand, the minimum and the maximum of testicular volume and plasma testosterone concentrations were also observed respectively in summer and winter, indicating a seasonal rhythm in the reproductive cycle parallel to that of BW. Theses variations were probably related to environmental changes, particularly the photoperiod. Indeed, during the elongation of the daylength (late winter), the concentration of testosterone was lowest, while the highest value was observed during the day shortening (late summer), showing that this male goat is a "short day breeder". It is known that the pineal melatonin, an endocrine index of daylength, is used to relay photoperiodic information to the reproductive axis and serves as a master regulator of breeding. The day shortening increase melatonin, causing decreased TSH-β subunit expression in pituitary pars-tuberalis, which affects sex hormone levels [16]. In our study, no clear change in plasma TSH between seasons. The lack of rhythm probably reflects unimportant role of peripheral TSH in the regulation of seasonal reproduction, confirming the findings of several authors who report that peripheral TSH secreted by pituitary pars-distalis, from the classical hypothalamic-pituitary-thyroid axis, does not depend on the photoperiod [17]. However, the TH follows a seasonal pattern, the minimum being observed in summer and the maximum in winter, which was inverse to that of testicular activity. The increase observed in winter, probably promotes changes in the neuroendocrine axis, which result in transition from the breeding to the non-breeding season, as reported by Yasuo et al.[18]. Moreover, the reduction in summer may reflect a metabolic adaptation to harsh environment, characterizing arid regions. In effect, in a previous work done on the same breed, we have reported high levels of cortisol in summer [19], thus decreasing the release of TH in order to reduce basal metabolism [2]. It is difficult to discriminate between the respective role of temperature and photoperiod on the seasonality of thyroid activity, in different environmental conditions [20]. However, these variations affect the energy metabolism that results in seasonal changes in BW, which is positively correlated with reproductive success. Knowledge on such physiological adaptive strategies, allows the monitoring and manipulation of testicular and thyroid activities, in order to improve animal health, welfare and production of this indigenous buck.

In conclusion, the buck native to Algerian Sahara Desert is a "short day breeder", it follows annual and seasonal rhythms of its reproductive activity correlated to BW, and opposed to that of thyroid activity. This species limits its reproductive activity to specific period of time in a year in order to survive and to maximize the success of reproduction and survival of their offspring.

Availabity of Data and Materials

The authors declare that data supporting the study findings are also available to the corresponding author.

Acknowledgements

We thank Hocine SALMI and Mohamed YAICH for their technical help at the experimental station of Béni-Abbès, the medical teams of the hospital and the polyclinic of Béni-Abbès. The authors dedicate this work to the memory of their colleague Yahia LAKHDARI, who contributed in the experimental part of this work.

Financial Support

The authors declared that there is no financial support

Conflict of Interest

The authors declared that there is no conflict of interest.

Author Contributions

N. Chergui: Conceptualization, Methodology, Validation, Formal analysis, Investigation, Writing - Original Draft, Writing - Review & Editing, Visualization. N. Boukenaoui-Ferrouk: Visualization, Review & Editing. S. Charallah-Cherif: Methodology & Visualization. F. Khammar: Resources, Methodology & Visualization. Z. Amirat: Conceptualization, Methodology, Investigation, Resources, Writing - Original Draft, Visualization, Review & Editing, Supervision. P. Mormede: Conceptualization, Writing - Original Draft, Review & Editing, Visualization.

References

1. Bertolini F, Servin B, Talenti A, Rochat E, Kim ES, Oget C, Palhière I, Crisà A, Catillo G, Steri R, Amills M, Colli L, Marras G, Milanesi M, Nicolazzi E, Rosen BD, Van Tassell CP, Guldbrandtsen B, Sonstegard TC, TosserKlopp G, Stella A, Rothschild MF, Joost S, Crepaldi P, AdaptMap consortium: Signatures of selection and environmental adaptation across the goat genome post-domestication. *Genet Sel Evol,* 50:57, 2018. DOI: 10.1186/s12711-018-0421-y

2. Joy A, Dunshea FR, Leury BJ, Clarke IJ, DiGiacomo K, Chauhan SS: Resilience of small ruminants to climate change and increased

environmental temperature: A review. *Animals*, 10 (5): 867, 2020. DOI: 10.3390/ani10050867

3. Swelum AAA, Saadeldin IM, Ba-Awadh H, Alowaimer AN: Shortened daily photoperiod during the non-breeding season can improve the reproductive performance of camel bulls *(Camelus dromedarius)*. *Anim Reprod Sci,* 195, 334-344, 2018. DOI: 10.1016/j.anireprosci.2018.06.014

4. Schneider JE, Wise JD, Benton NA, Brozek JM, Keen-Rhinehart E: When do we eat? Ingestive behavior, survival, and reproductive success. *Horm Behav*, 64 (4): 702-728, 2013. DOI: 10.1016/j.yhbeh.2013.07.005

5. Lomet D, Cognié J, Chesneau D, Dubois E, Hazlerigg D, Dardente H: The impact of thyroid hormone in seasonal breeding has a restricted transcriptional signature. *Cell Mol Life Sci*, 75, 905-919, 2018. DOI: 10.1007/s00018-017-2667-x

6. Gupta M, Mondal T: Heat stress and thermoregulatory responses of goats: A review. *Biol Rhythm Res*, 52 (3): 407-433, 2021. DOI: 10.1080/09291016.2019.1603692

7. Mader TL, Davis MS, Brown-Brandl T: Environmental factors influencing heat stress in feedlot cattle. *J Anim Sci*, 84 (3): 712-719, 2006. DOI: 10.2527/2006.843712x

8. Howard JG, Wildt DE, Chakraborty PK, Bush M: Reproductive traits including seasonal observations on semen quality and serum hormone concentrations in the Dorcas gazelle. *Theriogenology*, 20 (2): 221-234, 1983. DOI: 10.1016/0093-691X(83)90218-2

9. Ritar AJ: Seasonal changes in LH, androgens and testes in the male Angora goat. *Theriogenology*, 36 (6): 959-972, 1991. DOI: 10.1016/0093-691X(91)90321-4

10. Darbeïda H, Brudieux R: Seasonal variations in plasma testosterone and dihydrotestosterone levels and in metabolic clearance rate of testosterone in rams in Algeria. *J Reprod Fertil*, 59 (1): 229-235, 1980. DOI: 10.1530/jrf.0.0590229

11. Allaoui A, Safsaf B, Tlidjane M, Djaalab I, Mansour HD: Effect of increasing levels of wasted date palm in concentrate diet on reproductive performance of Ouled Djellal breeding rams during flushing period. *Vet World*, 11 (5): 712-719, 2018. DOI: 10.14202/vetworld.2018.712-719

12. Gherissi DE, Afri-Bouzebda F, Bouzebda Z: Seasonal changes in the testicular morphology and interstitial tissue histomorphometry of Sahraoui camel under Algerian extreme arid conditions. *Biol Rhythm Res*, 49 (2): 291-301, 2018. DOI: 10.1080/09291016.2017.1357331

13. Zarazaga LA, Guzman JL, Dominguez C, Perez MC, Prieto R: Effects of season and feeding level on reproductive activity and semen quality in Payoya buck goats. *Theriogenology*, 71 (8): 1316-1325, 2009. DOI: 10.1016/j.theriogenology.2009.01.007

14. Charallah S, Lakhdari Y, Amirat Z, Khammar F, Sempere A: Variations saisonnières hormonales de l'activité sexuelle chez la chèvre bédouine. *Bull Soc Ecophysiol*, 18 (1-2): 67-70, 1993.

15. Chakhma A, Khaldoun-Benabbas M, Charallah-Cherif S, Kassouri S, Khammar F, Amirat Z: Annual changes in plasma progesterone and estradiol-17β concentrations compared to pituitary-adrenal axis activity in the female goat reared under arid environment. *Biol Rhythm Res*, 52, 1394-1411, 2021. DOI: 10.1080/09291016.2019.1630920

16. Chemineau P, Bodin L, Migaud M, Thiery JC, Malpaux B: Neuro-endocrine and genetic control of seasonal reproduction in sheep and goats. *Reprod Domest Anim*, 45 (s3): 42-49, 2010. DOI: 10.1111/j.1439-0531.2010.01661.x

17. Ertek S: Molecular economy of nature with two thyrotropins from different parts of the pituitary: Pars tuberalis thyroid-stimulating hormone and pars distalis thyroid-stimulating hormone. *Arch Med Sci,* 17 (1): 189-195, 2021. DOI: 10.5114/aoms/102476

18. Yasuo S, Nakao N, Ohkura S, Iigo M, Hagiwara S, Goto A, Ando H, Yamamura T, Watanabe M, Watanabe T, Oda S, Maeda K, Lincoln GA, Okamura H, Ebihara S, Yoshimura T: Long-day suppressed expression of type 2 deiodinase gene in the mediobasal hypothalamus of the Saanen goat, a short-day breeder: implications for seasonal window of thyroid hormone action on reproductive neuroendocrine axis. *Endocrinology*, 147 (1): 432-440, 2006. DOI: 10.1210/en.2005-0507

19. Chergui N, Mormede P, Foury A, Khammar F, Amirat Z: Seasonal effects on plasma cortisol concentrations in the Bedouin buck: Circadian studies and response to ACTH. *Animal*, 11 (3): 445-451, 2017. DOI: 10.1017/S1751731116001671

20. Todini L: Thyroid hormones in small ruminants: Effects of endogenous, environmental and nutritional factors. *Animal*, 1 (7): 997-1008, 2007. DOI: 10.1017/S1751731107000262

Kafkas Universitesi Veteriner Fakultesi Dergisi
ISSN: 1300-6045 e-ISSN: 1309-2251
Journal Home-Page: http://vetdergikafkas.org

Kafkas Univ Vet Fak Derg
27 (6): 733-740, 2021
DOI: 10.9775/kvfd.2021.26203

RESEARCH ARTICLE

Identification of LncRNA Expression in the Estrous Cycle of Qira Black Sheep and Its Combination with miRNA Analysis

Xi CHEN [1,†,a] Hanying CHEN [2,†,b] Song JIANG [1,c] Hong SHEN [1,d] Xiancun ZENG [1,e (*)]

[†] *These authors contributed equally to this study*
[1] College of Animal Science and Technology, Shihezi University, 832003 Shihezi, Xinjiang, CHINA
[2] School of Pharmacy, Shihezi University, 832002 Shihezi, Xinjiang, CHINA
ORCIDs: [a] 0000-0003-0457-1823; [b] 0000-0002-3792-0316; [c] 0000-0002-1690-3939; [d] 0000-0002-6672-5480; [e] 0000-0002-4250-7817

Article ID: KVFD-2021-26203 Received: 09.04.2021 Accepted: 19.10.2021 Published Online: 27.10.2021

Abstract

In order to investigate the expression of lncRNAs in the ovaries of Qira black sheep at different stages of the estrous cycle, Qira black sheep were used as experimental materials in this experiment, and after estrus synchronization, ovarian tissues at four different stages of the estrous cycle were collected to extract total RNA.The samples at different stages were first subjected to genome-wide analysis using RNA-seq technology; target genes of lncRNAs were predicted using co-expression methods; and then GO and KEGG analysis of target genes was performed. Genes related to the estrous cycle of Qira black sheep were also selected to study their transcriptional differences. Finally, lncRNA-miRNA and mRNA-lncRNA-miRNA interaction networks were established to further analyze the effect of lncRNA alignment on Qira black sheep reproduction. The results showed that in the differentially expressed part, 14 lncRNAs were differentially expressed in Estrous VS Diestrus; the differential expression levels of lncRNAs in the two comparison groups of Estrous VS Metestrus and Estrus VS Proestrus were 18 and 24, respectively. The results of GO and KEGG functional enrichment analysis showed that differentially expressed lncRNAs and their target genes were mainly involved in reproduction-related pathways such as retinol metabolism, ovarian sterol production and endosterol biosynthesis. In the combined analysis of lncRNA-miRNA and mRNA-lncRNA-miRNA, genes related to reproduction, such as LNC011583, LNC003443 and bta-miR-202, were found, thus it can be seen that lncRNAs have some effect in the reproduction of Qira black sheep.

Keywords: *Estrous, Ovary, LncRNA, Qira black sheep*

Qira Kara Koyunlarında Östrus Siklusunda LncRNA Ekspresyonunun Belirlenmesi ve miRNA Analizi İle Kombinasyonu

Öz

Bu çalışmada, Qira kara koyunlarının ovaryumlarında lncRNA'ların ekspresyonunun araştırılması için materyal olarak östrus siklusunun farklı aşamalarında olan Qira kara koyunları kullanıldı. Total RNA eldesi amacıyla, östrus senkronizasyonunu takiben siklusun dört farklı aşamasından ovaryum dokuları toplandı. Farklı aşamalardaki örnekler, önce RNA-seq teknolojisi kullanılarak genom çapında analize tabi tutuldu, lncRNA'ların hedef genleri birlikte ifade edilme yöntemleri kullanılarak tahmin edildi ve takiben hedef genlerin analizi GO ve KEGG ile gerçekleştirildi. Qira kara koyunlarında östrus siklusu ile ilgili genler, transkripsiyonel farklılıklarının araştırılması amacıyla seçildi. Son olarak, lncRNA hizalamasının Qira kara koyunlarında üreme üzerine etkisini daha fazla analiz etmek için lncRNA-miRNA ve mRNA-lncRNA-miRNA etkileşim ağları kuruldu. Sonuçlar, çeşitli ekspresyon bölgelerinde, 14 lncRNA'nın diöstrusa göre östrusta farklı şekillerde eksprese edildiğini gösterdi ve metöstrusa karşı östrus ve proöstrusa karşı östrus gruplarında lncRNA'ların diferansiyel ekspresyon seviyeleri sırasıyla 18 ve 24 saptandı. GO ve KEGG fonksiyonel zenginleştirme analizleri, farklı şekilde eksprese edilen lncRNA'ların ve bunların hedef genlerinin, esas olarak retinol metabolizması, yumurtalık sterol üretimi ve endosterol biyosentezi gibi üreme ile ilgili fonksiyonlarda yer aldığını gösterdi. lncRNA-miRNA ve mRNA-lncRNA-miRNA'nın kombine analizi sonucu, LNC011583, LNC003443 ve bta-miR-202 gibi üreme ile ilgili genler saptandı, dolayısıyla lncRNA'ların Qira kara koyunlarının üremesinde bir miktar etkisinin olduğu görülebilir.

Anahtar sözcükler: *Östrus, Ovaryum, LncRNA, Qira kara koyunu*

INTRODUCTION

In general, the boundary of mammalian singleton and multiple birth traits is relatively obvious, but there is diversity in this trait in sheep, and it is of great scientific value to study the mechanism of multiple birth in sheep [1].

How to cite this article?

Chen X, Chen H, Jiang S, Shen H, Zeng X: Identification of LncRNA expression in the estrous cycle of Qira black sheep and its combination with miRNA analysis. *Kafkas Univ Vet Fak Derg,* 27 (6): 733-740, 2021.
DOI: 10.9775/kvfd.2021.26203

(*) **Corresponding Author**

Tel: +86 137 79204376
E-mail: zengxiancun@163.com (X. Zeng)

Qira black sheep is a multiparous fine landrace mainly producing lamb skin and is a characteristic sheep in Xinjiang. Due to its special ecological environment, it is characterized by resistance to coarse feeding, early sexual maturity, perennial estrus, and high fertility [2-4]. Among them, annual estrus and high reproductive rate are prominent breed characteristics of Qira black sheep and these characteristics are rare among sheep breeds in Xinjiang. Therefore, it is important to fully study and develop the excellent performance and multiparity of Qira black sheep for the long-term development of Xinjiang sheep.

Long non-coding RNAs (lncRNAs) are non-coding RNAs greater than 200 nucleotides in length. Studies have shown that lncRNAs play an important role in regulating cellular processes, including transcriptional regulation, intracellular substance transport and chromosome remodeling [5]. Their low expression, poor conservation between species and cellular expression specificity of lncRNAs, make them hot spots [6,7]. LncRNAs are involved in the regulation of various processes in the nucleus and cytoplasm, involving biological development processes such as immunology, neurobiology, cancer and stress [8], so the majority of studies on lncRNAs are still the related regulation and effects of lncRNAs on human cancers.

In recent years, more and more studies have shown that lncRNAs play an important role in sheep reproduction [9]. During the estrous cycle, follicles undergo multiple processes such as development, maturation, ovulation, and luteinization, and the development of follicles is regulated by many regulatory factors [10]. Zheng et al.[11] demonstrated the role of lncRNAs in the initial stages of follicular development. But the expression of lncRNAs in various stages of follicles is unknown. The aim of this study was to analyze and compare the expression of lncRNAs in the ovaries of Qira black sheep at different stages of the estrous cycle. To understand the regulatory mechanism of lncRNAs on follicles at different stages of their growth and development. And the effect of lncRNA countermeasures on the fecundity of Qira black sheep. It provides some reference for future studies on the regulation of follicular growth and development and the effect of lncRNAs on fertility.

Material and Methods

Ethics Statement

All experimental procedures were approved (A2016-085) by the Ethics Committee of Animal Experimental of the First Affiliated Hospital, Shihezi University School of Medicine. All methods were carried out in accordance with relevant guidelines and regulations. During the experiment, every effort was made to minimize suffering by the animals.

Sample Collection and Preparation

In this experiment, Xinjiang Qira Black Sheep, which is multiparous and productive, was selected as the experimental animal. Twelve healthy Qira black sheep (about 3-4 years old and weighing about 35-40 kg and all of them are multiparous) were selected from sheep farms in Qira County, Xinjiang Province, China. All sheep were kept under the same conditions with free access to food and treated with a vaginal sponge (injected with human synthetic progesterone) to synchronize the estrous cycle. Estrus was monitored twice daily by oestrus rams and vaginal examination. After determination of the second estrus, ovarian tissues were collected separately according to the following criteria according to groups: day 0 is estrus; 9-10 days before estrus is diestrus; 1-2 days before estrus is proestrus; and 2-3 days after estrus is diestrus. Then follow the test needs, follicular development rules and reproductive endocrine changes, the ovaries of the four periods were divided into four groups with three replicates in each group: these were diestrus (QD1, QD2, QD3), proestrus (QP1, QP2, QP3) estrus (QE1, QE2, QE3), and metestrus (QM1, QM2, QM3) *(Table 1)*. After the test sheep were slaughtered, ovarian tissue with follicles was obtained.

RNA Library Construction and Sequencing

Total RNA was extracted from each sheep ovarian tissue according to the manufacturer's recommendations, and the extracted RNA was then subjected to quality testing and integrity assessment (Agilent Technologies, CA, USA). A total of 3 μg RNA was used for each sample as input material for RNA sample preparation, for a total of 12 samples. First, ribosomal RNA was removed by the Epicenter-Ribo-zero rRNA Removal Kit (Epicentre, USA), and residues without rRNA were cleared by ethanol precipitation. Subsequently, sequencing libraries were generated using rRNA depleted RNA using the NEBNext Ultra Directed RNA Library Preparation Kit for Illumina (NEB, USA) according to the manufacturer's recommendations. Finally, sequencing libraries constructed using appropriate PCR cycles were sequenced by Novogene (Beijing, China) on an Illumina genome analyzer. Samples were averaged for subsequent assays.

Table 1. *Experimental grouping*

Grouping	Diestrus (QD)			Proestrus (QP)			Estrus (QE)			Metestrus (QM)		
Reoeat	QD1	QD2	QD3	QP1	QP2	QP3	QE1	QE2	QE3	QM1	QM2	QM3
Quantity	1	1	1	1	1	1	1	1	1	1	1	1

Data Analysis

Quality Control and Screening of lncRNAs: Raw data in fastq format (raw reads) were first processed through an in-house perl script to obtain clean data, then bowtie2 (v2.2.8) *(http://bowtie-bio.sourceforge.net/bowtie2/manual.shtml)* was used to build the index of the reference genome, and finally HISAT2(v2.0.4) [12] *(http://daehwankimlab.github.io/hisat2/)* was used to align the clean reads at the paired ends to the reference genome (reference genome and gene model annotation files were downloaded directly from the genome website). StringTie (v1.3.1) [13] *(http://ccb.jhu.edu/software/stringtie/#contact)* was used, the mapped reads for each sample were assembled. Finally, we predicted target genes by co-expression.

Differential Expression and Functional Enrichment: First, by observing the distribution of differential transcripts on the chromosome, and the linked expression of their surrounding transcripts, we can pick out the target genes related to the study. Then, hierarchical cluster analysis was performed by FPKM expression levels of differential transcripts under different experimental conditions. Finally, through the volcano plot, the overall distribution of differential transcripts or genes can be visually seen. In this experiment, we selected candidate lncRNAs for subsequent analysis based on the transcriptional assembly results of lncRNAs, combined with the functional characteristics of lncRNA non-coding proteins as well as their structural characteristics. Differential expression in gene expression data was determined using Cuffdiff (v2.1.1) *(http://cole-trapnell-lab.github.io/cufflinks/manual/)* software and the Ballgown suite, where transcripts with $P<0.05$ were designated as differentially expressed.

Gene Ontology (GO) enrichment analysis of differentially expressed genes or lncRNA target genes was implemented by the GOseq R software package. We used KOBAS software to test the statistical enrichment of differential expression genes or lncRNA target genes in KEGG pathways [14]. KEGG is a database resource for understanding high-level functions and utilities of the biological system [15] *(http://www.genome.jp/kegg/)*.

lncRNA-miRNA-mRNA Association Analysis: LncRNAs, as a type of ceRNAs (competing endogenous RNAs) [16,17], can competitively bind miRNAs with genes, so we searched for lncRNA-miRNA-gene pairs that also possess miRNA binding sites for combined analysis.

qRT-PCR: QRT-PCR was used in this experiment to validate gene expression levels. The amplification procedure was performed using a two-step method: 95°C 30 s; 95°C 5s, 60°C 30 s, for 45 cycles in total. Each sample was repeated three times for a total of 12 samples. Information about primers for qRT-PCR using GAPDH as the reference gene is shown in *Table 2*. Finally, the statistical analysis of the test data was performed using the $2^{-\triangle\triangle ct}$ method for relative quantitative analysis, and the statistical software SPSS 17.0 was used for significance test.

Result

Overview of Sequencing Data

In total, there were 12 libraries in this study, as shown in *Table 1*, resulting in 1,694,019,460 raw reads. In order to ensure the quality of the data and remove the adapter-bearing, low-quality reads inside, 1,647,629,538 clean reads were obtained after screening. Among them, clean reads accounted for 99.99% of raw reads.91.73% ~ 93.99% of clean reads in all libraries were successfully mapped to the reference genome *(Table 3)*. To further validate the data, we selected 2 differentially expressed lncRNAs targeting reproduction-related genes and determined their expression levels by qRT-PCR, and the results were verified to be consistent with those obtained by sequencing *(Fig. 1)*.

Screening of lncRNAs

A total of 11981 lncRNAs, 13,831 TUCPs and 22,824 mRNAs were identified in all samples for further analysis *(Fig. 2-A)*. We obtained Pearson correlation coefficients between 0.875 and 0.949 among the samples, of which the highest correlation with QD1 is QM3 (0.949) *(Fig. 2-B)*. The results showed that the expression levels of ovaries were almost consistent during the four stages of the estrous cycle *(Fig. 3-A)*, while the expression levels of lncRNAs and TUCP were much lower than those of mRNAs *(Fig. 3-B)*.

Differential Expression Analysis

In this experiment, we identified 11981 lncRNAs and 22,824 mRNAs from the ovaries of Qira Black sheep for further

Table 2. *Lnc-010801, lnc-008562 and internal reference amplification primers*

Primer	Gene Sequence	Fragment Size/bp
GAPDH-F	CCTGCCAAGTATGATGAGAT	119
GAPDH-R	TGAGTGTCGCTGTTGAAGT	
LNC-010801-F	GCGGGAAGTCCTGTCCTCT	124
LNC-010801-R	CGAAAAGTCCGAAACACCAG	
LNC_008562-F	CGCCAAATCGGAGTAAACA	100
LNC_008562-R	AATTCATCCAGGCAGGGTC	

Table 3. *The summary of sample data quality*

Sample Name	Raw Reads	Clean Reads	Clean Bases	Error Rate(%)	Q20 (%)	Q30 (%)	GC Content (%)
He1	90840870	88180586	13.23G	0.01	97.79	94.2	49.09
He2	120787312	117362696	17.6G	0.01	97.7	93.94	48.18
He3	114504810	111147030	16.67G	0.01	97.88	94.37	48.6
QD1	121671830	118548894	17.78G	0.01	97.73	94.03	48.26
QD2	111730482	108979944	16.35G	0.01	97.8	94.18	47.82
QD3	123522800	121471712	18.22G	0.01	97.15	93.23	48.47
QE1	109926982	106702328	16.01G	0.01	97.66	93.95	48.42
QE2	115505728	112006036	16.8G	0.01	97.75	94.15	48.63
QE3	121606340	118252002	17.74G	0.01	97.72	94.08	47.17
QM1	113856982	110990072	16.65G	0.01	97.78	94.15	49.28
QM2	121209526	117616398	17.64G	0.01	97.62	93.8	47.37
QM3	116530402	113689300	17.05G	0.01	97.75	94.1	47.42
QP1	110697120	107454358	16.12G	0.01	97.85	94.35	50.25
QP2	103318274	100061160	15.01G	0.01	97.82	94.27	49.01
QP3	98310002	95167022	14.28G	0.01	97.44	93.39	47.96

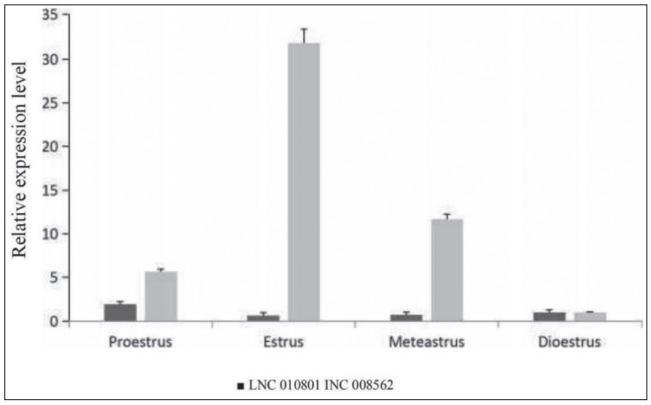

Fig 1. QRT-PCR validation of differentially expressed genes

was the most differentially expressed, with 15 up-regulated and 9 down-regulated. The remaining two comparison groups also had up- and down-regulated genes, respectively. From the lncRNA differential expression clustering results plot *(Fig. 4-D)*, we can see that the three proestrus groups (QP1/2/3) and the three estrus groups (QE1/2/3) were clustered, indicating that the differences between these two groups were quite different.

GO and KEGG Enrichment Analysis

In this experiment, target genes were predicted by means of co-expression. A total of 13,0152 potential target genes were identified by co-expression, and GO and KEGG analyses were performed on these potential target genes.

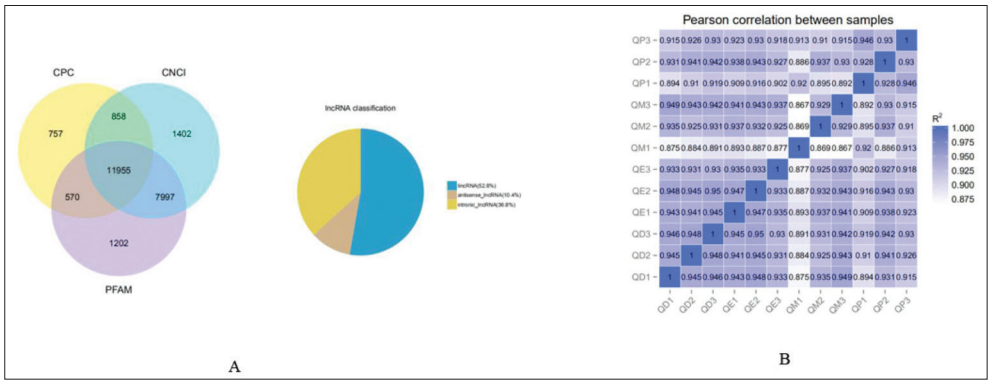

Fig 2. Screening results **(A)** and correlation expression **(B)**

analysis. Differential expression analysis was performed using Ballgown. In this experiment, we will elaborate the overall differential expression of lncRNAs from three comparison groups: QE_VS_QD, QE_VS_QM and QE_VS_QP.

We obtained differential expression results for the three comparison groups *(Fig. 4-A,B,C)*. Among them, QE_VS_QP

After obtaining the 56 differentially expressed lncRNAs, the target genes of these lncRNAs were subjected to GO enrichment analysis and their functions were described. GO analysis showed that all were divided into BP (biological process), CC (cellular component) and MF (molecular function). From the GO enrichment histogram *(Fig. 5-A)*, the GO terms of these differentially expressed lncRNA

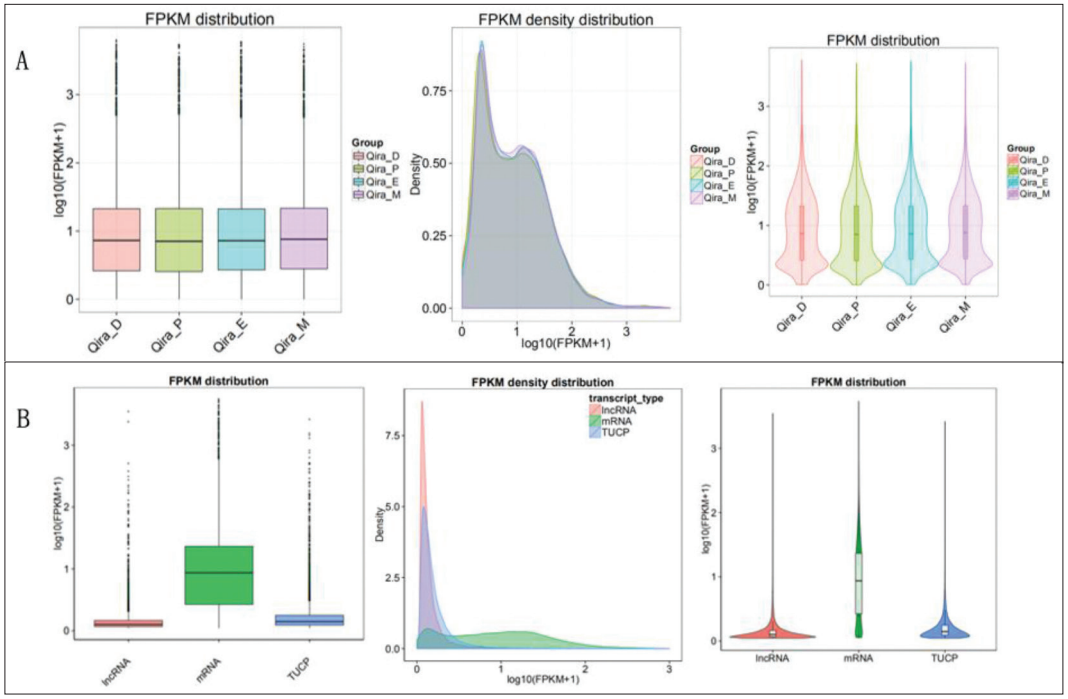

Fig 3. Comparison of expression levels of each group **(A)** and each gene **(B)**

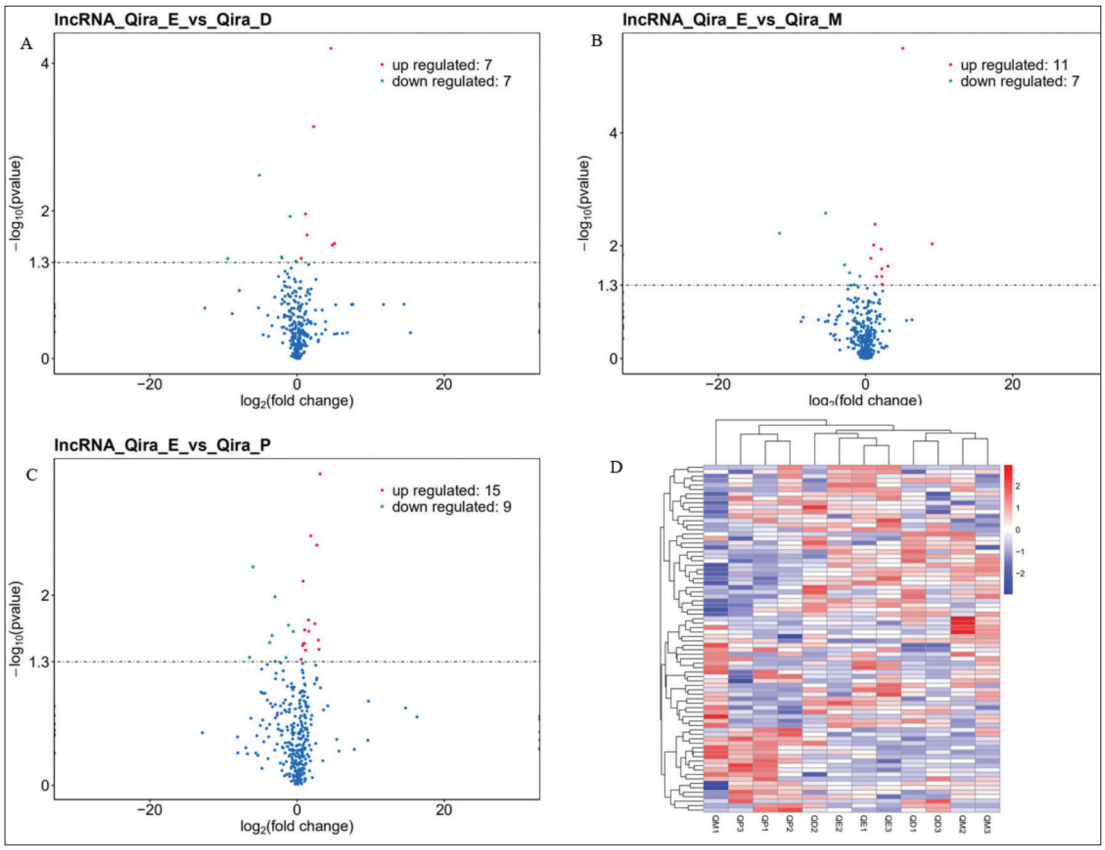

Fig 4. Differential expression in each comparison group **(A,B,C)** and differential expression clustering results **(D)**

target genes are enriched for several processes, such as: transcription, DNA-dependent, RNA biosynthetic process, neutral lipid catabolic process, etc.

The scatter plot is a graphical presentation of the KEGG enrichment analysis results, and we picked the 20 pathway entries with the most significant enrichment for

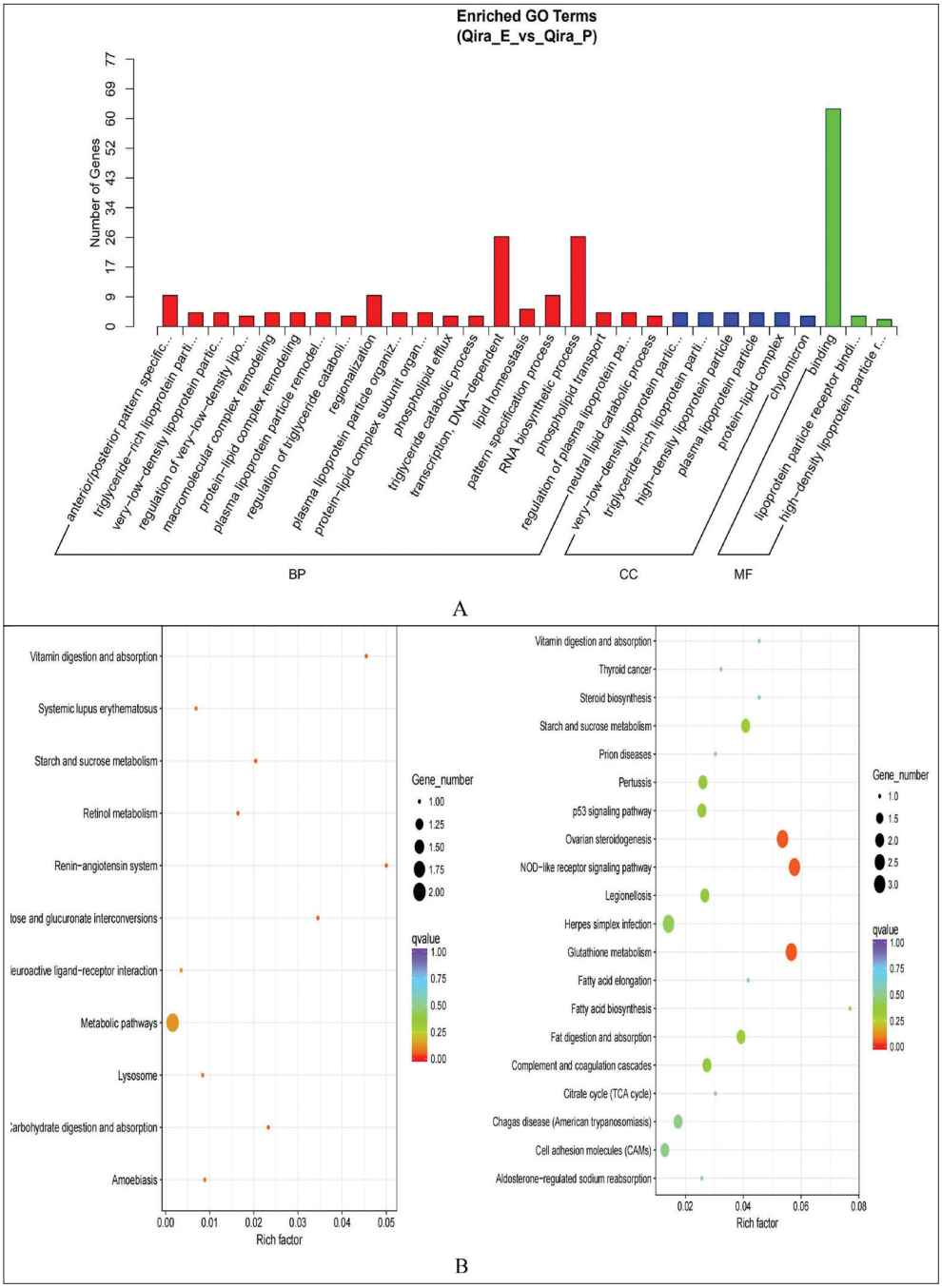

Fig 5. GO **(A)** and KEGG **(B)** analysis results of differentially expressed lncRNA target genes

presentation in this plot. KEGG analysis of heterologously expressed co-expressed lncRNA target genes showed that they were rich in pathways related to reproduction: Jak-STAT signaling pathway, retinol metabolism, Ovarian steroidogenesis, etc. *(Fig. 5-B)*.

LncRNA-miRNA-mRNA Association Analysis

By constructing an interactive network diagram of miRNA-lncRNAs (miRNAs have been proposed in other literature), we can better understand the involvement and function of lncRNAs in the estrous cycle of Qira Black Sheep. We constructed the interaction network of miRNA-lncRNAs separately for the three comparison groups *(Fig. 6-A,B,C)*. We obtained 248 miRNA-lncRNA interaction combinations with potential relationship compared by QE_VS_QP, of which LNC001917, LNC011056, LNC003367, LNC009395, LNC003443, etc. could interact with multiple different miRNAs, so they were in the middle position, and it can be speculated that these genes play a role in the regulation of estrous cycle in Qira black sheep. However, in the QE_VS_QD and QE_VS_QM comparison groups, we also obtained 175 and 22 interaction network graphs with potential relationships, respectively.

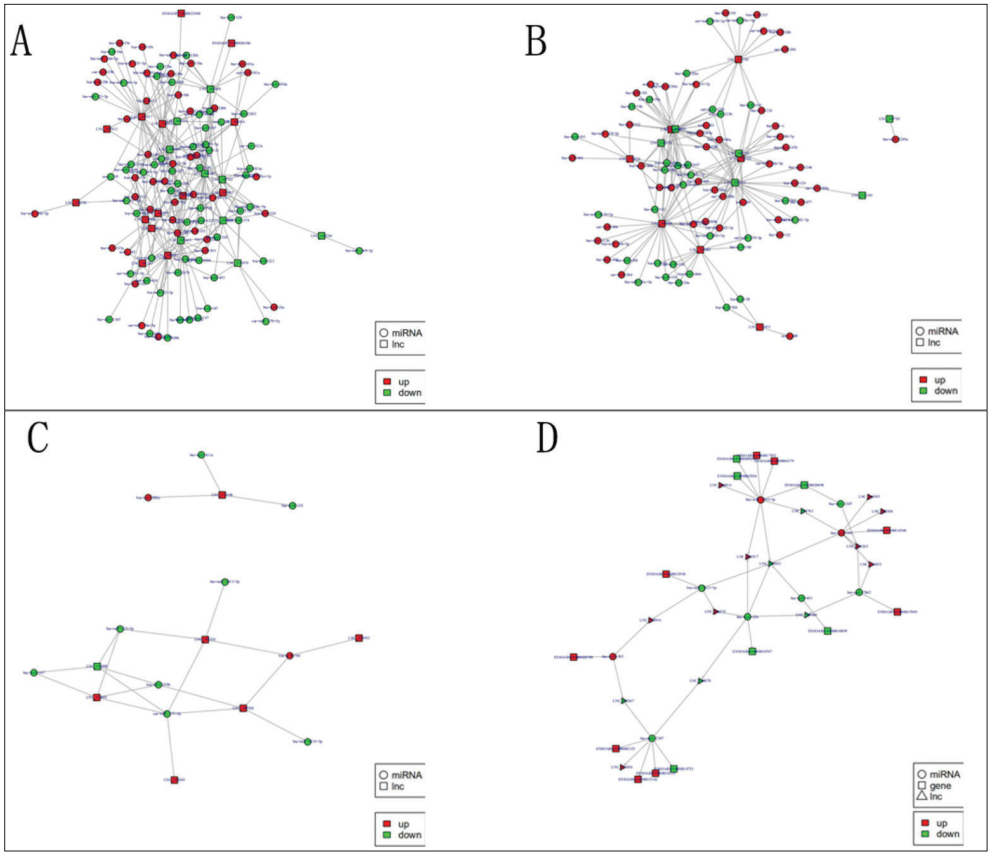

Fig 6. Target lncRNA-miRNA interaction net **(A,B,C)** and Target miRNA-lncRNA-mRNA interaction net **(D)**

We also constructed an interaction network map of miRNA-lncRNA-mRNA *(Fig. 6-D)*. We obtained that in QE_VS_QP, bta-miR-1343-5p, bta-miR-2411-5p, bta-miR-2387, etc. are at the comparative core position because they are able to interact with the most genes. Among them, LNC001917, LNC003443 and LNC001763 can interact with multiple different miRNAs, so we speculated that these genes may play a role in the regulation of the estrous cycle in Qira Black sheep.

Discussion

From the results of GO and KEGG enrichment analysis in this experiment, it can be seen that the most significantly different GO term is the term of the cofactor. However, it has been shown that [18], the cofactors may catalyze the synthesis of steroid hormones by increasing enzyme activity. In the results of KEGG enrichment analysis of lncRNAs, there is also a pathway of cytochrome P450 enzymes, which are expressed in both ovarian testes and play an important role in the synthesis of anabolic steroids and maintenance of sex hormones [19]. In KEGG enrichment analysis of lncRNA target genes, we obtained pathways related to fecundity as: retinol metabolism, ovarian endosterol production and endosterol biosynthesis. Studies have found that retinol and its derivatives play an important role in ovarian steroidogenesis, oocyte maturation and early embryonic development, are abundant in cumulus granulosa cells, and are involved in signaling related to ovarian development [20-22].

In the combined analysis of lncRNA-miRNAs, we obtained that bta-miR-26b was present in the gene interacting with LNC011583 in the QE_VS_QD comparison, which was pointed out by [23] that it belongs to the miR-26 family and plays a key role in estrogen stimulation [24]. So we speculated that LNC011583 gene, which interacts with bta-miR-26b, may play a role in estrogen stimulation, thereby affecting the content of estrogen. We also obtained oar-miR-432 and bta-miR-202 genes interacting with LNC003443 gene in QE_VS_QP comparison. Among them, the oar-miR-432 gene is likely to function by directly or indirectly affecting gonadotropin-releasing hormone (GnRH) activity associated with reproductive hormone release [25]. It has been proposed [26] that the bta-miR-202 gene is expressed only in the gonads. On the one hand, we can speculate that when LNC003443 gene interacts with oar-miR-432, it may have an effect on the reproduction of Qira Black sheep by affecting the activity of gonadotropin-releasing hormone (GnRH); on the other hand, when LNC003443 gene interacts with bta-miR-202 gene, it may have an effect on the ovary and thus affect the reproduction of Qira Black sheep.

In this experiment, the target genes of lncRNA-controlled

reproduction-related pathways were obtained by GO and KEGG enrichment analysis. The results showed that the target genes of lncRNAs had an effect on reproductive hormone synthesis such as steroids and retinol, thus we speculated that lncRNAs had some effect on Qira black sheep reproduction. Finally, we also performed a combined analysis combining mRNA and miRNA, speculating on genes that may be associated with reproduction, such as LNC011583 and LNC003443. It further illustrates the expression of lncRNAs during the estrous cycle in Qira black sheep. This experiment provides some reference for the study of fertility in Qira black sheep.

Availability of Data and Materials

The datasets during and/or analyzed during the current study available from the corresponding author on reasonable request.

Acknowledgements and Funding Information

This research was supported by the National Natural Science Foundation of China (31660643 and 31260536). The authors have no competing interests.

Conflict of Interest

The authors declared that there is no conflict of interest.

Author Contributions

XC Zeng designed the study, conducted the experiments, analysed the data, and drafted the manuscript. HY Chen and X Chen designed the study and drafted the manuscript. S Jiang, H Shen conducted parts of the experiments and collected samples.

References

1. Bai J: Candidate Genes of Multiparity in Xinjiang Qira Black Sheep and Duolang Sheep. Shihezi University, 2007. DOI: 10.7666/d.y1165085

2. Yu J, Dong H, Ji Y, Kong Y, Guligena, Meizi B, Yang F, Yassen K, Wen Q, Mizinisha: Current situation of sheep breed resources and protection and utilization measures in Hotan. *Gra-fee Livest*, 2, 7-9, 2011. DOI: 10.3969/j.issn.1003-6377.2011.02.003

3. Tan R, Cong LY, Yang QY, Xu CS: Study on protection and utilization scheme of Qira Black Sheep. *Gra-fee Livest*, 3, 31-33, 2011. DOI: 10.3969/j.issn.1003-6377.2011.03.011

4. Shao YY, Megenisha K, Yan MY, Yan MY, Fan QX, Yuan XF, Zeng XC: Expression of LNC-010801 and LNC-008562 in the ovary of Qira Black Sheep at different stages of estrous cycle. *Chin Herb Sci*, 38 (6): 9-12, 2018. DOI: 10.3969/j.issn.2095-3887.2018.06.003

5. Gong Y, Ma HM: Progress in transcriptional LncRNA in pigs. *Swine Ind Sci*, 296 (2): 100-106, 2020.

6. Birney E, Stamatoyannopoulos JA, Dutta A, Roderic Guigó, Gingeras TR, Margulies EH, Weng Z, Snyder M, Dermitzakis ET: Identification and analysis of functional elements in 1% of the human genome by the ENCODE pilot project. *Nature*, 447, 799-816, 2007. DOI: 10.1038/nature05874

7. Chen LL, Feng SS, Fan ZS, Gong C, Liu BY, Liu ZH, Li CW, Song EW, Sun SH, Wu GZ, Wu H, Wu M, Xu G, Yuan JH, Zeng CY, Zhu YM: Progress in non-coding RNA research. *Sci Sin Vita*, 49 (12): 1573-1605, 2019. DOI: 10.1360/SSV-2019-0179

8. Niu CY, Xue LL, Ji H, Li SZ: Progress in the biological function of lncRNAs. *Chin J Biol Prod*, 32 (2): 228-232, 2019.

9. Feng X, Li F, Wang F, Zhang G, Pang J, Ren C, Zhang T, Yang H, Wang Z, Zhang Y: Genome-wide differential expression profiling of mRNAs and lncRNAs associated with prolificacy in Hu sheep. *Biosci Rep*, 38 (2): BSR20171350, 2018. DOI: 10.1042/BSR20171350

10. Han DX, Sun XL, Wang CJ, Yu ZW, Zheng Y, Huang YJ, Wang WH, Jiang H, Gao Y, Yuan B: Differentially expressed lncRNA-m433s1 regulates FSH secretion by functioning as a miRNA sponge in male rat anterior pituitary cells. *Biol Reprod,* 101, 416-425, 2019. DOI: 10.1093/biolre/ioz100

11. Zheng LP, Luo RC, Su T, Hu LL,Gao FX, Zhang XN: Differentially expressed lncRNAs after the activation of primordial follicles in mouse. *Reprod Sci*, 26 (8): 1094-1104, 2019. DOI: 10.1177/1933719118805869

12. Langmead B, Salzberg SL: Fast gapped-read alignment with Bowtie 2. *Nat Methods*, 9 (4): 357-359, 2012. DOI: 10.1038/nmeth.1923

13. Pertea M, Daehwan K, Geo MP, Jeffrey TL, Salzberg SL: Transcript-level expression analysis of RNA-seq experiments with HISAT, StringTie and Ballgown. *Nat Protoc*, 11 (9): 1650-1667, 2016. DOI: 10.1038/nprot.2016.095

14. Mao XZ, Cai T, Olyarchuk JG, Wei LP: Automated genome annotation and pathway identification using the KEGG Orthology (KO) as a controlled vocabulary. *Bioinformatics*, 21 (19): 3787-3793, 2005. DOI: 10.1093/bioinformatics/bti430

15. Minoru K, Michihiro A, Susumu G, Masahiro H, Mika H, Masumi I, Toshiaki K, Shuichi K, Shujiro O, Toshiaki T: KEGG for linking genomes to life and theenvironment. *Nucleic Acids Res*, 36, D480-D484, 2018. DOI: 10.1093/nar/gkm882

16. Salmena L, Poliseno L, Tay Y, Kats L, Pandolf PP: A ceRNA hypothesis: The rosetta stone of a hidden RNA language. *Cell,* 146, 353-358, 2011. DOI: 10.1016/j.cell.2011.07.014

17. Tay Y, Rinn J, Pandolf PP: The multilayered complexity of ceRNA crosstalk and competition. *Nature*, 505, 344-352, 2014. DOI: 10.1038/nature12986

18. Xie J: Analysis of lncRNA and mRNA in Goat Ovary at Different Stages of Estrous Cycle. *Fuyang Normal University*, 2019.

19. Hakki T, Silvia Z, Dragan CA, Bureik M, Bernhardt R: Coexpression of redox partners increases the hydrocortisone (cortisol) production efficiency in CYP11B1 expressing fission yeast *Schizosaccharomyces pombe*. *J Biotechnol,* 133, 351-359, 2008. DOI: 10.1016/j.jbiotec.2007.06.022

20. Brown JA, Eberhardt DM, Schrick FN, Roberts MP, Godkin JD: Expression of retinol-binding protein and cellular retinol-binding protein in the bovine ovary. *Mol Reprod Dev*, 64 (3): 261-269, 2003. DOI: 10.1002/mrd.10225

21. Mohan M, Thirumalapura NR, Malayer J: Bovine cumulus granulosa cells contain biologically active retinoid receptors that can respond to retinoic acid. *Reprod Biol Endocrin*, 1:104, 2003. DOI: 10.1186/1477-7827-1-104

22. ZhaoYY, Zhang YM, Liu Y, Li WT, Yang YL: Progress in the role of retinol in ovarian development. *Chin J Anim Husb*, 55 (5): 1-5, 2019.

23. Gu B, Liu H, Han Y, Chen Y, Jiang HZ: Integrated analysis of miRNA and mRNA expression profiles in 2-, 6-, and 12-month-old Small Tail Han Sheep ovaries reveals that oar-miR-432 downregulates RPS6KA1 expression. *Gene,* 710, 76-90. 2019. DOI: 10.1016/j.gene.2019.02.095

24. Maillot G, Lacroix-Triki M, Pierredon S, Gratadou L, Schmidt S, Bénès V, Roché H, Dalenc F, Auboeuf D, Millevoi S, Vagner S: Widespread estrogen-dependent repression of micrornas involved in breast tumor cell growth. *Cancer Res,* 69, 8332-8340, 2009. DOI: 10.1158/0008-5472.can-09-2206

25. Zhang ZB, Tang JS, Di R, Liu QY, Hu W: Integrated hypothalamic transcriptome profiling reveals the reproductive roles of mRNAs and miRNAs in sheep. *Front Genet*, 10:1296, 2020. DOI: 10.3389/fgene.2019.01296

26. Sontakke SD, Mohammed BT, McNeilly AS, Donadeu FX: Characterization of microRNAs differentially expressed during bovine follicle development. *Reproduction*, 148 (3): 271-283, 2014. DOI: 10.1530/rep-14-0140

Kafkas Universitesi Veteriner Fakultesi Dergisi
ISSN: 1300-6045 e-ISSN: 1309-2251
Journal Home-Page: http://vetdergikafkas.org

Kafkas Univ Vet Fak Derg
27 (6): 741-747, 2021
DOI: 10.9775/kvfd.2021.26239

RESEARCH ARTICLE

Detection of Bacterial Isolation and Antimicrobial Resistance Profiles in Goat Mastitis

Seyyide SARIÇAM İNCE [1,a (*)] Ayhan BAŞTAN [2,b] Seçkin SALAR [2,c]
Ezgi DİKMEOĞLU [2,d] Tuğba OĞUZ [2,e] Mehmet AKAN [1,f]

[1] Ankara University, Faculty of Veterinary Medicine, Department of Microbiology, TR-06110 Ankara - TURKEY
[2] Ankara University, Faculty of Veterinary Medicine, Department of Obstetrics and Gynaecology, TR-06110 Ankara - TURKEY
ORCIDs: [a] 0000-0002-2386-6857; [b] 0000-0001-8291-1147; [c] 0000-0001-9303-6253; [d] 0000-0002-9146-7321; [e] 0000-0002-9359-0366
[f] 0000-0002-7342-1450

Article ID: KVFD-2021-26239 Received: 05.07.2021 Accepted: 15.10.2021 Published Online: 15.10.2021

Abstract

Mastitis is one of the most common infections worldwide. This infection poses risks to animal and public health. Therefore, determination of mastitis pathogens is important for the prevention of the infection. Generally, the combination of antimicrobials is an effective, reliable and common treatment approach. In this study, it was aimed to determine the bacterial mastitis pathogens in goat's milk and antimicrobial resistance profiles of these pathogens. A total of 190 goat milk samples were examined with standard microbiological analysis in the period of 2018-2019. Bacterial mastitis pathogens were obtained in 33.2% of all samples. Totally, 79 different bacterial agents were isolated due to multiple-bacterial isolation. Major genus was detected as *Staphylococcus* spp. (66%): coagulase-negative *Staphylococcus* (CNS) 44% and coagulase-positive *Staphylococcus* (CPS) 22%. This group was followed by respectively *Bacillus* spp. (17.6%), catalase-negative cocci (PNC) (14%), *Mannheimia* spp. (1.2%) and *Micrococcus* spp. (1.2%). The most prevalent species were identified *Staphylococcus caprae* (27%), *Staphylococcus aureus* and *Staphylococcus chromogenes* (13%), *Aerococcus viridans* and *Bacillus cereus* (7.6%). Considering the antimicrobial resistance test, tetracycline has the highest resistance rate (31%) among the tested antimicrobials. A total of 4 multi-drug resistant isolates were found: an *Enterococcus faecalis* and three *Streptococcus uberis* isolates. The highest resistance rate (35.7%) was observed for penicillin in all *Bacillus* spp. isolates.

Keywords: *Coagulase-negative Staphylococcus, Goat milk, Mastitis, Staphylococcus caprae*

Keçi Mastitisinde Bakteriyel İzolasyon ve Antimikrobiyal Direnç Profillerinin Tespiti

Öz

Mastitis, dünya çapında en yaygın enfeksiyonlardan biridir. Bu enfeksiyon, hayvan ve halk sağlığı açısından risk oluşturmaktadır. Bu nedenle, mastitis patojenlerinin belirlenmesi enfeksiyonun önlenmesi açısından önemlidir. Antimikrobiyal tedavi, bakteriyel mastitis tedavisinde en güvenilir ve en yaygın olanıdır. Genel olarak birden fazla antimikrobiyalin kombinasyonu, etkili bir tedavi yaklaşımıdır. Bu çalışmada, keçi sütündeki bakteriyel mastitis patojenlerinin saptanması ve bu patojenlerin antimikrobiyal direnç profillerinin belirlenmesi amaçlanmıştır. 2018-2019 yılları arasında toplam 190 keçi sütü örneği standart mikrobiyolojik analizler ile incelendi. Tüm numunelerinin %33.2'sinde bakteriyel mastitis patojenleri tespit edildi. Çoklu bakteriyel izolasyonu nedeniyle toplam 79 farklı bakteri izole edildi. Major bakteri cinsi, %44 koagülaz-negatif Staphylococcus (CNS) ve %22 koagülaz-pozitif *Staphylococcus* (CPS) olmak üzere *Staphylococcus* spp. (%66) olarak belirlendi. *Staphylococcus* cinsini takiben sırasıyla *Bacillus* spp. (%17.6), katalaz-negatif koklar (PNC) (%14), *Mannheimia* spp. (%1.2) ve *Micrococcus* spp. (%1.2) izole edildi. En yüksek prevelansa sahip türler *Staphylococcus caprae* (%27), *Staphylococcus aureus* ve *Staphylococcus chromogenes* (%13), *Aerococcus viridans* ve *Bacillus cereus* (%7.6) olarak tanımlandı. Antimikrobiyal direnç testi dikkate alındığında, test edilen antimikrobiyaller arasında en yüksek direnç tetrasiklinde (%31) tespit edildi. Bir *Enterococcus faecalis* ve üç *Streptococcus uberis* olmak üzere toplam 4 adet çoklu-ilaç dirençli izolat bulundu. Tüm *Bacillus* spp. izolatlarında en yüksek direnç oranı (%35.7) penisilin için gözlendi.

Anahtar sözcükler: *Keçi sütü, Koagülaz-negatif Staphylococcus, Mastitis, Staphylococcus caprae*

How to cite this article?

Sarıçam İnce S, Baştan A, Salar S, Dikmeoğlu E, Oğuz T, Akan M: Detection of bacterial isolation and antimicrobial resistance profiles in goat mastitis. *Kafkas Univ Vet Fak Derg,* 27 (6): 741-747, 2021.
DOI: 10.9775/kvfd.2021.26239

(*) Corresponding Author

Tel: +90 312 317 0315/4372 Cellular phone: +90 551 993 8384 Fax: +90 312 317 60017
E-mail: ssaricam@ankara.edu.tr (S. Sarıçam İnce)

Introduction

Goat milk is a highly nutritious milk containing proteins, minerals and vitamins. The production of goat milk is approximately 19 million tons worldwide [1]. However, milk quality is negatively affected by many factors such as mastitis. Mastitis (intramammary infections, IMI), is one of the most common infections worldwide. IMI affects animals and decreases productivity, quality in milk production industry. This infection also causes economic problems due to treatment and yield decline. Therefore, determination of IMI pathogens is important to control and prevent the infection.

A wide range of, approximately 140, microorganisms are the cause of IMI [2]. The major bacterial pathogens of IMI are coagulase-negative *Staphylococccus* spp., *Staphylococcus aureus, Streptococcus uberis, Streptococcus dysgalactiae, Corynebacterium* spp., *Escherichia coli, Klebsiella* spp.[3]. *Staphylococcus* food poisoning is defined as one of the common foodborne diseases around worldwide. Especially, *S. aureus* IMI is a risk to public health via secretion of enterotoxins [4]. Gram-positive catalase-negative cocci (PNC) have also been responsible for goat IMI. The most common PNC species isolated in IMI are *S. uberis, S. dysgalactiae, Streptococcus agalactiae, Enterococcus faecalis* and *Aerococcus viridans*. Frequently, they have been defined as environmental pathogens in IMI and they are transmitted to ruminants via farm equipment [5]. One of the environmental mastitis pathogens is *Bacillus* spp. has also been identified in clinical and subclinical IMI in previous studies. It poses a risk to producers and consumers of milk in terms of causing zoonotic disease [4,6]. *Bacillus cereus, Bacillus subtilis, Bacillus licheniformis, Bacillus thuringiensis* and *Bacillus circulans* are observed in goat IMI [7]. *Mannheimia* species are frequently observed in pneumonia, they are rarely detected in IMI cases. *M. haemolytica*, *M. glucosida* and *M. ruminalis* was previously investigated in IMI cases as studied by Poulsen et al.[8]. Especially in small ruminants, they have negatively affected animal welfare, productivity, production and quality of meat/milk. Even Omaleki et al.[9] have reported that *Mannheimia* species can be more important than *S. aureus* as a cause of IMI. Considering all these bacterial pathogens, antimicrobial treatment is commonly used to control bacterial IMI in small ruminants as a reliable method. The efficiency of treatment is dependent on the bacterial pathogen, susceptibility of antimicrobial, breed, clinical and environmental conditions. Generally, a combination of more than one antimicrobial is effective to control IMI than using of a single antimicrobial [6,10].

The present study was aimed to determine bacterial mastitis pathogens in goat's milk and antimicrobial resitance profiles of these pathogens. For this purpose, a total of 190 goat milk samples were examined by standard bacteriological analysis and tested for antimicrobials.

Material and Methods

Collection of Samples

The goat milk samples were obtained from a dairy goat farm in the period 2018-2019 located in Ankara, Turkey. A physical examination and California Mastitis Test (CMT) was used to detect mastitis. The samples were taken from positives in the CMT, according to aseptic techniques using sterile gloves, overall and tubes after the cleaning of teats with 70% ethyl alcohol [2]. After drying of alcohol, the first streams were discarded. Approximately 15 mL of individual milk samples were collected from each teat to sterile tube horizontally. In total, 190 milk samples were collected from 190 goats and immediately transported at cold chain. The samples were stored at 4°C until bacteriological analysis [1].

Bacterial Isolation and Identification

Mastitis causing pathogens were identified using standard bacteriological methods. For each milk sample, a loopful sample [~10 µL] was plated on 5% sheep blood agar plates and the plates were incubated at 37°C 24-72 s in aerobic conditions [1]. After incubation, bacterial colonies were separated according to morphological features such as pigmentation, colony form, hemolytic characteristics and purified on new plates. All isolates were examined by Gram staining, catalase, oxidase and oxidation-fermentation (OF) tests. The bacteria were identified using the methods described by Markey et al.[11]. *Staphylococcus* spp. isolates were identified to species based on coagulase tube test, urease production, DNase activity, mannitol fermentation test, polymixin-B test (300 U/disc), novobiocin test (5 µg/disc). Gram-positive cocci in clusters, catalase-positive, coagulase-negative, oxidative, bacitracin test (0.04 U/disc) susceptible bacteria were classified in *Micrococcus* spp. Gram-positive, catalase-negative cocci (PNC), were identified at genus level based on cultures of Edwards agar, MacConkey agar. For PNC, species-level identification was performed by 16S *rRNA* gene sequence analysis. *Enterococcus* spp. isolates were separated by esculin hydrolysis on Edwards agar and growth on MacConkey agar from *Streptococcus* spp. *Bacillus* spp. isolates were identified based on sporulation, nitrate reduction, motility test, hemolysis, MacConkey agar, urease production, Voges-Proskauer, citrate, glucose, penicillin susceptibility. *Mannheimia* spp. isolate was identified based on indole production, nitrate reduction, hemolysis, motility test, growth on MacConkey agar, urease production [7,8,11]. The conventional identification results were confirmed with the BD Phoenix M50 Instrument (BD, USA). Specific identification kits were used for Gram positive and Gram negative taxa in this automated micro-biology system.

16S rRNA Gene Sequence Analysis

DNA extraction was performed with GeneJET Genomic DNA Purification kit, Gram Positive Bacterial DNA extraction protocol (Thermo Fisher Scientific, USA). PCR amplification

of the 16S rRNA gene was performed using a 25 µL PCR reaction, which contained 12.2 µL PCR-grade water, 2.5 µL of 10xbuffer, 0.5 µL 10 mM dNTPs, 2.5 µL $MgCl_2$, 1 µL of each 10 mM primer, 0.3 µL Taq (2U/ µL) and 5 µL template DNA (Thermo Fisher Scientific, USA). For amplification and sequencing, 27F and 1492R universal primers were used [12]. The PCR conditions were as follows: pre-denaturation at 94°C for 4 min, then 35 cycles of 94°C for 30 s, 58°C for 30 s, 72°C for 1 min and final extension at 72°C for 6 min. The PCR products were purified with Exosap-IT (Thermo Fisher Scientific, USA) by incubation at 37°C for 45 min and 80°C for 15 min. BigDye Terminator v3.1 Cycle Sequencing Kit was used for sequence analysis (Thermo Fisher Scientific, USA). The cycle PCR products were purified with Sephadex gel filtration (Oxoid, UK). DNA samples were sequenced on ABI 3500 genetic analyzer system (Applied Biosystems, USA) and were aligned by CLC Main Workbench v.8.0.1 sequence analysis program (Qiagen, USA). DNA sequences were compared by National Centre for Biotechnology Information (NCBI, USA) BLASTN server for identification at the species level (≥99% sequence similarity).

Antimicrobial Resistance Test

Kirby-Bauer Disc Diffusion method was used following the recommendations of the Clinical and Laboratory Standards Institute (CLSI, 2008) [13]. Ampicillin (AMP, 10 µg/disc), cefoxitin (FOX, 30 µg/disc), ciprofloxacin (CIP, 5 µg/disc), clindamycin (DA, 2 µg/disc), cefotaxime (CTX, 30 µg/disc), ceftriaxone (CRO, 30 µg/disc), doxycycline (DO, 30 µg/disc), erythromycin (E, 15 µg/disc), gentamycin (CN, 10 µg/disc), kanamycin (K, 30 µg/disc), ofloxacin (OFX, 5 µg/disc), penicillin-G (P, 10 µg/disc), rifampin (RD, 5 µg/disc), tetracycline (TE, 30 µg/disc), trimethoprim (W, 5 µg/disc) and vancomycin (VA, 30 µg/disc) antimicrobial agents were tested. Ten antimicrobials were tested for *Staphylococcus* spp. isolates: FOX, CIP, DA, E, CN, K, P, TE, W and VA. The methicillin-resistant *Staphylococcus* (MRS) was determined with cefoxitin because cefoxitin is more sensitive detection of mecA-positive isolates [14]. Nine antimicrobials were tested for *Streptococcus* spp. isolates: AMP, DA, CTX, CRO, E, OFX, P, TE and VA. Seven antimicrobials were tested for *Enterococcus* spp. isolates: AMP, CIP, DO, E, RD, TE and VA. After incubation at 35°C±2°C 16-24 s, zone of inhibition was measured (mm). For *Bacillus* spp. isolates, MICs of seven antimicrobial agents (CIP, DA, E, CN, P, TE and VA) were determined by the Broth Microdilution method. The evaluation of results were performed according to the CLSI, 2008. Antimicrobial resistance (AMR) test of *A. viridans, Micrococcus luteus* and *Mannheimia ruminalis* isolates were not performed because of which organisms have excluded from CLSI protocol. Multi-drug resistant (MDR) isolates were detected by resistance to three or more classes of antimicrobials [15].

Results

A total of 190 milk samples were examined with standard microbiological analysis. The conventional identification results were 100% compatible with the results of BD Phoenix M50 automated microbiology system. Sixty three milk samples (33.2%) were found positive for bacterial IMI agents. Totally, 79 different bacterial agents were isolated due to the isolation of more than one bacteria in 15 samples. The combination of different two species were obtained at 14 samples, while the combination of different three species was obtained in one sample *(Table 1)*. The isolates were CNS (44%), CPS (22%), *Bacillus* spp. (17.6%), PNC (14%), *Mannheimia* spp. (1.2%) and *Micrococcus* spp. (1.2%). As a result of 16S rRNA sequence analysis performed for PNC, 6 *A. viridans* and 3 *S. uberis* were determined. The most common species identified were *Staphylococcus caprae* (27%, 21/79), *S. aureus* (13%, 10/79) and *S. chromogenes* (13%, 10/79). The other isolates were identified as belonging to *A. viridans* and *B. cereus* (7.6%, 6/79); *B. pumilis, S. intermedius* and *S. kloosii (*5%, 4/79); *S. hyicus* and *S. uberis* (3.8%, 3/79); *B. licheniformis* and *E. faecalis* 2.6%; *B. thuringiensis, B. circulans, M. luteus,* and *M .ruminalis* (1.2%, 1/79) *(Table 2)*.

Antimicrobial resistance test of the *Staphylococcus* isolates

Table 1. *Species combination and number of positive samples*

Species Combination		Number of Positive Samples
One species	*S. caprae*	11
	S. aureus	9
	B. cereus	6
	A. viridans	5
	S. uberis	3
	E. faecalis	2
	S. intermedius	2
	S. hyicus	2
	B. circulans	1
	B. licheniformis	1
	B. pumilis	1
	B. thuringiensis	1
	M. luteus	1
	M. ruminalis	1
	S. chromogenes	1
	S. kloosii	1
Two species	*S. caprae, S. chromogenes*	4
	S. caprae, S. kloosii	3
	S. chromogenes, B. pumilis	2
	S. chromogenes, S. intermedius	2
	S. aureus, S. caprae	1
	S. caprae, B. pumilis	1
	S. hyicus, A. viridans	1
Three species	*S. caprae, S. chromogenes, B. licheniformis*	1
Total		63 (33.2%)

Table 2. *Prevalence and etiology of bacterial IMI in goat milk*

Group (%)	Species	Number of Isolates (%)
CNS[a] (44)	*S. caprae* *S. chromogenes* *S. kloosii*	21 (27) 10 (13) 4 (5)
CPS[b] (22)	*S. aureus* *S. intermedius* *S. hyicus*	10 (13) 4 (5) 3 (3.8)
Bacillus (17.6)	*B. cereus* *B. pumilis* *B. licheniformis* *B. circulans* *B. thuringiensis*	6 (7.6) 4 (5) 2 (2.6) 1 (1.2) 1 (1.2)
PNC[c] (14)	*A. viridans* *S. uberis* *E. faecalis*	6 (7.6) 3 (3.8) 2 (2.6)
Micrococci (1.2)	*M. luteus*	1 (1.2)
Mannheimia (1.2)	*M. ruminalis*	1 (1.2)
Total		79 (100)

[a] *coagulase-negative Staphylococcus,* [b] *coagulase-positive Staphylococcus,* [c] *catalase-negative cocci*

indicated that they were susceptible to ciprofloxacin, clindamycin, cefoxitin, erythromycin, gentamycin, trimethoprim, and vancomycin *(Table 3)*. Among the *Staphylococcus* species, tetracycline has the highest resistance rate (32.6%, 17/52) among the tested antimicrobials. There was no detection of MRS and MDR among *Staphylococcus* isolates. The resistance to maximum two antimicrobials (penicillin and tetracycline) was detected for an *S. caprae* and an *S. chromogenes*. The *S. hyicus* isolates were susceptible to all antimicrobials. All of the *Bacillus* isolates were found susceptible to clindamycin, erythromycin, gentamycin, tetracycline and vancomycin *(Table 3)*. Among the tested antimicrobials, Beta lactam antimicrobial such as penicillin has the highest resistance rate (35.7%, 5/14). There is no detection of MDR between *Bacillus* isolates. The resistance to maximum two antimicrobials (penicillin and ciprofloxacin) was detected for a *B. cereus*. AMR test of the *Enterococcus* isolates indicated that they were susceptible to ampicillin, ciprofloxacin, penicillin *(Table 3)*. Among the tested antimicrobials, tetracycline has the highest resistance rate (100%, 2/2). An *E. faecalis* MDR isolate was found with resistance to rifampin, tetracycline and vancomycin. The other *E. faecalis* isolate was found

Table 3. *The AMR test profiles of isolates*

Antimicrobials[a]	Species	Number of Isolates (%)	
		Susceptibles	AMR Profiles
CIP, CN, DA, E, FOX, K, P, TE, VA, W	*S. caprae* (n=21)	15 (71.4)	TE, 4 (19) K, 1 (4.8) TE-P, 1 (4.8)
	S. aureus (n=10)	7 (70)	TE, 3 (30)
	S. chromogenes (n=10)	2 (20)	TE, 6 (60) TE-P, 1 (10) DA, 1 (10)
	S. intermedius (n=4)	3 (75)	TE, 1 (25)
	S. kloosii (n=4)	2 (50)	TE, 1 (25) K, 1 (25)
	S. hyicus (n=3)	3 (100)	-
	B. cereus (n=6)	4 (66.6)	P, 1 (16.7) CIP-P, 1 (16.7)
CIP, CN, DA, E, P, TE, VA	*B. pumilis* (n=4)	4 (100)	-
	B. circulans (n=1)	-	P, 1 (100)
	B. licheniformis (n=2)	1 (50)	P, 1 (50)
	B. thuringiensis (n=1)	-	P, 1 (100)
AMP, CRO, CTX, DA, E, OFX, P, TE, VA	*S. uberis* (n=3)	-	E-TE-DA, 3 (100)
AMP, CIP DO, E, RD, TE, VA	*E. faecalis* (n=2)	-	TE-VA-RD, 1 (50) E-TE, 1 (50)

[a] ***AMP:*** *Ampicillin;* ***CIP;*** *ciprofloxacin;* ***CN:*** *gentamycin,* ***CRO:*** *ceftriaxone;* ***CTX:*** *cefotaxime;* ***DA:*** *clindamycin;* ***DO:*** *doxycycline;* ***E:*** *erythromycin;* ***FOX:*** *cefoxitin;* ***K:*** *kanamycin,* ***OFX:*** *ofloxacin;* ***P:*** *penicillin-G;* ***RD:*** *rifampin;* ***TE:*** *tetracycline;* ***VA:*** *vancomycin;* ***W:*** *trimethoprim*

Table 4. *The AMR test profiles of isolates from a single milk sample*

Species Combination	Number of Samples	Common Resistance Profile (%)
S. caprae, S. chromogenes	4	Tetracycline (26.6)
S. caprae, S. kloosii	3	Tetracycline and Penicillin (20)
S. chromogenes, B. pumilis	2	Tetracycline and Penicillin (13.3)
S. chromogenes, S. intermedius	2	Tetracycline and Clindamycin (13.3)
S. aureus, S. caprae	1	-
S. caprae, B. pumilis	1	-
S. hyicus, A. viridans	1	-
S. caprae, S. chromogenes, B. licheniformis	1	Tetracycline (13.3)

resistant to erythromycin and tetracycline. Considering the AMR test of *S. uberis* isolates, they were susceptible to ampicillin, cefotaxime, ceftriaxone, ofloxacin, penicillin and vancomycin. All three *S. uberis* isolates were found MDR with resistance to erythromycin, clindamycin and tetracycline. Different agents isolated from a single milk sample showed some common resistance in the AMR test. Tetracycline resistance was common in 86.5% of multiple isolations, penicillin resistance in 33.3% of multiple isolations, and clindamycin resistance in 13.3% *(Table 4)*.

Discussion

This study was carried out to detect prevalence, diversity and antimicrobial resistance of the bacterial IMI agents in goat milk. Bacteria isolation was performed in 33.2% of the samples. 66% of all isolates were identified as *Staphylococccus*. These rates are in consistent to reports by Ebrahimi et al.[16] and Omar et al.[4]. CNS were detected 44% and CPS were detected 22% among *Staphylococcus* isolates. Cremonesi et al.[17] had reported CNS are part of microbiota, they can be considered as minor-mastitis pathogen in IMI and have become predominant pathogens causing IMI [8]. This study has shown that CNS are major bacteria causing IMI in goats. *S. epidermidis* was reported as the most dominant CNS species in the goat mastitis study carried out by Danmallam and Pimenov [18]. Similarly, Ebrahimi et al.[16] and Ruiz et al.[19] had also reported that *S. epidermidis* was the dominant CNS. However, in this study, *S. caprae* was found to be the most common CNS with a prevalence of 27%. This situation was thought to be due to the survival capacity of *S. caprae* during lactation and dry period. There are several studies that support this finding and report *S. caprae* is dominant in subclinical and clinical cases [20,21]. Moreover, *S. caprae,* the human pathogen, is known to cause hospital infections such as endocarditis, meningitis, bone infections, peritonitis, pneumonia and urinary infections. This situation reveals the importance of goat milk pasteurization or IMI treatment for public health [8]. *S.aureus* was detected as the most common CPS with prevalence of 13%, which is an agent of all samples. It is in concordance with Ebrahimi et al.[16], Danmallam and Pimenov [18] and Ruiz et al.[19] who also found that *S. aureus* was the most common CPS. *S. aureus* IMI is a potential risk for public health due to the fact that it can cause food poisoning with enterotoxins and virulence factors. Therefore, the high prevalence of *S. aureus* is considerable. As a result of this study, the most prevalent second genus was *Bacillus* spp. *Bacillus* spp. has also been identified in clinical IMI and subclinical IMI in many previous studies [1,6]. *Bacillus* spp. are known as the environmental mastitis pathogens. They cause milk contamination by direct contact to teats or indirect contact with materials. However, they pose risk to producers and consumers of milk in terms of causing zoonotic diseases [4]. This study has shown that 17.6% of all bacterial isolates were *Bacillus* spp. The high prevalence can be probably related to low hygienic conditions. *Bacillus* isolates were identified as *B. cereus, B. pumilis, B. licheniformis, B. thuringiensis and B. circulans*. *B. cereus* was reported as a causative agent of food poisoning and gangrenous IMI in goats as mentioned by Aruwa et al.[7] and Mavangira et al.[22]. Besides, Mavangira et al.[22] has reported that *B. cereus* causes gastrointestinal and non-gastrointestinal infections in humans. After *Bacillus* spp., PNC was the fourth mostly isolated group in this study. They can cause clinical or subclinical IMI and have also been isolated in goat IMI by previous studies [2,6,8,23]. While *S. agalactiae* was determined to be major PNC in many other IMI studies, however it was not detected in this study [2]. However, Raemy et al.[5] stated that *S. uberis* was the dominant PNC in their IMI study. This finding is consistent with our rate. Finally, we isolated *M. luteus* and *M. ruminalis* with prevalence of 1%. These species are generally reported with low prevalence in IMI studies of goats. For example, 2.5% prevalence for *M. luteus* was reported by Danmallam et al.[18] *M. ruminalis* was reported with 1.2% prevalence by Omaleki et al.[9] in small ruminant IMI. *Mannheimia* species naturally exist in the upper respiratory system of small ruminants. They are also rarely detected in IMI cases. There are several studies on the investigation of the *Mannheimia* species such as *M. haemolytica*, *M. glucosida* and *M. ruminalis* in IMI cases [8,16]. Especially in small ruminants, they negatively affect animal welfare, productivity, production and quality of meat/milk [9].

IMI was considered the main economic problem in dairy goats [1]. Therefore, its treatment is important to prevent

loss of value and efficiency. Antimicrobial treatment is commonly used as an appropriate and reliable method to control bacterial IMI in small ruminants. Generally, a combination of more than one antimicrobial is effective to control IMI than just using a single antimicrobial [10,24]. The antimicrobial resistance test of the isolates showed that the highest resistance rate (31%) was seen in tetracycline. Ebrahimi et al.[16] reported was average 26.8% MRS; Bochev and Russenova [25] reported 20% MRS in *Staphylococcus* isolated from goat IMI. However, there is no detection of MRS and MDR among *Staphylococcus* isolates in the present study. A total of 4 MDR isolates were detected in PNC: an *E. faecalis* isolate resistant to rifampin, tetracycline, vancomycin and three *S. uberis* isolates resistant to erythromycin, clindamycin, tetracycline. AMR test of the *Bacillus* isolates indicated that they were susceptible to clindamycin, erythromycin, gentamycin, tetracycline and vancomycin. Penicillin has the highest resistance rate (35.7%). This rate showed that Beta lactams can be used successfully in the treatment of *Bacillus* in acute IMI, rather than other antimicrobials. There was no detection of MDR among *Bacillus* isolates.

In this study, *S.caprae S.chromogenes* and *S.aureus* were determined as the most prevalent mastitis agents in dairy goats. CNS species were found to have a higher prevalence than CPS species.

Unlike the most mastitis studies performed on goat milk, it was determined that the dominant CNS species was *S. caprae* instead of *S. epidermidis*. This is thought to be due to high persistence of *S. caprae*. CNS species are considered as minor pathogens in goats due to their limited pathogenicity. *S. aureus* is considered risky for public health and animal health due to its high pathogenicity. *S. aureus* prevalence was found to be low in this study. The isolation of environmental factors such as *Bacillus* spp. and *Streptococcus* spp., low hygienic conditions have shown that the prevalence of IMI agents is increased. AMR results showed that treatment with more than one antimicrobial combination would be a necessary and effective treatment for goat mastitis. It was found that a successful treatment is possible, given the multiple bacterial isolations and the high resistance of tetracycline and penicillin.

Availability of Data and Materials

The authors declare that data supporting the findings of this study are available upon request.

Financial Support

This research received no grant from any funding agency/ sector.

Conflict of Interest

The authors declared that there is no conflict of interest.

Author Contributions

SSI, contributed to writing, reviewing and methodology of manuscript. AB and SS are responsible of sampling. ED and TO contributed draft preparation. MA contributed editing and study design. All authors have approved the final manuscript.

References

1. Lima MC, Sousa MCC, Espeschit IF, Maciel PACC, Souza JE, Moraes GF, Filho JDR, Moreira MAS: Mastitis in dairy goats from the state of Minas Gerais, Brazil: Profiles of farms, risk factors and characterization of bacteria. *Pesq Vet Bras,* 38 (9): 1742-1751, 2018. DOI: 10.1590/1678-5150-PVB-5698

2. Krukowski H, Lassa H, Zastempowska E, Smulski S, Bis-WenceL H: Etiological agents of bovine mastitis in Poland. *Med Weter,* 76, 221-225, 2020. DOI: 10.21521/mw.6339

3. Dufour S, Labrie J, Jacques M: The mastitis pathogens culture collection. *Microbiol Resour Announc,* 8:e00133-19, 2019.

4. Omar S, Mat-Kamir NF: Isolation and identification of common bacteria causing subclinical mastitis in dairy goats. *Int Food Res J,* 25, 1668-1674, 2018.

5. Raemy A, Meylan M, Casati S, Gaia V, Berchtold B, Boss R, Anja Wyder, Graber HU: Phenotypic and genotypic identification of streptococci and related bacteria isolated from bovine intramammary infections. *Acta Vet Scand,* 55:53, 2013.

6. Amer S, Galvez FLA, Fukuda Y, Tada C, Jımenez IL, Valle WFM, Nakai Y: Prevalence and etiology of mastitis in dairy cattle in El Oro Province, Ecuador. *J Vet Med Sci,* 80, 861-868, 2018. DOI: 10.1292/jvms.17-0504

7. Aruwa CE, Olatope SOA: Characterization of *Bacillus* species characterization of *Bacillus* species from convenience foods with conventional and API kit method: A comparative analysis. *J Appl Life Sci Int,* 3, 42-48, 2015. DOI: 10.9734/JALSI/2015/17406

8. Poulsen LL, Reinert TM, Sand RL, Bisgaard M, Christensen H, Olsen JE, Stuen S, Bojesen AM: Occurrence of haemolytic *Mannheimia* spp. in apparently healthy sheep in Norway. *Acta Vet Scand,* 48:19, 2006. DOI: 10.1186/1751-0147-48-19

9. Omaleki L, Browning GF, Barber SR, Allen JL, Srikumaran S, Markham PF: Sequence diversity, cytotoxicity and antigenic similarities of the leukotoxin of isolates of *Mannheimia* species from mastitis in domestic sheep. *Vet Microbiol,* 174, 172-179, 2014. DOI: 10.1016/j.vetmic.2014.08.009

10. Gutierrez-Chavez AJ, Martinez-Ortega EA, Valencia-Posadas M, León-Galván MF, Fuente-Salcido NM, Bideshi DK, Barboza-Corona JE: Potential use of *Bacillus thuringiensis* bacteriocins to control antibiotic-resistant bacteria associated with mastitis in dairy goats. *Folia Microbiol,* 61, 11-19, 2016. DOI: 10.1007/s12223-015-0404-0

11. Markey B, Leonard F, Archambault M, Cullinane A, Maguire D: Clinical Veterinary Microbiology. 2nd ed., 105-453, Mosby Elsevier, Dublin, 2013.

12. Zhang W, Chen Y, Shi Q, Hou B, Yang Q: Identification of bacteria associated with periapical abscesses of primary teeth by sequence analysis of 16S rDNA clone libraries. *Microb Pathog,* 141:103954, 2020. DOI: 10.1016/j.micpath.2019.103954

13. Clinical and Laboratory Standards Institute: Performance Standards for Antimicrobial Disk and Dilution Susceptibility Tests for Bacteria Isolated from Animals: Approved Standard. CLSI. 3rd ed., Wayne, Pennsylvania, 2008.

14. Chuang CC, Hasio CH, Tan HY, Ma DHK, Lin KK, Chang CJ, Huang YC: *Staphylococcus aureus* ocular infection: Methicillin-resistance, clinical features, and antibiotic susceptibilities. *PLoS ONE,* 8(8):e42437, 2012. DOI: 10.1371/journal.pone.0042437

15. Magiorakos AP, Srinivasan A, Carey RB, Carmeli Y, Falagas ME, Giske CG, Harbarth S, Hindler JF, Kahlmeter G, Olsson-Liljequist B,

Paterson DL, Rice LB, Stelling J, Struelens MJ, Vatopoulos A, Weber JT, Monnet DL: Multidrug-resistant, extensively drug-resistant and pandrugresistant bacteria: An international expert proposal for interim standard definitions for acquired resistance. *Clin Microbiol Infect,* 18, 268-281, 2012. DOI: 10.1111/j.1469-0691.2011.03570.x

16. Ebrahimi A, Shams N, Shahrokh S, Mirshokraei P: Characteristics of Staphylococci isolated from mastitic goat milk in Iranian dairy herds. *Vet World,* 3, 205-208, 2010.

17. Cremonesi P, Pisoni G, Severgnini M, Consolandi C, Moroni P, Raschetti M, Castiglioni B: Pathogen detection in milk samples by ligation detection reaction-mediated universal array method. *J Dairy Sci,* 92, 3027-3039, 2009. DOI: 10.3168/jds.2008-1773

18. Danmallam FA, Pimenov NV: Study on prevalence, clinical presentation, and associated bacterial pathogens of goat mastitis in Bauchi, Plateau, and Edo states, Nigeria. *Vet World,* 12, 638-645, 2019. DOI: 10.14202/vetworld.2019.638-645

19. Ruiz P, Barragan I, Sesena S, Palop ML: Is Staphyloccoci population from milk of healty goats safe? *Int J Food Microbiol,* 238, 146-152, 2016. DOI: 10.1016/j.ijfoodmicro.2016.08.033

20. Sanchez A, Fernandez C, Contreras A, Luengo C, Rubert J: Effect of intramammary infection by *Staphylococcus caprae* on somatic cell counts and milk composition in goats. *J Dairy Res,* 69, 325-328, 2002. DOI: 10.1017/S0022029902005496

21. Contreras A, JC Corrales, Sanchez A, Sierra D: Persistence of subclinical intramammary pathogens in goats throughout lactation. *J Dairy Sci,* 80, 2815-2819, 1997. DOI: 10.3168/jds.S0022-0302(97)76245-3

22. Mavangira V, Angelos JA, Samitz EM, Rowe JD, Byrne BA: Gangrenous mastitis caused by *Bacillus* species in six goats. *J Am Vet Med Assoc,* 242, 836-843, 2013.

23. Dore S, Liciardi M, Amatiste S, Bergagna S, Bolzoni G, Caligiuri V, Cerrone A, Farina G, Montagna CO, Saletti MA, Scatassa ML, Sotgiu G, Cannas EA: Survey on small ruminant bacterial mastitis in İtaly, 2013-2014. *Small Ruminant Res,* 141, 91-93, 2016. DOI: 10.1016/j.smallrumres.2016.07.010

24. Clinical and Laboratory Standards Institute: Clinical and Laboratory Standards: M45-A2 Methods for Antimicrobial Dilution and Disk Susceptibility Testing of Infrequently Isolated or Fastidious Bacteria; Approved Guideline. 2nd ed., Wayne, Pennsylvania 2011.

25. Bochev I, Russenova N: Resistance of *Staphylococcus* spp. strains isolated from goats with subclınıcal mastitis. *Bulg J Vet Med,* 8, 109-118, 2005.

Kafkas Universitesi Veteriner Fakultesi Dergisi
ISSN: 1300-6045 e-ISSN: 1309-2251
Journal Home-Page: http://vetdergikafkas.org

Kafkas Univ Vet Fak Derg
27 (6): 749-754, 2021
DOI: 10.9775/kvfd.2021.26247

RESEARCH ARTICLE

Morphological, Morphometrical and Histological Structure of the Interdigital Gland in Norduz Sheep

Semine DALGA [1,a (*)] Serap İLHAN AKSU [2,b] Kadir ASLAN [1,c]
Turgay DEPREM [2,d] Reşit UĞRAN [2,e] Rezzan BAYRAM [1,f]

[1] Kafkas University, Faculty of Veterinary Medicine, Department of Anatomy, TR-36100 Kars - TURKEY
[2] Kafkas University, Faculty of Veterinary Medicine, Department of Histology and Embryology, TR-36100 Kars - TURKEY
ORCIDs: [a] 0000 -0001-7227-2513; [b] 0000-0003-3100-498X; [c] 0000-0002-7617-0175; [d] 0000-0002-5523-8150; [e] 0000-0003-3431-8351
[f] 0000-0002-0464-7333

Article ID: KVFD-2021-26247 Received: 07.07.2021 Accepted: 01.10.2021 Published Online: 07.10.2021

Abstract

In this study, it was aimed to determine the morphological, morphometric, and histological features of the interdigital gland in Norduz sheep. In our study, the interdigital gland in the fore and hind feet of 12 male and 12 female Norduz sheep were examined by first dissecting and removing the interdigital glands from the feet. The study material was used for morphometric and histological examinations after fixation in 10% formaldehyde solution. It was determined that the interdigital gland, located between two digits, has a large corpus located on the corpus of the phalanx media and consists of a long excretory duct opening to the anterior end of the joint between the phalanx proximalis and phalanx media extending from the corpus. The gland had pipe-like appearance. The length and diameter of excretory duct and diameter of the orifice of excretory duct were measured using a digital caliper through the excretory duct of the interdigital gland. The proximal, middle, and distal diameter of the corpus and the length of the corpus were measured using the same method through the corpus of the glands. The mean corpus length of the interdigital gland was 15.05±4.80 mm on the right side, 15.90±4.39 mm on the left side in females, and 15.58±4.00 mm on the right side and 16.14±3.02 mm on the left side in males. The length of the excretory duct was determined as 20.98±4.50 mm, 21.39±5.51 mm in females, and 21.94±2.61 mm and 21.94±2.91 mm in males. L2 and L7 parameters of the fore-feet and hind feet in male Norduz sheep were statistically significant. Tissue sections were stained with Crossmann's modified triple staining technique (Triple staining), hematoxylin and eosin (H&E), and Periodic acid-Schiff (PAS) staining methods. It was observed that the interdigital gland consisted of epidermis, dermis, and a capsule. Apocrine glands were found to be located close to the capsule in the dermis. It was determined that PAS+ areas in male sheep were more intense than in female sheep. There was no histological difference in the interdigital glands of female and male Norduz sheep.

Keywords: *Interdigital gland, Norduz sheep, Morphometry, Morphology, Histology*

Norduz Koyunlarında Interdigital Bezin Morfolojik, Morfometrik ve Histolojik Yapısı

Öz

Bu çalışma Norduz koyunlarında interdigital bezin morfolojik, morfometrik ve histolojik özelliklerini belirlemek amacıyla yapıldı. Bu amaçla 12 adet erkek ve 12 adet dişi Norduz koyununun ön ve arka ayaklarındaki interdigital bezler kullanıldı. Öncelikle ayaklardan interdigital bezler diseke edilerek alındı. %10 luk formaldehit solüsyonunda tespit edildikten sonra morfometrik ve histolojik incelemeler için kullanıldı. İki parmak arasında bulunan interdigital bezin phalanx media'nın corpus'u üzerinde yerleşmiş geniş bir gövdeye (corpus) sahip olduğu ve gövdeden uzanan phalanx proximalis ile phalanx media arasındaki eklemin ön kısmına açılan uzun bir boşaltım kanalından oluştuğu tespit edildi. Bez şekilsel olarak pipoya benzetildi. İnterdigital bezlerin akıtıcı kanal kısmının üzerinden digital kumpas yardımı ile akıtıcı kanalın uzunluğu, çapı ve kanal açıklığının çapı ölçüldü. Bezlerin corpus'u üzerinden ise corpus'un proximal, orta ve distal çapı ile corpus'un uzunluğu aynı yöntem ile ölçüldü. Dişilerde interdigital bezin ortalama gövde (corpus) uzunluğu sağ tarafta 15.05±4.80 mm, sol tarafta 15.90±4.39 mm, erkeklerde ise sağ tarafta 15.58±4.00 mm, sol tarafta 16.14±3.02 mm olarak tespit edildi. Akıtıcı kanal uzunluğu ise dişilerde 20.98±4.50 mm, 21.39±5.51 mm, erkeklerde 21.94±2.61 mm, 21.94±2.91 mm olarak tespit edildi. Erkek Norduz koyunlarının ön ve arka ayaklarından ölçülen L2 ve L7 parametreleri istatistiksel olarak anlamlıydı. Doku kesitlerine Triple, Hematoksilen&Eozin (H&E) ve Periodik Asit Schiff (PAS) boyamaları uygulandı. İnterdigital bezin epidermis, dermis ve kapsül bölümlerinden oluştuğu görüldü. Dermis'in kapsüle yakın olan bölümünde apokrin bezler ayırt edildi. Erkek koyunlarda PAS+ alanların dişi koyunlarına göre daha yoğun olduğu belirlendi. Dişi ve erkek Norduz koyunlarının interdigital bezlerinde histolojik olarak herhangi bir farklılık saptanmadı.

Anahtar sözcükler: *İnterdigital bez, Norduz koyunu, Morfometri, Morfoloji, Histoloji*

How to cite this article?

Dalga S, İlhan Aksu S, Aslan K, Deprem T, Uğran R, Bayram R: Morphological, morphometrical and histological structure of the interdigital gland in Norduz sheep. *Kafkas Univ Vet Fak Derg,* 27 (6): 749-754, 2021.
DOI: 10.9775/kvfd.2021.26247

(*) Corresponding Author

Tel: +90 474 242 6839-5308 Cellular phone: +90 541 582 0218
E-mail: seminedalga@kafkas.edu.tr (S. Dalga)

Introduction

Norduz sheep, a domestic sheep breed, are reared in rural areas in Norduz region in Gürpınar county of Van province, Turkey. The whole neck of the sheep is covered with fleece. White, followed by ashen color is frequently seen, a small amount of gray-white and brown-white colors are also observed [1]. Mammals have skin glands that differ in size, shape, and location. In ungulates, reproductive activity is thought to be mediated by odors associated with cutaneous glands, localized in specific parts of the body including infraorbital, tarsal, and interdigital areas [2,3]. The interdigital gland within the artiodactyla is a hoof-skin organ which involved in apocrine and holocrine secretion. The interdigital gland, which contributes to the elasticity of the skin in the surrounding tissues, provides protection against ultraviolet rays, and also has fungicidal and bactericidal effects [4,5]. In addition, these glands act as olfactory glands that produce odorous signals and pheromones that play important biological roles in chemical communication, such as active demarcation of territory and expressing social behavior [5,6]. Although these glands are found on all four limbs in sheep, in some species they are only observed in the hind feet [7]. Due to their location on the body, infections such as interdigital sinusitis occur, particularly in spring owing to poor hygienic conditions and high humidity levels, as well as mechanical injuries caused by foreign bodies entering the gland [8]. Pourlis [9] reported that although number of studies has increased recently, detailed morphological data on the functionality of sheep interdigital glands are not available.

Studies on the anatomical location, morphological, morphometric, and histological structure of interdigital glands in small ruminants are available in the literature [6,10-16]. The present study aimed to conduct morphological, morphometric, and histological examination of the interdigital glands in the fore and hind feet of male and female Norduz sheep *(Ovis aries)*, which is of great importance and widely reared in the region, as well as to identify the location and structure of the interdigital glands, thereby providing data related to practice patterns for operative intervention.

Material and Methods

Ethical Approval

This study was approved by the Kafkas University Animal Experiments Local Ethics Committee [KAÜ-HADYEK] (Approval no: 2021/087).

Animals

The interdigital gland samples used in the study were collected from Norduz sheep (age, 1-2 years) slaughtered in the commercial abattoirs of Van province in November-December. The interdigital glands in the fore and hind feet of 12 female and 12 male Norduz sheep were analyzed anatomically and histologically.

Anatomical Method

In total, samples from nine of the sheep were used for morphometric measurements and from three for histological examinations. The interdigital gland between the two digits was first dissected and then fixed in 10% formaldehyde solution *(Fig. 1)*. After the fixation procedures, 7 parameters were measured using the digital caliper on the photographed interdigital glands *(Fig. 2)*.

Parameters

L1: Diameter of excretory duct, **L2:** Length of excretory duct, **L3:** Diameter of corpus proximal end, **L4:** Medium diameter of corpus, **L5:** Diameter of corpus distal end, **L6:** Body length, **L7:** Duct opening diameter.

Histological Method

Histological examinations were performed by obtaining the interdigital gland tissues from the fore and hind feet of female and male Norduz sheep, and fixing the samples in 10% formaldehyde solution for 24 h. Afterwards, the tissues were embedded in paraffin blocks through routine histological tissue processing solutions. 6 µm thick sections of the paraffin-embedded blocks were prepared. To evaluate the tissues histologically, tissue sections were stained with Crossmann's modified triple staining technique (Triple staining), hematoxylin and eosin (H&E), and Periodic acid-Schiff (PAS). Blocks were examined under a light microscope (Olympus BX51, Japan).

Radiological Method

The glandular secretions were emptied by massaging the feet. Then, contrast agent was injected into the gland with a plastic cannula placed at the orifice of the excretory duct using saline solution. Sagittal and coronal images were taken *(Fig. 3)*.

Statistical Analysis

For statistical analysis, the data were subjected to Independent-Samples T Test, using the SPSS 22.0 software package. A P-value of <0.05 was considered statistically significant while evaluating the significance of the differences between the mean values of the sheep interdigital gland.

Results

Macro-anatomical Findings

It was determined that the interdigital gland was located on the corpus of the phalanx media between 2 toes in the fore and hind feet in Norduz sheep. It was observed that the interdigital gland consisted of a corpus, an excretory duct, and an orifice of the excretory duct *(Fig. 1, 2, 3)*. It was

observed that the corpus of the gland was on the phalanx media. The excretory duct had an opening at the anterior edge of the junction of the phalanx proximalis and phalanx media. A large amount of hair was seen in the corpus and excretory duct forming the gland. It was determined that the interdigital gland in male Norduz sheep was larger than the gland in female animals.

Morphometric Analysis

In the statistical analysis between the fore and hind feet in Norduz sheep according to sex, the length of the excretory duct (L2) and the orifice diameter of the excretory duct (L7) were statistically significant in male Norduz sheep ($P<0.05$). There was no difference between other parameters in male animals and between all parameters in female animals. According to the statistical analysis of the sides (right/left) between the sexes, the mean corpus length was 15.05±4.80 mm on the right side 15.90±4.39 mm on the left side in females and 15.58±4.00 mm on the right side and 16.14±3.02 mm on the left side in males. It was determined that the mean values of left side measurements of the parameters were larger than that of right side the in both sex *(Table 1)*.

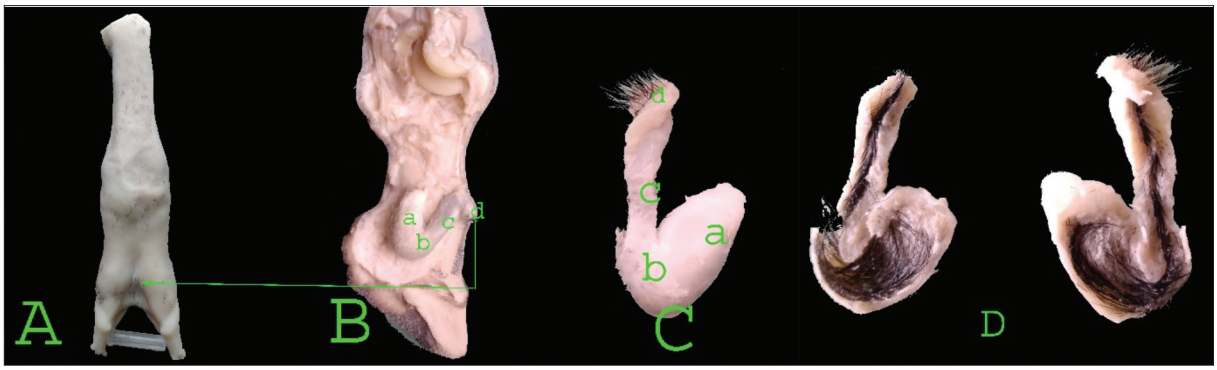

Fig 1. Location, morphological state and excretory duct of interdigital gland in Norduz sheep; **(A)** Cranial, **(B, C)** lateral appearance of the gland, **(D)** Sagital section of gland in Norduz Sheep, **a:** body, **b:** flexure, **c:** excretory duct, **d:** orifice

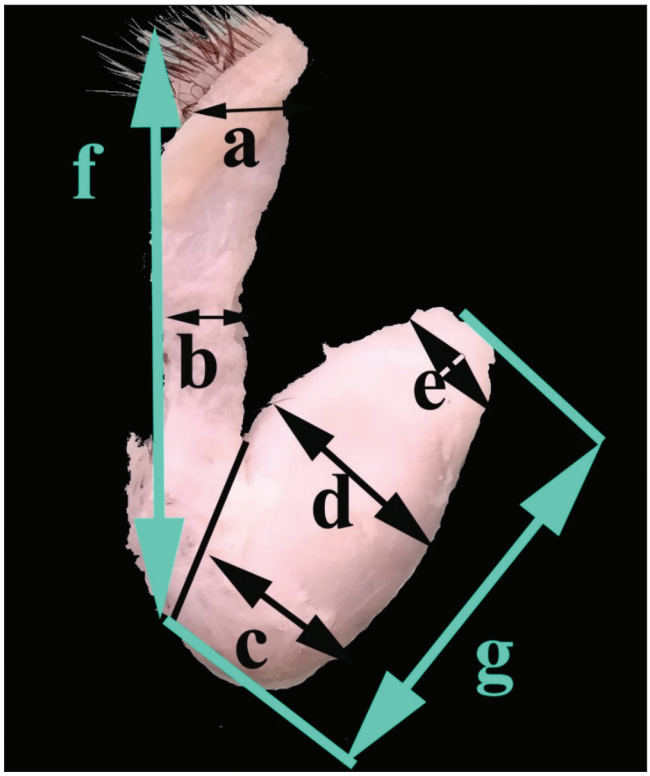

Fig 2. Morphometric measurement points of lateral appearance of the interdigital gland in Norduz sheep, **a:** duct opening diameter (L7), **b:** diameter of excretory duct (L1), **c:** diameter of corpus distal end (L5), **d:** medium diameter of corpus (L4), **e:** diameter of corpus proximal end (L3), **f:** length of excretory duct (L2), **g:** body length (L6)

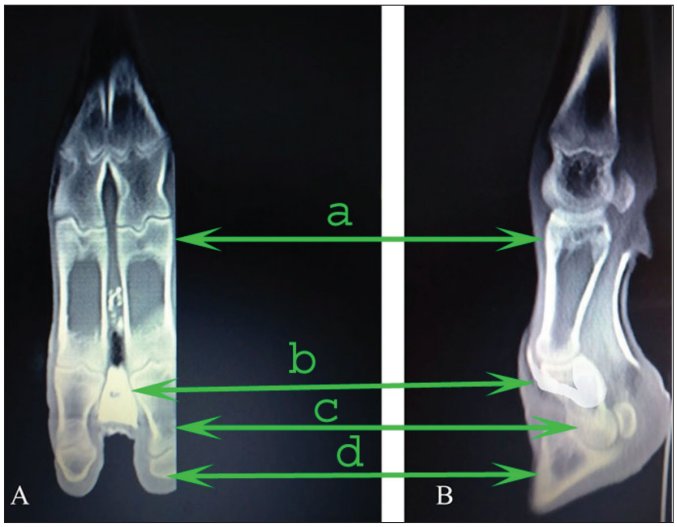

Fig 3. Radiological appearence of interdigital gland in Norduz sheep; **(A)** Dorsopalmar, **(B)** mediolateral, **a:** proximal phalanx, **b:** interdigital gland, **c:** medial phalanx, **d:** distal phalanx

Histological and Histochemical Examination

Interdigital glands sampled from both fore and hind feet of Norduz female and male sheep were examined histologically. The epidermis, dermis, and a capsule of the interdigital gland were distinguished in all samples *(Fig. 4-A,B)*. It was observed that the epidermis surrounding the lumen consisted of stratified squamous keratinized epithelium. In the dermis, intense collagen fibers around

Table 1. *Morphometric measurements of interdigital gland in Norduz sheep*

Parameters	Female Norduz Sheep (mean±standard deviation)		Male Norduz Sheep (mean±standard deviation)		Female Norduz Sheep (mean±standard deviation)		Male Norduz Sheep (mean±standard deviation)	
	Right	Left	Right	Left	Fore	Hind	Fore	Hind
L1	3.91±0.49	4.43±1.10	4.27±0.46	4.52±0.83	3.85±0.26	4.49±1.14	4.13±0.74	4.66±0.48
L2[a]	20.98±4.50	21.39±5.51	21.94±2.61	21.94±2.91	23.11±1.98	19.26±6.21	23.28±2.70[a]	20.60±2.01[a]
L3	5.27±1.02	5.92±1.36	5.49±0.96	5.52±0.58	5.99±0.74	5.21±1.5	5.48±0.82	5.63±0.77
L4	6.69±1.37	7.43±2.25	6.92±1.54	6.83±1.31	7.32±1.06	6.81±2.44	7.14±1.61	6.61±1.16
L5	5.73±1.72	7.36±2.79	6.79±1.68	6.51±1.25	6.48±1.95	6.61±2.90	6.31±1.43	6.99±1.46
L6	15.05±4.80	15.90±4.39	15.58±4.00	16.14±3.02	16.29±2.49	14.66±3.92	16.03±2.80	15.69±4.18
L7[b]	3.79±0.66	3.63±0.91	4.59±0.77	4.62±0.81	3.70±0.65	3.72±0.92	4.26±0.65[b]	4.95±0.74[b]

*[a,b] P<0.05; **L1:** Diameter of excretory duct; **L2:** Length of excretory duct; **L3:** Diameter of corpus proximal end; **L4:** Medium diameter of corpus; **L5:** Diameter of corpus distal end; **L6:** Body length; **L7:** Duct opening diameter*

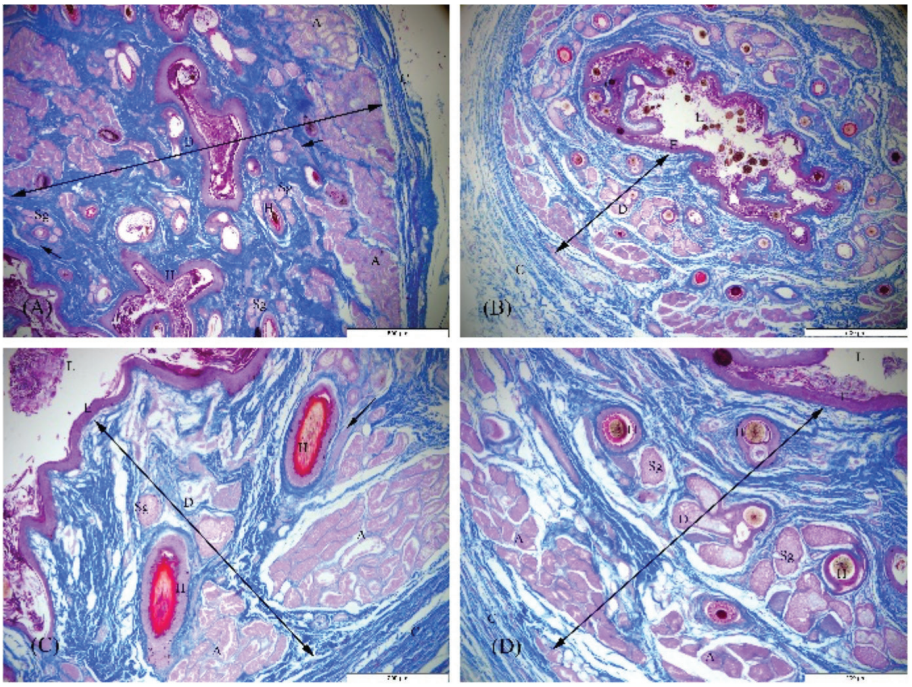

Fig 4. Histological structure of interdigital gland in Norduz sheep. **(A-C):** Male Norduz sheep, **(B-D):** Female Norduz sheep. **L:** Lumen, **E:** Epidermis, **D:** Dermis, **A:** Apocrine gland, **C:** Capsule, **H:** Hair follicle, **Sg:** Sebaceous gland, *Arrows:* m. erector pili; Triple stain

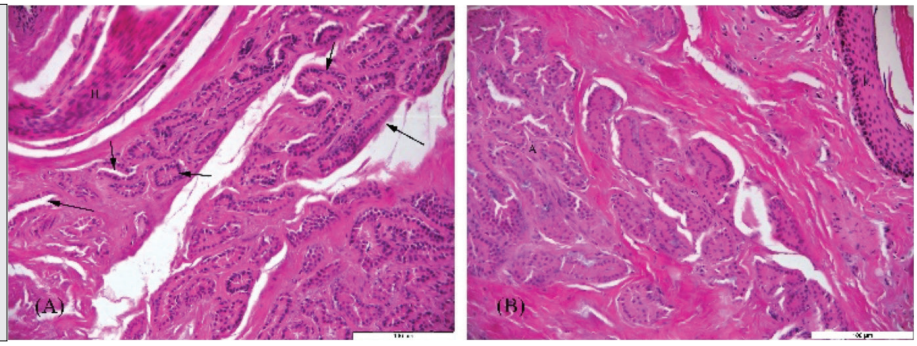

Fig 5. Apocrine gland structure. **(A):** Male Norduz sheep, **(B):** Female Norduz sheep. **E:** Epidermis, **H:** Hair follicle, **A:** Apocrine gland, *Arrows:* Apocrine gland unit; H&E stain

the sebaceous glands, hair follicles, arrector pili muscle, blood vessels, and nerve plexuses were observed *(Fig. 4-C,D)*. The hair follicles surrounded by sebaceous glands were intense in the dermis. Secretory units with narrow lumen and consisting of a single row of cubic cells surrounded by myoepithelial cells were identified in the dermis mostly close to the capsule *(Fig. 5-A,B)*. It was determined that the outermost layer of the gland, the capsule, had a loose connective tissue structure and contained blood vessels, nerve plexuses, and adipose cells. PAS staining showed that PAS+ was observed in the basal membranes of the apocrine glands in the interdigital gland. PAS+ areas were

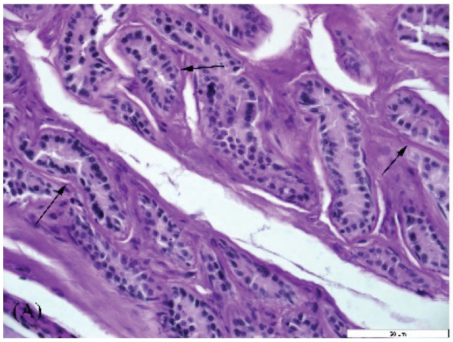

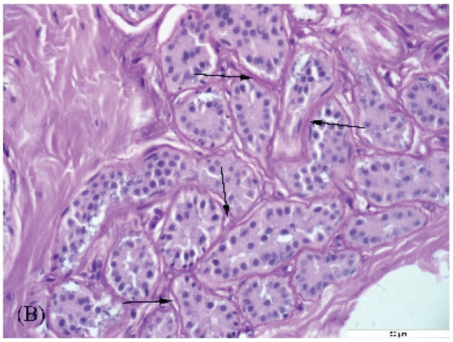

Fig 6. PAS stain for apocrine glands. **(A):** Male Norduz sheep, **(B):** Female Norduz sheep. *Arrows:* PAS+ areas; PAS stain

Fig 7. Neck area of interdigital gland. **(A):** Male Norduz sheep, **(B):** Female Norduz sheep. **L:** Lumen, **E:** Epidermis, **D:** Dermis, **A:** Apocrine gland, **C:** Capsule, **H:** Hair follicle, **Sg:** Sebaceous gland; Triple stain

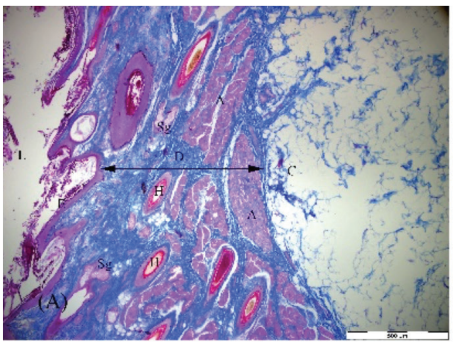

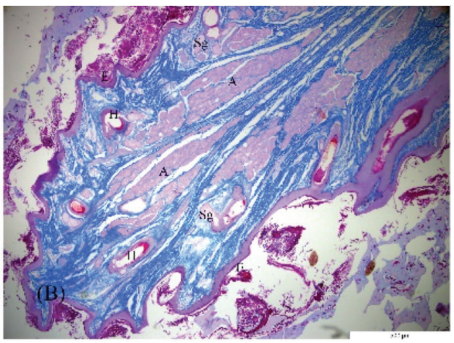

not found in the lumens of the secretion units. It was determined that PAS+ areas were more intense in male sheep than in female sheep *(Fig. 6-A,B)*. Histologically, the neck regions of the interdigital gland composed of similar structures as the corpus region *(Fig. 7-A,B)*. There was no histological difference in the interdigital glands of female and male Norduz sheep. It was observed that the interdigital glands of the fore and hind legs consisted of the same structures.

Discussion

In this study, morphological, morphometric and histological features of interdigital gland were determined in Norduz sheep. Accordingly, Gürbüz et al.[17] have reported that the length of the gland was 30.18±1.93 mm in the fore-feet and 25.67±1.77 mm in hind feet in male Hemshin sheep. They also have stated that the interdigital gland in fore-feet was significantly larger than that of the hind-feet its collected in December. In our study, it was observed that measurements of hind-feet were greater than that of the fore-feet, and intersex comparisons showed males have larger gland parameters than females. This result is similar to Lori's sheep [4]. Süzer et al.[10] have examined the morphological and immunohistochemical features of the sinus interdigitalis in Kivircik sheep and reported that the sinus has a tube-like appearance and is located between the proximal and distal interphalangeal joints between the two toes. In Norduz sheep, it was observed that the gland has a corpus located on the phalanx media between two toes and a long excretory duct opening to the distal edge of the phalanx proximalis in both sexes. Interdigital glands had a pipe-like appearance in our study, which was consistent with the literature [4,14].

Kara et al.[15] reported that the corpus and excretory duct lengths of the interdigital gland were 17.25±1.09 mm, 26.39±2.22 mm in fore-feet and 13.67±0.85 mm, 22.64±2.30 mm in hind feet in Hasmer sheep and 16.33±0.92 mm, 29.65±0.82 mm in fore-feet, 12.89±0.66 mm, 23.51±1.21 mm in hind feet Hasak sheep, respectively. Similarly, in the study Yılmaz et al.[14] investigating the effects of sex and breeding season (June-July) on the morphological and histological structures of the interdigital gland in Awassi sheep, the corpus and excretory duct lengths of the gland were 19.87±0.39 mm and 29.47±0.5 mm in fore-feet and 14.96±0.26 mm and 24.14±0.34 mm in hind feet, respectively. In addition, Yılmaz et al.[14] have stated that all parameters of the gland in Awassi sheep have higher values in males compared to females. Similarly, it was observed in our study that the values of parameters in males were higher among Norduz sheep.

The histological examinations of Norduz sheep revealed that interdigital gland wall structure consists of epidermis, dermis and a capsule as observed in Lori's sheep [4], Kivircik sheep [11], Baladi sheep [18], Hemshin sheep [17], Awassi sheep [14], Hasmer and Hasak sheep [15]. As in other sheep breeds, the interdigital gland of Norduz sheep was composed of stratified keratinized epithelium, and sebaceous glands, hair follicles, arrector pili muscle, blood vessels, and nerve plexuses were observed in the dermis.

Abbasi et al.[4] have reported the presence of sweat glands located close to the capsule and surrounded by myoepithelial cells, and that sweat glands occupy more

space in the interdigital gland compared to the sebaceous glands located in the superficial area. In Norduz sheep, it was observed that the apocrine glands were located close to the capsule and occupy a large area in the interdigital gland. Unlike other studies, we determined that the apocrine gland units consisted of a single row of cubic cells but had a narrow lumen. This suggests that the interdigital gland, which has been reported to have activity during the reproductive period, may cause periodic or age-dependent changes in the histology of apocrine glands [5,14].

Janicki et al.[7] in their study examining the interdigital gland structure of roe deer, reported that the interdigital gland structure is not surrounded by connective tissue (capsule) and has no sweat glands. Similar to other studies [4,11,18], we determined that the interdigital gland of Norduz sheep was surrounded by a capsule formed by connective tissue, and there were blood vessels, nerve plexuses and fat cells in the capsule. In our study, PAS staining showed no neutral glycoprotein in the lumen of apocrine glands in contrast to Kivircik sheep [11] and similar to Lori's sheep [4]. In addition, no histological difference was observed between male and female interdigital glands.

Interdigital gland in Norduz sheep is considered to be similar in shape and structure to other sheep breeds, but different in terms of morphometrics. The similarities and differences of the morphological, morphometric and histological features of the interdigital gland will form the basis of future sexual function studies in Norduz sheep.

Availability of Data and Materials

The authors declare that data supporting the study findings are also available to the corresponding author.

Funding Support

This work was not supported by any institution.

Competing Interest

The authors declare that they have no competing interests.

Author Contributions

SD and SİA designed the study. SD, KA, and RB performed the macro-anatomical and morphometric analysis. SİA, TD, and RU carried out histological examination. SD and SİA carried out the statistical analysis. SD, SİA, and KA performed the imaging all section. The manuscript was written by SD, SİA, and RU. All authors approved the final version.

References

1. Koyuncu M: Norduz Koyunu. **In**, Koyuncu M (Ed): Koyun Yetiştiriciliği, 43, Dora Yayınevi, Bursa, 2019.

2. König HE, Liebich HG: Veterinary Anatomy of Domestic Mammals, Textbook and Colour Atlas. 3rd ed., 609-615, Stuttgart, Germany, Schattauer Gmbh, 2007.

3. Alexandre-Pires G, Martins C, Galvão AM, Correia M, Ramilo D, Quaresma M, Ligeiro D, Nunes T, Caldeira RM, Ferreira-Dias G: Morphological aspects and expression of estrogen and progesterone receptors in the interdigital sinus in cyclic ewes. *Microsc Res Tech*, 77 (4): 313-325, 2014. DOI: 10.1002/jemt.22345

4. Abbasi M, Gharzi A, Mohammadzadeh S, Karimi H: Morphology and histology of the interdigital gland in an Iranian native breed of sheep. *J Anim Vet Adv*, 8, 1157-1161, 2009.

5. Parillo F, Diverio S: Glycocomposition of the apocrine interdigital gland secretions in the fallow deer *(Dama dama)*. *Res Vet Sci*, 86, 194-199, 2009. DOI: 10.1016/j.rvsc.2008.08.004

6. Aslan K, Kürtül I, Nazlı M, Ateş S: Morphologic features of the interdigital sinus of the Tuj sheep. *Kafkas Univ Vet Fak Derg,* 16, 623-626, 2010. DOI: 10.9775/kvfd.2009.1307

7. Janicki Z, Hraste A, Slavica A, Konjeviæ D, Marinoviæ Z, Stubièan D: Morphohistological characteristics of the interdigital gland in the roebuck *(Capreolus capreolus* L.). *Vet Arhiv,* 73, 27-37, 2003.

8. Uğurlu S: Koyunlarda sinus interdigitalislerin ışık mikroskobik yapısı üzerine incelemeler. *İstanbul Univ Vet Fak Derg*, 17, 1-7, 1991.

9. Pourlis AF: Functional morphological characteristics of the interdigital sinus in the sheep. *Folia Morphol,* 69, 107-111, 2010.

10. Süzer B, Özgüden Akkoç CG, Arıcan İ, Yıldız H: Morphological and immunohistochemical features of interdigital sinus in Kivircik sheep. *Kafkas Univ Vet Fak Derg*, 22, 69-73, 2016. DOI: 10.9775/kvfd.2015.13902

11. Demiraslan Y, Akbulut Y, Deprem T, Karadağ Sarı E, Aslan K: Morphological and morphometrical characteristics of the interdigital gland in Kivircik sheep. *Turk J Vet Anim Sci,* 38, 485-489, 2014. DOI: 10.3906/vet-1403-21

12. Bahadır A, Yakışık M: Yerli kıl keçisinde sinus interdigitalis'in (sinus biflexe) morfolojisi. *Uludag Univ Vet Fak Derg*, 7, 87-92, 1988.

13. Calislar T: Sinus interdigitalis'in morfolojik özellikleri. *Ankara Univ Vet Fak Derg*, 18, 38-40, 1971.

14. Yılmaz B, Yılmaz R, Demircioglu I, Arıcan I: Morphological and histological structure of the interdigital gland in Awassi sheep *(Ovis aries)*. *Turk J Vet Anim Sci*, 41, 380-386, 2017. DOI: 10.3906/vet-1605-8

15. Kara H, Gedikli S, Özüdogru Z, Özdemir D, Balkaya H: A morphological, morphometrical and histological investigation of the interdigital gland in Hasmer and Hasak sheep. *Folia Morphol*, 79 (4): 742-747, 2020. DOI: 10.5603/FM.a2020.0014

16. Maya S, Sreeranjini AR, Leena C, Sunil Kumar NS, Sumena KB, Irshad A: Histology, lectin histochemistry and ultrastructure of interdigital gland in crossbred sheep. *J Food Anim Sci*, 01 (02): 112-116, 2020. DOI: 10.51128/jfas.2020.A020

17. Gürbüz I, Demiraslan Y, Karadağ Sarı E, Aslan K: Morphologic and morphometric structure and arterial vascularization of glandula interdigitalis in male Hemshin sheep. *Kafkas Univ Vet Fak Derg*, 23 (2): 241-246, 2017. DOI: 10.9775/kvfd.2016.16359

18. Awaad AS, Tawfiek MG, Moawad UK, Abdel Razek AH, Abedellah BA: Morphohistological and surgical anatomy of the sinus interdigitalis in Egyptian native breeds of sheep. *J Basic Appl Sci,* 4, 157-166, 2015. DOI: 10.1016/j.bjbas.2015.05.010

Kafkas Universitesi Veteriner Fakultesi Dergisi
ISSN: 1300-6045 e-ISSN: 1309-2251
Journal Home-Page: http://vetdergikafkas.org

Kafkas Univ Vet Fak Derg
27 (6): 755-762, 2021
DOI: 10.9775/kvfd.2021.26281

RESEARCH ARTICLE

Evaluation of Oxidative Stress, Immune System and Mineral Concentrations in Milk and Serum of Cows with Clinical and Subclinical Mastitis Naturally Infected by *Staphylococcus aureus*

Serdal KURT [1,a (*)] Funda ESKI [2,b] Leyla MIS [3,c] Pinar AYVAZOGLU DEMIR [4,d]

[1] Kahramanmaras Istiklal University, Elbistan Vocational School, Department of Veterinary, TR-46300 Kahramanmaras - TURKEY
[2] Cukurova University, Faculty of Ceyhan Veterinary Medicine, Department of Obstetrics and Gynecology, TR-01330 Adana - TURKEY
[3] Van Yuzuncu Yil University, Veterinary Medicine, Department of Veterinary Physiology, TR-65080 Van - TURKEY
[4] Kafkas University, Faculty of Veterinary Medicine, Department of Livestock Economic and Management, TR-36100 Kars - TURKEY
ORCIDs: [a] 0000-0002-0191-3245; [b] 0000-0002-9242-9271; [c] 0000-0002-5110-2862; [d] 0000-0002-7010-0475

Article ID: KVFD-2021-26281 Received: 13.07.2021 Accepted: 15.11.2021 Published Online: 16.11.2021

Abstract

The aim of this study was to investigate effect of *Staphylococcus aureus* on oxidative stress status (TAS, TOS, OSI), immune system (IL-1β, IL-6, TNF-α), and mineral (Mg, Fe, Zn, Cu, Na and Ca) concentrations in milk and serum of cows with mastitis. The cows were allocated to three groups according to mammary health status as follows: healthy (Group 1), clinical (Group 2) and subclinical mastitis cows (Group 3). IL-1β levels in serum and milk increased in Group 2 compared to Group 1 and Group 3 (P<0.001; P<0.05). Milk IL-6 level was greater in Group 3 and Group 2 than in Group 1 (P<0.01). Blood TNF-α (P<0.001), TOS and OSI levels (P<0.01) were higher in Group 2 than other groups. Milk TNF-α level increased and blood TAS level decreased in Group 2 compared to Group 1 (P<0.05). Milk TOS (P<0.01) and OSI (P<0.05) levels increased in Group 3 compared to Group 1. Blood and milk Mg levels increased in Group 1 (P<0.05) and Group 2 (P<0.001), respectively. Milk Fe (P<0.01) and Na levels were greater in Group 2 (P<0.001). Blood Zn level was lower in Group 2 compared to Group 3 (P<0.05). While blood Cu level decreased in Group 1 compared to other groups, milk Cu level decreased in Group 3 compared to other groups (P<0.001). In conclusion, *S. aureus* had significant effects on oxidative stress, cytokine and mineral levels in milk and blood serum of cows with clinical and subclinical mastitis. However, since there were specific changes only in milk OSI and IL-6 levels according to other parameters, it is thought that milk IL-6 and OSI levels may be a diagnostic tool in the detection of subclinical mastitis.

Keywords: *Cytokine, Mastitis, Mineral substance, Oxidative stress, Staphylococcus aureus*

Staphylococcus aureus İle Doğal Olarak Enfekte Olan Klinik ve Subklinik Mastitisli İneklerin Süt ve Serumlarında Oksidatif Stres, Bağışıklık Sistemi ve Mineral Konsantrasyonlarının Değerlendirilmesi

Öz

Bu çalışmanın amacı, *Staphylococcus aureus*'un mastitisli ineklerin süt ve kan serumlarında oksidatif stres durumu (TAS, TOS, OSI), bağışıklık sistemi (IL-1β, IL-6, TNF-α) ve mineral (Mg, Fe, Zn, Cu, Na ve Ca) konsantrasyonları üzerine etkisini araştırmaktı. Çalışma sağlıklı (Grup 1), klinik (Grup 2) ve subklinik mastitisli (Grup 3) inekler olmak üzere üç grup üzerinde yürütüldü. Grup 1 ve Grup 3'e göre Grup 2'de kan ve sütteki IL-1β düzeyleri arttı (P<0.001; P<0.05). Grup 1'e göre Grup 3 ve Grup 2'de süt IL-6 düzeyi daha yüksekti (P<0.01). Diğer gruplara göre Grup 2'de kan TNF-α (P<0.001), TOS ve OSI düzeyleri (P<0.01) daha yüksekti. Grup 1'e göre Grup 2 de süt TNF-α düzeyi yükseldi ve kan TAS düzeyi azaldı (P<0.05). Grup 1'e kıyasla Grup 3'te süt TOS (P<0.01) ve OSI (P<0.05) düzeyleri yükseliş gösterdi. Diğer gruplara göre kan ve süt Mg düzeyleri sırasıyla Grup 1 (P<0.05) ve Grup 2'de (P<0.001) arttı. Diğer gruplara göre Grup 2'de süt Fe (P<0.01) ve Na düzeyleri arttı (P<0.001). Grup 3'e göre Grup 2'de kan Zn düzeyi düşüş gösterdi (P<0.05). Kan Cu düzeyi diğer gruplara göre Grup 1'de düşerken, süt Cu düzeyi diğer gruplara kıyasla Grup 3'te azaldı (P<0.001). Sonuç olarak, *S. aureus*'un klinik ve subklinik mastitisli ineklerin süt ve kan serumlarında oksidatif stres, sitokin ve mineral seviyeleri üzerinde önemli etkileri olduğu görülmüştür. Ancak diğer parametrelere göre sadece süt OSI ve IL-6 düzeylerinde spesifik değişiklikler olduğu için süt IL-6 ve OSI düzeylerinin subklinik mastitisin saptanmasında tanı aracı olabileceği düşünülmektedir.

Anahtar sözcükler: *Mastitis, mineral madde, Oksidatif stres, Sitokinler, Staphylococcus aureus*

How to cite this article?

Kurt S, Eski F, Mis L, Ayvazoglu Demir P: Evaluation of oxidative stress, immune system and mineral concentrations in milk and serum of cows with clinical and subclinical mastitis naturally infected by *Staphylococcus aureus. Kafkas Univ Vet Fak Derg,* 27 (6): 755-762, 2021.
DOI: 10.9775/kvfd.2021.26281

(*) Corresponding Author

Tel: +90 541 420 1892
E-mail: serdal.kurt@hotmail.com (S. Kurt)

Introduction

Mastitis, which is one of the costliest problems for the dairy industry [1], is defined as inflammation of the mammary gland against infectious and non-infectious factors [2]. It affects the milk composition and quality [3], and accounts for about 38% of the total costs caused by major production diseases in dairy cows [2]. One of the most important bacterial agents that cause bovine mastitis is *Staphylococcus aureus* [2,4], and it is associated with the clinical and subclinical mastitis [4,5]. Since *S. aureus* found on the normal skin flora, it is impossible to eradicate from the herds. It is also very difficult to combat because it can produce exotoxins, biofilms, bacterial superantigens and proteases, and adhere to mammary epithelial cells [6]. It can also survive within the phagocytes and epithelial cells, so antibiotic treatments are often ineffective [7]. Therefore, alternative methods are needed to increase the treatment rate for mastitis caused by *S. aureus* [6]. In order to achieve success in the combat against *S. aureus*, some studies have been conducted to investigate its effects on the defense system [8,9]. Immune response of a mammary gland infected by *S. aureus* is controlled by lymphocyte subpopulations, other leukocytes and some cytokines released by them. The virulence factors of S. *aureus* such as enterotoxin and toxic shock syndrome toxins allow it to deceive and escape from the immune system [10], however it can affect the levels of proinflammatory cytokines [11] such as interleukin 1 beta (IL-1β), interleukin 6 (IL-6) [12] and tumor necrosis factor alpha (TNF-α) [11]. These cytokines induce an immune response by stimulating phagocytic cells to the inflammation [13]. Therefore, the production of reactive oxygen species (ROS), the most abundant oxidant in the biological system, increases as a result of the destruction of pathogens during mastitis [14]. If the level of ROS produced in the body exceeds the antioxidant capacity, oxidative stress occurs. Oxidative stress causes damage to cells' macromolecules such as DNA, lipids and proteins [15,16], and thus it may exacerbate mastitis. More clearly, there is a relationship among oxidative stress, cytokine release and mastitis [15,17], and these changes can be observed in both milk and systemic circulation [18]. On the other hand, since mastitis causes deterioration in the blood-milk barrier, it causes extracellular fluid to enter the mammary gland [19]. Therefore, it affects the mineral and trace element level in the milk and blood [20]. Some mineral substances are involved in the antioxidant system [21,22] and are important in monitoring udder health [23]. In recent studies, it has been emphasized that proinflammatory cytokines [24] and oxidative stress [25] are critical in the fight against mastitis. However, this needs to be further elaborated in order to effectively combat *S. aureus* mastitis.

We hypothesized that mastitis caused by *S. aureus* has significant influences on oxidative stress, some cytokine and mineral levels in milk and blood serum of cows. Therefore, the presented study aimed to investigate oxidative stress status, immune system (IL-1β, IL-6, TNF-α), and mineral (Mg, Fe, Zn, Cu, Na and Ca) concentrations in milk and serum of cows with clinical and subclinical mastitis caused by *S. aureus*.

Material and Methods

Ethical Statement

The present study was carried out in compliance with the National Research Council's guide for animal use and approved by the Local Ethics Committee of Ceyhan Veterinary Faculty, Cukurova University, Adana, Turkey (Approval no: 27/07/2020-04/01).

Animal and Management

This study was carried out on a total of 30 multiparous Holstein dairy cows at a medium-scale commercial farm in Adana, Turkey, in August. All cows had a similar age, milk yield, body condition score and parity, and they were managed in free stall barns under the same conditions, milked twice a day using an automatic milking system and had free access to water. All cows were in mid-lactation period and fed with same total mixed ration (TMR) arranged for mid-lactation period. The mid-lactation ration content is given in the *Table 1*. The farm had evaporative and ventilated air-cooling systems against heat stress. Moreover, pre- and post-milking udder disinfection procedures [26], and mastitis screenings were routinely performed in the farm.

Groups and Experimental Design

The dairy cows were divided into three groups as healthy (Group 1; n=10), clinical (Group 2; n=10) and subclinical (Group 3; n=10) mastitis. No treatment was performed before and during the study. First, the days in milking (DIM) of all cows were recorded to evaluate the similarity in terms of lactation days between the groups. The groups were

Table 1. *The ration content of the cows in the mid lactation period*

Ration Content	Percantage (%)
Corn silage	46.16
Clover	13.02
Wheat straw	4.73
Soy meal	6.62
Cottonseed	5.20
Barley	2.60
Corn grain	11.83
Corn gluten meal	0.47
Corn bran	1.18
Soybean grain	5.77
Other	2.36
Total	100

formed according to California mastitis test (CMT), udder examination and bacteriological identification in milk. The CMT was performed according to the manufacturer's instructions (California mastitis test kit, ImmuCell). The CMT reaction of each quarter was recorded as negative (0), trace, 1+, 2+ and 3+ [27,28]. If one of the 1+, 2+, and 3+ values was obtained, it was considered positive. All tests were performed for 4 teats of each cow. The clinical symptoms of mastitis, as previously described, were considered as changes in milk appearance, heat, swelling and pain of affected udder [18]. Before collecting the milk, the udder and the teat ends were washed, cleaned and dried, and samples were taken after the foremilk was discarded [23]. The healthy group consisted of cows with the negative CMT test, no clinical signs of mastitis and no bacteria was isolated in their milk samples. Subclinical mastitis group consisted of cows with the positive CMT test, no clinical signs of mastitis and only *S. aureus* was isolated in their milk samples. Clinical mastitis group consisted of cows with the positive CMT test, typical signs of clinical mastitis [12] and only *S. aureus* was isolated in their milk samples. A total of 560 teats were examined until the number of animals in all groups was completed.

Blood and Milk Samples

All blood and milk samples were taken before morning milking and feeding. In all groups, blood samples (5 mL) were collected from the jugular vein into sterile vacutainer tubes with clot activator (Hema & Tube®, Italy). Immediately after the blood collection process, milk samples (15 mL; two samples per cows) were taken from individual quarters with healthy, subclinical and clinical mastitis groups into sterile falcon tubes (Isolab®, Germany) under aseptically conditions, according to the Laboratory Handbook on Bovine Mastitis of the National Mastitis Council [29]. One milk sample per cow was transported to the laboratory at +4°C for microbiological and mineral substance analyzes. Other milk and blood samples were centrifuged at 4.000 ×g (for 15 min) and 1500 x g (for 10 min), respectively. After the milk and blood serums were harvested, they were immediately stored at -20°C until IL-1β, IL-6, TNF-α, total antioxidant status (TAS), total oxidant status (TOS), mineral substance analyzes. While milk analyzes were performed on the same day, serum analyzes were performed within 14 days after storage at -20°C.

IL-1β, IL-6 and TNF-α Analysis in Milk and Blood Serum

Milk and blood serum IL-1β, IL-6 and TNF-α levels were determined using a microplate reader (Stat Fax-2100, Awareness®, USA) and commercial kits (IL-1β cat no: CSB-E12019B-bovine IL-1 ELISA kit; IL-6 cat no: CSB-E12899B-bovine IL-6 ELISA kit; TNF-α cat no: CSB-E12020B-bovine TNF-α ELISA kit).

TAS and TOS Analysis in Milk and Blood Serum

Milk and blood serum TAS and TOS levels were measured by same as above (Stat Fax-2100, Awareness®, USA) using commercial kits (Rel Assay Diagnostics®, Turkey), according to the method developed by Erel [30] and Erel [31]. The test principle is a colorimetric method that can be determined spectrophotometrically.

Calculation of Oxidative Stress Index (OSI)

OSI was accepted as percent ratio of TOS level to TAS level. After the resulting unit of TAS (mmol Trolox equivalent/L) was converted to μmol Trolox equivalent/L, the OSI was calculated according to the following formula: TOS (μmol H_2O_2 Eq/L)/TAS (mmol Trolox Eq/L) x 100 [32].

Mineral Substance Analysis

- Preparation of Milk Samples

All milk serum samples were dried in a forced stove at 100°C to obtain a constant weight. They were brought to room temperature, and 4 mL of HNO_3 (65%, Merck, Germany) and 2 mL of H_2O_2 (30%, Merck, Germany) were added onto 2 mL milk serum sample. The samples were solubilized at 180°C and 270 bar pressure. After this process, they were allowed to cool for 15-20 min. Subsequently, they were filtered from filter papers and taken into balloon flasks. Their volumes were completed to 25 mL with ultra-pure water.

- Preparation of Blood Serum Samples

Serum samples in 1 mL volumes were taken into glass tubes. Then, a 3% HNO_3 solution was prepared from 65% HNO_3 (Merck, Germany) and added onto serum samples in a volume of 1 mL. Finally, the resulting mixture was centrifuged at 3000 rpm for 10 min. The remaining particles in the tubes were filtered, 1 mL of 1% Triton-X was added to them and their volume were completed to 10 mL using deionized pure water.

- Mineral Substance Analysis in Milk and Blood Serum

Analysis of copper (Cu), iron (Fe), zinc (Zn), calcium (Ca), sodium (Na), magnesium (Mg) was performed using an atomic absorption spectrophotometer (ICE 3000, Thermo).

Microbiological Examination

Microbiological examinations were performed according to standard procedure of National Mastitis Council [29] to identify gram-negative and gram-positive bacteria. The *S. aureus* identify procedures were summarized below.

Culture

The milk samples were individually inoculated into blood agar (Oxoid, CM0055) and MacConkey agar (Oxoid, CM0007) using a quadrant streaking method, and they were incubated at 37°C for 24-48 h. Blood agar and MacConkey agar were used for bacteriological isolation; morphologic characteristics of isolated microorganisms were observed

on these primary cultures. Additionally, Gram staining was applied to define the gram reaction and shape of the cultures. Coagulase test (Coagulase Plasma Lyophilized. Rabbit plasma w/EDTA, Catalog number: R21052, Thermo Fisher Scientific, MA, USA) was applied to differentiate staphylococcus species.

Statistical Analysis

In this study, the group sizes were determined as 10, according to the results of the power analysis using 80% power and 5% margin of error. All statistical calculations were done with SPSS software (Version: 23.0; IBM, USA). The normality tests of data were performed using the Kolmogorov-Smirnov test. One-way analysis of variance test (ANOVA) was used to compare group means. The differences among all groups were analyzed with Duncan's multiple comparison test. Significance level was accepted as $P<0.05$ in all analyses. The results were given as the mean±standard error of mean (mean±SEM).

Results

It was found that DIM was similar between all groups ($P>0.05$). The DIM averages in Group 1, Group 2, and Group 3 were 143.7±6.7, 146.2±6.1, and 140.0±10.2, respectively ($P>0.05$).

Pro-inflammatory Cytokine Concentrations

IL-1β levels in blood and milk serums significantly increased in the Group 2 compared to Group 1 and Group 3 ($P<0.001$; $P<0.05$). While the IL-6 levels in blood were similar between the groups ($P>0.05$), its level in milk was higher in the Group 3 and Group 2 than in the Group 1 ($P<0.01$). Blood TNF-α level was higher in the Group 2 group than in the other groups ($P<0.001$). Milk TNF-α level was higher in the Group 2 than in the Group 1 ($P<0.05$).

Oxidative Stress Markers

Milk TAS levels were found to be similar between groups ($P>0.05$); however, blood TAS level significantly increased in the Group 1 compared to the Group 2 ($P<0.05$). Blood oxidative stress index (OSI) and TOS levels were significantly higher in the Group 2 compared to the Group 1 and Group 3 ($P<0.01$). On the other hand, an increase was observed in the milk TOS ($P<0.01$) and OSI ($P<0.05$) levels of the Group 3 compared to the Group 1.

Mineral Substance Concentrations

Blood and milk Mg levels were significantly higher in the Group 1 ($P<0.05$) and Group 2 ($P<0.001$), respectively, than in the other group. While the blood Fe levels were similar between the groups ($P>0.05$), milk Fe level was found higher in the Group 2 than in the Group 1 and Group 3 ($P<0.01$). There was no significant difference between the groups in terms of milk Zn levels ($P>0.05$), but the blood Zn level was lower in the Group 2 than in the Group 3 ($P<0.05$). Blood and milk Cu levels were found to be significantly lower in the Group 1 and Group 3, respectively, compared to the other group ($P<0.001$). Blood Na levels were similar in all groups; however, milk Na levels was found to be higher in the Group 2 compared to other groups, and also significantly higher in the Group 3 than in the Group 1 ($P<0.001$). No difference was found between the groups in terms of blood and milk Ca levels ($P>0.05$). The levels of proinflammatory cytokines (IL-1β, IL-6, TNF-α), oxidative stress markers (TAS, TOS, OSI) and mineral substance (Mg, Fe, Zn, Cu, Na, Ca) obtained from blood and milk serums of all groups are presented in *Table 2* and *Table 3*, respectively.

Table 2. *The levels of some proinflammatory cytokines and oxidative stress markers obtained from blood and milk serums of all groups*

Parameters		Group 1	Group 2	Group 3
IL-1β ng/L	Blood	$0.96\pm0.05^{b***}$	$1.59\pm0.22^{a***}$	$0.62\pm0.08^{b***}$
	Milk	$0.76\pm0.04^{b*}$	$1.09\pm0.11^{a*}$	$0.69\pm0.13^{b*}$
IL-6 ng/L	Blood	3.31±0.07	3.09±0.09	3.11±0.02
	Milk	$3.01\pm0.03^{b**}$	$3.16\pm0.02^{a**}$	$3.1\pm0.00^{a**}$
TNF-α ng/L	Blood	$0.97\pm0.14^{b***}$	$2.0\pm0.03^{a***}$	$0.96\pm0.12^{b***}$
	Milk	$0.58\pm0.06^{b*}$	$0.89\pm0.06^{a*}$	$0.76\pm0.07^{b*}$
TAS mmol/L	Blood	$1.22\pm0.02^{a*}$	$1.07\pm0.02^{b*}$	$1.12\pm0.04^{ab*}$
	Milk	1.07±0.00	1.07±0.03	1.12±0.01
TOS µmol/L	Blood	$0.96\pm0.04^{b**}$	$1.49\pm0.20^{a**}$	$0.78\pm0.15^{b**}$
	Milk	$1.03\pm0.01^{b**}$	$1.20\pm0.07^{ab**}$	$1.46\pm0.14^{a**}$
OSI	Blood	$0.08\pm0.00^{b**}$	$0.14\pm0.01^{a**}$	$0.07\pm0.01^{b**}$
	Milk	$0.10\pm0.00^{b*}$	$0.12\pm0.00^{ab*}$	$0.13\pm0.01^{a*}$

*^{a,b,c} Different letters in the same column indicate the statistical difference ($P<0.05$); * $P<0.05$, ** $P<0.01$, *** $P<0.001$; **IL-1β:** Interleukin 1 beta; **IL-6:** Interleukin 6; **TNF-α:** Tumor necrosis factor alpha; **TAS:** Total antioxidant status; **TOS:** Total oxidant status; **OSI:** Oxidative stress index; **Group 1:** Healthy; **Group 2:** Clinical mastitis; **Group 3:** Subclinical mastitis*

Table 3. *The levels of some mineral substance obtained from blood and milk serums of all groups*

Parameters		Group 1	Group 2	Group 3
Mg	Blood	$14.45\pm0.9^{a*}$	$12.30\pm0.45^{b*}$	$11.76\pm0.27^{b*}$
	Milk	$43.37\pm0.70^{b***}$	$50.02\pm3.24^{a***}$	$37.40\pm1.49^{b***}$
Fe	Blood	0.47±0.04	0.64±0.11	0.63±0.02
	Milk	$0.07\pm0.00^{b***}$	$0.13\pm0.01^{a***}$	$0.08\pm0.00^{b***}$
Zn	Blood	$0.23\pm0.01^{ab*}$	$0.21\pm0.00^{b*}$	$0.26\pm0.01^{a*}$
	Milk	0.45±0.02	0.51±0.10	0.58±0.04
Cu	Blood	$0.03\pm0.00^{b***}$	$0.15\pm0.00^{a***}$	$0.14\pm0.00^{a***}$
	Milk	$0.05\pm0.01^{a***}$	$0.04\pm0.00^{a***}$	$0.01\pm0.00^{b***}$
Na	Blood	372.39±0.15	371.05±1.66	373.78±1.78
	Milk	$158.67\pm3.82^{c***}$	$303.96\pm3.68^{a***}$	$200.97\pm5.74^{b***}$
Ca	Blood	45.73±1.0	42.66±1.38	42.21±0.75
	Milk	300.13±3.9	213.08±41.43	273.23±17.08

*^{a,b,c} Different letters in the same column indicate the statistical difference (P<0.05); * P<0.05; *** P<0.001;* ***Group 1:*** *Healthy;* ***Group 2:*** *Clinical mastitis;* ***Group 3:*** *Subclinical mastitis*

Discussion

In the present study, healthy dairy cows and those diagnosed with subclinical and clinical mastitis naturally infected by *S. aureus* were used. Levels of oxidative stress markers (TAS, TOS, OSI), proinflammatory cytokines (IL-1β, IL-6, TNF-α) and mineral substances (Mg, Fe, Zn, Cu, Na, Ca) were compared in the blood and milk serums of all groups. Since environmental and management differences such as heat stress, lactation period, and ration content can affect both oxidative stress and cytokine levels [13,33-35], the present study was carried out in mid-lactation cows fed the same ration in same season.

During mastitis, immune cells struggle to eliminate invading pathogens [13]. Cytokines are the important mediators in establishing immune response against intramammary infection [36], and proinflammatory cytokines including TNF-α, IL-1β and IL-6 are critical for activation of the innate immune system in epithelial cells, macrophages or monocytes [37]. It was reported that levels of TNF-α, IL-1β and IL-6 are significantly elevated in infected mammary glands [38] within clinical and subclinical mastitis [18], and they are not only produced locally but also released into the circulation [24]. Guo et al.[39] noted that there is an association between *S. aureus*-induced mastitis and TNF-α, IL-1β and IL-6 levels. Early changes in cytokine transcription may be useful as a predictive tool in the detection of *S. aureus*-induced mastitis [10]. Alluwaimi [11] reported that *S. aureus* may affect TNF-α release due to their immunosuppressive effect, while Osman et al.[12] stated that IL-1 and IL-6 levels increased in the early stage of *S. aureus* mastitis. Considering the findings of the presented study, it was observed that *S. aureus*-induced mastitis did not affect IL-1β and TNF-α levels in blood and milk serum of the Group 3, but their levels increased significantly in the Group 2. Similarly, Yang et al.[40] stated that *S. aureus,* which causes subclinical infections, results in only a very low level of proinflammatory cytokine response. On the other hand, it was reported that milk IL-6 level could be used in the early diagnosis of subclinical mastitis and significantly increased in the milk of cows with subclinical mastitis [41]. In addition, Kleczkowski et al.[17] noted that IL-6 is required to initiate the systemic inflammatory response. To clarify this situation, many studies have investigated the changes in cytokine levels, especially IL-6, in cases of mastitis caused by different bacteria [42-45]. Hagiwara et al.[43] reported that IL-6 is an important inflammatory mediator in cases of endotoxin-induced mastitis. On the other hand, Shaheen et al.[45] reported that IL-6 levels were similar between cows with healthy and subclinical mastitis without bacterial isolation. Similarly, Ohtsuka et al.[46] stated that the severity of the disease did not affect the level of IL-6 in cases of mastitis caused by coliform bacteria. However, staphylococcal enterotoxins stimulate lymphocytes and leukocytes rapidly and thus immediately trigger IL-6 release in the early stage of mastitis [12]. Therefore, we think that IL-6 level is more specific in *S. aureus*-induced subclinical mastitis because of the strong stimulation of IL-6 release as a defense mechanism in the early stage of staphylococcal mastitis. However, the relationship between IL-6 and mastitis cases caused by *S. aureus* or other bacterial species has not been clarified in terms of specificity and sensitivity. In a previous study, milk IL-6 levels were found higher in cows with *S. aureus*-induced subclinical mastitis compared to healthy cows and those with clinical mastitis. In the present study, while blood IL-6 level was similar in all groups, its milk serum level was higher in the Group 3 and Group 2 compared to the Group 1. It is known that systemic inflammation and oxidative stress occurs in cows with subclinical and clinical mastitis [14], and inflammatory response and oxidative stress are closely related [47]. Similarly, it was informed that there is a relationship between mastitis and oxidative stress [48].

It was also reported that total oxidant capacity increased and total antioxidant capacity decreased in clinical and subclinical mastitis [21]. Moreover, it was stated that total oxidant capacity of milk increased in cow with subclinical mastitis [25]. However, Sadek et al.[18] reported that while serum total antioxidant capacity decreased in subclinical mastitis, both milk and serum total antioxidant capacity decreased in clinical mastitis. So, oxidative stress status can be evaluated as a systemic or local finding in cases of mastitis caused by different bacterial species, including *S. aureus* [18,47,49-51]. However, since *S. aureus* can survive for a long time in host cells [52], it has a greater importance than other bacteria in terms of creating oxidative stress in subclinical mastitis cases. Nevertheless, sensitivity and specificity of OSI in the diagnosis of subclinical mastitis cases caused by *S. aureus* or other bacteria need to be investigated in further studies. In our study, *S. aureus*-induced mastitis did not affect milk TAS levels. However, it decreased the blood TAS level in the Group 2 compared to the Group 1. The reason for this is considered to be an intense antioxidant transition from blood to milk in cows with *S. aureus* mastitis, but the milk TAS level does not change as they are used to inactivate ROS in udder. TOS and OSI results obtained in this study support the above-mentioned information. *S. aureus*-induced mastitis resulted in increased blood TOS and OSI levels in the Group 2 than in other groups. In addition, it was associated with increased milk TOS and OSI levels in the Group 3 compared to the Group 1. On the other hand, it has been reported that there is a relationship between the antioxidant defense system and the number of bacterial colonies in cows with mastitis [53]. It is also known that the milk quality of treated or recovered cows is improved and oxidative stress is reduced by increasing the antioxidant defense system [54]. This can be assessed by taking a second milk sample after the first bacteriologically positive sample for infection stability. However, since the main purpose of our study was to instantly evaluate some biochemical changes in blood and milk levels in cows with mastitis caused by *S. aureus*, and no treatment was applied, repeated sampling was not performed. In addition, in the presented study, only milk samples from which aureus was clearly isolated were included in the study. In doubtful cases, cows from which milk samples were taken were excluded from the study. It was recorded that antioxidant levels decreased, a systemic oxidative stress and inflammation response were observed in cows with subclinical and clinical mastitis [14], and it is thought that the increase in oxidant level of milk with mastitis is related with the increase of epithelial cells such as macrophages, eosinophiles, neutrophiles and lymphocytes and some cytokines (IL-1β, IL-6, IL-8, TNF-α) [55].

Amiri et al.[25] stated that oxidative stress indices are current markers used in the determination of subclinical mastitis, and the antioxidant and oxidant levels in milk can be a diagnostic tool for the early diagnosis of mastitis. However, systemic oxidative stress level can increase in many diseases stress [48], so we considered that the milk OSI level would be more specific for the evaluation of mastitis. In addition, we believe that blood and milk mineral and macro element levels are important in mastitis studies. It is known that the blood-milk barrier and function of epithelial cells are disrupted during mastitis, and accordingly, it changes the levels of most components in udder secretion [20,56]. Therefore, in the presented study, the level of some mineral substances in blood and milk serums was measured to evaluate the effect of clinical and subclinical mastitis caused by *S. aureus* on the blood-milk barrier. A previous study indicated that while milk and blood levels of Ca, Mg, Fe and Zn significantly decreased in cows with subclinical mastitis, concentration of Na significantly increased; however, Cu level was not affected [23]. Another study demonstrated that while plasma Ca levels increased, Na and Mg levels did not change in cows with clinical and subclinical mastitis [20]. Moreover, Al-Autaish [57] revealed that serum Mg, Ca and Fe levels decreased, but Zn level increased in cows with subclinical mastitis. However, our study revealed that Ca level did not change in any group. Gera et al.[58] also reported that mastitis increased milk Zn and Fe levels, but not Cu level. As can be understood from the information above, mastitis may have different effects on the mineral values in milk and blood. In presented study, while non-significant changes in levels of Mg, Fe and Zn in the milk serum and in levels of Fe, Zn and Na the blood serum were observed in the Group 3 compared to the Group 1, Mg level in blood and Cu level in milk decreased, and Na level in milk increased. Cu is associated with humoral immune response [59], its deficiency reduces neutrophil killing capacity and increases susceptibility to bacterial infections [49]. Therefore, it is thought that decreased milk Cu level may affect the case of subclinical mastitis caused *by S. aureus*. It was also stated that the change in milk Na level in mastitis may be related with the mastitis pathogen, the severity of inflammation, milk fraction and a decrease in lactose production [28]. In this study, significant increases were observed in only milk levels of Mg, Fe and Na in the Group 2, while a decrease in blood level of Mg was observed. Since Na level has an effect on milk osmolality [60], we assumed that it could also affect the level of other minerals. Considering the above information, it is understood that *S. aureus* has different degrees of local and systemic effects on these observed parameters in cows with clinical and subclinical mastitis.

In conclusion, the present study revealed that *S. aureus* increased IL-1β and TNF-α levels in blood and milk serum of cows with clinical mastitis. IL-6 level increased only in milk serum of cows with both clinical and subclinical mastitis. So, while differences in IL-1β, IL-6 and TNF-α levels were observed in cows with clinical mastitis, only IL-6 level was the discriminant factor in cows with subclinical mastitis. On the other hand, *S. aureus* caused an increase in blood OSI levels in cows with clinical mastitis. OSI level increased in milk serum of cows with subclinical mastitis, according to healthy cows. Therefore, it can be emphasized that the

milk OSI level is of critical importance in terms of subclinical mastitis. *S. aureus* also caused some important changes in Mg, Fe, Na and Cu levels. While these parameters were affected at different levels in milk or blood serum, more specifically, milk Mg and Fe levels increased only in cows with clinical mastitis and milk Cu level decreased only in cows with subclinical mastitis.

Availability of Data and Materials

The data that support the findings of the present study are available from the corresponding author upon reasonable request.

Acknowledgements

The authors thank Prof. Dr. Armağan Erdem ÜTÜK for his generous assistance in fieldwork.

Funding Support

Financial support not received.

Competing Interests

The authors declare that they have no conflicts of interest.

Author Contributions

This work was carried out in collaboration between all authors. Serdal KURT and Funda ESKI conceptualized the hypothesis of this manuscript. Serdal KURT and Funda ESKI conducted research. Leyla MIS conducted laboratory experiments and analyzed data. Serdal KURT and Funda ESKI together wrote the manuscript. Pinar AYVAZOGLU DEMIR made statistical analysis. Serdal KURT and Funda ESKI critically reviewed the manuscript. All authors read and approved the final manuscript.

References

1. Ma W, Wang Y, Gao F, Ning M, Liu A, Li Y, Gao Y, Lu P, Chen D: Development of a monoclonal antibody against bovine α-casein to evaluate functional status of mammary epithelial cells during mastitis. *Kafkas Univ Vet Fak Derg*, 25, 445-450, 2019. DOI: 10.9775/kvfd.2018.20897

2. Bradley AJ: Bovine mastitis: An evolving disease. *Vet J*, 164, 116-128, 2002. DOI: 10.1053/tvjl.2002.0724

3. Rusenova N, Gebreyes W, Koleva M, Mitev J, Penev T, Vasilev N, Miteva T: Comparison of three methods for routine detection of *Staphylococcus aureus* isolated from bovine mastitis. *Kafkas Univ Vet Fak Derg*, 19, 709-712, 2013. DOI: 10.9775/kvfd.2013.8753

4. Kurt S, Çolakoğlu HE, Yazlık MO, Vural MR, Küplülü, Ş: Sütçü ineklerde mastitis yönünden kuru ve geçiş dönemlerinin önemi. *Atatürk Üniversitesi Vet Bil Derg*, 14, 107-113, 2019. DOI: 10.17094/ataunivbd.407022

5. Saidi R, Cantekin Z, Khelef D, Ergün Y, Solmaz H, Kaidi R: Antibiotic susceptibility and molecular identification of antibiotic resistance genes of staphylococci isolated from bovine mastitis in Algeria. *Kafkas Univ Vet Fak Derg,* 21, 513-520, 2015. DOI: 10.9775/kvfd.2014.12836

6. Peralta OA, Carrasco C, Vieytes C, Tamayo MJ, Muñoz I, Sepulveda S, Tadich T, Duchens M, Melendez P, Mella A, Torres CG: Safety and efficacy of a mesenchymal stem cell intramammary therapy in dairy cows with experimentally induced *Staphylococcus aureus* clinical mastitis. *Sci Rep*, 10:2843, 2020. DOI: 10.1038/s41598-020-59724-7

7. Pereira UP, Oliveira DGS, Mesquita LR, Costa GM, Pereira LJ: Efficacy of *Staphylococcus aureus* vaccines for bovine mastitis: A systematic review. *Vet Microbiol,* 148, 117-124, 2011. DOI: 10.1016/j.vetmic.2010.10.003

8. Niedziela DA, Murphy MP, Grant J, Keane OM, Leonard FC: Clinical presentation and immune characteristics in first-lactation Holstein-Friesian cows following intramammary infection with genotypically distinct *Staphylococcus aureus* strains. *J Dairy Res*, 103, 8453-8466, 2020. DOI: 10.3168/jds.2019-17433

9. Zhang L, Hou X, Sun L, He T, Wei R, Pang M, Wang R: *Staphylococcus aureus* bacteriophage suppresses LPS-induced inflammation in MAC-T bovine mammary epithelial cells. *Front Microbiol,* 9:1614, 2018. DOI: 10.3389/fmicb.2018.01614

10. Alluwaimi AM, Leutenegger CM, Farver TB, Rossitto PV, Smith WL, Cullor JS: The cytokine markers in *Staphylococcus aureus* mastitis of bovine mammary gland. *J Vet Med B Infect Dis Vet Public Health*, 50, 105-111, 2003. DOI: 10.1046/j.1439-0450.2003.00628.x

11. Alluwaimi AM: The cytokines of bovine mammary gland: Prospects for diagnosis and therapy. *Res Vet Sci*, 77, 211-222, 2004. DOI: 10.1016/j.rvsc.2004.04.006

12. Osman KM, Hassan HM, Ibrahim IM, Mikhail MMS: The impact of staphylococcal mastitis on the level of milk IL-6, lysozyme and nitric oxide. *Comp Immunol Microbiol Infect Dis,* 33, 85-93, 2010. DOI: 10.1016/j.cimid.2008.08.009

13. Ibrahim HMM, El-Seedy YY, Gomaa NA: Cytokine response and oxidative stress status in dairy cows with acute clinical mastitis. *J Dairy Vet Anim Res*, 3 (1): 00064, 2016. DOI: 10.15406/jdvar.2016.03.00064

14. Turk R, Piras C, Kovačić M, Samardžija M, Ahmed H, De Canio M, Urbani A, Meštrić ZF, Soggiu A, Bonizzi L, Roncada P: Proteomics of inflammatory and oxidative stress response in cows with subclinical and clinical mastitis. *J Proteomics*, 75, 4412-4428, 2012. DOI: 10.1016/j.jprot.2012.05.021

15. Abuelo A, Hernández J, Benedito JL, Castillo C: The importance of the oxidative status of dairy cattle in the periparturient period: Revisiting antioxidant supplementation. *J Anim Physiol Anim Nutr,* 99, 1003-1016, 2015. DOI: 10.1111/jpn.12273

16. Cenesiz S: The role of oxidant and antioxidant parameters in the infectious diseases: A systematic literature review. *Kafkas Univ Vet Fak Derg*, 26, 849-858, 2020. DOI: 10.9775/kvfd.2020.24618

17. Kleczkowski M, Kluciński W, Czerski M, Kudyba E: Association between acute phase response, oxidative status and mastitis in cows. *Vet Stanica*, 48, 177-186, 2017.

18. Sadek K, Saleh E, Ayoub M: Selective, reliable blood and milk biomarkers for diagnosing clinical and subclinical bovine mastitis. *Trop Anim Health Prod,* 49, 431-437, 2017. DOI: 10.1007/s11250-016-1190-7

19. Zhao X, Lacasse P: Mammary tissue damage during bovine mastitis: Causes and control. *J Anim Sci*, 86, 57-65, 2008. DOI: 10.2527/jas.2007-0302

20. Singh M, Yadav P, Sharma A, Garg VK, Mittal D: Estimation of mineral and trace element profile in bubaline milk affected with subclinical mastitis. *Biol Trace Elem Res,* 176, 305-310, 2017. DOI: 10.1007/s12011-016-0842-9

21. Abd Ellah MR: Role of free radicals and antioxidants in mastitis. *J Adv Vet Res*, 3, 1-7, 2013.

22. Spears JW, Weiss WP: Role of antioxidants and trace elements in health and immunity of transition dairy cows. *Vet J*, 176, 70-76, 2008. DOI: 10.1016/j.tvjl.2007.12.015

23. Qayyum A, Khan JA, Hussain R, Avais M, Ahmad N, Khan MS: Investigation of milk and blood serum biochemical profile as an indicator of sub-clinical mastitis in Cholistani cattle. *Pak Vet J*, 36, 275-279, 2016.

24. Kuhla B: Review: Pro-inflammatory cytokines and hypothalamic inflammation: implications for insufficient feed intake of transition dairy cows. *Animal,* 14, 65-77, 2020. DOI: 10.1017/S1751731119003124

25. Amiri P, Rad AHF, Heidarpour M, Azizzadeh M, Khoramian B: Diagnostic accuracy of milk oxidation markers for detection of subclinical mastitis in early lactation dairy cows. *Comp Clin Pathol*, 29, 95-101, 2020. DOI: 10.1007/s00580-019-03024-8

26. Williamson JH, Lacy-Hulbert SJ: Effect of disinfecting teats post-

milking or pre-and post-milking on intramammary infection and somatic cell count. *N Z Vet J*, 61, 262-268, 2013. DOI: 10.1080/00480169.2012.751576

27. Baştan A, Kaçar C, Acar DB, Şahin M, Cengiz M: Investigation of the incidence and diagnosis of subclinical mastitis in early lactation period cows. *Turk J Vet Anim Sci,* 32, 119-121, 2008.

28. Kandeel SA, Morin DE, Calloway CD, Constable PD: Association of California mastitis test scores with intramammary infection status in lactating dairy cows admitted to a veterinary teaching hospital. *J Vet Intern Med*, 32, 497-505, 2018. DOI: 10.1111/jvim.14876

29. Hogan JS, Gonzalez RN, Harmon RJ, Nickerson SC, Oliver SP, Pankey JW, Smith KL: Laboratory handbook on bovine mastitis. National Mastitis Council, Madison, Wisconsin, 1999.

30. Erel O: A novel automated direct measurement method for total antioxidant capacity using a new generation, more stable ABTS radical cation. *Clin Biochem*, 37, 277-285, 2004. DOI: 10.1016/j.clinbiochem.2003.11.015

31. Erel O: A new automated colorimetric method for measuring total oxidant status. *Clin Biochem*, 38, 1103-1111, 2005. DOI: 10.1016/j.clinbiochem.2005.08.008

32. Eşki F, Kurt S, Demir-Ayvazoğlu P: Effect of different estrus synchronization protocols on estrus and pregnancy rates, oxidative stress and some biochemical parameters in hair goats. *Small Ruminant Res,* 198:106348, 2021. DOI: 10.1016/j.smallrumres.2021.106348

33. Pedernera M, Celi P, García SC, Salvin HE, Barchia I, Fulkerson WJ: Effect of diet, energy balance and milk production on oxidative stress in early-lactating dairy cows grazing pasture. *Vet J*, 186, 352-357, 2010. DOI: 10.1016/j.tvjl.2009.09.003

34. Trevisi E, Jahan N, Bertoni G, Ferrari A, Minuti A: Pro-inflammatory cytokine profile in dairy cows: Consequences for new lactation. *Ital J Anim Sci*, 14 (3): 3862, 2015. DOI: 10.4081/ijas.2015.3862

35. Colakoglu HE, Kuplulu O, Vural MR, Kuplulu S, Yazlik MO, Polat IM, Oz B, Kaya U, Bayramoglu R: Evaluation of the relationship between milk glutathione peroxidase activity, milk composition and various parameters of subclinical mastitis under seasonal variations. *Vet Arhiv*, 87, 557-570, 2017. DOI: 10.24099/vet.arhiv.160728

36. Bannerman DD: Pathogen-dependent induction of cytokines and other soluble inflammatory mediators during intramammary infection of dairy cows. *J Anim Sci*, 87, 10-25, 2009. DOI: 10.2527/jas.2008-1187

37. Yang C, Liu P, Wang S, Zhao G, Zhang T, Guo S, Jiang K, Wu H, Deng G: Shikonin exerts anti-inflammatory effects in LPS-induced mastitis by inhibiting NF-κB signaling pathway. *Biochem Biophys Res Commun,* 505, 1-6, 2018. DOI: 10.1016/j.bbrc.2018.08.198

38. Akhtar M, Guo S, Guo YF, Zahoor A, Shaukat A, Chen Y, Umar T, Deng PG, Guo M: Upregulated-gene expression of pro-inflammatory cytokines (TNF-α, IL-1β and IL-6) via TLRs following NF-κB and MAPKs in bovine mastitis. *Acta Trop,* 207:105458, 2020. DOI: 10.1016/j.actatropica.2020.105458

39. Guo YF, Xu NN, Sun W, Zhao Y, Li CY, Guo MY: Luteolin reduces inflammation in *Staphylococcus aureus*-induced mastitis by inhibiting NF-κB activation and MMPs expression. *Oncotarget,* 8, 28481-28493, 2017. DOI: 10.18632/oncotarget.16092

40. Yang W, Zerbe H, Petzl W, Brunner RM, Günther J, Draing C, von Aulock S, Schuberth HJ, Seyfert HM: Bovine TLR2 and TLR4 properly transduce signals from *Staphylococcus aureus* and *E. coli*, but *S. aureus* fails to both activate NF-κB in mammary epithelial cells and to quickly induce TNFα and interleukin-8 (CXCL8) expression in the udder. *Mol Immunol,* 45, 1385-1397, 2008. DOI: 10.1016/j.molimm.2007.09.004

41. Sakemi Y, Tamura Y, Hagiwara K: Interleukin-6 in quarter milk as a further prediction marker for bovine subclinical mastitis. *J Dairy Res*, 78, 118-121, 2011. DOI: 10.1017/S0022029910000828

42. Nakajima Y, Mikami O, Yoshioka M, Motoi Y, Ito T, Ishikawa Y, Yasukawa K: Elevated levels of tumor necrosis factor-α, (TNF-α) and interleukin-6 (IL-6) activities in the sera and milk of cows with naturally occurring coliform mastitis. *Res Vet Sci,* 62, 297-298, 1997. DOI: 10.1016/S0034-5288(97)90209-5

43. Hagiwara K, Yamanaka H, Hisaeda K, Taharaguchi S, Kirisawa R, Iwai H: Concentrations of IL-6 in serum and whey from healthy and mastitic cows. *Vet Res Commun*, 25, 99-108, 2001. DOI: 10.1023/a:1006400801305

44. Bochniarz M, Zdzisińska B, Wawron W, Szczubiał M, Dąbrowski R: Milk and serum IL-4, IL-6, IL-10, and amyloid A concentrations in cows with subclinical mastitis caused by coagulase-negative staphylococci. *J Dairy Sci*, 100, 9674-9680, 2017. DOI: 10.3168/jds.2017-13552

45. Shaheen T, Ahmad SB, Rehman MU, Muzamil S, Bhat RR, Hussain I, Bashir N, Mir MUR, Paray BA, Dawood MAO: Investigations on cytokines and proteins in lactating cows with and without naturally occurring mastitis. *J King Saud Univ Sci*, 32 (6): 2863-2867, 2020. DOI: 10.1016/j.jksus.2020.07.009

46. Ohtsuka H, Kudo K, Mori K, Nagai F, Hatsugaya A, Tajima M, Tamura K, Hoshi F, Koiwa M, Kawamura SI: Acute phase response in naturally occurring coliform mastitis. *J Vet Med Sci*, 63, 675-678, 2001. DOI: 10.1292/jvms.63.675

47. Fusco R, Cordaro M, Siracusa R, Peritore AF, D'Amico R, Licata P, Crupi R, Gugliandolo E: Effects of hydroxytyrosol against lipopolysaccharide-induced inflammation and oxidative stress in bovine mammary epithelial cells: A natural therapeutic tool for bovine mastitis. *Antioxidants,* 9(8):693, 2020. DOI: 10.3390/antiox9080693

48. Sordillo LM, Aitken SL: Impact of oxidative stress on the health and immune function of dairy cattle. *Vet Immunol Immunopathol,* 128, 104-109, 2009. DOI: 10.1016/j.vetimm.2008.10.305

49. Yang FL, Li XS: Role of antioxidant vitamins and trace elements in mastitis in dairy cows. *J Adv Vet Anim Res,* 2, 1-9, 2015. DOI: 10.5455/javar.2015.b48

50. Puppel K, Kalińska A, Kot M, Slósarz J, Kunowska-Slósarz M, Grodkowski G, Kuczyńska B, Solarczyk P, Przysucha T, Gołębiewski M: The effect of *Staphylococcus* spp., *Streptococcus* spp. and Enterobacteriaceae on the development of whey protein levels and oxidative stress markers in cows with diagnosed mastitis. *Animals*, 10 (9):1591, 2020. DOI: 10.3390/ani10091591

51. Tabatabaee N, Heidarpour M, Khoramian B: Milk metabolites, proteins and oxidative stress markers in dairy cows suffering from *Staphylococcus aureus* subclinical mastitis with or without spontaneous cure. *J Dairy Res*, 88, 326-329, 2021. DOI: 10.1017/S0022029921000613

52. Chen SJ, Zhang CY, Yu D, Lin CJ, Xu HJ, Hu CM: Selenium alleviates inflammation in *Staphylococcus aureus*-induced mastitis via MerTK-dependent activation of the PI3K/Akt/mTOR pathway in mice. *Biol Trace Elem Res*, 2021 (in press). DOI: 10.1007/s12011-021-02794-z

53. Andrei S, Matei S, Fit N, Cernea C, Ciupe S, Bogdan S, Groza IS: Glutathione peroxidase activity and its relationship with somatic cell count, number of colony forming units and protein content in subclinical mastitis cows milk. *Rom Biotechnol Lett*, 16, 6209-6217, 2011.

54. Mahapatra A, Panigrahi S, Patra RC, Rout M, Ganguly S: A study on bovine mastitis related oxidative stress along with therapeutic regimen. *Int J Curr Microbiol App Sci*, 7, 247-256, 2018. DOI: 10.20546/ijcmas.2018.701.027

55. Dalanezi FM, Joaquim SF, Guimaraes FF, Guerra ST, Lopes BC, Schmidt EMS, Cerri RLA, Langoni H: Influence of pathogens causing clinical mastitis on reproductive variables of dairy cows. *J Dairy Sci*, 103, 3648-3655, 2020. DOI: 10.3168/jds.2019-16841

56. Singh R, Bhardwaj RK, Azad MS, Beigh SA: Effect of mastitis on haemato-biochemical and plasma mineral profile in crossbred cattle. *Indian J Anim Res*, 48, 63-66, 2014. DOI: 10.5958/j.0976-0555.48.1.013

57. Al-Autaish HHN: Clinical, hematological and serological study of sub-clinical mastitis in local cows in Basrah Province. *QJVMS*, 18, 99-104, 2019.

58. Gera S, Guha A, Sharma A, Manocha V: Evaluation of trace element profile as an indicator of bovine sub-clinical mastitis. *Intas Polivet*, 12, 9-11, 2011.

59. Enjalbert F, Lebreton P, Salat O: Effects of copper, zinc and selenium status on performance and health in commercial dairy and beef herds: Retrospective study. *J Anim Physiol Anim Nutr (Berl),* 90, 459-466, 2006. DOI: 10.1111/j.1439-0396.2006.00627.x

60. Kandeel SA, Megahed AA, Constable PD: Evaluation of hand-held sodium, potassium, calcium, and electrical conductivity meters for diagnosing subclinical mastitis and intramammary infection in dairy cattle. *J Vet Intern Med*, 33, 2343-2353, 2019. DOI: 10.1111/jvim.15550

Kafkas Universitesi Veteriner Fakultesi Dergisi
ISSN: 1300-6045 e-ISSN: 1309-2251
Journal Home-Page: http://vetdergikafkas.org

Kafkas Univ Vet Fak Derg
27 (6): 763-769, 2021
DOI: 10.9775/kvfd.2021.26292

RESEARCH ARTICLE

Can Gestational Age be Determined by Placentome Diameter, Placentome Blood Flow Pixel Area and Progesterone Concentration During Pregnancy in Kivircik Ewes?

Sinem Özlem ENGİNLER [1,a (*)] Gamze EVKURAN DAL [1,b]
Ali Can ÇETİN [1,c] Ahmet SABUNCU [1,d] Kerem BAYKAL [2,e]

[1] Istanbul University-Cerrahpasa, Faculty of Veterinary Medicine, Department of Obstetrics and Gynecology, TR-34320 Istanbul - TURKEY
[2] Istanbul University-Cerrahpasa, The Institute of Graduate Education, TR-34320 Istanbul - TURKEY
ORCIDs: [a] 0000-0001-6522-285X; [b] 0000-0002-9996-3290; [c] 0000-0003-4617-8544; [d] 0000-0001-7905-421X; [e] 0000-0003-2200-403X

Article ID: KVFD-2021-26292 Received: 13.07.2021 Accepted: 21.10.2021 Published Online: 27.10.2021

Abstract

The information obtained about the gestational age allows ewes to be grouped and fed with appropriate rations for pregnancy. The aims of this study are to evaluate the relationship between placentome diameter (PD), placentome blood flow pixel area (PBFPA) and progesterone (P4) concentrations during pregnancy and to determine which parameter/s is/are effective in determining the gestational age better in sheep whose gestational age is unknown. In the study, 50 singleton pregnant Kivircik ewes were used. The day that the sheep mated with the ram was considered as day 0 of pregnancy. Ultrasonographic examinations and blood sample collections were done on the same day; once a week between 26-40 days, once every two weeks between 41-130 days, and once a week from day 130 of gestation until parturition. The power Doppler images of the biggest 3 placentomes were recorded. ImageJ software program was used for analysis of the area of colored pixels of placentome. The gestational day accurately determined up to 40th, 84th and 96th day of pregnancy according to the PD, PBFPA and P4 concentration, respectively. In conclusion, no relationship (except for PBFPA 40 and PD 40; $P<0.05$) between PD, PBFPA and P4 concentration on same time segments were detected in Kivircik ewes during pregnancy in this study. It was determined that P4 concentration measurements in sheep with unknown breeding time were the most useful parameter for determining the day of gestation, rather than PBFPA and PD, until day 96 of gestation in this study. However, while progesterone allowed for a more accurate determination of the gestational age up to day 96, this method is not yet successful in accurately determining the exact day of gestation beyond day 96 and until the end of pregnancy.

Keywords: *Gestational age, Placentome diameter, Placentome blood flow pixel area, Progesterone, Sheep*

Kıvırcık Koyunlarında Gebelikte Plasentom Çapı, Plasentom Kan Akışı Piksel Alanı ve Progesteron Konsantrasyonu İle Gebelik Yaşı Belirlenebilir mi?

Öz

Gebelik yaşı hakkında elde edilen bilgiler, koyunların gruplanarak gebelik için uygun rasyonlarla beslenmesini sağlar. Bu çalışmanın amacı gebelikte plasentom çapı (PÇ), plasentom kan akımı piksel alanı (PKAPA) ve progesteron (P4) konsantrasyonları arasındaki ilişkiyi değerlendirmek ve gebelik yaşı bilinmeyen koyunlarda gebelik yaşını daha iyi belirlemede hangi parametre/lerin etkili olduğunu tespit etmektir. Çalışmada 50 adet tekiz gebe Kıvırcık koyun kullanıldı. Koyunların koçla çiftleştiği gün gebeliğin 0. günü olarak kabul edildi. Ultrasonografik incelemeler ve kan örneklerinin toplanması 26-40 gün arasında haftada bir, 41-130 gün arasında iki haftada bir, gebeliğin 130. gününden doğuma kadar haftada bir olmak üzere aynı gün yapıldı. En büyük 3 plasentomun power Doppler görüntüleri kaydedildi. Plasentomun renkli piksel alanlarının analizi için ImageJ yazılım programı kullanıldı. PÇ, PKAPA ve P4 konsantrasyonuna göre gebelik günleri sırasıyla 40., 84. ve 96. gebelik günlerine kadar doğru olarak belirlendi. Sonuç olarak, bu çalışmada Kıvırcık koyunlarında gebelik sırasında PÇ, PKAPA ve aynı zaman dilimlerindeki P4 konsantrasyonu arasında (PKAPA 40 ve PD 40 hariç; $P<0.05$) ilişki saptanmadı. Bu çalışmada gebeliğin 96. gününe kadar PKAPA ve plasentom çapından ziyade çiftleşme zamanı bilinmeyen koyunlarda P4 konsantrasyon ölçümlerinin gebelik gününü belirlemede en yararlı parametre olduğu belirlendi. Bununla birlikte, progesteron, 96. güne kadar gebelik yaşının daha doğru bir şekilde belirlenmesine izin verirken, bu yöntem, 96. günden sonra ve gebeliğin sonuna kadar kesin gebelik gününün belirlenmesinde henüz başarılı değildir.

Anahtar sözcükler: *Gebelik yaşı, Plasentom çapı, Plasentom kan akışı piksel alanı, Progesteron, Koyun*

How to cite this article?

Enginler SÖ, Evkuran Dal G, Çetin AC, Sabuncu A, Baykal K: Can gestational age be determined by placentome diameter, placentome blood flow pixel area and progesterone concentration during pregnancy in Kivircik ewes? *Kafkas Univ Vet Fak Derg,* 27 (6): 763-769, 2021.
DOI: 10.9775/kvfd.2021.26292

(*) Corresponding Author

Tel: +90 212 473 7070-17137 Celular Phone: + 90 555 511 7304
E-mail: enginler@iuc.edu.tr (S.Ö. Enginler)

Introduction

Placentomes, approximately 80 per placenta, are the combination of interdigitated fetal cotyledonary and maternal caruncular microvilli; they are also the site of maternal-fetal nutrient exchange in ruminant animals [1-3]. The placentomes can be detected on the surface of the endometrium as particular echogenic areas at days 28 to 30 of gestation by transrectal ultrasonography; as pregnancy further progresses, they maturate into cup-shaped hyperechogenic areas around day 42 in cross-section [4]. Anwar et al.[5] started to examine the placentome scanning on day 26 twice weekly till 60th day of pregnancy transabdominally, using a 3.5 mHZ probe, and observed the maturation of placentomes on days 51 and 55 of pregnancy. Rasheed [6] found that ultrasonographically placentomes can be measured starting from day 35 of pregnancy until day 135, but this measurement is not reliable in determining the gestational age after day 90 of pregnancy. Jones et al.[7] defined perfusion as the volume of blood flowing through a mass of tissue per unit of time. Lemley [8] reported that some tissues and organs can have inadequate amounts of blood flow or the arteries may be too small to maintain their blood flow; therefore the power flow of the Doppler instrument can overcome this difficulty. Power mode is an advanced method of scanning blood flow compared with the traditional color Doppler technique [9], which allows recording blood flow independently of blood flow velocity and direction. This is essential for tissues with low blood flow velocity and numerous blood vessels such as placentomes [10]. Serum progesterone hormone is essential for the maintanance of pregnancy in animals [11,12]. In sheep, serum progesterone has a regular pattern during pregnancy and tends to decline in the prepartum period and at birth [12,13].

For high reproductive efficiency in sheep, basic procedures such as accurate pregnancy diagnosis, determination of gestational age, determination of fetal numbers and removal of non-pregnant females from the herd are required. In particular, the information obtained about the gestation period allows ewes to be grouped and to be fed with appropriate rations according to their nutritional needs for pregnancy; it allows for monitoring females that are close to calving and providing sufficient time to dry off the lactating females [4,14,15].

One of the aims of this study is to evaluate the relationship between PD, PBFPA and P4 concentrations during pregnancy in Kivircik ewes. Another aim of this study is to determine which of these parameter/s is/are effective in determining the gestational age better (until the later day of pregnancy) in sheep whose gestational age is unknown. Thus, with this study, blood flow pixel area in placentomes and placentome diameters during pregnancy of ewes and progesterone concentrations in maternal serum were evaluated.

Material and Methods

Ethical Statement

Ethical approval for the study was obtained from the Istanbul University-Cerrahpaşa Veterinary Faculty Ethics Committee Unit (2019/54, 19.12.2019).

Animals and Management

A total of 170 Kivircik ewes were synchronized with progesterone-based protocol during breeding season and 50 singleton pregnant ewes were selected according to the first pregnancy examination day. Ewes were between 2-6 years old, which were fed semi-intensively. Progesterone-containing intravaginal sponges (30 mg flurorogestone acetate, Chronogest, Intervet, Turkey) were used for 11 days in the breeding season for oestrus synchronization in sheep. Further, 400 IU PMSG (PMSG, Intervet, Turkey) were applied on the day of sponge withdrawal, and fertile rams were added to the sheep herd 48 h later. The day that the sheep mated with the ram was considered as day 0 of pregnancy. Pregnancy diagnosis was made by transrectal ultrasonography between days 17-19 in sheep that were synchronized and were placed with rams, and out of them, 50 singleton pregnant sheep were selected randomly and included to the study.

Study Design

The animals were placed in the standing position, and both sides of the inguinal region in the early period of pregnancy and the more cranial side of the ventral abdomen in later periods were shaved; then the probe was positioned to display the maximum size of the placentomes ultrasonographically (Esaote, MyLab One, Italy). In the current study, the biggest three placentomes were measured, and mean diameter of these placentomes were calculated in centimeters (cm). Ultrasonographic examinations were conducted with a 5 mHz microconvex probe transabdominally once a week between days 26 to 40, once every two weeks between days 41 to 130, and once a week from day 130 of gestation until parturition. In order to obtain the maximum number of colored pixels captured in power Doppler examination in the placentomes, the probe was adjusted in place by light manipulation before freezing *(Fig. 1)*. Using the power flow function of the Doppler ultrasound, 3 placentomes were imaged transabdominally for blood perfusion. Ultrasound images were uploaded from the Esaote, MyLab One ultrasound device and a software program was used for analysis of the area of colored pixels of placentome tissue in sheep in gravid horn. Ultrasound images firstly were set scaled from pixels to mm, and then the placentome was selected via the freehand tool then the images were edited to distinguish the blood perfusion area, the surroundings of the placentome were all being cleared with "clear outside" tool. The colored perfusion areas were saturated with threshold function of ImageJ program (ImageJ, version

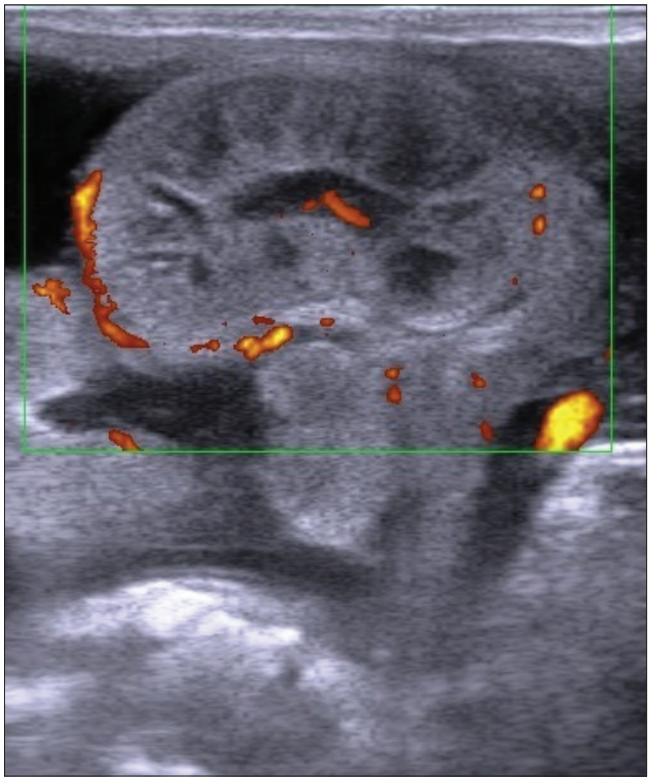

Fig 1. The ultrasound probe was adjusted in place by light manipulation before freezing, and maximum number of colored pixels was captured in a power Doppler examination in the placentomes

1.50e, US National Institutes of Health, USA). These areas were measured using the "Analyse" function of ImageJ for each placentome. From these data, the mean pixel areas of the biggest three placentomes were recorded for each animal in mm^2.

On the ultrasonographic examination days, 10 mL blood samples were collected from the jugular vein into anti-coagulant tubes. Blood samples were centrifuged at 1000 x g for 10 min for serum retrieval and the obtained sera were kept at -20°C until progesterone analysis. The progesterone concentration in serum samples were determined by the quantitative sandwich enzyme immunoassay technique using commercial kits (Sheep progesterone ELISA, Bioassay Technology Laboratory, Shanghai, China) according to the manufacturer's instructions with a sensitivity of 0.027 ng/mL. The intra- and inter-assay coefficients of variation for the kit were <8 and <10%.

Statistical Analysis

The relationship between placentome diameter, placentome blood flow pixel area and progesterone concentration were analyzed using the Pearson correlation analysis method.The Shapiro-Wilk test was used to check the normality of data. Statistical analyses of the parameters were measured with ANOVA for, repeated measures. The SPSS 13.0 package program was used for analysis. For all statistical analyses performed, $P<0.05$ was accepted as significant.

Results

Although there was statistical significance ($P<0.05$) between some features in general, a relationship that allow to make a meaningful interpretation could not be determined. Besides, according to the same time segments no relationship among PD, PBFPA and P4 concentration were detected in Kivircik ewes during pregnancy in this study, except for PBFPA 40 and PD 40 ($P<0.05$) *(Table 1)*. In this study, it was observed that placentome diameters increased until day 84 of gestation and reached its maximum value (3.69 cm) on day 84. Then, it decreased to 1.57 cm by day 145 of gestation. Although the gestational day can be accurately determined up to day 40 of pregnancy according to the PD, the exact day of gestation beyond day 40 cannot be determined. Placentome blood flow pixel area increased until day 124 of gestation and reached its maximum value (39.46 mm^2). From that point, it started to decrease and reached to its final value 21.92 mm^2 by the end of pregnancy. According to the PBFPA, it is evident that until day 84 of pregnancy, gestational age can be accurately determined, but after that point, the exact day of pregnancy cannot be clearly determined till the end of gestation. Based on the PBFPA measurement, gestational age can only be established as lying between days 84 to 145.

In this study, P4 concentration in maternal serum was found to increase until day 124 of gestation with its maximum concentration at 13.85 ng/mL, and from that point on, the P4 concentration decreased (11.50 ng/mL) at the end of gestation. It was observed that, based on the P4 concentration, the pregnancy can be accurately determined until day 96 of pregnancy. By obtaining the P4 concentration in pregnancies after 96 days, the pregnancy can be foreseen only between 96-145 days. According to the statistical analysis, the effects of the features depending on the time of pregnancy were found to be different ($P<0.001$) *(Table 2)*.

Discussion

Pregnancy might be recognized as early as 17-19 days post breeding using B-Mode ultrasonography in sheep [16,17]. Jyothi et al.[18] observed placentomes first on day 22 of gestation by transabdominal ultrasonography as an echogenic dense line in Nellore brown ewes. Due to the visualization of placentomes by transabdominal ultrasonography, we performed ultrasonographic examinations on day 26 and further until the end of gestation to predict the most effective parameter --PD, PBFPA and/or P4 concentration-- to detect the exact gestational age in the ewes in this study. According to the same time segments, only one positive relationship between PBFPA 40 and PD 40 ($P<0.05$) was found. However, it would not be correct to reveal a meaningful relationship between the study parameters by determinig at this result alone. It was reported that the mean diameters of placentomes

Table 1. *Correlation analysis of placentome diameter, placentome blood flow pixel area and progesterone concentration*

Parameter	PBFPA 26	PBFPA 33	PBFPA 40	PBFPA 54	PBFPA 68	PBFPA 84	PBFPA 96	PBFPA 110	PBFPA 124	PBFPA 131	PBFPA 138	PBFPA 145	P 26	P 33	P 40	P 54	P 68	P 84	P 96	P 110	P 124	P 131	P 138	P 145	PD 26	PD 33	PD 40	PD 54	PD 68	PD 84	PD 96	PD 110	PD 124	PD 131	PD 138	PD 145
PBFPA26	1.0	0.7	0.0	-0.2	0.1	0.0	0.0	0.0	0.1	-0.1	0.0	-0.1	-0.1	-0.1	-0.2	-0.2	0.0	-0.1	0.2	0.0	0.3	0.1	0.1	-0.2	0.1	0.2	**0.3**	**0.3**	0.1	0.1	-0.1	0.1	0.1	0.1	0.1	0.0
PBFPA33		1.0	0.3	0.0	0.2	0.1	0.1	0.1	-0.2	0.1	0.1	0.1	-0.2	0.0	0.0	-0.1	-0.1	-0.1	0.1	**0.4**	**0.5**	**0.3**	0.2	-0.3	-0.1	0.2	**0.3**	0.2	-0.1	0.0	-0.1	0.0	0.1	0.1	0.1	0.0
PBFPA40			1.0	**0.3**	**0.4**	**0.3**	**0.4**	**0.3**	-0.2	0.2	-0.1	0.0	-0.1	0.0	0.0	-0.2	-0.1	0.1	0.2	0.1	0.3	0.2	0.2	-0.3	-0.1	**0.4**	**0.3**	0.2	0.0	0.2	0.1	0.0	0.0	0.1	0.1	0.0
PBFPA54				1.0	0.1	0.1	0.1	-0.1	0.0	0.0	0.1	0.1	-0.1	0.1	0.0	-0.1	-0.1	0.3	0.1	0.2	0.1	0.1	0.1	0.0	0.0	0.2	-0.1	0.0	-0.1	-0.1	-0.1	-0.1	0.0	0.0	0.0	-0.1
PBFPA68					1.0	**0.4**	0.1	0.0	**-0.4**	0.1	-0.1	0.0	0.0	0.1	0.0	0.1	-0.1	0.0	0.2	0.1	0.3	0.2	0.2	-0.1	-0.1	**0.3**	**0.4**	**0.4**	0.1	0.3	0.1	0.0	-0.2	-0.2	-0.2	-0.2
PBFPA84						1.0	0.2	0.1	**-0.3**	0.0	0.0	-0.1	0.0	-0.1	-0.2	0.1	-0.2	0.1	0.1	0.2	**0.3**	0.2	0.2	-0.2	-0.1	0.2	0.2	0.0	0.0	0.2	0.0	-0.1	-0.2	-0.2	-0.1	-0.1
PBFPA96							1.0	0.2	-0.1	0.2	0.0	-0.2	0.1	0.1	0.2	0.1	-0.1	0.2	0.1	0.1	0.2	**0.3**	**0.3**	0.0	0.0	0.1	0.2	0.2	0.1	0.2	0.0	0.2	0.0	0.0	-0.1	-0.2
PBFPA110								1.0	0.0	0.2	0.1	-0.2	0.2	-0.1	0.0	0.0	0.1	0.0	-0.2	-0.1	0.1	0.0	0.1	-0.1	0.2	0.0	0.2	-0.1	-0.1	-0.1	-0.2	-0.1	-0.3	-0.3	**-0.3**	**-0.3**
PBFPA124									1.0	-0.2	-0.1	0.0	0.0	-0.1	0.0	-0.1	0.2	0.1	0.1	0.0	0.0	0.1	0.1	0.1	0.0	-0.1	-0.3	-0.1	0.1	-0.1	-0.1	-0.2	-0.1	-0.1	-0.1	0.0
PBFPA131										1.0	0.0	0.0	0.0	0.1	0.1	0.1	0.0	-0.1	0.0	0.1	0.2	0.3	0.3	0.1	-0.1	-0.1	-0.2	0.1	0.1	0.1	0.1	0.3	0.1	0.1	0.1	0.0
PBFPA138											1.0	**0.5**	-0.1	-0.1	0.0	-0.1	-0.2	-0.2	-0.2	0.0	0.0	0.0	0.0	0.2	0.1	-0.1	**-0.4**	**-0.3**	-0.1	-0.1	0.0	-0.1	0.0	0.0	-0.1	-0.2
PBFPA145												1.0	**-0.3**	0.0	-0.1	0.0	0.1	-0.1	-0.1	0.0	0.0	-0.1	-0.1	-0.1	-0.2	-0.1	-0.2	0.0	0.0	0.0	0.0	0.0	0.1	0.0	0.0	-0.1
P26													1.0	**0.5**	**0.4**	0.2	0.0	0.0	0.0	-0.2	-0.2	-0.1	0.0	0.1	0.2	0.0	0.0	0.0	0.0	-0.1	-0.1	-0.1	0.0	0.0	0.0	0.0
P33														1.0	**0.8**	**0.3**	0.1	0.0	0.0	0.0	0.0	0.0	-0.1	0.1	0.1	0.0	0.1	0.3	0.0	0.1	-0.1	-0.1	0.0	0.0	0.0	-0.1
P40															1.0	**0.3**	0.1	-0.1	-0.1	0.0	0.0	0.0	0.0	**0.3**	0.1	0.0	0.1	0.2	0.1	0.1	-0.1	0.0	0.1	0.0	-0.1	-0.1
P54																1.0	0.2	0.2	0.1	0.0	0.1	0.0	0.1	0.2	0.0	0.0	0.1	**0.4**	0.1	0.2	0.2	0.1	0.1	0.1	0.1	0.0
P68																	1.0	0.0	0.0	-0.1	0.0	0.0	0.1	0.2	-0.1	-0.3	0.0	0.1	0.2	0.1	-0.1	0.0	0.0	0.0	0.0	0.0
P84																		1.0	**0.5**	0.2	0.1	0.1	0.1	-0.1	-0.2	-0.2	0.0	0.1	-0.3	-0.2	-0.2	-0.3	-0.2	-0.2	-0.2	-0.2
P96																			1.0	**0.5**	**0.4**	**0.5**	**0.4**	0.0	**-0.4**	-0.1	-0.1	0.1	0.0	0.1	0.1	-0.1	0.0	0.0	0.0	-0.1
P110																				1.0	**0.7**	**0.7**	**0.6**	0.0	**-0.4**	-0.2	-0.1	-0.2	0.0	0.1	0.0	-0.1	0.0	-0.1	-0.1	-0.2
P124																					1.0	**0.8**	**0.8**	-0.1	-0.2	0.1	0.1	0.2	0.2	**0.4**	0.1	0.1	0.0	0.1	0.0	-0.1
P131																						1.0	**0.9**	0.1	-0.2	0.0	0.0	0.0	0.3	**0.3**	0.1	0.0	0.0	0.0	0.0	-0.1
P138																							1.0	0.1	-0.2	0.0	0.0	0.1	**0.3**	**0.4**	0.1	0.1	0.1	0.1	0.0	0.0
P145																								1.0	0.1	-0.2	**-0.3**	-0.1	0.0	0.0	0.0	0.1	-0.1	-0.1	-0.1	-0.1
PD26																									1.0	**0.6**	**0.3**	0.1	0.2	0.1	0.1	0.2	0.1	0.2	0.2	0.2
PD33																										1.0	**0.7**	**0.5**	0.2	**0.4**	**0.4**	**0.3**	0.2	0.2	0.2	0.3
PD40																											1.0	**0.5**	0.2	**0.3**	0.3	0.3	0.0	0.1	0.0	0.1
PD54																												1.0	**0.3**	**0.5**	**0.3**	**0.3**	**0.3**	0.3	0.3	0.2
PD68																													1.0	**0.9**	**0.7**	**0.6**	**0.5**	**0.5**	**0.5**	**0.5**
PD84																														1.0	**0.7**	**0.6**	**0.4**	**0.5**	**0.5**	**0.4**
PD96																															1.0	**0.7**	**0.6**	**0.6**	**0.6**	**0.5**
PAD110																																1.0	**0.7**	**0.7**	**0.6**	**0.6**
PD124																																	1.0	**1.0**	**0.9**	**0.8**
PD131																																		1.0	**1.0**	**0.8**
PD138																																			1.0	**0.9**
PD145																																				1.0

Those written in bold are statistically significant (P<0.05); PBFPA: Placentome blood flow pixel area, P: Progesterone concentration, PD: Placentome diameter

Table 2. *The results of mean placentome diameter, placentome blood flow pixel area and progesterone concentration throughout pregnancy in Kivircik ewes*

Gestational Days	Placentome Diameter Mean ± SE (cm)	Placentome Blood Flow Pixel Area Mean ± SE (mm^2)	Progesterone Concentration Mean ± SE (ng/mL)
26	0.72 ± 0.03^{a}	1.10 ± 0.10^{a}	2.41 ± 0.08^{a}
33	0.95 ± 0.02^{b}	2.09 ± 0.08^{b}	2.89 ± 0.08^{b}
40	1.23 ± 0.03^{c}	4.60 ± 0.10^{c}	3.24 ± 0.07^{c}
54	2.33 ± 0.06^{g}	8.03 ± 0.07^{d}	6.58 ± 0.10^{d}
68	3.33 ± 0.06^{i}	11.25 ± 0.12^{e}	8.52 ± 0.10^{e}
84	3.69 ± 0.07^{j}	17.20 ± 0.15^{f}	11.33 ± 0.14^{f}
96	2.77 ± 0.05^{h}	25.73 ± 0.26^{h}	12.39 ± 0.09^{g}
110	2.25 ± 0.04^{g}	32.89 ± 0.37^{j}	13.46 ± 0.06^{i}
124	1.79 ± 0.02^{f}	39.46 ± 0.21^{k}	13.85 ± 0.07^{j}
131	1.74 ± 0.02^{ef}	30.66 ± 0.19^{i}	13.50 ± 0.06^{i}
138	1.66 ± 0.02^{de}	21.61 ± 0.18^{g}	13.06 ± 0.06^{h}
145	1.57 ± 0.02^{d}	21.92 ± 0.21^{g}	11.50 ± 0.05^{f}
P	P<0.001	P<0.001	P<0.001

$^{a\text{-}k}$ The significant differences between time in the columns is shown in different letters

as approximately 3.0 cm and remained unchanged from the first scanning (day 60 of pregnancy) until lambing on Santa Ines ewes with 9 females carried twins and 4 ewes had single pregnancies [19]. Mean PDs in the similar examining days were detected lower in ewes carrying single offspring in this study. In another study, Dwyer et al.[20] reported that placental weight, placental cotyledons and mean placental weight were lower in singleton pregnant sheep than in twins. Placentomes began to appear as buds on the endometrium surface, giving an echogenic appearance on day 28 of pregnancy in Merinos ewes [15]. Doize et al.[4] detected the placentomes on days 28-30 ultrasonographically in their study in mixed-breed ewes. In this study, the ultrasonographic examinations were started on day 26 after controlled mating, and the placentomes were detected as buds giving an echogenic appearance on this day - results reported by Aydın et al.[15] and Doize et al.[4] were very close to those results also. Alexander [21] observed that placentome sizes can vary in relation to their location in the uterine horn, where the smallest placentomes were found at the tips of the horns and the largest near the junction of both horns. In this study, placentome diameter increased and until day 84 of gestation, after which their size started to decrease; the maximal size of the placentomes was recorded on day 84 of gestation. Doize et al.[4] reported the maximum size of the placentomes detected by transrectal ultrasonography method on day 74 of gestation. The variation of placental development in relation to season has also been reported previously [22], the number of developed placentomes and their total weight was much greater in females bred during the normal breeding season than those bred during the anestrus season [4]. In the present study, examinations were performed on females bred during the normal breeding season in line with a previous study [4]. Waziri et al.[23] reported a high correlation between PD and gestatinal age in sheep. However, the mean diameter of placentomes was not statistically different during the last 7 weeks before parturition. The authors concluded that PD measurement can be used as an indicator of gestational age only at midgestation. In the present study, the gestational day can be accurately determined up to day 40 of pregnancy according to the PD.

Doppler ultrasonography is as extremely useful tool for small ruminant reproduction [24]. Power Doppler sonography is a new scanning method that displays the strength of the Doppler signal in color rather than the speed and direction of blood flow. Therefore, it is approximately three times more sensitive than a conventional color Doppler for detecting blood flow; therefore especially useful for those with small blood vessels and low-velocity flow [25]. In a study [26], pregnancy can be diagnosed accurately by semiquantitative assessment of corpus luteum vascularization as early as 17 days post breeding in ewes. Besides, placentome blood flow pixel area can be detected by power Doppler ultrasonography as this method facilitates the evaluation of capillary blood flow. Still images or recordings obtained during power/color Doppler examinations can be stored for later for analysis with various image analytical programs. The vascularized (colored) area of an ultrasonogram can be taken as a proportion or percentage of the total cross-sectional area of the organ or tissue, and the pixels corresponding to blood flow velocities can be measured [25,27,28]. In this study, PBFPA was measured using a software program to eliminate the errors that may arise from subjective evaluations. The vascularization of placentome tissue is an important feature for the gestational process, and the increase in blood flow in these structures throughout pregnancy is

related to the nutritional requirements of the foetus and the proximity of parturition [29]. Lemley et al.[30] examined the changes in placentome blood perfusion that occurred due to vasoactive medications and determined acute fluctuations in placentome blood perfusion in singleton pregnant ewes. Da Silva et al.[31] evaluated fetomaternal structures throughout pregnancy by ultrasonography in ewes. The values achieved from gray-scale analysis of the placentomes decreased gradually. As gestation progressed, the echogenity of placentomes changed from hyperechoic to hypoechoic structures, especially from the 18th week of pregnancy. However, the echotexture of the tissue remained homogeneous. Although Doppler ultrasonography was not performed, the reduction of placental echogenicity was suggested to be associated with an increase in the blood volume, which is in line with the highest pixel area calculated on day 124 in our study.

Progesterone with other hormones directly related to pregnancy, and P4 is necessary for the continuation of pregnancy in domestic animals, including sheep. Hamon and Heap [32] reported an increase during the early gestational period and a reduction in the P4 concentration between days 30 to 50; afterwards the P4 concentration was found to increase again. Kalkan et al.[33] reported a mean P4 concentration of 2.02 ng/mL begininig from 30 day of gestation in blood samples collected every 20 days till parturition in sheep with single offspring, besides they indicated that when the number of fetuses increases, P4 level increases in maternal serum and also P4 measurement can be used to predict the fetal number after the second half of pregnancy. Progesterone concentration is approximately 10.02 ng/mL during the same gestational period in current study. Yotov [34] reported P4 concentrations of 15.0 ng/mL and 19 ng/mL and 17.3 ng/mL and 23.3 ng/mL in Trakia Merino and Pleven Blackhead sheep on days 40 and 60, respectively, during pregnancy. In this study, the P4 concentration was found to be 3.24 ng/mL and 8.52 ng/mL on days 40 and 68 of gestation, respectively, in Kivircik ewes. The P4 concentration was observed to increase until day 124 of gestation, and it was measured as 13.85 ng/mL at that point, after which it decreased until parturition in this study. Manalu and Sumaryadi [35] reported the mean P4 concentration as 16.9 ng/mL between weeks 8-20 of pregnancy in sheep with a single fetus. Dramatic increase in maternal serum P4 concentration during the fetal phase (8-20 week) of pregnancy is due to the role of placental P4 [36,37]. The P4 concentration measured by RIA method in their study was higher during the same gestational period. Stabenfeldt et al.[38] reported a decline in P4 concentration beginning around days 130-135 (week 19) and continued to the day of parturition; this suggests that endocrine preparation for delivery begins about 2 weeks prior to parturition. The P4 concentration started to decrease on day 131 and continued to the day of parturition in our current study, which is in line with their study.

In conclusion, according to the same time segments, only one positive relationship between PBFPA 40 and PD 40 was found. It was associated with the increased blood supply due to the increase in placentome diameter. Although, statistically significant differences by time were found in terms of PD, PBFPA and P4 concentration, according to the results of this study, it was determined that P4 concentration measurements in sheep with unknown breeding time were more useful parameters in determining the day of gestation than PBFPA or PD. However, while progesterone allowed for a more accurate determination of the gestational age up to day 96, this method is not yet successful in accurately determining the exact day of gestation beyond day 96 and until the end of pregnancy.

Availability of Data and Materials

The datasets during and/or analyzed during the current study available from the corresponding author on reasonable request.

Acknowledgements

We want to thank to Prof. Dr. Ömür Koçak from Department of Animal Breeding and Husbandry, Faculty of Veterinary Medicine, Istanbul University-Cerrahpasa for his valuable contributions for statistical analysis of this study. The authors are also grateful to Dr. Koray Gürkan from Department of Electrical and Electronics Engineering, Faculty of Engineering, Istanbul University-Cerrahpasa for the help of ImageJ analysis. The manuscript was edited by WordsRU; OnlineEnglish Editing and Proofreading Service.

Funding Support

This research did not receive any specific grant from funding agencies in the public, commercial, or not-for-profit sectors.

Conflict of Interest

The authors declare that they have no conflict of interests.

Author Contributions

S.Ö. Enginler: Project administration, conceptualization, methodology, software, visualization, investigation, writing - original draft, writing- review & editing. G. Evkuran Dal: Methodology, visualization, data curation, software. A.C. Çetin: Conceptualization, investigation, data curation, software. A. Sabuncu and K. Baykal: Methodology, investigation, visualization.

References

1. Reynolds LP, Redmer DA: Utero-placental vascular development and placental function. *J Anim Sci,* 73,1839-1851, 1995. DOI: 10.2527/1995.7361839x

2. Reynolds LP, Redmer DA: Angiogenesis in the placenta. *Biol Reprod,*

64, 1033-1040, 2001. DOI: 10.1095/biolreprod64.4.1033

3. Laurent A, Wassef M, Namur J, Martal J, Labarre D, Pelage JP: Recanalization and particle exclusion after embolization of uterine arteries in sheep: A long-term study. *Fertil Steril,* 91, 884-892, 2009. DOI: 10.1016/j.fertnstert.2007.12.015

4. Doize F, Vaillancourt D, Carabin H, Belanger D: Determination of gestational age in sheep and goats using transrectal ultrasonographic measurement of placentomes. *Theriogenology,* 48, 449-460, 1997. DOI: 10.1016/s0093-691x(97)00254-9

5. Anwar M, Riaz A, Ullah N, Rafiq M: Use of ultrasonography for pregnancy diagnosis in Balkhi sheep. *Pak Vet J,* 28 (3): 144-146, 2008.

6. Rasheed YM: Ultrasonic estimation of gestation age in goats via plancentomes diameter. *Iraqi J Vet Med,* 40 (2): 100-106, 2016. DOI: 10.30539/iraqijvm.v40i2.120

7. Jones NW, Raine-Fenning N, Bugg G: 3D Power Doppler in obstetrics. *Fetal Matern Med Rev,* 22, 1-24, 2011.

8. Lemley CO: Investigating reproductive organ blood flow and blood perfusion to ensure healthy offspring. *Anim Front,* 7 (3): 18-24, 2017. DOI: 10.2527/af.2017-0124

9. Bollwein H, Heppelmann M, Lüttgenau J: Ultrasonographic Doppler use of female reproduction management. *Vet Clin North Am Food Anim Pract,* 32, 149-164, 2016. DOI: 10.1016/j.cvfa.2015.09.005

10. Bude RO, Rubin JM: Power Doppler sonography. *Radiology,* 200, 21-23, 1996. DOI: 10.1148/radiology.200.1.8657912

11. Izhar M, Pasmanik M, Shemesh M: Bovine placental progesterone synthesis: Comparison of first and second trimesters of gestation. *Biol Reprod,* 46, 846-852, 1992. DOI: 10.1095/biolreprod46.5.846

12. Silver M: Placental progestagens in sheep and horse and the changes leading to parturition. *Exp Clin Endocrinol Diabetes,* 102, 203-211, 1994. DOI: 10.1055/s-0029-1211284

13. Smith FJ: Principles of reproduction. **In,** Wickham GA, McDonald MF (Eds): Breeding and Reproduction. Sheep Production. 211-228, Ray Richards Publisher, Auckland, 1982.

14. Goel AK, Agrawal KP: A review of pregnancy diagnosis techniques in sheep and goats. *Small Ruminant Res,* 9, 255-264, 1992. DOI: 10.1016/0921-4488(92)90155-W

15. Aydın İ, Celik HA, Şendag S, Dinç DA: Koyunlarda plasentomların ultrasonografik ölçümleri ile plasentom gelişimi ve gebelik yaşının belirlenmesi. *Vet Bil Derg,* 24, 29-34, 2008.

16. Garcia A, Neary MK, Kelly GR, Pierson RA: Accuracy of ultrasonography in early pregnancy diagnosis in the ewe. *Theriogenology,* 39 (4): 847-861, 1993. DOI: 10.1016/0093-691X(93)90423-3

17. Arashiro EKN, Ungerfeld R, Clariget RP, Pinto PHN, Balaro, MFA, Bragança GM, Riberio LSR, da Fonseca JF, Brandao FZ: Early pregnancy diagnosis in ewes by subjective assessment of luteal vasularization using colour Doppler ultrasonography. *Theriogenology,* 106, 247-252, 2018. DOI: 10.1016/j.theriogenology.2017.10.029

18. Jyothi K, Sudha G, Krishna KM, Sahadev A, Swamy MN, Rao S, Kshama MA: Transabdominal ultrasonographic measurement of placentome length to estimate and validate gestational age in Nellore broen ewes. *J Entomol Zool Stud*, 8 (6): 1460-1467, 2020.

19. Vannucchi CI, Veiga GAL, Silva LCG, Lucio CF: Relationship between fetal biometric assessment by ultrasonography and neonatal lamb vitality, birth weight and growth. *Anim Reprod*, 16 (4): 923-929, 2019. DOI: 10.21451/1984-3143-AR2019-0006

20. Dwyer CM, Calvert SK, Farish M, Donbavand J, Pickup HE: Breed, litter and parity effects on placental weight and placentome number, and consequences for the neonatal behaviour of the lamb. *Theriogenology,* 63, 1092-1110, 2005. DOI: 10.1016/j.theriogenology.2004.06.003

21. Alexander G: Studies on the placenta of the sheep *(Ovis aries):* Placental size. *J Reprod Fertil,* 7, 289-305, 1964. DOI: 10.1530/jrf.0.0070289

22. Jenkinson CMC, Peterson SW, Mackenzie DDS, McCutcheon SN: The effects of season on placental development and fetal growth. *Proc N Z Soc Anim Prod,* 54, 227-230, 1994.

23. Waziri MA, Ikpe AB, Bukar MM, Ribadu AY: Determination of gestational age htrough trans-abdominal scan of placentome diameter in Nigerian breed sheep and goats. *Sokoto J Vet Sci,* 15 (2): 49-53, 2017. DOI: 10.4314/sokjvs.v15i2.7

24. Bartlewski PM: Applications of Doppler ultrasonography in reproductive health and physiology of small ruminants. *Rev Bras Reprod Anim,* 43 (2): 122-125, 2019.

25- El-Sherry TM, Derara R, Bakry R: Changes in blood flow in ovine follicles and serum concentration of estradiol 17 beta (E2) and nitric oxide (NO) around the time of ovulation in Ossimi ewes. *Anim Reprod Sci,* 138, 188-193, 2013. DOI: 10.1016/j.anireprosci.2013.02.019

26. Evkuran Dal G, Enginler SO, Baykal K, Sabuncu A. Early pregnancy diagnosis by semiquantitative evaluation of luteal vascularity using power Doppler ultrasonography in sheep. *Acta Vet Brno,* 88, 19-23, 2019. DOI: 10.2754/avb201988010019

27. Oliveira MEF, Feliciano MAR, D'Amato CC, Oliveira LG, Bicudo SD, Fonseca JF, Vicente WRR, Visco E, Bartlewski PM: Correlations between ovarian follicular blood flow and superovulatory responses in ewes. *Anim Reprod Sci,* 144, 30-37, 2014. DOI: 10.1016/j.anireprosci.2013.10.012

28. Figueira LM, Fonseca JF, Arashiro EKN, Souza-Fabjan JMG, Ribeiro ACS, Oba E, Viana JHM, Brandão FZ: Colour Doppler ultrasonography as a tool to assess luteal function in Santa Inês ewes. *Reprod Domest Anim,* 50, 643-650, 2015. DOI: 10.1111/rda.12543

29. Cunningham JG: Tratado de Fisiologia Veterinária. 2nd ed., Rio de Janeiro: Guanabara Koogan, 1999.

30. Lemley CO, Bowers KJ, Yankey KC, Tu ML, Hart CG, Steadman CS, McCarty KJ, Owen MPT: Investigating ovine placentome blood perfusion using power flow Doppler ultrasonography. *Small Ruminant Res,* 184:106051, 2020. DOI: 10.1016/j.smallrumres.2020.106051

31. da Silva PDA,Uscategui RAR, Santos VJC, Taira AR, Mariano RSG, Rodrigues MGK, Simões APR, Maronezi MC, Avante ML, Vicente WRR, Feliciano MAR: Qualitative and quantitative ultrasound attributes of maternal-foetal structures in pregnant ewes. *Reprod Domest Anim,* 53, 725-732, 2018. DOI: 10.1111/rda.13163

32. Hamon MH, Heap RB: Progesterone and estrogen concentrations in plasma of Barbary sheep (audad, *Ammotragus lervia)* compared with those domestic sheep and goats during pregnancy. *J Reprod Fertil,* 90, 207-211, 1990. DOI: 10.1530/jrf.0.0900207

33. Kalkan C, Cetin H, Kaygusuzoglu E, Yılmaz B, Ciftci M, Yıldız H, Yıldız A, Deveci H, Apaydın AM, Ocal H: An investigation on plasma progesterone levels during pregnancy and parturition in the Ivesi sheep. *Acta Vet Hung,* 44, 335-340, 1996.

34. Yotov S: Determination of the number of fetuses in sheep by means of blood progesterone assay and ultrasonography. *Bulg J Vet Med,* 10 (3): 185-193, 2007.

35. Manalu W, Sumaryadi MY: Maternal serum progesterone concentration during pregnancy and lamb birth weight at parturition in Javanese Thin-Tail ewes with different litter sizes. *Small Ruminant Res,* 30, 163-169, 1998. DOI: 10.1016/S0921-4488(98)00100-X

36. Ricketts AP, Flint APF: Onset of synthesis of progesterone by ovine placenta. *J Endocrinol,* 86, 337-347, 1980. DOI: 10.1677/joe.0.0860337

37. Sheldrick EL, Ricketts AP, Flint APF: Placental production of 5β-pregnane-3α, 20α-diol in goats. *J Endocrinol,* 90, 151-158, 1981. DOI: 10.1677/joe.0.0900151

38. Stabenfeldt GH, Drost M, Franti CE: Peripheral plasma progesterone levels in the ewe during pregnancy and parturition. *Endocrinology,* 90, 144-150, 1972. DOI: 10.1210/endo-90-1-144

Kafkas Universitesi Veteriner Fakultesi Dergisi
ISSN: 1300-6045 e-ISSN: 1309-2251
Journal Home-Page: http://vetdergikafkas.org

Kafkas Univ Vet Fak Derg
27 (6): 771-779, 2021
DOI: 10.9775/kvfd.2021.26300

RESEARCH ARTICLE

The Effect of Midazolam and Its Reversal Flumazenil on Sedative and Cardiopulmonary Variables in Sheep

Ünal YAVUZ [1,a (*)] Kerem YENER [1,b] Adem ŞAHAN [2,c]

[1] Department of Surgery, Faculty of Veterinary Medicine, Harran University, TR-63200 Şanlıurfa - TURKEY
[2] Department of Internal Medicine, Faculty of Veterinary Medicine, Harran University, TR-63200 Şanlıurfa - TURKEY
ORCIDs: [a] 0000-0002-4981-2355; [b] 0000-0002-6947-0356; [c] 0000-0002-4779-0893

Article ID: KVFD-2021-26300 Received: 15.07.2021 Accepted: 11.11.2021 Published Online: 16.11.2021

Abstract

The aim of this study was to investigate the effects of flumazenil antagonism after midazolam administration on sedative and cardiopulmonary variables in ewes. Six Awassi ewes were studied at least 14 days apart. The ewes were randomly divided into two groups as midazolam/saline (MDS) and midazolam/flumazenil (MDF). Hemodynamic values, blood gas, metabolic and electrolyte variables and reflex values were determined in both groups before midazolam (0.6 mg/kg, IV) administration (baseline) and after the 5th (T5) and 25th min (T25) of administration. At T25, saline was injected into the MDS and flumazenil (0.02 mg/kg, IV) into the MDF. The same measurements were repeated at the 5th min (T30), 35th min (T60), and 65th min (T90) of saline and flumazenil applications. Midazolam produced deep sedation and a significant increase in reflex scores in both groups at the indicated times ($P<0.05$). It caused an increase in heart rate (HR), a decrease in systemic and diastolic arterial pressure (SAP, DAP), hypoventilation, mild respiratory acidosis, and adverse effects on metabolic variables at a transient and clinically acceptable level. It was observed that these effects returned to baseline within 5 min with the use of flumazenil in MDF. Flumazenil (0.02 mg/kg, IV) was sufficient to reverse cardiopulmonary adverse effects within 5 min during deep sedation by high-dose midazolam (0.6 mg/kg, IV) in ewes.

Keywords: *Cardiopulmonary, Flumazenil, Midazolam, Sedation, Sheep*

Koyunda Midazolam ile Reversali Flumazenilin Sedatif ve Kardiyopulmoner Değişkenlere Etkisi

Öz

Bu çalışmada koyunlarda midazolam uygulamasının ardından flumazenil antagonizmasıyla sedatif ve kardiyopulmoner değişkenlerdeki etkilerin değerlendirilmesi amaçlanmıştır. Çalışmada en az 14 gün aralıkla İvesi ırkı 6 erkek koyun kullanıldı. Koyunlar midazolam/izotonik serum (MDS) ve midazolam/flumazenil (MDF) olarak rastgele 2 gruba ayrıldı. Her iki grupta midazolam (0.6 mg/kg, IV) uygulamasından önce (baseline) ve uygulamanın 5. (T5) ve 25. dk'sında (T25) hemodinamik değerler ile kan gazı, metabolik ve elektrolit değişken değerleri belirlendi ve refleks değerleri ölçüldü. T25'de MDS'ye izotonik serum solüsyonu, MDF'ye flumazenil (0.02 mg/kg, IV) enjekte edildi. İzotonik serum ve flumazenil uygulamalarının 5. dk (T30), 35. dk (T60) ve 65. dk (T90)'larında aynı ölçümler tekrarlandı. Belirlenen zamanlarda midazolam her iki grupta derin sedasyon ve refleks değerlerde önemli yükselme sağladı ($P<0.05$). Kalp vurum sayısında (HR) artış, sistemik ve diastolik arteriyel basınç (SAP, DAP)'da azalma, hipoventilasyon, hafif şekilde respiratorik asidoz ve metabolik değişkenler üzerinde geçici ve klinik olarak kabul edilebilir düzeyde olumsuz etkilere neden oldu. MDF'de flumazenil uygulanmasıyla bu etkilerin 5 dk içinde başlangıç seviyesine döndüğü görüldü. Flumazenil (0.02 mg/kg, IV) koyunlarda yüksek doz midazolamın (0.6 mg/kg, IV) oluşturduğu derin sedasyon ile kardiyopulmoner olumsuz etkilerin 5 dk içinde tersine çevrilmesine yeterli oldu.

Anahtar sözcükler: *Flumazenil, Kardiyopulmoner, Koyun, Midazolam, Sedasyon*

INTRODUCTION

Thanks to their skeletal growth in a short time, their similarity to humans in weight, size, and anatomical and physiological aspects, ewes are a frequently used large animal model for *in vivo* biomedical studies, especially in surgical sciences [1-3]. Between 2015 and 2017, 60.158 ewes were used for experimental and scientific purposes in the EU Member States [4]. The complexity of surgical research, preoperative preparation, anesthetic protocols,

How to cite this article?

Yavuz Ü, Yener K, Şahan A: The effect of midazolam and its reversal flumazenil on sedative and cardiopulmonary variables in sheep. *Kafkas Univ Vet Fak Derg,* 27 (6): 771-779, 2021.
DOI: 10.9775/kvfd.2021.26300

(*) **Corresponding Author**

Tel: +90 414 318 3921 Cellular phone: +90 505 311 4310
E-mail: unalyavuz@harran.edu.tr (Ü. Yavuz)

and monitoring, and postural changes (lateral position) can lead to significant morbidity and mortality in ewes [2,5]. These procedures require close monitoring of anesthesia and hemodynamic parameters [3].

Sedatives are commonly used in small ruminants. The most commonly used sedatives for this purpose are α2-adrenoceptor agonists. However, α2-adrenoceptor agonists have many side effects such as hypoventilation and hypoxemia as well as cardiopulmonary depression [5-8]. Small ruminants are more vulnerable to the pulmonary side effects of α2-adrenoceptor agonists. Since they are thought to have minimal adverse effects on the cardiovascular and respiratory systems, many anesthesiologists recommend benzodiazepines (BDZs) as an alternative sedative agent in ewes [8-11].

Midazolam, a benzodiazepine with a high margin of safety, produces anxiolytic and muscle relaxant effects by interacting with anticonvulsant and sedative effects, as well as glycine-mediated inhibitory routes in the brain and spinal cord. It acts indirectly by optimizing an existing physiological inhibitory route rather than directly suppressing neuronal activity, and rapidly crosses the blood-brain barrier [12-15]. While its low doses (0.05-0.1 mg/kg IV) can be used to induce mild sedation during painless procedures (e.g., X-ray, ultrasound) in ewes, major surgery can be performed by adding local analgesia to the high-dose (0.4 mg/kg and above, IV) midazolam injection or midazolam-opioid combination [8,16-18]. One of its main advantages is that its effects can be reversed by using flumazenil, a benzodiazepine antagonist [8,14]. Flumazenil has a high affinity for the benzodiazepine receptor site of the $GABA_A$ receptor and reverses the effects of benzodiazepines throughout the central nervous system (CNS) [19,20]. This increases the importance of flumazenil as a clinical antagonist in ewes.

The aim of this study was to investigate the effects of reversal administration of flumazenil (0.02 mg/kg, IV) in ewes after high-dose midazolam (0.6 mg/kg, IV) administration on sedative effects and cardiopulmonary, arterial blood gas, metabolic, and electrolyte variables. We hypothesized that in healthy ewes, IV administration of midazolam would produce a rapid and deep induction of sedation with minimal changes in cardiopulmonary variables, followed by the administration of flumazenil, these changes would soon return to baseline values.

Material and Methods

Ethical Statement

The study was conducted at Experimental Animal Implementation and Research Center (HDAM) Farm Animals Unit with the permission of Harran University Animal Experiments Local Ethics Committee (HRU-HADYEK) with the number 2020/003/11.

Animals

Six male Awassi ewes aged 6-8 months and weighing 34-41 kg (38.6±2.6 kg) were studied. The health status of the ewes to be included in the study was checked by clinical examination and complete blood count. One month prior to the study, ewes were divided into pairs or groups of three and housed in wide boxing. During this time, they were fed *ad libitum* with hay and concentration. Because the ewes were extremely anxious and restless when separated from flock, they were kept in pairs in the experimental room for 1 h at least 2 times per week for 2 weeks before the start of the study to minimize stress, and they were allowed to acclimate to environmental conditions. Meanwhile, physiological changes in the ewes were measured and electrocardiogram (ECG) leads were introduced in the baseline apex configuration for habituation. The hair at the withers was shaved and ewes were adapted to the application of a clamp modified to the withers and metacarpus. For 12 h prior to each experiment, ewes were not allowed to eat food, but water was available *ad libitum*.

Instrumentation

The experiment was conducted at a constant ambient temperature of 22°C, in a quiet, air-cooled closed cabin with fluorescent lighting, without attempting to maintain the body temperature of the sheep. To ensure standardization, injections were performed during the light phase of the cycle between 09:00 and 11:00 am. In the experimental room, two ewes were placed together in adjacent cabins of sufficient width to perform the procedure. Catheterization (Bıçakçılar®, Istanbul, Turkey) was performed with a 20 G branule in the left jugular vein for drug injections, with a 22 G branule in the left auricular artery for blood sampling, and with a 22 G branule in the right auricular artery for IBP measurement. 5% lidocaine (Sandoz® İlaç, Istanbul, Turkey) was pomaded to the auricular artery 45 min before catheter insertion to facilitate catheter placement. Just before the injection of midazolam (baseline, T0), a multi-parameter monitor (Mindray® uMEC12VET, Shenzen Mindray Bio-Medical Electronics Co, Shenzhen, China) was used to monitor values for hemodynamic parameters such as heart rate (HR, beats per minute), systemic arterial pressure (SAP, mmHg), diastolic arterial pressure (DAP, mmHg), respiratory rate (RR, breaths per minute), Oxy-hemoglobin saturation (SpO_2, %), end- tidal CO_2 ($EtCO_2$, %), and body temperature (BT, °C) values with ECG lead II. SpO_2 was monitored using a pulse oximeter with a clip placed in the ear, and BT was monitored via an electronic rectal probe from the rectum. Epoc® Blood Analysis device (Epocal Inc, Ottawa, Canada) and the BGEM® Test Card kit (Epocal Inc, Ottawa, Canada) were used to measure the values of arterial blood gas and metabolic and electrolyte variables such as arterial pH, partial pressure of carbon dioxide in arterial blood (pCO_2), partial pressure of oxygen in arterial blood (pO_2), bicarbonate (HCO_3^-), base excess

(BE), hematocrit (Hct), hemoglobin (Hb), lactate, glucose, sodium (Na^+), potassium (K^+), chloride (Cl^-).

Experimental Design

Ewes were randomly divided into 2 groups as MDS and MDF. The study was conducted in two phases with a minimum interval of 14 days. The MDS group was studied first followed by the MDF group. In both groups, the hemodynamic changes were recorded at the 5th (T5) and 25th min (T25) after slow IV injection of midazolam (Zolamid® 5 mg/5 mL IV ampul, Defarma İlaç, Ankara, Turkey) at a dose of 0.6 mg/kg within 15 sec, and for the analysis of arterial blood gases and metabolic and electrolyte variables, 1 mL blood samples were taken from the auricular artery.

At the 25th min of midazolam administration (immediately after blood collection, T25), saline (Kanfleks® 0.9% isotonic sodium chloride solution, Kansuk Laboratory, Istanbul, Turkey) was slowly injected within 15 sec into the sheep of the MDS group (n:6) via the IV route in an amount equal to the volume of flumazenil.

At the 25th min of midazolam administration (immediately after blood collection, T25), benzodiazepine antagonist flumazenil (Mazenil® 0.5 mg/5 mL IV ampul, VEM İlaç, Ankara, Turkey) was slowly injected within 15 sec into the sheep of the MDF group (n:6) via the IV route at the dose of 0.02 mg/kg.

The hemodynamic parameters were re-recorded at the 5th (T30), 35th (T60), and 65th (T90) min after the injection of saline to the ewes in MDS and flumazenil to the ewes in MDF, later, 1 mL blood samples were collected for analysis of arterial blood gasses and metabolic and electrolyte variables. The collected blood samples were processed without delay via the Epoc® Blood Analysis instrument and the results were recorded.

Degree of Sedation

The scoring system proposed by Carroll et al.[21] was used to determine sedation and posture degree. Accordingly, the degree of sedation was scored as 0 = No sedation (A normal warning attitude; can be frightened, moves the ears in response to toy gun firing); 1 = Mild sedation (A depressive attitude; may be frightened, movements may be observed in the ears or face in response to the sound of the toy gun); 2 = Moderate sedation (A depressive attitude and sternal recumbency. May be aware of the sound of the toy gun, but has little reaction); 3 = Profound sedation (Lateral recumbency), and the degree of posture was scored as 0 = Standing; 1 = Recumbency (without movement). Scorings were recorded by the same observer, who had no knowledge of the study materials or methods. Sedation and postural scoring and behavioral scores were determined immediately after baseline (T0), T5, T25, T30, T60, and T90 hemodynamic values and blood sample collection.

Sedation scores were determined by firing a toy gun from a distance of 1 m from the head of the ewe. A modified tester with an adapted electronic force transducer was used to measure the applied isometric force when determining changes in mechanical threshold, similar to the modified hoof tester proposed by Carroll et al.[21]. The modified tester, powered by two batteries, was about 30 cm long and had a tester gap diameter of 7 cm. The accuracy of the tester was 1 N and it was capable of measuring up to a maximum of 1 kN. In baseline, T5, T25, T30, T60 and T90, pressure was applied using the modified tester to the withers and metacarpus of the ewe in less than 5 sec and the force applied could be visualized by a signal processor. If the sheep made a purposeful movement or emitted a sound during the application of force, the force was terminated and the reading was recorded as a force tolerance test value.

The ewes were also monitored for signs of agitation (vocalization, piloerection, rolling), salivation, ruminal tympany, and urination.

Statistical Analysis

Because the data did not meet the parametric test assumptions, the difference between groups (MDS and MDF) for all quantitative traits measured was compared using the Mann-Whitney U test. The difference between repeated measurements made on the same ewe as a function of time was compared separately within each group using the Freidman test. Pairwise comparisons of variables with significant differences as a result of the Freidman test were made using the Wilcoxon test, only the differences between the baseline measurement and the later measurements. Changes were considered significant when $P<0.05$. All values were given as median.

Results

Time-dependent median results of the MDS and MDF groups in sedation and postural scoring and changes in mechanical threshold of reflexes were summarized in *Table 1*.

The difference between the MDS and MDF groups in sedation and postural variables proved significant ($P<0.05$) in scoring (T30, T60 and T90) after the administration of flumazenil. In the within-group evaluation, lateral recumbency and deep sedation (220 sec in MDS, up to 260 sec in MDF) occurred with the absence of the palpebral reflex from the administration of midazolam to T5 in both groups and the return of the Bulbus oculi to the full ventromedial position ($P<0.05$).

At the onset of sedation, stargazing and mydriasis were observed in all sheep in both group, but no signs of apnea, agitation (vocalization, piloerection, rolling), or convulsions were observed.

Table 1. *Time-dependent median results of sedation and postural and analgesia levels determined by force application at the withers and metacarpus in 6 ewes receiving MDS and MDF by the IV route*

Time Points	Sedation		Posture		Withers		Metacarpus	
	MDS	MDF	MDS	MDF	MDS	MDF	MDS	MDF
BL (T0)	0.0	0.0	0.0	0.0	9.5	10.5	3.5	4.0
T5	3.0*	3.0*	1.0*	1.0*	41.0*	43.5*	11.0*	11.5*
T25	3.0*	3.0*	1.0*	1.0*	44.5*	47.5*	14.0*	13.0*
T30	3.0*	0.0#	1.0*	0.0#	44.5*	11.0#	14.0*	4.0#
T60	3.0*	0.0#	1.0*	0.0#	35.5*	10.5#	10.5*	4.0#
T90	2.0*	0.0#	1.0*	0.0#	22.5*	10.0#	6.5*	4.0#

Sedation and postural scoring and changes in mechanical reflex threshold were evaluated after blood collection with determination of cardiopulmonary variables; ***MDS:*** *injection of saline solution equal to the volume of flumazenil 25 min (T25) after midazolam (0.6 mg/kg, IV) injection;* ***MDF:*** *injection of flumazenil (0.02 mg/kg, IV) 25 min (T25) after midazolam (0.6 mg/kg, IV) injection;* ***BL (T0):*** *Baseline measurement value immediately before midazolam injection;* ***T5:*** *Measured value 5 min after midazolam injection;* ***T25:*** *Measured value 25 min after midazolam injection, immediately before flumazenil injection;* ***T30:*** *30 min after midazolam injection and 5 min after flumazenil injection;* ***T60:*** *Measured value 60 min after midazolam injection and 35 min after flumazenil injection;* ***T90:*** *Measured value 90 min after midazolam injection and 65 min after flumazenil injection;* ***#:****Significantly different from MDS at indicated times, (P<0.05);* ***** *Significantly different from baseline (T0), (P<0.05)*

Table 2. *Time-dependent median results for cardiopulmonary variables in 6 ewes receiving MDS and MDF by the IV route*

Time Points	HR (beats per min)		SAP (mmHg)		DAP (mmHg)		RR (breaths per min)		SpO_2 (%)		$EtCO_2$ (%)		BT (˚C)	
	MDS	MDF	MDS	MDF	MDS	MDF	MDS	MDF	MDS	MDF	MDS	MDF	MDS	MDF
BL (T0)	97.5	95.5	141.0	129.0	93.0	92.5	34.5	31.5	94.0	94.5	40.5	38.0	39.4	39.1
T5	106.0*	104.5	127.0	124.0	57.0	74.5*	27.0*	25.0*	91.5*	90.5*	43.5*	40.5*	39.2*	38.9
T25	110.0*	109.0	112.5	129.0	64.0	69.5*	29.0*	26.0*	88.5*	86.0*	40.5	37.5*	39.2*	38.6*
T30	112.0*	88.5#	110.0	144.0	68.5	113.0	29.0*	34.0*	86.5*	95.0#	45.0*	33.5#	39.0*	39.0
T60	93.0	95.0	106.5	119.0	68.5	93.5#	31.5*	35.0	89.5*	96.0#	42.5	37.5#	38.8*	39.1
T90	97.5	95.0	114.0	122.0	58.5	86.5#	33.5*	33.0	93.5	95.0	44.0	39.5	38.9*	39.0

MDS: *injection of saline solution equal to the volume of flumazenil 25 min (T25) after midazolam (0.6 mg/kg, IV) injection;* ***MDF:*** *injection of flumazenil (0.02 mg/kg, IV) 25 min (T25) after midazolam (0.6 mg/kg, IV) injection;* ***BL (T0):*** *Baseline measurement value immediately before midazolam injection;* ***T5:*** *Measured value 5 min after midazolam injection;* ***T25:*** *Measured value 25 min after midazolam injection, immediately before flumazenil injection;* ***T30:*** *30 min after midazolam injection and 5 min after flumazenil injection;* ***T60:*** *Measured value 60 min after midazolam injection and 35 min after flumazenil injection;* ***T90:*** *Measured value 90 min after midazolam injection and 65 min after flumazenil injection;* ***HR:*** *heart rate;* ***SAP:*** *systolic arterial pressure;* ***DAP:*** *diastolic arterial pressure;* ***RR:*** *respiratory rate;* ***SpO_2:*** *oxy-haemoglobin saturation;* ***$EtCO_2$:*** *end-tidal CO_2;* ***BT:*** *body temperature;* ***#*** *Significantly different from MDS at indicated times (P<0.05);* ***** *Significantly different from baseline (T0), (P<0.05)*

The difference between the MDS and MDF groups in analgesia scores measured at the withers and metacarpus was significant (P<0.05) for measurements after the administration of flumazenil (T30, T60, and T90), as well as for sedation and posture scores. In the within-group evaluation related to analgesia scores (both in withers and metacarpus), the measured increase from baseline to T90 in MDS was significant (P<0.05), while the increase in MDF from baseline to flumazenil administration (T5 and T25) was significant (P<0.05). In MDS, two ewes were standing (ewes 2 and 4) and did not lie down again in T90, whereas in MDF, one ewe for 36 sec (ewe 11), two ewes for 44 sec (ewes 9 and 12), and three ewes for 53 sec after flumazenil (ewes 7, 8 and 10) were standing and not lying down again (at T30, T60 and T90) (P<0.05). During the recovery period, mild agitation was observed in two ewes (ewes 5 and 6) in MDS, but no signs of agitation were observed in MDF.

Hypersalivation was noted in all ewes in both groups. Hypersalivation, which started at the 6th min in ewes in MDS, continued until the 34th min. In MDF, on the other hand, hypersalivation, which started at the 8th min, ended after flumazenil application (T30). It was observed that hypersalivation was higher in the first 10 min and gradually decreased. Mild ruminal tympany was observed between 16 and 60 min in the MDS in 2 ewes (ewes 2 and 4) and between 12 and 30 min in the MDF in 3 ewes (ewes 9, 11 and 12). Urination was observed between 22 and 70 min in MDS in 3 ewes (ewes 2, 3 and 6) and between 27 and 64 min in MDF in 2 ewes (ewes 7 and 9).

The time-dependent median results of the MDS and MDF groups in relation to cardiopulmonary variables and BT were summarized in *Table 2*.

With regard to cardiovascular variables, the difference

Table 3. *Time-dependent median results for blood gases and metabolic variables in 6 ewes receiving MDS and MDF by the IV route*

Time Points	pHa		pCO_2 (mmHg)		pO_2 (mmHg)		HCO_3^- (mmol/L)		BE (mmol/L)		Hct (%)		Hb (g/dL)		Lactate (mmol/L)		Glucose (mg/dL)	
	MDS	MDF	MDS	MDF	MDS	MDF	MDS	MDF	MDS	MDF	MDS	MDF	MDS	MDF	MDS	MDF	MDS	MDF
BL (T0)	7.481	7.513	30.50	31.15	81.75	80.25	24.65	25.40	3.65	4.65	33.50	32.50	8.00	7.60	1.50	2.33	95.00	88.50
T5	7.458	7.462	31.30*	31.80*	78.90*	78.20*	24.15	24.40	1.90*	2.30*	32.50	31.50	7.65	7.20	1.32*	1.86*	97.00	89.00
T25	7.426*	7.454	31.75*	33.10*	76.15*	77.20*	24.10	24.75	1.30*	1.25*	33.50	32.50	8.05	7.60	1.25*	1.34*	103.50*	94.00
T30	7.446*	7.462#	32.05*	30.30*	76.25*	81.60	25.60	26.10	2.70	2.20	34.00	32.00	8.30	7.45	1.18*	1.69*	102.50*	97.00
T60	7.453	7.534*#	32.40*	29.35*#	77.75*	83.45#	25.50	27.85*	2.40	3.30	34.50	32.50	8.45	7.60	1.20*	2.10#	100.50*	91.00#
T90	7.461	7.521*#	31.90*	30.20*	81.50	82.60	25.75	29.35*	2.10	4.05#	35.50	32.00	8.70	7.15	1.29*	2.06#	108.50*	91.50#

MDS: *injection of saline solution equal to the volume of flumazenil 25 min (T25) after midazolam (0.6 mg/kg, IV) injection;* ***MDF:*** *injection of flumazenil (0.02 mg/kg, IV) 25 min (T25) after midazolam (0.6 mg/kg, IV) injection;* ***BL (T0):*** *Baseline measurement value immediately before midazolam injection;* ***T5:*** *Measured value 5 min after midazolam injection;* ***T25:*** *Measured value 25 min after midazolam injection, immediately before flumazenil injection;* ***T30:*** *30 min after midazolam injection and 5 min after flumazenil injection;* ***T60:*** *Measured value 60 min after midazolam injection and 35 min after flumazenil injection;* ***T90:*** *Measured value 90 min after midazolam injection and 65 min after flumazenil injection;* ***pHa:*** *arterial pH;* ***pCO_2:*** *partial pressure of carbon dioxide in arterial blood;* ***pO_2:*** *partial pressure of oxygen in arterial blood;* ***HCO_3:*** *bicarbonate;* ***BE:*** *base excess;* ***Hct:*** *hematocrit;* ***Hb:*** *hemoglobin; # Significantly different from MDS at indicated times (P<0.05); * Significantly different from baseline (T0), (P<0.05)*

Table 4. *Time dependent median results of electrolyte variables in 6 ewes receiving MDS and MDF by the IV route*

Time Points	Na^+ (mmol/L)		K^+ (mmol/L)		Cl^- (mmol/L)	
	MDS	MDF	MDS	MDF	MDS	MDF
BL (T0)	144.50	144.00	4.10	4.20	108.00	110.00
T5	145.50	144.00	3.75*	3.70*	108.00	108.50
T25	145.00	144.50	3.75*	3.90*	108.50*	109.00
T30	144.00	144.00	3.90	3.90	107.50	109.00
T60	145.00	144.00	4.20	4.05	108.50	108.50
T90	145.00	144.50	4.40	4.05	110.00	108.00

MDS: *injection of saline solution equal to the volume of flumazenil 25 min (T25) after midazolam (0.6 mg/kg, IV) injection;* ***MDF:*** *injection of flumazenil (0.02 mg/kg, IV) 25 min (T25) after midazolam (0.6 mg/kg, IV) injection;* ***BL (T0):*** *Baseline measurement value immediately before midazolam injection;* ***T5:*** *Measured value 5 min after midazolam injection;* ***T25:*** *Measured value 25 min after midazolam injection, immediately before flumazenil injection;* ***T30:*** *30 min after midazolam injection and 5 min after flumazenil injection;* ***T60:*** *Measured value 60 min after midazolam injection and 35 min after flumazenil injection;* ***T90:*** *Measured value 90 min after midazolam injection and 65 min after flumazenil injection;* ***Na^+ (mmol/L):*** *sodium,* ***K^+ (mmol/L):*** *potassium,* ***Cl^- (mmol/L):*** *chloride; # Significantly different from MDS at indicated times (P<0.05); * Significantly different from baseline (T0), (P<0.05)*

between the MDS and MDF groups in HR was significant (P<0.05) only immediately after flumazenil administration (T30). The increase in HR, which began immediately after midazolam administration in both groups, continued in MDS until T30 (P<0.05) and remained at a level close to baseline from T60. A sudden drop was observed in MDF after flumazenil administration, and all changes within the group were found to be insignificant compared with baseline (P>0.05). No arrhythmia was monitored in ECG in either group. The difference between and within groups in SAP was insignificant (P>0.05). While a decrease was observed in MDS up to T60, a decrease was seen in MDF at T5, and after flumazenil administration (T30), it increased with a sudden rise above baseline. The difference between the groups in DAP at T60 and T90 was found to be significant (P<0.05). It was observed to be lower than the baseline value from T5 to T90 in MDS (P>0.05). While a decrease (P<0.05) was observed in MDF until the application of flumazenil (T25), the sudden increase that started at T30 continued until T90 at a level close to baseline. Midazolam was observed to cause mild, transient, but statistically significant cardiovascular depression and insignificant hypotension in MDS, and these effects were normalized by flumazenil administration in MDF.

With respect to respiratory variables, midazolam resulted in transient and nondramatic changes. The difference between the MDS and MDF groups in RR was insignificant (P>0.05). It was observed that RR in T5 showed a sudden decrease in both groups (P<0.05). This decrease in MDS remained below baseline until the end of anesthesia (P<0.05). In contrast, in MDF, a decrease (P<0.05) was observed until the administration of flumazenil (T25), whereas the sudden increase (P<0.05) that began at T30 was above baseline at T90. The difference between groups in SpO_2 at T30 and T60 was significant (P<0.05). It was observed that SpO_2 in MDS remained below baseline until T60 (P<0.05), while it decreased in MDF until flumazenil application (T25) and increased from T30 (P>0.05). For $EtCO_2$, the difference between groups was significant only at T30 and T60 (P<0.05). It was observed to be higher than baseline at T5 and T30 in MDS and in the period

until flumazenil application in MDF (T5 and T25) (P<0.05). Although significant changes in RR, SpO_2, and $EtCO_2$ were observed in both groups after midazolam administration, it was assessed that these changes were clinically insignificant and returned to normal with flumazenil administration in MDF.

The difference between the MDS and MDF groups in BT was insignificant (P>0.05). BT decreased significantly in both groups after midazolam administration (P<0.05), but hypothermia was not observed. A new increase (P>0.05) was observed after flumazenil administration (T30) in MDF.

The time-dependent median results of the MDS and MDF groups with respect to arterial blood gas and metabolic variables were summarized in *Table 3*.

With regard to arterial blood gases, although a partial decrease in pH, a statistically significant increase in pCO_2, and a significant decrease in pO_2 were observed in both groups, these changes were close to the reference ranges. Midazolam was found to cause mild respiratory acidosis in both groups. It was observed that pH, pCO_2, and pO_2 values returned to the normal range with the increase in RR and SpO_2 ≥95% from T30 on MDF. It was assessed that the decrease in HCO_3^- and BE was consistent with mild respiratory acidosis, but these changes were not clinically significant.

The difference between and within groups in Hct and Hb was not significant (P>0.05). The difference between MDS and MDF groups in terms of lactate and glucose was significant at T60 and T90 (P<0.05). In MDS, lactate was lower than baseline (P<0.05) and glucose was higher than baseline (P<0.05, except T5) up to T90 at a statistically significant level.

The time-dependent median results of the MDS and MDF groups with respect to the electrolyte variables were summarized in *Table 4*.

With respect to Na^+, K^+, and Cl^- levels, the difference between the MDS and MDF groups was insignificant (P>0.05). In both groups, midazolam had no effect on Na^+, caused a decrease in K^+ until T25 (P<0.05), while Cl^- remained stable (observed only at T25 in MDS (P<0.05)). It was observed that flumazenil had no effect on electrolyte variables in MDF.

Discussion

Although changes in cardiopulmonary variables and behavioral reflexes caused by IV injection of midazolam in the range of 0.05-0.5 mg/kg in ewes have been studied [14,18,22], the effect of flumazenil antagonism has been reported only on behavioral reflexes [14]. Stegmann et al.[23] reported that benzodiazepine dosages for ewes and goats were similar. In the current study, considering studies in goats, dose selection was made for midazolam according to the preliminary studies [10,22,24,25] and for flumazenil according to the preliminary study [14]. In light of the literature, IV administration of 0.6 mg/kg midazolam [18,26] and IV administration of 0.02 mg/kg flumazenil [27,28] were considered high doses. This study evaluated changes in mechanical threshold of reflexes in ewes and their effects on cardiopulmonary, arterial blood gas, metabolic, and electrolyte variables with a single high-dose (0.02 mg/kg, IV) injection of flumazenil, a benzodiazepine antagonist, 25 min (T25) after a single high-dose injection of midazolam, whose cardiopulmonary effects were considered minimal.

Flumazenil is well tolerated even in amounts exceeding recommended doses in humans. According to Food and Drug Administration (FDA), the first dose of 0.2 mg of flumazenil should be administered IV within 15 sec. If the desired level of consciousness is not achieved within 60 sec of the first IV administration, a sec dose of 0.1 mg may be injected. It is recommended that this be repeated as necessary at 60-sec intervals up to a total dose of 1 mg [29]. Flumazenil has been reported to have virtually no intrinsic pharmacological activity in animals and does not produce tachypnea, CNS agitation, or behavioral changes even in the absence of benzodiazepines [13,14]. In this study, a single IV administration of 0.02 mg/kg flumazenil was sufficient to reverse the effects of midazolam smoothly in a very short time, but there is insufficient information on the pharmacodynamic and pharmacokinetic effects of flumazenil in animals. Because the drug doses and number of ewes used in this study were limited, there is a need to further investigate the different dose rates of midazolam and flumazenil, as well as repeated doses of flumazenil, to uncover the clinical effects of flumazenil.

Simon et al.[22] emphasized that IV administration of midazolam (0.5 mg/kg) resulted in profound sedation in 5 of the 8 ewes within 5 min, profound ataxia was observed in all ewes, and sedation scores were significantly different from baseline in the first 15 min. Upton et al.[18] found that lower doses of midazolam showed minimal sedative effects in ewes, and midazolam produced variable but longer term sedation with increasing dose. Kyles et al.[14] reported that administration of midazolam in ewes resulted in a dose-dependent increase in thermal and mechanical thresholds and that these effects of midazolam, which resulted in dose-dependent sedation and ataxia, could be attenuated by IV administration of flumazenil. Flumazenil has been reported to be used IV, IM, sublingually, endotracheally, or rectally to reverse benzodiazepine-induced sedation, but the most rapid effect may be obtained via IV administration [30]. Because no surgery was performed in the present study, the mechanical stimulus apparatus defined by Carroll et al.[21] was modified and used to determine changes in the mechanical threshold of reflexes. Deep sedation in ewes in both groups within the first 5 min after administration of high-dose midazolam and

recovery from deep sedation shortly after (standing within 53 sec) administration of flumazenil were consistent with the findings of the aforementioned researchers [14,18,22]. As Heniff et al.[30] noted; IV administration of both drugs was thought to induce the onset of deep sedation and a rapid response, and it was suggested that this effect might be due to the fact that midazolam, with its lipophilic structure, rapidly crosses the blood-brain barrier and flumazenil has a high affinity for benzodiazepine receptors.

Because flumazenil has a very short half-life and a shorter duration of action than benzodiazepines, resedation may occur if long-acting benzodiazepines were used [28,31,32]. The absence of repeated sedation in any of the ewes in the study was explained by the presence of a short-acting benzodiazepine in its midazolam.

The combination of IV injection of midazolam (0.025-0.05 mg/kg) and ketamine (5-7 mg/kg) is used to induce general anesthesia and enhance muscle relaxation for endotracheal intubation in small ruminants [8,33]. Hypersalivation was observed in 4 of 6 ewes following IV administration of midazolam by Simon et al.[22] and in all goats by Stegmann and Bester [10]. The main side effect observed in the study was hypersalivation, which was seen in all ewes, consistent with the researchers' [10,22] findings. In ewes put under general anesthesia with midazolam premedication, it should be kept in mind that aspiration of large amounts of saliva can lead to complications if the trachea is left unprotected.

Anesthesia-induced brainstem depression has been reported to cause cardiovascular and respiratory depression, and the extent of depression in the brain is proportional to the depth of sedation, cardiovascular, and respiratory depression [18,34,35]. It has been reported that IV administration of lower doses of midazolam in ewes had minor cardiovascular and respiratory effects compared with baseline, whereas higher doses of midazolam increased HR up to 47% after 10 min, and that cardiovascular depression occurs as a function of dose, but the extent of cardiovascular depression in ewes is not life-threatening [18]. Simon et al.[22] discovered that after IV administration of midazolam in ewes, there was an increase of about 22% to HR by the 30th min, which was below baseline at the 90th min. Other studies performed with benzodiazepines in ewes have reported that diazepam tends to increase HR, that there is an increase in the first 10 min and then a decrease [11], and that remimazolam (CNS 7056), a new benzodiazepine, dose-dependently increases HR up to 53% after 5 min [18]. In the study, high doses of midazolam were observed to induce deep sedation and have profound effects on the cardiovascular system. In line with the findings of the researchers [11,18,22,34], it was observed that the HR increased with deep sedation in the first 30 min of anesthesia and immediately decreased with injection of flumazenil. The longer duration of the increase in HR compared to other studies was attributed to the high dose.

It has been reported that the depth of anesthesia and cardiovascular depression may be directly proportional regardless of the drug causing the sedation, and that low arterial blood pressure, one of the signs of cardiovascular depression, may cause decreased oxygenation of vital organs due to malperfusion of tissues [3,18,36]. Invasive SAP is defined as normotension when the pressure is between 90 and 120 mmHg, hypotension when it is below 90 mmHg, and hypertension when it is above 120 mmHg [3,36]. Upton et al.[34] found that midazolam significantly reduced MAP in ewes in the first 35 min (excluding 8th and 20th min) compared with baseline, but this decrease was only about 8%. Upton et al.[18] reported that midazolam causes a dose-dependent decrease of up to 11% in MAP in ewes. In the study, it was remarkable that the baseline median values in both groups were higher than the normotension values reported in the literature [3,36] with respect to SAP and DAP. It was observed that the decrease occurred at SAP and DAP in MDS in the normotensive range and sudden hypertension developed at T30 in MDF. It was considered that the results were compatible with studies conducted with ewes administered IV midazolam [18,34], that hypotension was caused by the central effects of midazolam on vasomotor centers, and that SAP values recorded above 90 mmHg during sedation were high enough to ensure perfusion of vital organs. As noted by Upton et al.[18], the reason for the increase in HR was explained as a compensatory response to the decrease in SAP and DAP.

It has been highlighted that BDZs can reduce RR in animals but rarely affect ventilation and oxygenation, and at high doses can cause dose-dependent respiratory depression or exacerbate existing respiratory depression [37]. Midazolam has been shown to inhibit the central respiratory system in humans, and respiratory depression during conscious sedation has been reported as the most significant adverse effect [38,39], and it has been noted that RR usually returns to normal after BDZs when flumazenil is used [40,41]. It has been reported that there was a transient, dose-dependent reduction in RR of more than 50% after IV administration of midazolam in ewes [18,22], that SpO_2 decreased by approximately 10% at the 10th min [34] and that RR and decrease in SpO_2 at the measurement periods and the temporal changes in the $EtCO_2$ data were compatible [18]. Time to reversal of respiratory depression induced by IV flumazenil and midazolam in dogs was reported to be 120±25 sec [30]. In the study, as reported by the investigators [18,22,34,35], the decrease in RR and decrease in SpO_2 and changes in $EtCO_2$ were consistent with time. The extent of reduction in SpO_2 with concomitant reduction in paO_2 in both groups did not indicate the need for oxygen therapy. It has been observed that transient and nondramatic changes in the respiratory system disappeared with the use of flumazenil, as noted by Heniff et al.[30] and Shalansky et al.[40]. It has been suggested that respiratory depression occurred as a result of further brainstem suppression by high doses of midazolam [18], and that the increase in RR

with the use of flumazenil may have been achieved by the disappearance of sedation and the improvement of consciousness [40].

It has been reported that IV administration of BDZs in ewes and goats can result in significant decreases in BT, but these decreases are within the normal range [10,18,22,35]. In the current study, it was suggested that the reduction in BT, which occurred in relatively normal ranges in agreement with results in the literature and was not considered clinically significant, might be related to the vasodilation that developed after midazolam administration, as noted by Upton et al.[18].

The values of arterial blood gasses and metabolic variables obtained in this study differed, although only partially, from the literature on conscious values in ewes [42-44]. Midazolam has been reported to cause changes in blood gas levels and small fluctuations in HCO_3 and BE in goats while these changes were minimal [24,25], whereas there was a significant decrease in paO_2 at 10th min in ewes [34]. Upton et al.[18] indicated that it caused a decrease in pH, an increase in $paCO_2$, and a decrease in paO_2 concurrently cause mild but significant respiratory acidosis in ewes, and these effects were more significant with remimazolam (CNS 7056) compared to with midazolam. Other studies conducted with benzodiazepines in ewes reported that diazepam decreased paO_2 at the onset of sedation (at the 2nd min) but remained close to the control group after the 15th min, but had no significant effect on $paCO_2$ and acid-base variables [11]. Midazolam caused mild respiratory acidosis in the present study, which was not considered clinically significant, with a decrease in pH and paO_2 and an increase in $paCO_2$. It improved in a short time with the increase in RR and SpO_2 after the administration of flumazenil in MDF. In line with the findings of the aforementioned investigators [11,18,24,25,34], high dose midazolam was observed to cause a clinically acceptable level of transient respiratory depression in healthy ewes.

De Carvalho et al.[45] reported that although significant changes occurred in HR and arterial blood gases, no significant electrolyte abnormalities were noted. While mild hypoventilation and decreases in HCO_3^- and BE, which were associated with hypoxemia, resulted in findings supporting respiratory acidosis, the changes in metabolic and electrolyte variables were clinically insignificant. As noted by De Carvalho et al.[45], the mechanism of such changes in ewes remains unclear.

In conclusion, single and slow administration of 0.6 mg/kg midazolam via the IV route in ewes resulted in beneficial effects on sedation depth and reflex scores, but transient and clinically acceptable adverse effects on cardiopulmonary, blood gas and metabolic variables. A single and slow administration of 0.02 mg/kg flumazenil via the IV route was sufficient to shorten the recovery time and reverse the adverse effects within 5 min. It was concluded that further studies at different doses are needed to better understand the potential role of flumazenil as a clinical antagonist in ewes, and that midazolam and flumazenil at these doses can be used in ewes that are expected to recover from sedation in a short time.

Availability of Data and Materials

The datasets during and/or analyzed during the current study available from the corresponding author on reasonable request.

Acknowledgements

The authors thank Prof. Dr. Şükrü GÜRLER for his valuable contribution to the statistical analysis of the study results.

Funding Support

This research did not receive any specific grant from funding agencies in the public, commercial, or not-for profit sectors.

Conflict of Interest

The authors declared that there is no conflict of interest.

Author's Contributions

Ü.Y.: Experimental design, data collections, data analysis, manuscript writing. K.Y. and A.Ş.: Data collections, data analysis.

References

1. Häger C, Biernot S, Buettner M, Glage S, Keubler LM, Held N, Bleich EM, Otto K, Müller CW, Decker S, Talbot SR, Bleich A: The sheep grimace scale as an indicator of post-operative distress and pain in laboratory sheep. *Plosone,* 12 (4): e0175839, 2017. DOI: 10.1371/journal.pone.0175839

2. Di Vincenti Jr L, Westcott R, Lee C: Sheep *(Ovis aries)* as a model for cardiovascular surgery and management before, during, and after cardiopulmonary bypass. *J Am Assoc Lab Anim Sci*, 53 (5): 439-448, 2014.

3. Almeida D, Barletta M, Mathews L, Graham L, Quandt J: Comparison between invasive blood pressure and a non-invasive blood pressure monitor in anesthetized sheep. *Res Vet Sci,* 97 (3): 582-586, 2014. DOI: 10.1016/j.rvsc.2014.10.004

4. Report from the Commission to the Europe an Parliament and the Council: 2019 Report on the Statistics on the Use of Animals for Scientific Purposes in the Member States of the European Union in 2015-2017. https://op.europa.eu/en/publication-detail/-/publication/04a890d4-47ff-11ea-b81b-01aa75ed71a1; *Accessed:* 02.06.2021.

5. Lin HC: Comparative anesthesia and analgesia of ruminants and swine. **In,** Grimm KA, Lamont LA, Tranquilli WJ, Greene SA, Robertson SA (Eds): Veterinary Anesthesia and Analgesia. The fifth edition of Lumb and Jones, 5th ed., 743-753, John Wiley&Sons, USA, 2015.

6. Kästner SBR: A2-agonists in sheep: A review. *Vet Anaesth Analg*, 33 (2): 79-96, 2006. DOI: 10.1111/j.1467-2995.2005.00243.x

7. Carroll GL, Hartsfield SM: General anesthetic techniques in ruminants. *Vet Clin North Am Food Anim Pract,* 12 (3): 627-661, 1996. DOI: 10.1016/s0749-0720(15)30391-1

8. Seddighi R, Doherty TJ: Field sedation and anesthesia of ruminants. *Vet Clin North Am Food Anim Pract,* 32 (3): 553-570, 2016. DOI: 10.1016/j.cvfa.2016.05.002

9. Lin HC: Commonly used preanesthetics. **In,** Lin HC, Walz P (Eds): Farm Animal Anesthesia. 17-38, Oxford: Wiley-Blackwell, USA, 2014.

10. Stegmann GF, Bester L: Sedative-hypnotic effects of midazolam in goats after intravenous and intramuscular administration. *Vet Anaesth Analg,* 28 (1): 49-55, 2001. DOI: 10.1046/j.1467-2987.2000.00034.x

11. Celly CS, McDonell WN, Black WD, Young SS: Cardiopulmonary effects of clonidine, diazepam and the peripheral α2 adrenoceptor agonist ST-91 in conscious sheep. *J Vet Pharmacol Ther,* 20 (6): 472-478, 1997. DOI: 10.1046/j.1365-2885.1997.00098.x

12. Rankin DC: Sedatives and tranquilizers. **In,** Grimm KA, Lamont LA, Tranquilli WJ, Greene SA, Robertson SA (Ed): Veterinary Anesthesia and Analgesia. The fifth edition of Lumb and Jones, 5th ed., 196-206, John Wiley&Sons, USA, 2015.

13. Klein LV, Klide AM: Central α_2 adrenergic and benzodiazepine agonists and their antagonists. *J Zoo Wildl Med*, 20, 138-153, 1989.

14. Kyles AE, Waterman AE, Livingston A: Antinociceptive activity of midazolam in sheep. *J Vet Pharmacol Ther,* 18 (1): 54-60, 1995. DOI: 10.1111/j.1365-2885.1995.tb00551.x

15. Erol M, Erol H, Atalan G, Ceylan C, Yönez MK: The effects of propofol-sevoflurane, midazolam-sevoflurane and medetomidine ketamine -sevoflurane anesthetic combinations on intraocular pressure in rabbits. *Kafkas Univ Vet Fak Derg,* 26 (4): 477-481, 2020. DOI: 10.9775/kvfd.2019.23557

16. White K, Taylor P: Anaesthesia in sheep. *In Practice,* 22 (3): 126-135, 2000. DOI: 10.1136/inpract.22.3.126

17. Lizarraga I, Chambers JP: Use of analgesic drugs for pain management in sheep. *N Z Vet J,* 60 (2): 87-94, 2012. DOI: 10.1080/00480169.2011.642772

18. Upton RN, Martinez AM, Grant C: Comparison of the sedative properties of CNS 7056, midazolam, and propofol in sheep. *Br J Anaesth,* 103 (6): 848-857, 2009. DOI: 10.1093/bja/aep269

19. Gangwar AK, Kumar N, Devi KS: Preanesthetic agents. **In,** General Animal Surgery and Anesthesiology. 207-222, New India Publishing Agency New Delphi, India, 2020.

20. Posner LP: Sedatives and tranquilizers. **In,** Riviere JE, Papich MG (Eds): Veterinary Pharmacology and Therapeutics. 10th ed., 324-368, John Wiley&Sons, USA, 2018.

21. Carroll GL, Hartsfield SM, Champney TH, Geller SC, Martinez EA, Haley EL: Effect of medetomidine and its antagonism with atipamezole on stress-related hormones, metabolites, physiologic responses, sedation, and mechanical threshold in goats. *Vet Anaesth Analg*, 32 (3): 147-157. 2005. DOI: 10.1111/j.1467-2995.2005.00187.x

22. Simon BT, Scallan EM, Odette O, Ebner LS, Cerullo MN, Follette C, Cox SK, Doherty TJ, Lizarraga I: Pharmacokinetics and pharmacodynamics of midazolam following intravenous and intramuscular administration to sheep. *Am J Vet Res,* 78 (5): 539-549, 2017. DOI: 10.2460/ajvr.78.5.539

23. Stegmann GF: Observations on the use of midazolam for sedation, and induction of anaesthesia with midazolam in combination with ketamine in the goat. *J S Afr Vet Assoc,* 69 (3): 89-92, 1998. DOI: 10.4102/jsava.v69i3.823

24. Stegmann GF: Observations on some cardiopulmonary effects of midazolam, xylazine and a midazolam/ketamine combination in the goat. *J S Afr Vet Assoc,* 70 (3): 122-126, 1999. DOI: 10.4102/jsava.v70i3.771

25. Dzikiti TB, Stegmann GF, Hellebrekers LJ, Auer REJ, Dzikiti LN: Sedative and cardiopulmonary effects of acepromazine, midazolam, butorphanol, acepromazine-butorphanol and midazolam-butorphanol on propofolanaesthesia in goats. *J S Afr Vet Assoc,* 80 (1): 10-16, 2009. DOI: 10.4102/jsava.v80i1.162

26. Izwan A, Snelling EP, Seymour RS, Meyer LCR, Fuller A, Haw A, Mitchell D, Farrell AP, Costello MA, Maloney SK: Ameliorating the adverse cardiorespiratory effects of chemical immobilization by inducing general anaesthesia in sheep and goats: implications for physiological studies of large wild mammals. *J Comp Physiol B,* 188 (6): 991-1003, 2018. DOI: 10.1007/s00360-018-1184-z

27. Douglas H, Hopster K, Cerullo M, Hopster-Iversen C, Stefanovski D, Driessen B: The effects of flumazenil on ventilatory and recovery characteristics in horses following midazolam-ketamine induction and isoflurane anaesthesia. *Equine Vet J,* 53 (6): 1257-1267, 2021. DOI: 10.1111/evj.13391

28. Ilkiw JE, Farver TB, Suter C, McNeal D, Steffey EP: The effect of intravenous administration of variable-dose flumazenil after fixed-dose ketamine and midazolam in healthy cats. *J Vet Pharmacol Ther,* 25 (3): 181-188, 2002. DOI: 10.1046/j.1365-2885.2002.00402.x

29. Flumazenil-US Food and Drug Administration: https://www.accessdata.fda.gov/drugsatfda_docs/label/2007/020073s016lbl.pdf; *Accessed:* 10.06.2021.

30. Heniff MS, Moore GP, Trout A, Cordell WH, Nelson DR: Comparison of routes of flumazenil administration to reverse midazolam-induced respiratory depression in a canine model. *Acad Emerg Med,* 4 (12): 1115-1118, 1997. DOI: 10.1111/j.1553-2712.1997.tb03692.x

31. Seelhammer TG, DeGraff EM, Behrens TJ, Robinson JC, Selleck KL, Schroeder DR, Sprung J, Weingarten TN: The use of flumazenil for benzodiazepine associated respiratory depression in postanesthesia recovery: risks and outcomes. *Braz J Anesthesiol*, 68 (4): 329-335, 2018. DOI: 10.1016/j.bjan.2017.12.012

32. James SB, Cook RA, Raphael BL, Stetter MD, Kalk P, MacLaughlin K, Calle PP: Immobilization of babirusa *(Babyrousa babyrussa)* with xylazine and tiletamine/zolazepam and reversal with yohimbine and flumazenil. *J Zoo Wildl Med*, 30, 521-525, 1999.

33. Galatos AD: Anesthesia and analgesia in sheep and goats. *Vet Clin North Am Food Anim Pract,* 27 (1): 47-59, 2011. DOI: 10.1016/j.cvfa.2010.10.007

34. Upton RN, Ludbrook GL, Grant C, Martinez A: *In vivo* cerebral pharmacokinetics and pharmaco-dynamics of diazepam and midazolam after short intravenous infusion administration in sheep. *J Pharmacokinet Pharmacodyn*, 28 (2): 129-153, 2001. DOI: 10.1023/a:1011550915515

35. Upton RN, Martinez AM, Grant C: A dose escalation study in sheep of the effects of the benzodiazepine CNS 7056 on sedation, the EEG and the respiratory and cardiovascular systems. *Br J Pharmacol,* 155 (1): 52-61, 2008. DOI: 10.1038/bjp.2008.228

36. Riebold TW: Ruminants. **In,** Grimm KA, Lamont LA, Tranquilli WJ, Greene SA, Robertson SA (Eds): Veterinary Anesthesia and Analgesia. The fifth edidtion of Lumb and Jones, 5th ed., 912-927, John Wiley&Sons, USA, 2015.

37. McDonell WN, Kerr CL: Physiology, pathophysiology, and anesthetic management of patients with respiratory disease. **In,** Grimm KA, Lamont LA, Tranquilli WJ, Greene SA, Robertson SA (Eds): Veterinary Anesthesia and Analgesia. The fifth edition of Lumb and Jones, 5th ed., 513-558, John Wiley&Sons, USA, 2015.

38. Reves GJ, Glass PSA, Lubarsky DA: Nonbarbiturate intravenous anesthetics. **In,** Cucchiara RF, Miller ED, Reves JG, Roizen MF, Savarese JJ (Eds): Anesthesia. Vol. 1 4th ed., 247-290, Churchill Livingstone New York, 1994.

39. Vuyk J, Sitsen E, Reekers M: Intravenous anesthetics. *Miller's Anesthesia*, 8, 821-863, 2015.

40. Shalansky SJ, Naumann TL, Englander FA: Effect of flumazenil on benzodiazepine-induced respiratory depression. *Clin Pharm*, 12 (7): 483-487, 1993.

41. Flögel CM, Ward DS, Wada DR, Ritter JW: The effects of large-dose flumazenil on midazolam-induced ventilatory depression. *Anaesth Analg*, 77 (6): 1207-1214, 1993.

42. Silva LP, Lourenço ML, Paula RA, Verdugo MR, Pereira KH, Chiacchio SB: Assessment of serum lactate levels, blood glucose values and blood gas values in sheep, newborn lambs and placenta. *Pesq Vet Bras,* 38 (9): 1878-1884, 2018. DOI: 10.1590/1678-5150-PVB-5689

43. Izer J, Mattern E, Ellwanger J, Wilson R: Comparison of arterial and venous blood-gas values in anesthetized Dorset cross-bred lambs (*Ovis aries*) using a point-of-care analyzer. *Vet Anaesth Analg,* 46 (2): 209-213, 2019. DOI: 10.1016/j.vaa.2018.12.003

44. Onmaz AC, Gunes V, Atalan G, Gelfert CC, Atalan G: Comparison of arterial and venous blood gas values in sheep before and during isoflurane anaesthesia. *Revue Méd Vét,* 160 (7): 356-361, 2009.

45. De Carvalho LL, Nishimura LT, Borges LP, Cerejo SA, Villela IO, Auckburally A, de Mattos-Junior E: Sedative and cardiopulmonary effects of xylazine alone or in combination with methadone, morphine or tramadol in sheep. *Vet Anaesth Analg,* 43 (2): 179-188, 2016. DOI: 10.1111/vaa.12296

Kafkas Universitesi Veterinar Fakultesi Dergisi
ISSN: 1300-6045 e-ISSN: 1309-2251
Journal Home-Page: http://vetdergikafkas.org

Kafkas Univ Vet Fak Derg
27 (6): 781-786, 2021
DOI: 10.9775/kvfd.2021.26315

RESEARCH ARTICLE

Identification and Phylogenetic Positioning of *Salmonella* Dublin from Aborted Cattle Materials

Berna YANMAZ [1,a (*)] Ediz Kağan ÖZGEN [1,b]

[1] Republic of Turkey Ministry of Agriculture and Forestry, Erzurum Veterinary Control Institute, TR-25070 Erzurum - TURKEY
ORCIDs: [a] 0000-0002-4176-9487; [b] 0000-0002-5665-6864

Article ID: KVFD-2021-26315 Received: 19.07.2021 Accepted: 19.10.2021 Published Online: 18.10.2021

Abstract

This study was aimed to isolate, and characterize the *Salmonella* Dublin in the liver, lung tissues and the abomasum contents of 367 aborted cattle fetal samples obtained from four different cities (Ağrı, Erzincan, Erzurum and Kars) of Turkey by using molecular methods. After proper incubation of the tissues and contents, *Salmonella* spp. identification was performed. Colonies with suspicion of *Salmonella* were boiled on a dry heat block for DNA extraction, while multiplex PCR was used for species identification of *Salmonella* spp. and identification of *S.* Dublin. The multiplex PCR, 16S rDNA sequence, and phylogenetic analysis were performed on an isolate with a band profile specific to *S.* Dublin. The *S.* Dublin identification was performed according to BLAST analysis and similarity scores obtained from NCBI GenBank. Molecular prevalence of *S.* Dublin in the aborted fetal samples of cattle was 0.82%. The 16S rRNA sequence results of the isolate was found to be similar to many *S.* Dublin strains. The partial sequence of the 16S rRNA gene region of the isolate was recorded in the GenBank database with the name strain Erzurum VCRI and access number MZ452230. In conclusion, *S.* Dublin was identified in the aborted cattle fetuses and phylogenetic position was determined for *S.* Dublin using the sequence analysis of 16S rDNA gene region.

Keywords: *Cattle, Salmonella Dublin, Phylogenetic, Sequence*

Sığır Abort Materyallerinden *Salmonella* Dublin İdentifikasyonu ve Filogenetik Pozisyonlandırılması

Öz

Bu çalışmanın amacı Türkiye'nin dört farklı şehrinden (Ağrı, Erzincan, Erzurum ve Kars) alınan 367 adet sığır aborte fötus örneklerine ait karaciğer ve akciğer dokuları ile abomazum içeriklerinde *Salmonella* Dublin'i izole etmek ve moleküler yöntemlerle karakterizasyonunu sağlamaktır. Doku ve içeriklerin uygun inkübasyonu sonrasında *Salmonella* spp. identifikasyonu yapıldı. DNA ekstraksiyonu için *Salmonella* spp. şüpheli kolonilere kuru ısı bloğu üzerinde kaynatma metodu, *Salmonella* spp.'ların tür düzeyinde identifikasyonu ve *S.* Dublin teşhisi için ise multipleks PCR metodu kullanıldı. Multipleks PCR analizi sonucunda *S.* Dublin'e özgü bant profili gösteren bir izolatın 16S rDNA dizi analizi ile sekanslaması ve filogenetik analizi gerçekleştirildi. *S.* Dublin identifikasyonu ise BLAST analizine göre ve NCBI GenBank'tan elde edilen benzerlik skorlarına göre yapıldı. Sığır atık fötal örneklerinde *S.* Dublin'in moleküler prevalansı %0.82 olarak saptandı. İzolatın 16S rRNA sekans bulguları birçok *S.* Dublin suşu ile benzer olarak bulundu. İzolatın 16S rRNA gen bölgesinin sekansı Genbankasına MZ452230 erişim numarası ve Erzurum VKEM suş ismi ile kaydedilmiştir. Sonuç olarak sığır atık fötusundan *S.* Dublin tanımlanmış ve 16S rDNA gen bölgesinin dizi analizi ile de *S.* Dublin'e filogenetik pozisyon kazandırılmıştır.

Anahtar sözcükler: *Sığır, Salmonella Dublin, Filogenetik, Sekans*

INTRODUCTION

Salmonellosis is a disease which can cause digestive and urogenital system infections in cattle regardless of age [1]. *Salmonella enterica* subspecies *enterica serovar* Dublin (*Salmonella* Dublin) is a serotype hosted by cattle [2]. Due to having the *Salmonella* plasmid virulence (spv) gene, which plays a role in its pathogenesis, *S.* Dublin is different from many other *Salmonella* serotypes and this gene makes the microorganism resistant to phagocytosis [1]. In cattle establishments, clinically infected animals or asymptomatic carriers cause the bacteria to spread within the farm [1]. This type of animals shed the bacteria into the environment via discharges such as milk, saliva, faeces,

How to cite this article?

Yanmaz B, Özgen EK: Identification and phylogenetic positioning of *Salmonella* Dublin from aborted cattle materials. *Kafkas Univ Vet Fak Derg,* 27 (6): 781-786, 2021.
DOI: 10.9775/kvfd.2021.26315

(*) Corresponding Author

Tel: +90 442 316 8142, Fax: +90 442 317 0733
E-mail: bernayanmaz@gmail.com (B. Yanmaz)

vaginal discharge, urine, etc. [1,2]. Infection is generally transmitted via faecal-oral route [1].

In addition to causing diarrhea or septicemia in calves, *S.* Dublin causes significant economic losses due to the abortions in gestating animals [3]. Abortion may occur at any stage of gestation in cattle, however the abortions caused by *S.* Dublin are the most common in the 5th-9th months of gestation. Because *S.* Dublin rarely causes clinical symptoms, it has extremely negative effects on fertility and this causes significant economic losses in the cattle industry [4,5]. In clinical terms, abortions are reported to be caused by serotypes B, C and D. There are different mechanisms of abortions caused by *Salmonella* infection in cattle. One of them is the infection of the fetus by the bacteria, which reaches the uterus and the fetus, and eventually causes the death of the fetus. In this case, isolation of the agent from the internal organs of the aborted fetus enables us to put forward this mechanism. Endotoxemia, which causes the release of inflammatory mediators, causes a secondary luteolysis as a result of the release of prostaglandin. The body temperature increase is also responsible from the death of the fetus [1].

S. Dublin has been isolated at a prevalence of 5.6% (106/1877) in cattle fetal membrane samples and at a prevalence of 2.1% (4/190) in vaginal swab samples [5]. The abortion rate of *S.* Dublin has been reported as 0.66% in Australia (1/150) [6]. Anderson [7] analyzed 391 aborted cattle fetuses in USA using bacteriological culture, and isolated *Salmonella* spp. from 1.7% (7/391) of the samples while 5 (71.4%) of them has been identified as *S.* Dublin. It has been stated that abortion rate of *S.* Dublin is 26.7% in England [8]. Moreover, a previous study has reported the cattle abortions rate caused by *S.* Dublin as 80% throughout the world [9]. The aim of this study was to isolate, and characterize *Salmonella* Dublin in the liver and lung tissues, and the abomasum contents of 367 aborted cattle fetal samples obtained from four different cities (Ağrı, Erzincan, Erzurum and Kars) of Turkey by using molecular methods.

Material and Methods

Ethical Approval

The Atatürk University Animal Experiments Local Ethics Committee approved the study protocol of this study (decision no: 164/2021).

Study Material

The material of the study consisted of liver and lung tissues as well as abomasum contents of 367 aborted cattle fetuses brought to Ağrıı, Erzincan, Erzurum and Kars cities *(Fig. 1)* of Turkey. Samples were collected from February to April, 2021. After necropsy was performed properly on the aborted fetuses, at least 3 grams of the organs were taken into sterile sample containers, while abomasum content was soaked into the transport swab with Stuart's medium. *Salmonella Typhimurium* strain, which was isolated by our institute in the previous years, was used as positive control for bacteriological culture and multiplex PCR analyses.

Bacterial Isolation and Identification

Bacteriological culture was performed on the fetal tissues and abomasum contents for the analysis of *S.* Dublin. For *Salmonella* spp. isolation, fetal lung and liver tissues as well as abomasum contents were directly inoculated onto XLD agar and these media were incubated for 5 days under anaerobic conditions at 37°C. After incubation, the typical H_2S positive black colonies which formed on XLD agar and surrounded by a reddish-pink halo were assessed with suspicion of *Salmonella* spp. and later the preparations obtained from these colonies were gram-stained [10]. Bacterial colonies with a gram-negative *Bacillus* morphology were passaged into blood agar and left for incubation for 48 h at 37°C under aerobic conditions. After incubation, *Salmonella* spp. identification was performed using a Vitek-2 Compact (Biomerioux) GN ID card [11].

Fig 1. Number of samples studied by province

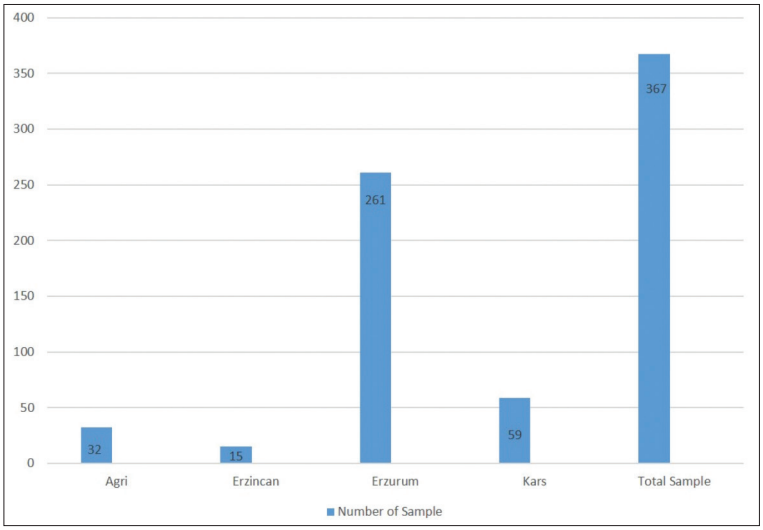

DNA Extraction

For DNA extraction, 4-5 bacterial colonies from *Salmonella* spp. suspected colonies were taken into sterile micro-centrifuge tubes containing 500 µL PBS. DNA extraction was performed by boiling on dry ice block [3].

Multiplex Polymerase Chain Reaction

Multiplex PCR method of previous work was used for species identification of *Salmonella* spp. and *S.* Dublin [12]. The *invA* gene region was used for type identification, and *SeD A1118* and *SeD A2283* primers were used for the identification of *S.* Dublin. PCR mixture was prepared with 12.5 µL Hotstart Master Mix (Qiagen, Hilden, Germany), 7.5 µL deionized ultrapure water, 2 µL primer mix and 3 µL target DNA, and the first denaturation was performed at 95°C for 15 min. Later, denaturation occurred for 30 sec at 95°C, annealing for 30 sec at 60°C and extension for 45 sec at 72°C, making 35 cycles in total. The mixture was kept at 72°C for 5 min for the final extension. Qiaxcel Advanced System (Qiagen, Germany) was used for the determination of the sizes of PCR amplicons. Electroforesis was performed according to OM500 protocol of DNA High Resolution kit. The detection of a 284 bp band for *invA* gene region only for *Salmonella* spp., and the detection of a 284 bp band for *invA* gene, a 378 bp band for *SeD A2283* gene and a 463 bp band for *SeD A1118* gene for *S.* Dublin led to assess these agents as positive.

16S rDNA Sequencing and Phylogenetic Analysis

After the multiplex PCR analysis, 16S rDNA sequence analysis was performed by BM Laboratory Systems. EurX GeneMATRIX Bacterial & Yeast DNA isolation kit (Poland) was used for the isolation of DNA from the colony in the pure culture. Spectrophotometric measurements were performed using Thermo Scientific Nanodrop 2000 (USA) to control the amount and purity of the DNA's. The gene region which was targeted for the identification of the type was amplified using a universal primer pair (27F -1492R) [13]. For amplification, 1X PCR buffer, 1.5 mM $MgCl_2$, 0.2 mM dNTP mix, 0.3 µM of each primer, 2 U Taq DNA polymerase and 3 µL template DNA were prepared to make a total volume of 35 µL and the first denaturation was performed for 5 min at 95°C. Later, denaturation occurred for 45 sec at 95°C, annealing for 45 sec at 57°C and extension for 60 sec at 72°C, making 35 cycles in total. The mixture was kept at 72°C for 5 min for the final extension. The amplified PCR product was purified from the single band samples using a MAGBIO "HighPrep™ PCR Clean-up System" (AC-60005) kit. The sequencing of 16S rDNA gene was performed using a BigDye Terminator v3.1 Cycle Sequencing Kit on an ABI 3730XL Sanger sequencer (Applied Biosystems, Foster City, CA). The readings taken from 27F and 1492R primers were assembled to a contig to create a consensus sequence. CAP contig assembly algorithm in the BioEdit software was used for this process. Sequence analysis results were assessed using BLAST analysis and similarity scores obtained from NCBI GenBank [14]. The genetic relationships between the 16S rRNA genes of one *S.* Dublin strain and representative strains from the *S.* Dublin were inferred using the maximum likelihood method based on Kimura's two-parameter model with 1000 bootstrap using the MEGA X software (Version 10.2.2) [15].

Results

Isolation and Identification Results

In this study, *Salmonella* spp. was identified in 16 (4.35%) of the liver and lung tissues and abomasum contents of 367 aborted cattle fetuses, which were analyzed using bacteriological culture, with the presence of agents with Gram-negative bacillus morphology, having typical colonies with black color in the middle and surrounded by a reddish-pink halo due to the H_2S positivity in XLD medium. In the analyses of *Salmonella* spp. isolates using Vitek-2 GN ID panel, all of their identifications were confirmed on a genus level *(Salmonella* spp.) *(Table 1)*.

Multiplex PCR Results

As a result of the genus-specific multiplex PCR analysis of 16 isolates, which were identified as *Salmonella* spp. using phenotypic methods and Vitek-2 automated identification system, all of these isolates were confirmed as *Salmonella* spp. with the presence of 284 bp PCR products that showed *invA* gene amplification. In multiplex PCR, 3 of the 16 isolates (18.75%) were identified as *S.* Dublin with the presence of 284 bp product belonging to the *invA* gene region specific to the *Salmonella* genus, as well as the presence of 378 bp *SeD A2283* and 463 bp *SeD A1118* genes *(Fig. 2)*. *S.* Dublin was equally isolated from organs, and these were not statistically different. The molecular prevalence of *S.* Dublin in aborted fetal samples of cattle was found to be 0.82%.

The Findings of 16S rDNA Sequencing and Phylogenesis

After Multiplex PCR, 16S rRNA sequence analysis was performed on one of the three isolates identified as *S.* Dublin positive. PCR analysis with the universal primers (27F and 1492R) showed the presence and successful amplification of the 16S rRNA gene region with the presence of 1465 bp bands in one *S.* Dublin isolate. The 100% similarity was not found between the DNA sequences of *S.* Dublin isolate analyzed and the DNA sequences uploaded to the gene bank. The similarities with the DNA sequences with the closest similarity were evaluated. The 16S rRNA sequence results of the isolate was found to be similar to those of many *S.* Dublin strains including CP032379, CP0324446, CP032449, CP032396, CP032390, CP032393, CP032387, CP032384, LK931502, CP075021, CP074229, CP063756, CP063754, CP019179, with 99.46%, CP0019179, CP0075113, CP074226, CP001144, with 99.39%, FJ997268,

Table 1. *Sample distribution and culture positivity rate by province (%)*

Province	Total Sample	Positive	Culture Positive (%)	Vitek 2 Diagnosis *Salmonella* spp.			*S.* Dublin Positive
				Very Good	Good	Medium	
Ağrı	32	0	0.0	-	-	-	-
Erzincan	15	2	15.4	2	0	0	0
Erzurum	261	8	3.1	6	2	0	2
Kars	59	6	10.2	5	1	0	1
Total	367	16	4.35	13	3	0	3

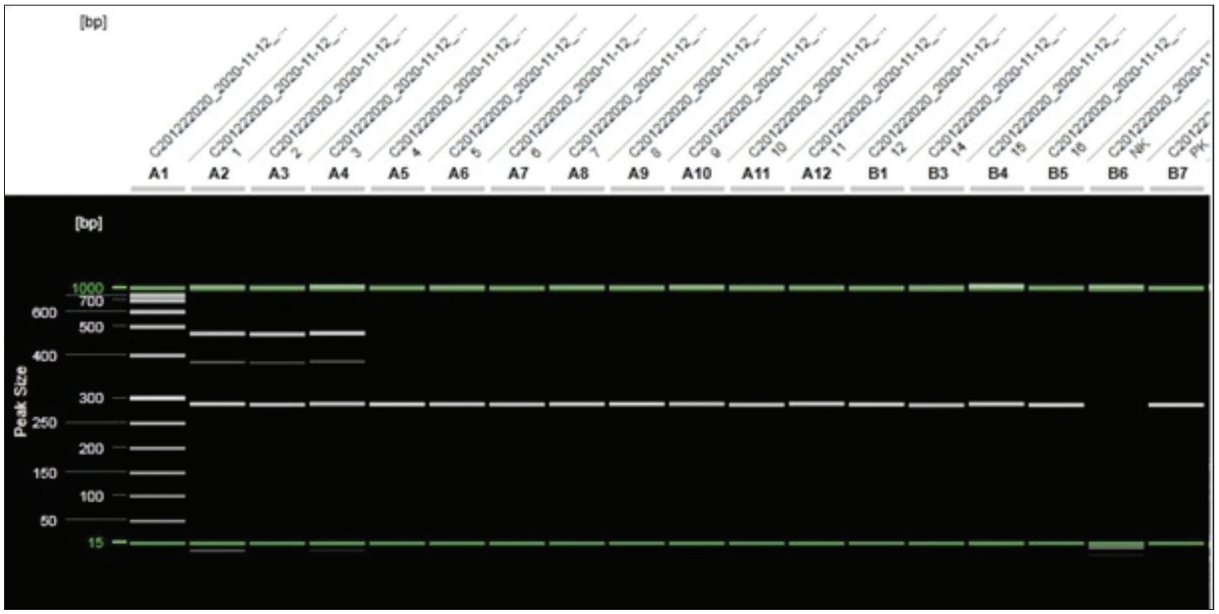

Fig 2. Capillary electrophoresis image of multiplex PCR; A4: *Salmonella* Dublin isolates (invA, SeD A1118 and SeD A2283 positive). A5-B5 *Salmonella* spp. isolates *(invA* positive only). B6: Negative Control. B7: Positive Control

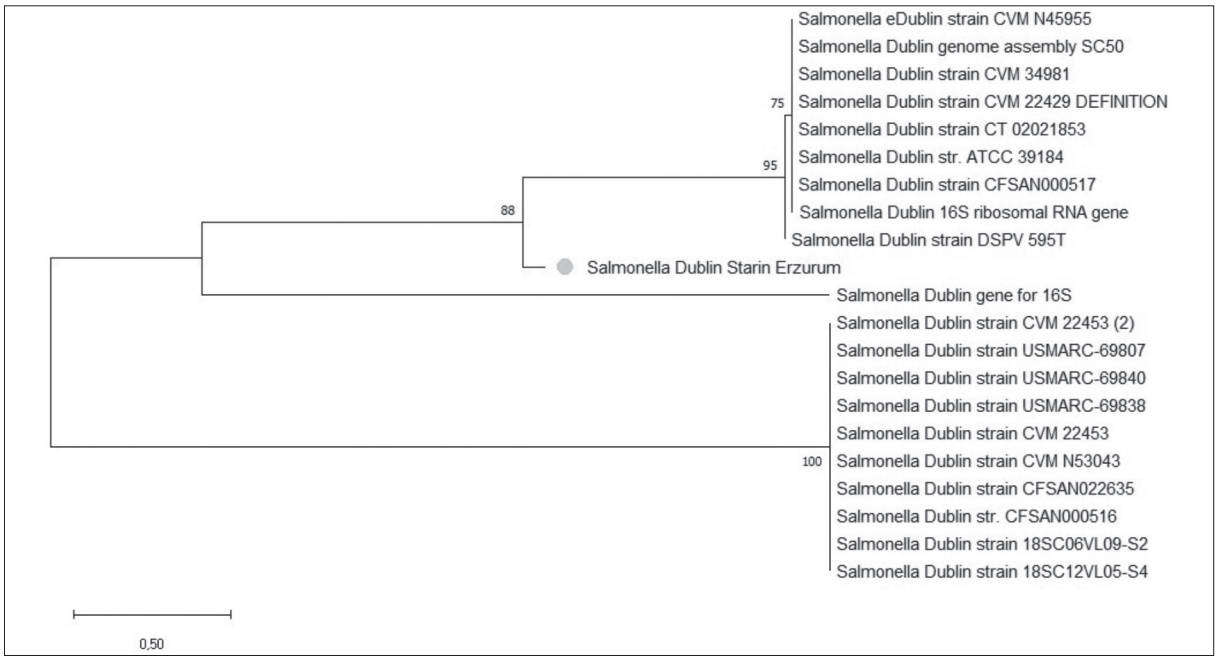

Fig 3. The dendrogram generated by the neighboring joining method for the *S. Dublin* isolate that was designated based on the sequence of the 16S rRNA gene region

with 99.16%, AF227868, with 99.39%, D12810 with 99.09% similarity index. The partial sequence of the 16S rRNA gene region of the isolate was recorded in the GenBank database with the name strain Erzurum VKEM and access number MZ452230.

The *S.* Dublin isolate identified in this study was found to be in the same cluster as the *S.* Dublin strains isolated from cattle. This isolate was positioned in the same branch with cattle and turkey isolates which were defined as cattle stool, ground turkey, ground beef *(Fig. 3)*.

Discussion

Salmonella species play a role in the etiology of abortions in cattle [9]. In this study, the roles of *Salmonella* types in the etiology of cattle abortions were investigated by using cultural method and *Salmonella* spp. positivity was found to be 4.35% (16/367), this finding was consistent with previous studies that reported the rate between 0% and 6.5% [7,16-19]. In this study, *S.* Dublin positivity was determined as 0.81%, this finding was consistent with previous studies that reported this rate as 0.66-5.6% [5,6,20]. In this study, three of the isolates (18.75%) were identified as *S.* Dublin after PCR analysis. A previous study that analyzed 391 aborted cattle fetuses in the United States of America using bacteriological culture isolated *Salmonella* spp. from 1.7% (7/391) of the samples, while 5 (71.4%) of them were identified as *S.* Dublin [17]. Another study has isolated *Salmonella* spp. from 24 (6.5%) of the samples while 2 (8.3%) of them were identified as *S.* Dublin [18]. It has been postulated that the prevalence of cattle abortions caused by *S.* Dublin in England was 3.6% in fattening cattle and 16.6% in dairy cattle [8].

Even though it has been recommended to inoculate fetal stomach content and fetal brain directly for culture [9,21], in this study *S.* Dublin was isolated from aborted fetal liver, lung and abomasum contents. The previous studies have similarly isolated *Salmonella* spp. in fetal tissues [22], placenta discharge [9,23], fetal stomach content and placental samples [24]. PCR-based analyses can be used in the identification of *Salmonella* serovars [10]. A previous study has developed a multiplex PCR which included primers specific to *S.* Dublin, namely *SeD _A1118* and *SeD_ A2283*, and primers specific to *invA* gene regions which are specific to *Salmonella* spp. [12]. Although PCR has some advantages in identification, bacteriological culture is necessary for advanced analyses [25].

A 16S rDNA sequence analysis can allow the phylogenetic analysis of the bacteria and it can allow the identification of microorganisms that can rarely be grown. In 16S rDNA sequence analyses, it is necessary to find a similarity rate less than 1% [26]. In the current research, by performing sequence analysis of one isolate of *S.* Dublin with 16S rDNA allowed genomic comparisons of *S.* Dublin strains isolated in previous studies. *S.* Dublin isolate, which was identified in this study was found to have; 99.46% similarity with the isolates which have been registered to the NCBI GenBank with the access codes CP032379, CP0324446, CP032449, CP032396, CP032390, CP032393, CP032387, CP032384, LK931502, CP075021, CP074229, CP063756, CP063754, CP019179, 99.39% similarity with the isolates which have been registered to the NCBI GenBank with the access codes CP0019179, CP0075113, CP074226, CP001144, 99.16% similarity with the isolate which has been registered to the NCBI GenBank with the access code FJ997268, 99.39% similarity with the isolate which is registered to the NCBI GenBank with the access code AF227868 and 99.09% similarity with the isolate which is registered to the NCBI GenBank with the access code D12810. While *S.* Dublin isolate was in the same set with the *S.* Dublin isolates with the code D12810 obtained from a sample of cattle origin in Japan, it was on the same branch with the *S.* Dublin isolates with the codes CP001144, CP074226, CP075113, CP019179, CP32396, CP032390, CP032387, LK931502, FJ997268 obtained from minced beef, minced turkey meat and cattle faeces samples from USA, France, Argentina, Nigeria and United Kingdom.

As a result, the number of cattle isolates were high on the branch of the phylogenetic tree where the isolate of cattle origin subject to 16S rDNA sequencing. At the same time, the origin of the isolates with phylogenetic relationship goes back to Europe, America, Africa and Asia shows that the geographical distribution of the agent is wide. In conclusion, definitive identification of *S.* Dublin was identified in aborted cattle foetuses. Furthermore, 16S rDNA gene region sequence analysis was performed, and phylogenetic position of *S.* Dublin isolate was determined.

Availability of Data and Materials

The authors declare that data supporting the study findings are also available to the corresponding author.

Funding Support

None declared.

Competing Interests

The authors declare that they have no competing interests.

Author Contributions

Both authors planned, designed and performed the analysis. The manuscript was written by both authors. Both authors have interpreted the data, revised the manuscript for contents, and approved the final version.

References

1. Holschbach CL, Peek SF: *Salmonella* in dairy cattle. *Vet Clin North Am Food Anim Pract,* 34 (1): 133-154, 2018. DOI: 10.1016/j.cvfa.2017.10.005

2. Nielsen LR: Review of pathogenesis and diagnostic methods of immediate relevance for epidemiology and control of *Salmonella* Dublin in cattle. *Vet Microbiol,* 162 (1): 1-9, 2013. DOI: 10.1016/j.vetmic.2012.08.003

3. Hezil D, Zaidi S, Benseghir H, Zineddine R, Benamrouche N, Ghalmi F: *Salmonella* Dublin associated with abortion in dairy cattle in Algiers and comparison of different diagnostic methods. *Afr J Clin Exp Microbiol,* 22 (2): 211-222, 2021. DOI: 10.4314/ajcem.v22i2.14

4. Peek SF, Mcguirk SM, Sweeney RW, Cummings KJ: Infectious diseases of the gastrointestinal tract. Rebhun's Diseases of Dairy Cattle. 3rd ed., 249-356, 2018. DOI: 10.1016/B978-0-323-39055-2.00006-1

5. Hinton M: The diagnosis of *salmonella* abortion in cattle with particular reference to *Salmonella* Dublin. A review. *Epidemiol Infect,* 79 (1): 25-38, 1977. DOI: 10.1017/s0022172400052815

6. Sodoma E, Mitterhuemer S, Krassnig G, Stellnberger K, Reisp K, Schmoll F, Dünser M: Infektiös bedingte Aborte beim Rind-eigene Erfahrungen und Untersuchungen aus dem Jahr 2018 (Januar-September). *Tierärztl Prax Ausg G: Grosstiere Nutztiere,* 47, 143-150, 2019. DOI: 10.1055/a-0896-0945

7. Anderson ML: Infectious causes of bovine abortion during mid-to late-gestation. *Theriogenology,* 68 (3): 474-486, 2007. DOI: 10.1016/j.theriogenology.2007.04.001

8. Carrique-Mas J, Willmington J, Papadopoulou C, Watson E, Davies R: *Salmonella* infection in cattle in Great Britain, 2003 to 2008. *Vet Rec*, 167 (15): 560-565, 2010. DOI: 10.1136/vr.c4943

9. Noakes DE, Parkinson TJ, England GC: Subfertility and infertility. **In,** Veterinary Reproduction and Obstetrics 9th ed., 393-646, Saunders Elseiver, England, 2018.

10. OIE Manual of Standards for Diagnostic Tests and Vaccines for Terrestrial Animals: Ch. 3.9.8. Salmonellosis (NB: Version adopted in May 2016), 2018.

11. Babacan O, Karadeniz H: Çiğ tavuk etlerinden izole edilen *Salmonella* spp. suşlarının antibiyotik duyarlılıklarının araştırılması. *Vet Hekim Der Derg,* 90 (2): 105-114, 2019. DOI: 10.33188/vetheder.497569

12. Zhai L, Kong X, Lu Z, Lv F, Zhang C, Bie X: Detection of *Salmonella enterica* serovar Dublin by polymerase chain reaction in multiplex format. *J Microbiol* Meth*ods,* 100, 52-57, 2014. DOI: 10.1016/j.mimet.2014.02.014

13. Fredriksson NJ, Hermansson M, Wilén BM: The choice of PCR primers has great impact on assessments of bacterial community diversity and dynamics in a wastewater treatment plant. *PloS One,* 8 (10): e76431, 2013. DOI: 10.1371/journal.pone.0076431

14. Petti CA, Brandt ME, Church DL, Emler S, Simmon K, Zelazny AM: Interpretive criteria for identification of bacteria and fungi by DNA target sequencing. **In,** CLSI guideline MM18, 2nd ed., 7-117, Clinical and Laboratory Standards Institute, Philadephia, 2018.

15. Nishimaki T, Sato K: An Extension of the Kimura two-parameter model to the natural evolutionary process. *J Mol Evol,* 87 (1): 60-67, 2019. DOI: 10.1007/s00239-018-9885-1

16. Barkallah M, Gharbi Y, Hassena AB, Slima AB, Mallek Z, Gautier M, Greub G, Gdoura R, Fendri I: Survey of infectious etiologies of bovine abortion during mid-to late gestation in dairy herds. *PLoS One,* 9 (3): e91549, 2014. DOI: 10.1371/journal.pone.0091549

17. Anderson ML, Blanchard PC, Barr BC, Hoffman RL: A survey of causes of bovine abortion occurring in the San Joaquin Valley, California. *J Vet Diagn Invest,* 2 (4): 283-287, 1990. DOI: 10.1177/104063879000200405

18. Halimi HA, Seifi HA, Rad M: Bovine salmonellosis in Northeast of Iran: Frequency, genetic fingerprinting and antimicrobial resistance patterns of *Salmonella* spp. *Asian Pac J Trop Biomed,* 4 (1): 1-7, 2014. DOI: 10.1016/S2221-1691(14)60199-4

19. Kirkbride CA: Bacterial agents detected in a 10-year study of bovine abortions and stillbirths. *J Vet Diagn Invest*, 5 (1): 64-68, 1993. DOI: 10.1177/104063879300500114

20. Derdour SY, Hafsi F, Azzag N, Tennah S, Laamari A, China B, Ghalmi F: Prevalence of the main infectious causes of abortion in dairy cattle in Algeria. *J Vet Res,* 61 (3): 337-343, 2017. DOI: 10.1515/jvetres-2017-0044

21. Reichel MP, Wahl LC, Hill FI: Review of diagnostic procedures and approaches to infectious causes of reproductive failures of cattle in Australia and New Zealand. *Front Vet Sci,* 5:222, 2018. DOI: 10.3389/fvets.2018.00222

22. Regional Veterinary Laboratories Report - November 2014: *Vet Ireland J*, 5, 79-84, 2015.

23. Geisbauer E, Stellnberger K, Krassnig G, & Dünser M: *Salmonella dublin* outbreak in cattle. Animal Hygiene and Sustainable Livestock Production. *Proceedings of the XVth International Congress of the International Society for Animal Hygiene,* Vienna, Austria, 575, 3-7 July2011.

24. Jerrett IV, McOrist S, Waddington J, Browning JW, Malecki JC, McCausland IP: Diagnostic studies of the fetus, placenta and maternal blood from 265 bovine abortions. *Cornell Vet,* 74 (1): 8-20, 1984.

25. Karatas Yeni D, Akca D: Evaluation of the analytical efficiency of Real-Time PCR in the diagnosis of Brucellosis in cattle and sheep. *Kafkas Univ Vet Fak Derg,* 27 (4): 503-509, 2021. DOI: 10.9775/kvfd.2021.25776

26. Drancourt M, Bollet C, Carlioz A, Martelin R, Gayral JP, Raoult D: 16S ribosomal DNA sequence analysis of a large collection of environmental and clinical unidentifiable bacterial isolates. *J Clin Microbiol,* 38 (10): 3623-3630, 2000. DOI: 10.1128/JCM.38.10.3623-3630.2000

Kafkas Universitesi Veteriner Fakultesi Dergisi
ISSN: 1300-6045 e-ISSN: 1309-2251
Journal Home-Page: http://vetdergikafkas.org

Kafkas Univ Vet Fak Derg
27 (6): 787-793, 2021
DOI: 10.9775/kvfd.2021.26332

RESEARCH ARTICLE

Calcium (Ca^{2+}) Oscillations and Intensity in Fresh Embryo and Vitrified Embryos Produced from Intra-cytoplasmic Sperm Injection (ICSI)

Widjiati WIDJIATI [1,a] Zakiyatul FAIZAH [2,b] Viski Fitri HENDRAWAN [3,c] Helly Nurul KARIMA [4,d] Choirunil CHOTIMAH [4,e] Sutiman Bambang SOEMITRO [5,f] A. A. Muhammad Nur KASMAN [6,g] Epy Muhammad LUQMAN [1,h (*)]

[1] Universitas Airlangga, Faculty of Veterinary Medicine, Department of Veterinary Science, 60115 Surabaya, INDONESIA
[2] Universitas Airlangga, Faculty of Medicine, Department of Biomedical Science, 60132 Surabaya, INDONESIA
[3] Universitas Brawijaya, Faculty of Veterinary Medicine, Department of Reproduction, 65151, Malang, INDONESIA
[4] Universitas Brawijaya, Bio-Science Central Laboratory, 65151, Malang, INDONESIA
[5] Universitas Brawijaya, Faculty of Science, Department of Biology, 65151, Malang, INDONESIA
[6] Universitas Muhammadiyah Mataram, Faculty of Health Science, 83115, Mataram, INDONESIA
ORCIDs: [a] 0000-0002-8376-1176; [b] 0000-0003-0962-9123; [c] 0000-0003-1089-0070; [d] 0000-003-2551-9303; [e] 0000-0001-6610-9306
[f] 0000-0001-8001-4338; [g] 0000-00003-2511-4920; [h] 0000-0001-7110-0939

Article ID: KVFD-2021-26332 Received: 26.07.2021 Accepted: 01.11.2021 Published Online: 05.11.2021

Abstract

This study aims to determine the intracellular calcium profile and viability of embryos produced by the Intra-Cytoplasmic Sperm Injection (ICSI) method. In this study, there were 2 groups (T1: fresh embryos, T2: embryos post vitrification). The stages of the study included medium preparation, goat oocyte collection, *in vitro* maturation of Kacang goat oocytes, fertilization using the ICSI method, and examination of the calcium (Ca^{2+}) intensity profile of fresh embryos and embryos post vitrification per unit time (sec). Measuring the intensity of Ca^{2+} using a Confocal Laser Scanning Microscope (CLSM) with time-lapse, taken at 3 points, namely point 1: edge, point 2: middle, and point 3: edge of the embryo sample. The fertilized embryos showed that the average calcium intensity of T1 was 334.62±8.60 and T2 was 408.2±13.67. The intensity of Ca^{2+} in embryos post vitrification is higher than that of in fresh embryos. The oscillation of Ca^{2+} in fresh embryos was in tune to the measurement point of 50 sec, while in embryos post vitrification the intensity from the 10^{th}, 20^{th} early sec and the 50^{th} end interval were not consistent. It can be concluded that the intensity of Ca^{2+} in embryos post vitrification is higher than that of in fresh embryos. The dynamics of Ca^{2+} in frozen embryos experiencing changes in intensity indicate a change in embryo quality due to vitrification.

Keywords: *Food production, Calcium, Embryo, Freezing, ICSI, Oscillation*

İntrasitoplazmik Sperm Enjeksiyonu (ICSI) İle Üretilen Taze Embriyoda ve Vitrifiye Embriyoda Kalsiyum (Ca^{2+}) Salınımları ve Yoğunluğu

Öz

Bu çalışma, Intra-Sitoplazmik Sperm Enjeksiyonu (ICSI) yöntemi ile üretilen embriyoların hücre içi kalsiyum profilini ve canlılığını belirlemeyi amaçlamıştır. Çalışmada 2 grup vardı (T1: taze embriyolar, T2: vitrifikasyon sonrası embriyolar). Çalışma, besiyeri hazırlama, keçi oositlerinin toplanması, Kacang keçi oositlerinin *in vitro* olgunlaştırılması, ICSI yöntemi kullanılarak embriyoların döllenmesi ve taze embriyoların ve vitrifiye embriyoların birim zamanda (sn) kalsiyum (Ca^{2+}) yoğunluk profillerinin incelenmesi aşamalarını içermiştir. Ca^{2+} yoğunluğu, time-lapse Lazer Taramalı Konfokal Mikroskobu (CLSM) kullanılarak 3 bölgede, bölge 1: kenar, bölge 2: orta ve bölge 3: embriyo numunesinin kenarı, gerçekleştirildi. Döllenen embriyolardan, T1'in ortalama kalsiyum yoğunluğu 334.62±8.60 ve T2'nin 408.2±13.67 olarak saptandı. Vitrifikasyon sonrası embriyolardaki Ca^{2+} yoğunluğu, taze embriyolardakinden daha yüksekti. Taze embriyolarda Ca^{2+} salınımlarının 50 sn'lik aralıktaki ölçümleri uyumluyken, vitrifikasyon sonrası embriyolarda 10 sn, 20 sn öncesi ve 50 sn'lik son aralıklara ait yoğunluklar uyumlu değildi. Vitrifikasyon sonrası embriyolardaki Ca^{2+} yoğunluğunun taze embriyolardakinden daha yüksek olduğu sonucuna varılabilir. Yoğunluk değişiklikleri yaşayan donmuş embriyolardaki Ca^{2+} dinamikleri, vitrifikasyon nedeniyle embriyo kalitesinde bir değişikliğe işaret eder.

Anahtar sözcükler: *Gıda üretimi, Kalsiyum, Embriyo, Dondurma, ICSI, Salınım*

How to cite this article?

Widjiati W, Faizah Z, Hendrawan VF, Karima HN, Chotimah C, Soemitro SB, Kasman AAMN, Luqman EM: Calcium (Ca^{2+}) oscillations and intensity in fresh embryo and vitrified embryos produced from intra-cytoplasmic sperm injection (ICSI). *Kafkas Univ Vet Fak Derg,* 27 (6): 787-793, 2021. DOI: 10.9775/kvfd.2021.26332

(*) Corresponding Author

Tel: +62 315 992785, Mobile: +62 812 3090594 Fax: +62 315 993015
E-mail: epy-m-l@fkh.unair.ac.id (E.M. Luqman)

Introduction

One of the assisted reproductive technologies that are now popular in tackling infertility problems is *in-vitro* fertilization (IVF). IVF is a very profitable method because besides being able to overcome infertility problems, this method can produce embryos of high quality and in large numbers. However, the drawbacks of this technology are poor oocyte quality and limited oocyte sources for *in vitro* embryo production [1].

An alternative breakthrough technology to produce embryos can be done *in vitro* using the Intra-Cytoplasmic Sperm Injection (ICSI) method. The ICSI method is a method by inserting sperm directly into the ooplasm of the metaphase II oocyte using a microscopic injector needle. This method is mostly used on humans and animal models to increase the reproducibility and productivity of livestock. The advantage of IVF and ICSI embryos is that they can be frozen using the cryopreservation method. During the freezing process, all cell metabolism stops and then return to normal when the embryo is thawed again. Drastic temperature changes in the cryopreservation of embryos cause damage to blastomere cells, sometimes causing blastomeric cell apoptosis [2,3].

In the ICSI process, oocyte activation is one of the factors that influence the success of fertilization. The oocyte activation occurs due to a complex interaction triggered by the entry of spermatozoa into the oocyte. An early indicator of oocyte activation is characterized by repeated increases in the intracellular calcium concentrations. The increase in intracellular calcium occurs due to a complex interaction triggered by the entry of spermatozoa cells into the oocyte during the fertilization process. During the fertilization process, the endoplasmic reticulum inside the oocyte releases Ca^{2+} ions as important triggers for development into embryos. Increased levels of calcium ions (Ca^{2+}) in the oocyte cytoplasm will initiate the formation of a pronucleus as a sign that the oocyte has been fertilized [4]. The most important principle of embryos cryopreservation is the removal of water from the cells (dehydration) before intracellular freezing. If dehydration does not occur, large ice crystals form in the cell and damage the cell. Reversely, if severe dehydration occurs the cell experiences membrane damage and dies [5]. Damage to the embryonic membrane during vitrification causes disruption of calcium oscillations and affects the process of embryonic development.

Calcium is important for embryonic development. If there is damage to the cell membrane, the released calcium will not re-enter the cell quickly. The dynamics of calcium uptake in cells greatly affect the quality and viability of the embryo. As a second messenger, intracellular calcium signals are capable of decoding and integrating into both chemical and physical environments. These calcium signals control cell division, differentiation, migration, and cell death. Calcium through signal transduction plays a role in the oocytes into embryos transition through the fertilization process, and in the embryo formation [6].

During the fertilization, the fusion of spermatozoa and oocytes triggers a repetitive calcium transient in the oocyte that normally responds to the initiation of embryogenesis. Calcium oscillations that occur due to the trigger by sperm-specific isozyme of phospholipase C (PLCζ) are expressed by the acrosomes of spermatozoa cells. Spermatozoa cells carrying PLCζ cleave phosphatidylinositol 4,5-bisphosphate (PIP2) in the oocyte to release InsP3 and calcium from storage in the endoplasmic reticulum. During embryogenesis, calcium is important in the process of left-right patterning and asymmetric morphogenesis, heart and vascular formation, and kidney formation. Calcium signaling is known to influence the nodal flow process from E7.5 by cilia-driven asymmetric fluid flow originating from the ventral node and transient to the middle during early somitogenesis. This process plays an important role in influencing the permeable channel polycystin-2 (PKD2) protein during the embryogenesis process [7].

It has been shown that calcium plays an important role in the formation of heart through the family of voltage-gated calcium, such as Cavβ2, NCX1, and ryanodine receptor type 2 (RyR2) which are essential for heart formation and embryonic heart function. In addition, calcium signaling plays an important role in the formation of the cardiovascular system with spontaneous calcium signaling for the first pulse transduced by PIEZO1 [8]. A previous research also reports that calcium ions as intracellular messengers play a role in kidney formation [9]. Using genetic and molecular biological approaches, it has been identified several Ca^{2+}-permeable ion channel families as important regulators of Ca^{2+} homeostasis in kidney. In addition, the role of Nuclear Factor Activated in T cells (NFAT) which has implications for signaling pathways for calcium invertebrates was also determined [10].

The dynamics of Ca^{2+} release and uptake greatly affect the cleavage process during embryonic development. If the post thawing blastomere cell death or degeneration occurs after vitrification due to temperature stress, Ca^{2+} released into the cytoplasm cannot be retracted into the cell so that it will affect the quality of the embryo. This study aims to determine the embryo's intracellular calcium profile and viability using the Intra Cytoplasmic Sperm Injection (ICSI) method among fresh embryo and embryo prior to vitrification produced.

Material and Methods

Ethical Approval

This research was conducted at the Biomedical Laboratory of the Faculty of Medicine, Universitas Airlangga, Surabaya

Indonesia. It has been ethically approved with no.1. KE.061.04.2019 issued by the Animal Care and Use Committee, Universitas Airlangga, Faculty of Veterinary Medicine Universitas Airlangga, Surabaya Indonesia.

Methods

This study used the Completely Randomized Design method and the sample used was a Kacang goat oocyte which was obtained from a slaughterhouse. The stages of this research included medium preparation, goat oocyte collection, *in vitro* maturation of Kacang goat oocytes, fertilization using the ICSI method. ICSI-produced embryos were divided into 2 groups, group T1 which was fresh embryos, and T2 which embryo with vitrification. Both of them then observed the intracellular calcium profile. Examination of the Ca^{2+} intensity profile of fresh embryos and vitrified embryos per unit time (sec). Measuring the intensity of Ca^{2+} using Confocal Laser Scanning Microscopy (CLSM) with time-lapse, taken at 3 points, namely point 1: edge, point 2: middle, and point 3: edge of the embryo sample.

- Medium Preparation

Media oocytes collection, maturation, and ICSI was prepared by making Earle's Balanced Salt Solution (EBSS) (E2888-Sigma-Aldrich) media drops with 7% Fetal Calf Serum (F7524-Sigma-Aldrich), HCG (Chorulon-Intervet), and PMSG (Folligon-Intervet) on disposable petridish (Nunc; Copenhagen, Denmark) with micropipette. The medium droplets were then covered with 2500-3000 µL mineral oil, and incubated in an incubator with 5% CO_2 at 38ºC for 22 h with 98% humidity before being used for *in vitro* maturation.

- Oocyte Collection

Kacang goat ovaries were obtained from a slaughterhouse and then brought to the laboratory in a flask containing 0.95% physiological NaCl at 37ºC (60 min). After arriving to the laboratory, the ovaries were sterilized and washed with physiological NaCl 0.95% + 100 µL gentamycin. Oocyte collection and aspiration using a syringe with an 18G needle containing 1 mL medium EBSS. The collected oocytes were inserted into a sterile petridish and then observed for the grade oocytes. Only oocytes surrounded with cumulus complexes of more than 3 layers were used for *in vitro* maturation.

- In Vitro Maturation

Oocytes with completed layers of cumulus washed 3 times with EBSS medium. Oocytes then transferred to the previously prepared maturation media and then incubated in a 5% CO_2 incubator at 38ºC for 22 h until the expansion of cumulus cells occurs. Then oocyte maturity level is examined.

After 22 h of culturation, the level of oocyte maturation was observed using a microscope with magnification of 100x and 400x to observe polar body I. The oocyte was immersed in a medium containing the hyaluronidase enzyme (HYASE-10x™, Vitrolife®) and left for 30 sec and then transferred to the culture medium [11,12].

- Spermatozoa Preparation Using Density Gradient Centrifugation

Frozen spermatozoa that have been collected and ready to be used were added with Sil-Select Plus medium (Fertipro, Beernem, Belgium) and centrifuged at 2500 rpm for 10 min, then put into a drop in the form of a well. Motile spermatozoa in small wells were used for fertilization [13].

- Fertilization Using Intra Cytoplasmic Sperm Injection (ICSI)

Oocytes that have been denuded in hyaluronidase enzyme to knock out the cumulus cells so the polar body would be visible. Good and motile spermatozoa that have been prepared are then immobilized by injuring the tail with an injector and then inserted into the injector and injected into the oocyte that has a polar body appearance. ICSI was carried out under mineral oil in 50x9 mm^2 Petri dishes (BD Falcon, Bedford, MA; Catalog No. 351006) using a Nikon Eclipse TE-2000-U microscope (Nikon, Melville, NY) equipped with manipulators (Eppendrof, Hamburg, Germany) [14-16].

- Embryo Vitrification

The ICSI embryos were exposed to a vitrified equilibration medium containing PBS + 15% ethylene glycol + 0.5 M sucrose + 15% PROH/propanediol (V2) with an exposure time of 18-20 min. The embryos were then put into M2 (Sigma, Saint-Quntin-Fallavier, France) (V3) medium for 30 sec. The embryos were then placed in a 0.25 mL transparent hemistraw, therefore exposed to nitrogen vapor for 10 sec, and placed in a liquid nitrogen container [17].

- Embryo Thawing

After being vitrified, the embryos were warmed (warming/thawing) in the air for 10 sec and then in a water bath at 35ºC for 30 sec. Embryos in hemistraw were poured and exposed to an equilibration medium containing PBS + 20% serum + 0.5 M sucrose (V4) for 2 min. Then the embryos were put into a medium containing PBS + 20% serum + 0.25M sucrose (V5) for 2 min then continued into PBS medium + 20% serum + 0.1M sucrose (V6) for 3 min [17].

- Embryo Ca^{2+} Oscillation Profile Examination

Fresh embryo and the thawed embryos were then fixed and washed with PBS 3 times for 5 min. The intensity of Ca^{2+} during activation embryo was observed by Fluo-3 staining with Confocal Laser Scanning Microscope (CLSM). Embryo were loaded with Fluo-3 AM Calcium indicator (Molecular Probes, Eugene, USA) (0.5 µg/mL in HEPES medium, at 37ºC

for 60 min). The cells were washed three times with Krebs-Ringer solution (K4002-Sigma-Aldrich) for 5 min and then incubated in Krebs-Ringer solution for 15 min to remove any non-specific staining on the cell surface. The embryo cell coverslips incubated with Fluo-3AM were placed in a special perfusion chamber of the laser scanning confocal microscope. After the perfusion apparatus was installed, the amount of injected and aspirated liquid was balanced at a speed of 2-3 mL/min; the temperature of the water bath was maintained at 37°C. The fluorescence was excited by an argon ion laser with an excitation wavelength of 506 nm and an emission wavelength of 525 nm. The cells were scanned in an XYT-plane fashion under the laser scanning confocal microscope using the Time Series program time-lapse. All of the results were analyzed using the TCS-SP2 CLSM software.

Statistical Analysis

Data were analyzed using the SPSS 21.0 software (IBM Corp., NY, USA) and first tested for normality using the Saphiro Wilk test then using T independent test with $P<0.05$ signification. If the distribution of the data abnormal, the data were verified using the Kruskall Wallis Test then intervariable using Mann Whitney U Test to find the differentiation of each group. $P\leq0.05$ was considered statistically significant.

Results

From the results of the average calcium intensity of T1 embryos treated with fresh embryos and T2 embryos post vitrification, *Table 1* data is obtained.

The mean result of fresh embryo calcium intensity was 334.62±8.60. Meanwhile, the average embryonic calcium intensity post vitrification in the T2 group was slightly higher at 408.2±13.67. The embryos in both groups were then examined for calcium intensity with a CLSM microscope per unit time. The examination of the calcium intensity of fresh embryos result was shown in *Fig. 1*.

Based on the results, it was known that the intensity of Ca^{2+} in the T1 group moves up and down as its activity goes in and out of cells freely. Changes in Ca^{2+} concentration are called changes in Ca^{2+} oscillations. At all three points, the Ca^{2+} oscillation profile shows a decreasing intensity with time. At point 1, the highest intensity is known to occur at the initial 10-sec interval (376.92) and the lowest at the 50-sec interval (279.89). At point 2, the highest Ca^{2+} intensity was at the 10th sec (335.97) and the lowest was at the 50th time (236.16). At point 3, the highest Ca^{2+} intensity was also at the 10th initial time interval (296.54) and the lowest at the 40th-sec interval (225.20).

In the T2 group, the Ca^{2+} intensity also moved up and down according to intracellular activity. At all three points, the Ca^{2+} oscillation profile shows an intensity that fluctuates over time. At point 1, the highest Ca^{2+} intensity was at the 40th-sec interval (310.77) and the lowest was at the 10th initial time interval (208.95). At point 2, the highest intensity is known to occur at the initial 10-sec interval (483.50) and the lowest at the end of the 50-sec interval (231.34). At point 3, the highest Ca^{2+} intensity was at the 20th time interval (311.77) and the lowest was at the 50th sec (112.34) *(Fig. 2)*.

Based on the different tests using ANOVA between points against time per 10 sec, in fresh embryos, there is a tangent approach to calcium intensity at point 2 (middle) and point 3 (edge) at the end of the 50th sec between 236.16-228.81. In embryos after vitrification, contact occurs more as much as 3 times. The tangent approach of calcium intensity occurs at the interval of 20 sec between point 1 (edge)

Table 1. *Calcium Intensity Kacang goat frozen embryo post vitrification and fresh embryo*

Group	Mean±SD*
T1 (Fresh embryo)	334.62±8.60^{a}
T2 (Frozen embryo)	408.2±13.67^{b}

** Different supercript in the same column have significant difference (P<0.05)*

Fig 1. Calcium Oscillation Profile in Fresh Embryo group (T1)

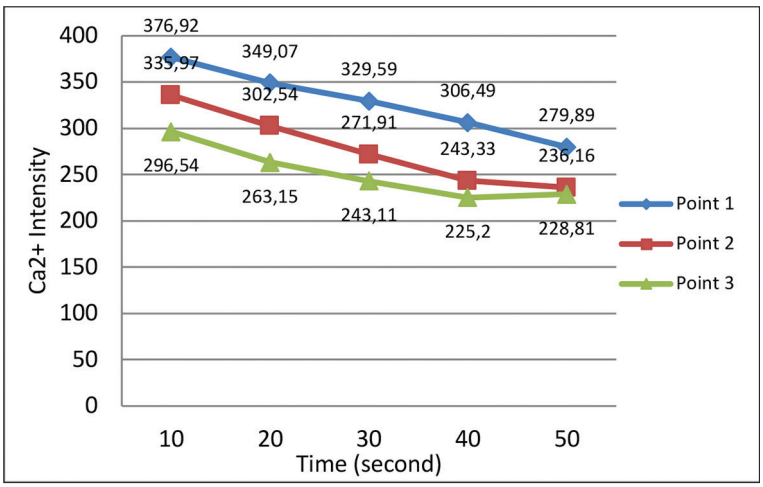

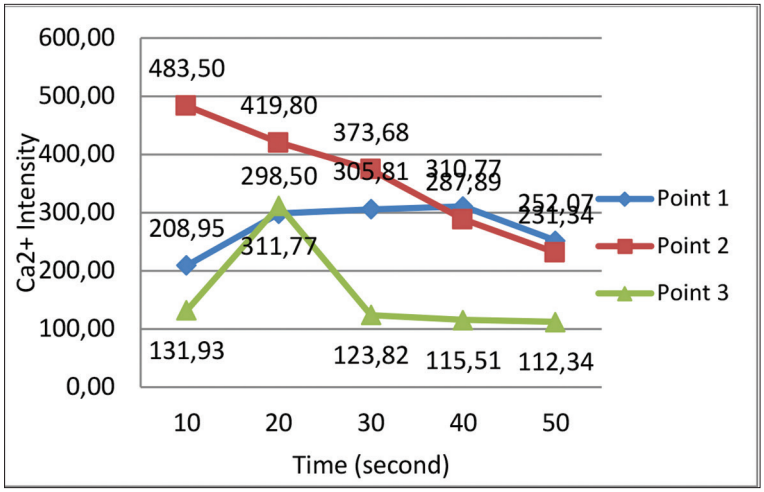

Fig 2. Calcium Oscillation Profile in Embryo post Vitrification (T2)

and point 3 (edge) between 298.50-311.77; at the 40th sec between point 1 (edge) and point 2 (middle) the range is 287.99-310.77, and the 50th sec between point 1 (edge) and point 2 (middle) of the intensity range from 231.34-252.07. Based on the LSD test, it was found that there was no significant difference between the 20th and 50th sec (p: 0.046; P<0.05) in both T1 and T2 embryos.

Discussion

The results of the average calcium intensity of fertilized embryos using the ICSI method showed that the calcium intensity of fresh embryos was 334.62±8.60. While the embryo after vitrification was slightly higher at 408.2±13.67. This is comparable to the report of Bonte et al.[18] which states that the frozen embryo recovery process during the warming process run quickly and optimally in the right medium. Cellularly in the endoplasmic reticulum, the storage of calcium ions after the warming process increases significantly compared to the fresh condition. This can be seen in the strong indicator of the SERCA pump and the calcium outlet valve. Excess release of calcium on the endoplasmic reticulum would start the process of calcium ions influx into the mitochondria to overload. The negative side if this happens also causes a high rate of cell apoptosis. Increase in intracellular calcium occurs after the clotting process followed by osmotic stress and regulatory volume decrease (RVD) due to calcium imbalance. The increase in optimal calcium is stimulated by the mitogen-activated protein kinase (MAP kinase) pathway. The extracellular-signal-regulated kinase (ERK) stimulation occurs after triggering hypoosmotic cell stress by increasing ERK phosphorylation and inhibiting RVD and keeping cells stable [18-20].

The Ca^{2+} intensity in the fresh embryo group had the characteristics of increasing and decreasing as Ca^{2+} activity entered and left the cells freely. At the three points, the Ca^{2+} oscillation profile shows the highest intensity in the first sec (10th sec) and the lowest in the last second (40-50 sec). Nikiforaki [21] reported according to their research that the characteristics of calcium oscillations in the first initiation transient were seen at the beginning of the phase with the highest amplitude of 1.1 (1-1.4) AU and initiation with the lowest amplitude of 0.6 (0.6-0.8) AU at the end of the phase. In the vitrified embryos group, the intensity of Ca^{2+} also moved up and down according to intracellular activity. The Ca^{2+} oscillation profile at points 2 and 3 of the highest intensity occurred in the initial phase time interval (10 sec and 20 sec) and the lowest at the final second phase (50 sec). While at point 1, the highest Ca^{2+} intensity was at the 40th-sec interval and the lowest was at the 10th initial time interval. Nikiforaki [21] explained in their research that the transition amplitude of calcium would significantly increase and slowly decrease after the vitrification process. In his study, frozen embryos showed an increase in the early phase of 1.8 (1.4-2.2) AU and decreased to 0.8 (0.7-0.9) AU [21].

In fresh embryos, there is a tangent approach to calcium intensity at the end of the 50th sec. In frozen embryos, the approximation of the tangent occurs at an interval of 20 sec; the 40th sec; and the 50th sec. Based on the LSD test, it was found that there was no significant difference between the initial and final sec (P: 0.046; P<0.05) both in fresh embryos and after vitrification, but in embryos post vitrification the calcium intensity points (Ca^{2+}) were not aligned and did not meet at one point at the end of the 50 sec measurement. Nikiforaki [21] explained that the source of the oocyte and the origin of its shape, both fresh and frozen *(in vitro* and *in vivo)* influences the pattern of calcium oscillations following ICSI. Direct comparison of the values of the calcium oscillation parameters results have been reported for failed fertilized.

In this study, the pattern of calcium oscillations also showed differences in the calcium oscillation model for 1 min which showed a calcium oscillation pulse 10-20 sec early and late. According to the study of Tesarik [22], calcium oscillations begin 2-12 h after ICSI and their intracellular initiation occurs every 1-5 min in the MII division of fresh

embryos. Micro intracellular oscillations occur every 20 sec and continue for 0.5-1 h. Different things were reported by Yanagida [23], who stated that calcium initiation occurred at 18.4±3.8 min after ICSI and was seen every 11 sec [21-23].

The difference in the results of each report on calcium analysis in oocytes and embryos do not depend on oocyte variability, differences in the use of spermatozoa, or the medium, but is also influenced by the use of calcium indicators. Shwann [24] who used the hydrolysis form of acetoxymethyl ester calcium reported that the indicator could diffuse into the organelles and vesicles longer during the measurement process so that the measurement time was also longer. In addition, the Fura-2 dextran indicator is also able to remain in the cytosol better so that the measurement is more accurate [24].

The pattern of calcium oscillations in vitrified embryos appears to be more likely to occur at contact and pulse oscillations. The same thing is comparable to the research of Nikiforaki [21] which showed that calcium oscillations with vitrification and warming started more slowly with a long period of time and high amplitude and low frequency. However, according to the different tests conducted in this study, it was shown that there was no significant difference in calcium intensity between fresh and vitrified embryos. This is also in accordance with the research of Kim [25], which showed that embryos vitrified using ethylene glycol and DMSO with fresh embryos do not show any significant difference in calcium oscillations after ICSI. However, this study also showed that calcium oscillations in fresh embryos appeared to be more stable when compared to the frozen embryos. Even though vitrified embryos can survive the freezing process and would be able to increase the survival rate and embryo development, sometimes there would be a slight decrease in quality during fertilization and embryo transfer when compared to fresh embryos. This is because calcium signaling affects not only oocyte activation, but is also required for the post-implantation formation [21,25-27].

In addition, embryos with a vitrification process would experience more calcium shocks or pulsations. This happens because the vitrification process would reduce and damage cortical granules and smooth endoplasmic reticulum. Disturbance in the mitochondria-endoplasmic smooth reticulum would interfere with the calcium signaling process and form wide endoplasmic reticulum vesicles and result in membrane rupture causing calcium leakage. Therefore, cryoprotectants are used as cell protective agents, such as 1,2-propanediol, ethylene glycol, and DMSO, which can induce an increase in intracellular calcium concentration. The release of calcium with cryoprotectants induces potentially oocyte activation, fertilization, and embryo formation. Calcium oscillations induce calcium entry into oocytes and embryos and affect meiosis activation and cell division [28-33].

The intensity of Ca^{2+} in embryos post vitrification is higher than in fresh embryos. The oscillations of Ca^{2+} in fresh embryos was aligned from the measurement point of 50 sec, while in embryos post vitrification the intensity from the initial 10^{th} and 20^{th}-sec intervals and the end of the 50^{th}-sec interval did not match the intensity. This is due to the dynamics of Ca^{2+} in frozen embryos experiencing changes in intensity indicating a change in embryo quality due to vitrification.

Availabity of Data and Materials

The authors declare that data supporting the study findings are also available to the corresponding author.

Acknowledgement

The authors are grateful to the authorities Faculy of Veterinary Medicine, Faculty of Medicine, Airlangga University and Dr. Soetomo General Hospital, Surabaya, Indonesia.

Funding Support

This research was funded by Universitas Airlangga with the Mandat Project number: 1520/UN3/2019.

Conflict of Interest

The authors report no conflicts of interest. The authors are responsible for the content and writing of paper.

Author Contributions

WW, SBS and EML conceived and supervised the study. WW, ZF and VFH collected and analyzed data. WW, HNK, CC and AAMNK made laboratory measurements. HNK and CC applied the embryo Ca^{2+} oscillation profile examination of the study. All authors contributed to the critical revision of the manuscript and have read and approved the final version.

References

1. Nasr-Esfahani MH, Razavi S, Mardani M, Shirazi R, Javanmardi S: Effects of failed oocyte activation and sperm protamine deficiency on fertilization post ICSI. *Reprod Biomed Online*, 14 (4): 422-429, 2007. DOI: 10.1016/s1472-6483(10)60888-7

2. Colombo M, Zahmel J, Jänsch S, Katarina Jewgenow K, Luvoni GC: Inhibition of apoptotic pathways improves DNA integrity but not developmental competence of domestic cat immature vitrified oocytes. *Front Vet Sci,* 7:588334, 2020. DOI: 10.3389/fvets.2020.588334

3. Hatırnaz S, Ata B, Hatırnaz ES, Dahan MH, Tannus S, Tan J, Tan SL: Oocyte *in vitro* maturation: A sytematic review. *Turk J Obstet Gynecol,* 15 (2): 112-125, 2018. DOI: 10.4274/tjod.23911

4. Karabulut S, Aksünger Ö, Ata C, Sağıroglu Y, Keskin I: Artificial oocyte activation with calcium ionophore for frozen sperm cycles. *Syst Biol Reprod Med,* 64 (5): 381-388, 2018. DOI: 10.1080/19396368.2018.1452311

5. Coticchio G, Borini A, Distratis V, Maione M, Scaravelli G, Bianchi V, Machiarelli G, Nottola SA: Qualitative and morphometric analysis of the ultrastructure of human oocytes cryopreserved by two alternative slow cooling protocols. *J Assist Reprod Genet,* 27 (4): 131-140, 2010. DOI: 10.1007/s10815-010-9394-7

6. Stewart TA, Davis FM: An element for development: Calcium signaling in mammalian reproduction and development. *Biochim Biophys Acta Mol Cell Res,* 1866, 1230-1238, 2019. DOI: 10.1016/j.bbamcr.2019.02.016

7. Yoshiba S, Hamada H: Roles of cilia, fluid flow, and Ca^{2+} signaling in breaking of left-right symmetry. *Trends Genet,* 30 (1): 10-17, 2014. DOI: 10.1016/j.tig.2013.09.001

8. Jiang F, Yin K, Wu K, Zhang M, Wang S, Cheng H, Zhou Z, Xiao B: The mechanosensitive Piezo1 channel mediates heart mechano-chemo transduction. *Nat Commun*, 12:869, 2021. DOI: 10.1038/s41467-021-21178-4

9. Zhou Y, Greka A: Calcium-permeable ion channels in the kidney. *Am J Physiol Renal Physiol*, 310 (11): F1157-F1167, 2016. DOI: 10.1152/ajprenal.00117.2016

10. Nonomura K, Lukacs V, Sweet D, Goddard L, Kanie A, Whitwam T, Ranade S, Fujimori T, Kahn M, Patapoutian A: Mechanically activated ion channel PIEZO1 is required for lymphatic valve formation, *Proc Natl Acad Sci U S A*, 115 (50): 12817-12822, 2018. DOI: 10.1073/pnas.1817070115

11. Bakri NM, Ibrahim SF, Osman NA, Hasan N, Jaffar FHF, Rahman ZA, Osman K: Embryo apoptosis identification: Oocyte grade or cleavage stage? *Saudi J Biol Sci,* 23 (1): S50-S55, 2016. DOI: 10.1016/j.sjbs.2015.10.023

12. de Moura BRL, Gurgel MCA, Machado SPP, Marques PA, Rolim JR, de Lima MC, Salgueiro LL: Low concentration of hyaluronidase for oocyte denudation can improve fertilization rates and embryo quality. *JBRA Assist Reprod*. 21 (1): 27-30, 2017. DOI: 10.5935/1518-0557.20170008

13. Suyono SS, Hinting A, Lunardhi H, I'tishom R: Density gradient centrifugation pra-freezing mengoptimalkan persentase morfologi normal spermatozoa pasca-thawing. *MKB*, 50 (3): 133-139, 2018. DOI: 10.15395/mkb.v50n3.1348

14. Pramesemara IGN, Faizah Z, Darsini N: The Intracytoplasmic sperm injection (ICSI) technique in an infertile man with hepatitis-B virus (HBV) infection: A case report. *Indo J Biomed Sci,* 14 (2): 82-85, 2020. DOI: 10.15562/ijbs.v14i2.231

15. Parmegiani L, Cognigni G, Filicori M: New advances in intracytoplasmic sperm injection (ICSI). **In,** Bin Wu (Ed): Advances in Embryo Transfer. 99-114, 2012. DOI: 10.5772/39227

16. Shadanloo F, Hasan M, Morteza NS, Sayyed H, Hosseini M, Hossein M, Nasr-Esfahani H, Hossein M, Nasr-Esfahani H: Sperm status and DNA dose play key roles in sperm/ICSI-mediated gene transfer in caprine. *Mol Reprod Dev,* 77 (10): 868-875, 2010. DOI: 10.1002/mrd.21228

17. Faizah Z, Aswin RH, Lunardhi H: Effect of oocyte vitrification before and after *in vitro* maturation towards Bcl-2, Bax and Bcl-2/Bax ratio expression. *Majalah Obstet Ginekol,* 24 (2): 56-60, 2016. DOI: 10.20473/mog.V24I22016.56-60

18. Bonte D, Thys V, De Sutter P, Boel A, Leybaert L, Heindryckx B: Vitrification negatively affects the Ca^{2+}-releasing and activation potential of mouse oocytes, but vitrified oocytes are potentially useful for diagnostic purposes. *Reprod Biomed Online,* 40 (1): 13-25, 2020. DOI: 10.1016/j.rbmo.2019.09.012

19. Wang N, Hao HS, Li CY, Zhao YH, Wang HY, Yan CL, Du WH, Wang D, Liu Y, Pang YW, Zhu HB, Zhao XM: Calcium ion regulation by BAPTA-AM and ruthenium red improved the fertilisation capacity and developmental ability of vitrified bovine oocytes. *Sci Rep,* 7:10652, 2017. DOI: 10.1038/s41598-017-10907-9

20. Zhao XM, Hao HS, Du WH, Zhao SJ, Wang HY, Wang N, Wang D, Liu Y, Qin T, Zhu HB: Melatonin inhibits apoptosis and improves the developmental potential of vitrified bovine oocytes. *J Pineal Res,* 60 (2): 132-141, 2016. DOI: 10.1111/jpi.12290

21. Nikiforaki D, Meerschaut FV, Qian C, De Croo I, Lu Y, Deroo T, den Abbeel EV, Heindryckx B, De Sutter P: Oocyte cryopreservation and *in vitro* culture affect calcium signalling during human fertilization. *Hum Reprod,* 29 (1): 29-40, 2014. DOI: 10.1093/humrep/det404

22. Tesarik J, Sousa M, Testart J: Human oocyte activation after intracytoplasmic sperm injection. *Hum Reprod*, 9 (3): 511-518, 1994. DOI: 10.1093/oxfordjournals.humrep.a138537

23. Yanagida K, Katayose H, Hirata S, Yazawa H, Hayashi S, Sato A: Influence of sperm immobilization on onset of Ca^{2+} oscillations after ICSI. *Hum Reprod,* 16 (1): 148-152, 2001. DOI: 10.1093/humrep/16.1.148

24. Swann K: Measuring Ca^{2+} oscillations in mammalian eggs. **In,** Homer H (Ed): Mammalian Oocyte Regulation Methods in Molecular Biology (Methods and Protocols). 231-248, 2013. DOI: 10.1007/978-1-62703-191-2_16

25. Kim BY, Yoon SY, Cha SK, Kwak KH, Fissore RA, Parys JB, Yoon TK, Lee DR: Alterations in calcium oscillatory activity in vitrified mouse eggs impact on egg quality and subsequent embryonic development. *Pflugers Arch*, 461 (5): 515-526, 2011. DOI: 10.1007/s00424-011-0955-0

26. Saragusty J, Arav A: Current progress in oocyte and embryo cryopreservation by slow freezing and vitrification. *Reproduction*, 141 (1): 1-19, 2011. DOI: 10.1530/REP-10-0236

27. Magli MC, Lappi M, Ferraretti AP, Capoti A, Ruberti A, Gianaroli L: Impact of oocyte cryopreservation on embryo development. *Fertil Steril*, 93 (2): 510-516, 2010. DOI: 10.1016/j.fertnstert.2009.01.148

28. Khalili MA, Maione M, Palmerini MG, Bianchi S, Macchiarelli G, Nottola SA: Ultrastructure of human mature oocytes after vitrification. *Eur J Histochem*, 56:e38, 2012. DOI: 10.4081/ejh.2012.e38

29. Shahedi A, Hosseini A, Khalili MA, Norouzian M, Salehi M, Piriaei A, Nottola SA: The effect of vitrification on ultrastructure of human *in vitro* matured germinal vesicle oocytes. *Eur J Obstet Gynecol Reprod Biol*, 167 (1): 69-75, 2013. DOI: 10.1016/j.ejogrb.2012.11.006

30. Miao YL, Stein P, Jefferson WN, Padilla-Banks E, Williams CJ: Calcium influx-mediated signaling is required for complete mouse egg activation. *Proc Natl Acad Sci U S A,* 109, 4169-4174, 2012. DOI: 10.1073/pnas.1112333109

31. Bonetti A, Cervi M, Tomei F, Marchini M, Ortolani F, Manno M: Ultrastructural evaluation of human metaphase II oocytes after vitrification: Closed versus open devices. *Fertil Steril*, 95 (3): 928-935, 2011. DOI: 10.1016/j.fertnstert.2010.08.027

32. Gardner DK, Sheehan CB, Rienzi L, Katz-Jaffe M, Larman MG: Analysis of oocyte physiology to improve cryopreservation procedures. *Theriogenology*, 67 (1): 64-72, 2007. DOI: 10.1016/j.theriogenology.2006.09.012

33. Ghetler Y, Skutelsky E, Ben Nun I, Ben Dor L, Amihai D, Shalgi R: Human oocyte cryopreservation and the fate of cortical granules. *Fertil Steril*, 86 (1): 210-216, 2006. DOI: 10.1016/j.fertnstert.2005.12.061

Kafkas Universitesi Veteriner Fakultesi Dergisi
ISSN: 1300-6045 e-ISSN: 1309-2251
Journal Home-Page: http://vetdergikafkas.org

Kafkas Univ Vet Fak Derg
27 (6): 795-802, 2021
DOI: 10.9775/kvfd.2021.26337

RESEARCH ARTICLE

Determination of Gender and Breed in Arabian Horses and Thoroughbred Horses Using Radiography of the Tarsal Region

Dilek OLGUN ERDIKMEN [1,a] Ozan GUNDEMIR [2,b] Gulsun PAZVANT [2,c] Mustafa Orhun DAYAN [3,d]
Sokol DURO [4,e] Hulya HARTOKA [5,f] William PÉREZ [6,g] Cagla PARKAN YARAMIS [7,h (*)]

[1] Department of Surgery, Faculty of Veterinary Medicine, Istanbul University-Cerrahpaşa, TR-34320 Avcılar/Istanbul - TURKEY
[2] Department of Anatomy, Faculty of Veterinary Medicine, Istanbul University-Cerrahpaşa, TR-34500 Büyükçekmece, Istanbul - TURKEY
[3] Department of Anatomy, Faculty of Veterinary Medicine, Selçuk University, TR-42003 Konya - TURKEY
[4] Faculty of Veterinary Medicine, Agricultural University of Tirana, Tirana, ALBANIA
[5] Jockey Club of Turkey, Istanbul Horse Hospital, TR-34144 Istanbul - TURKEY
[6] Unidad de Anatomía, Facultad de Veterinaria, Universidad de la República, Montevideo, URUGUAY
[7] Vocational School of Veterinary Medecine, Equine and Equine Training Programme, Istanbul University-Cerrahpaşa, TR-34320 Avcılar, Istanbul - TURKEY
ORCIDs: [a] 0000-0002-8190-8429; [b] 0000-0002-3637-8166; [c] 0000-0001-5986-3992; [d] 0000-0003-0368-4607; [e] 0000-0002-6075-7342
[f] 0000-0002-6666-1851; [g] 0000-0002-9647-4731; [h] 0000-0002-5048-9452

Article ID: KVFD-2021-26337 Received: 04.08.2021 Accepted: 04.11.2021 Published Online: 05.11.2021

Abstract

In this study, it was examined whether the radiographic measurements taken from the tarsal region, especially the calcaneus, can be used in sex determination. In addition, two different horse breeds were used and whether these values would cause any difference between the breed was examined. 213 race horses were used in this study. Radiographic images of the left tarsal joint of Arabian horses (30 females, 57 males) and Thoroughbred horses (57 females, 69 males) were taken from the lateromedial direction. The widest point of the trochlea was seen to be a determinant in sex determination of Arabian horses. In Thoroughbred horses, it was seen that the value of the calcaneus body was the most important factor in sex determination. As a result of the discriminant analysis, 71.26% of male and female Arabian horses and 66.67% of Thoroughbred horses, respectively were classified correctly. It was observed that 88.26% of the horses between the two breeds were classified correctly regardless of sex. In the correlation test between measurements, negative correlation value with age was seen in the talus measurement (correlation value: -0.139-099). In conclusion, radiological measurements of this clinically important region can be used as an alternative method for sex and breed discrimination.

Keywords: *Calcaneus, Discriminant analysis, Equine, Limbs, Radiometric, Talus*

Arap ve İngiliz Atlarında Tarsal Bölgenin Radyografisi Kullanılarak Irk ve Cinsiyetin Belirlenmesi

Öz

Bu çalışmada başta calcaneus olmak üzere, tarsal bölgeden alınan radyografik ölçümlerin cinsiyet tayininde kullanılıp kullanılamayacağı incelenmiştir. Ayrıca farklı iki at ırkı kullanılmış ve alınan bu değerlerin ırklar arasında herhangi bir farklılığa neden olup olmadığı incelenmiştir. Çalışmada 213 yarış atı kullanıldı. Safkan Arap (30 dişi, 57 erkek) ve İngiliz atlarının (57 dişi, 69 erkek) sol tarsal eklemlerinin lateromedial yönden radyografik görüntüleri alındı. Arap atlarının cinsiyet tayininde trochlea'nın en geniş noktasının belirleyici olduğu görüldü. İngiliz atlarında ise cinsiyet tayininde kalkaneus gövde ölçüm değerinin en önemli faktör olduğu görüldü. Diskriminant analizi sonucunda cinsiyet ayırımında erkek Arap atlarının %71.26'sının, İngiliz atlarının ise %66.67'sinin doğru olarak sınıflandırıldığı görüldü. İki ırk arasındaki atların %88.26'sının cinsiyet gözetmeksizin doğru sınıflandırıldığı gözlemlendi. Ölçümler arası korelasyon testinde, talus ölçümünde yaş ile negatif korelasyon değeri tespit edildi. (korelasyon değeri: -0.139-099). Sonuç olarak, klinik açıdan önemli olan bu bölgenin radyolojik ölçümleri, cinsiyet ve ırk ayrımı için alternatif bir yöntem olarak kullanılabilir.

Anahtar sözcükler: *Calcaneus, Diskriminant analizi, Tek tırnaklı, Uzuvlar, Radyometrik, Talus*

How to cite this article?

Olgun Erdikmen D, Gundemir O, Pazvant G, Dayan MO, Duro S, Hartoka H, Pérez W, Parkan Yaramis C: Determination of gender and breed in Arabian horses and thoroughbred horses using radiography of the tarsal region. *Kafkas Univ Vet Fak Derg,* 27 (6): 795-802, 2021.
DOI: 10.9775/kvfd.2021.26337

(*) Corresponding Author

Tel: +90 212 473 7070/17101 Cellular Phone: +90 530 645 7484
E-mail: cparkan@iuc.edu.tr (Ç. Parkan Yaramış)

Introduction

Using direct bone and living material measurements in taxonomy studies, the differences between sex and species have been revealed for years. However, in recent years, a different perspective has been brought to these studies by using the features of imaging systems. One of its most important features is that it can be sampled on live animals. Later, this data can be followed up on live animals. It is also ethically more advantageous compared to dissection studies. Moreover, thanks to modeling studies, tissue and bone sampling of endemic species can be made and these data can be stored electronically. In addition, with these studies in basic disciplines, results directly related to clinical sciences can be obtained. Because of these features, studies conducted with imaging systems in animals are preferred over the classical dissection method [1-4].

Tarsal articulation is a pelvic limb joint which is composed by cochlea of the tibia, fibula, tarsal and metatarsal bones. The number of tarsal bones is different depending on the animal species, which is six in the horses. The proximal tarsal row is composed by talus and calcaneus, the last is located in plantar and lateral side of the talus. This joint is clinically important in horses, especially Osteochondritis dissecans is an important pathological condition that causes lameness in horses. The radiological image of the tarsal region is very important in the diagnosis of most such diseases and pelvic limb lameness [5,6].

Radiological images have been used in studies such as determining the normal posture position of animals as well as determining bone-joint relations. Gonçalves et al.[7] obtained the parameters related to hoof balance using healthy animals in his study and provided the radiologically based database on this subject. Dorner et al.[8] on the other hand, conducted a radiological study in horses to explain the relationship between the distal phalanx angle and the radiological condition of the navicular bone.

There are studies examining the differences between genders in studies on the tarsal joint. Studies have been conducted on humans and measurements of gender differences have been reported [1,3,4]. The hypothesis of this study is that there are differences between two different horse breeds as well as between the sexes as examined the tarsal joint radiographs.

Material and Methods

Ethical Statement

The study was approved by the Local Ethics Committee of Faculty of Veterinary Medicine, İstanbul University-Cerrahpaşa (Approval no: 2020/41).

Animals

In this research, 213 horses from 2 to 12 years old and without pathological conditions in their tarsal joints were used. Radiographic images of the tarsal joint of the left pelvic limb of Arabian horses (30 females, 57 males) and Thoroughbred horses (57 females, 69 males) were taken from the lateromedial direction. Images were taken while the cassette was in contact with the tarsal joint as the X-ray beam was 70 cm distance. X-ray images were taken at the Istanbul horse Hospital of the Jockey Club of Turkey. Gierth X-ray (model TR90/30) model device was used.

Radiometric Analysis

In the study, a single image taken from the lateral direction was used for each animal. Nine measurements were made over the X-ray image of the tarsal joint *(Fig. 1)*. In addition, two angle values were recorded in the same image *(Fig. 2)*. Measurements were taken on the computer using the Radiant DICOM Viewer (version 2020.2.2) [4,9].

Cranial calcaneus length (CCL): The distance between the highest point of the tuber calcanei and the coracoid process of calcaneus.

Maximum calcaneus length (MCL): The distance between the highest point of the tuber calcanei and the most dorso-distal point of the calcaneus base.

Calcaneal body depth (CBD): The shortest distance between cranial and caudal border of the calcaneus body.

Tuber calcaneus length (TCL): The maximum length of the tuber calcaneus.

Cochlea of tibia´s depth (CTD): The distance from the most cranial margin of the distal part of the tibia to the most caudal border of the cochlea tibia.

Facies articulares talares´s length (FTL): The length between the distal endpoints of the CCL (Cranial calcaneus length) and MCL (Maximum calcaneus length).

Metatarsus depth (MD): The distance from the most cranial margin of the third metatarsal bone to the caudal margin of the fourth metatarsal bone.

Talus ridge´s length (TRL): The distance from the proximal to distal end point of talus ridge.

Talus high (TH): The distance from the talus tuberosity to the deepest point of the cochlea tibia´s.

Proximal angle (PA): The angle between the line drawn from most dorsal point of tuber calcaneus to the coracoid process and the line drawn in the direction of facies articulares talares´s length (FTL).

Distal angle (DA): The angle between the line drawn from most dorsal point of tuber calcaneus to the most dorso-distal point of the calcaneus base and the line drawn in the direction of facies articulares talares´s length (FTL).

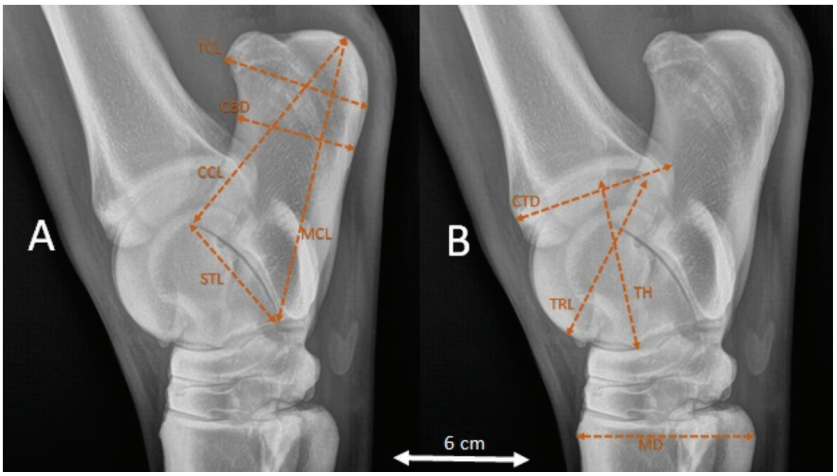

Fig 1. Measurement points (The x-ray image is of a 3-year-old female Thoroughbred horse) **Cranial calcaneus length (CCL):** The distance between the highest point of the tuber calcanei and the coracoideus process of calcaneus**, Maximum calcaneus length (MCL):** The distance between the highest point of the tuber calcanei and the most dorso-distal point of the calcaneus base, **Calcaneal body depth (CBD):** The shortest distance between cranial and caudal border of the calcaneus body, **Tuber calcaneus length (TCL):** The maximum length of the tuber calcaneus, **Cochlea of tibia´s depth (CTD):** The distance from the most cranial margin of the distal part of the tibia to the most caudal border of the cochlea tibia, **Facies articulares talares´s length (FTL):** The length between the distal endpoints of the CCL (Cranial calcaneus length) and MCL (Maximum calcaneus length), **Metatarsus depth (MD):** The distance from the most cranial margin of the third metatarsal bone to the caudal margin of the fourth metatarsal bone, **Talus ridges length (TRL):** The distance from the proximal to distal end point of talus ridge, **Talus high (TH):** The distance from the talus tuberosity to the deepest point of the cochlea tibia´s

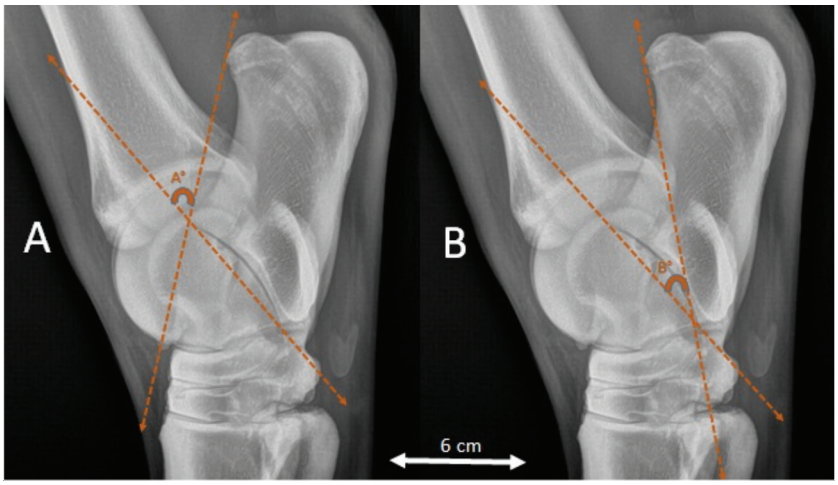

Fig 2. Angle measurements (The x-ray image is of a 3-year-old female British horse) **A: Proximal angle (PA):** The angle between the line drawn from most dorsal point of tuber calcaneus to the coracoid process and the line drawn in the direction of facies articulares talares´s length (FTL), **B: Distal angle (DA):** The angle between the line drawn from most dorsal point of tuber calcaneus to the most dorso-distal point of the calcaneus base and the line drawn in the direction of facies articulares talares´s length (FTL)

Statistical Analysis

Three different groups were created for statistical analysis. In the first group, male and female distinction for Arabian horse was examined. In the second group, male and female distinction was examined for the Thoroughbred horse. In the third group, the differences between the Arabian horse and the Thoroughbred horse were examined, ignoring the gender difference. T test was used to reveal the difference between the two breeds. Discriminant analysis was applied for each group among themselves. Functions in the discriminant analysis were written as formulas. Eigenvalue and Wilks Lambda values were taken. Correctly classified rates received. In addition, the correlations between the data were also taken and those that were statistically significant were indicated in the table. SPSS (version 22) was used for discriminant analysis, correlation test and T test. Visualizing the distribution of samples as a result of

discriminant analysis and for correctly classified values, the statistics program was obtained using Past (4.01).

Results

The mean values, standard deviations and the statistical differences for both Arabian and Thoroughbred horses are presented in *Table 1*. It was seen that only the TRL value made a statistical difference in gender discrimination for Arabian horses (P<0.05). In Thoroughbred horses, it was seen that only the MCL value was a determinant in gender discrimination (P<0.05). The results of the angle values received from this study were not an important factor in gender determination. The study showed that despite the sex differences between the two horse breeds it was observed that all measurements performed, except MCL length play a key role in determining the breed.

Distal angle (DA) measurement was also found to be a determining element in differentiating between these two breeds.

Discriminant analysis was performed for sex determination for both Arabian and Thoroughbred horses. The distribution of Arabian and Thoroughbred horses as a result of the discriminant analysis is plotted in *Fig. 3*.

The Wilks Lambda value between the sex of Arabian horses was 0.685 and the eigenvalue was 0.459.

Discriminant function score equation for stepwise analysis in sex determination of Arabian horse (Group centroids: F: 0,923, M: -0,486) is:

D: (0.413) x CCL + (1.086) x MCL + (-0.904) x CBD + (-0.122) x TCL + (1.996) x CTD + (-1.242) x FTL + (-.651) x MD + (-3.496) x TRL + (1.108) x TH + (0.026) x PA+ (0.107) x DA -1.887.

The Wilks Lambda value between the sex of Thoroughbred horses was 0.851. The eigenvalue was 0.174.

Discriminant function score equation for stepwise analysis in gender determination of Thoroughbred horses (Group centroids: F: 0,456, M: -0,377) is:

Table 1. *Female and male horses measurement values, averages and standard deviations (t test)*

Measurement (cm)	Arabian Horses			Significant	Thoroughbred Horses		
	Female N:30	Significant	Male N:57		Female N:57	Significant	Male N:69
CCL	9.97±0.45	NS	9.83±0.43	NS	10.26±0.53	NS	10.16±0.48
MCL	12.16±0.58	NS	12.02±0.58	***	12.76±0.57	*	12.52±0.61
CBD	5.34±0.23	NS	5.36±0.29	**	5.48±0.36	NS	5.48±0.37
TCL	6.53±0.29	NS	6.54±0.31	***	6.84±0.40	NS	6.80±0.38
CTD	6.53±0.43	NS	6.43±0.43	***	7.04±0.48	NS	7.02±0.46
FTL	5.61±0.39	NS	5.70±0.47	***	6.19±0.42	NS	6.08±0.52
MD	7.20±0.44	NS	7.17±0.50	***	7.87±0.45	NS	7.77±0.44
TRL	6.54±0.43	*	6.77±0.36	***	7.43±0.54	NS	7.54±0.54
TH	7.08±0.36	NS	7.12±0.35	***	7.83±0.44	NS	7.76±0.45
PA	53.85±4.84	NS	52.97±5.20	NS	52.85±4.90	NS	52.80±4.42
DA	31.20±3.19	NS	30.33±3.36	**	29.34±2.92	NS	29.02±2.80

NS: *Non significant, * P<0.05, ** P<0.01, *** P<0.001*
CCL, *cranial calcaneus length;* ***MCL****, maximum calcaneus length;* ***CBD****, calcaneal body depth;* ***TCL,*** *tuber calcaneus length;* ***CTD****, cochlea of tibia´s depth;* ***FTL,*** *facies articulares talares´s length;* ***MD,*** *metatarsus depth;* ***TRL****, talus ridge´s length;* ***TH,*** *talus high;* ***PA,*** *proximal angle;* ***DA,*** *distal angle*

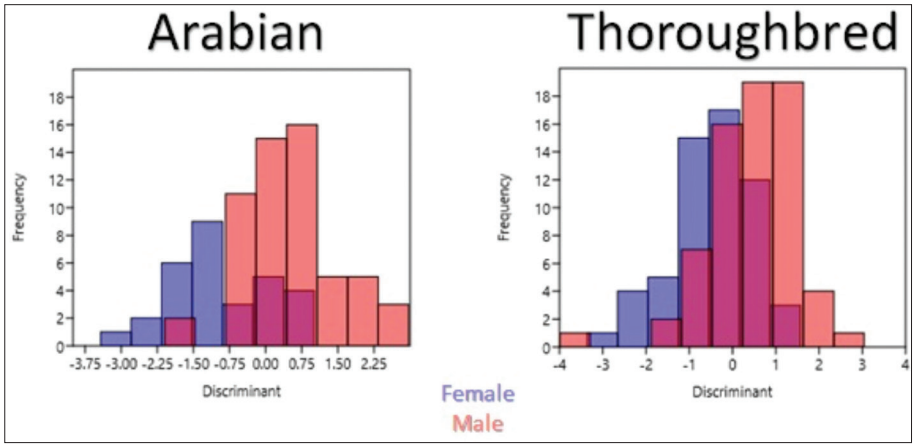

Fig 3. Distribution of female male discriminant analysis result in Arabian horses and Thoroughbred horses

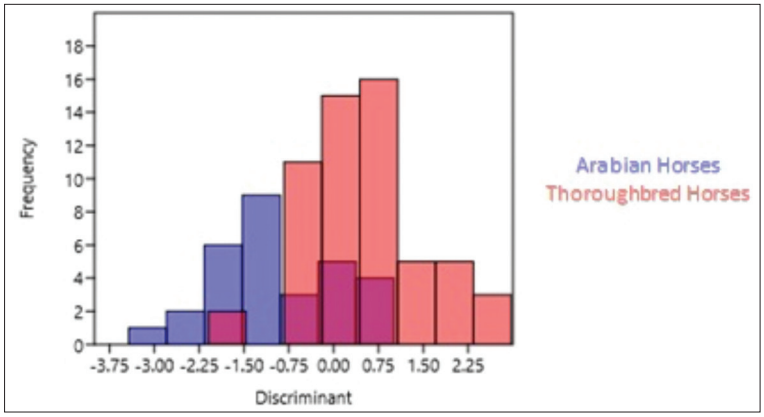

Fig 4. Distribution of discriminant analysis results between Arabian horses and Thoroughbred horses without discriminating between females and males

Table 2. *Confusion matrix. Percentage of initial classifications that were correct, shown by sex*

Breed	Sex	Female	Male	Total	Correctly Classified
Arabian	Female	21	9	30	71.26%
	Male	16	41	57	
Thoroughbred	Female	37	20	57	66.67%
	Male	22	47	79	

Percentages within rows sum to 100%

Table 3. *Confusion matrix. Percentage of initial classifications that were correct, shown by breed*

Breed	Arabian	Thoroughbred	Total	Correctly Classified
Arabian	81	6	87	88.26%
Thoroughbred	19	107	126	

Percentages within rows sum to 100%

D: (-1.499) x CCL + (1.973) x MCL + (-1.263) x CBD + (-1.88) x TCL + (0.685) x CTD + (0.561) x FTL + (0.866) x MD + (-1.544) x TRL + (0.899) x TH + (-0.036) x PA + (0.394) x DA - 21.491.

The distribution of individuals is given in *Fig. 4*, as a result of the discriminant analysis performed between the Arabian and the Thoroughbred horses regardless of gender. The Wilks Lambda was 0.395 and the eigenvalue was 1.530. Discriminant analysis results showed that the most determinant measurements were in the talus values (TRL and TH).

Discriminant function score equation for stepwise analysis between the two breeds. (Group centroids: Arabian horse: -1.482, Thoroughbred horses: 1.023) is:

D: (-0.582) x CCL + (-0.112) x MCL + (-1.854) x CBD + (-0.252) x TCL + (0.431) x CTD + (1.179) x FTL + (1.561) x MD + (1.208) x TRL + (0.402) x TH + (0.023) x PA + (-0.36) x DA – 14.543.

Using these measurements, it was observed that only 71.26% of Arabian horses were accurately classified between males and females. Whereas in Thoroughbred horses only 66.67% of them were correctly classified as males and female *(Table 2)*. The results showed that the exact differentiation of Arabian and Thoroughbred horse breeds was 88.26% regardless of the gender differences *(Table 3)*.

Correlation values between measurements results are given in *Table 4*. It was observed that age had a negative correlation with MCL, CTD, MD, TRL, TH and DA values. Among these values, the highest negative correlation value with age was seen in the TRL measurement (correlation value: -0.139). The correlation with the CBD value was positive and its value was higher than the other measurements (correlation value: 0.190). The correlation value between the two angles was positive and statistically significant. The highest correlation between length measurements was between TRL and CTD measurements (correlation value: 0.780). The correlation between the measurement values of MCL, TCL, MD and TH and the values of the angles were all negative.

Discussion

In this study, tarsal radiography of 213 horses was used and the measurement values of the tarsal region were revealed both between sex and breeds. Different measurement characteristics were seen in two breed types. Thoroughbred horses data was found to be higher

Table 4. *Correlation values between measurement values*

Parameters	CCL	MCL	CBD	TCL	CTD	FTL	MD	TRL	TH	PA	DA
Age	.160*	-.001	.190**	.036	-.014	.040	-.079	-.139*	-.099	.021	-.020
CCL		.291**	.291**	.246**	.262**	.184**	.123	.164*	.209**	.092	.070
MCL			.595**	.729**	.513**	.634**	.695**	.430**	.687**	-.284**	-.393**
CBD				.755**	.564**	.550**	.453**	.433**	.554**	.047	-.091
TCL					.575**	.564**	.636**	.507**	.685**	-.225**	-.306**
CTD						.614**	.412**	.780**	.665**	.267**	.066
FTL							.291**	.422**	.577**	.022	-.296**
MD								.513**	.736**	-.288**	-.365**
TRL									.752**	.178**	.037
TH										-.090	-.255**
PA											.798**

** Correlation is significant at the 0.05 level; ** Correlation is significant at the 0.01 level*
CCL, *cranial calcaneus length;* ***MCL,*** *maximum calcaneus length;* ***CBD,*** *calcaneal body depth;* ***TCL,*** *tuber calcaneus length;* ***CTD,*** *cochlea of tibia´s depth;* ***FTL,*** *facies articulares talares´s length;* ***MD,*** *metatarsus depth;* ***TRL,*** *talus ridge´s length;* ***TH,*** *talus high;* ***PA,*** *proximal angle*

than that of Arabian horses. Most of the differences between them were statistically significant. However, it was observed that the tarsal area measurements were not effective in sex discrimination between species. Correlation between joint measurement points was mostly positive. However, the negative correlation between age and tarsal measurement values was striking. This result may give an idea for future studies.

In this study, sex determination was examined within Thoroughbred horses and Arabian horses. While TRL measurement in Arabian horses was discriminatory for gender, it was found that only MCL measurement was determinant for Thoroughbred horses ($P<0.05$). The difference between gender for all other measurement values was statistically insignificant. In studies conducted in humans, it was stated that calcaneus length measurements in male were higher than that of females, and this difference was statistically significant [1,3]. In some measurements, females were found to be higher than males in both Thoroughbred horses and Arabian horses. Also, although the measurement of calcaneal body depth in horses does not play a decisive role for sex differentiation, however this measurement has been reported to play a determining role in terms of gender history in humans [2,4,9]. In addition, the angle values obtained from measurements in the calcaneus revealed that they were not crucial for sex determining in horses, as were the data presented in the literature [10].

The tarsal region is especially important for racing horses in terms of movement biomechanics. Tendo calcaneus communis is directly connected to the tuber calcanei of the calcaneus and plays a role in the active movement of this region. In this study, it was seen that the measurements of the tarsal region in Thoroughbred horses were higher in all of the longitudinal measurements and this difference was statistically significant. It can be said that the tarsal data should be evaluated together with the gait analysis data in order to comment on whether this difference affects active movement between two horse breeds. In another study, as a result of the gait analysis performed between these two horses, it was stated that there were also differences in the walking kinematics of the two horses, and that there were time differences between extensor and flexor muscle movements [11].

In this study, the difference between right and left was not examined, considering the possibility of a difference, only the lateromedial radiological image of the left side was used and it was examined whether there is only a sex and breed difference. There are studies that take symmetrical measurements of the right and left samples using radiographic images and examine the difference between them. In a study, distal phalanx radiological images of 10 Iranian Arabian horses were used and the difference between right and left measurements was examined. In this study, it was reported that there was no statistical difference between right and left measurements [12]. However, Sakaue [2] reported that he found a statistically significant difference between right and left measurements in his study using calcaneus measurements in humans.

There was a positive correlation between the measurements of the tarsal area in Thoroughbred horses and Arabian horses. However, the correlation between these measurements and age was negative. Especially the negative correlation between TRL measure and age was statistically significant. It was observed that TH value, which is another measurement of talus, had a negative correlation related with age. The talus bone is in the middle of the tarsal joint with respect to the calcaneus, and it transmits the animal's pelvic limb load directly to the metatarsal bone. This result can be discussed with exercise

and age. In the literature, the effects of age and exercise on the bones of horses were also examined in studies on this subject. In a study on bone in horses, changes in the microstructure of bones depending on age were mentioned [13]. The authors argued that this change was not affected by sex, but related to age. In another study conducted with British horses, it was stated that exercise and age can cause changes in the bone structure´s [6]. Cruz et al.[14] reported in his study on horses that differences in bone changes on the distal phalanx were as a result of exercise. In a study conducted on Labrador Retrievers dogs, it was found that age had an effect on the talus bone by increasing its density [15]. To make this information more comprehensive, repeated measurements can be made at different ages on the same horses, perhaps in other similar studies which may help to further clarify this idea.

In this study, radiometric measurements of the field region with lateromedial direction shooting were used. In this sense, just like the reference studies used in the article, only the lateral aspect of the calcaneus and talus, which are the main elements of the study, could be evaluated. In future studies, caudal images of calcaneus, which seems to be determinant among species, can be taken and measurements can be made about the width of the tuber calcanei. In addition, measurements of calcaneus can be taken and differences between two species can be revealed osteometrically. However, thanks to the radiographic method, which is the main material of this study, samples were taken from live animals and a large number of sample groups were reached. In this sense, we can say that radiometric measurements are more advantageous than osteometric measurements. In addition, with radiometric measurements, repeated measurements can be taken from the same horses after a certain period of time and repeated analyzes can be performed. In this way, bone development can also be recorded gradually.

In this study, it is seen that the radiological images of the tarsal region play an important role in sex and breed discrimination. It was observed that especially the calcaneus length measurements revealed a statistically significant difference, whereas the angle measurements did not make a significant difference in sex determination. As the results of this study show, radiological measurements of this clinically important region can be used as an alternative method to be used for sex and breed discrimination.

Availability of Data and Materials

The datasets during and/or analyzed during the current study available from the corresponding author on reasonable request.

Acknowledgements

We thank to Jokey Club of Turkey supports the work.

Funding Support

This research did not receive any specific grant from funding agencies in the public, commercial, or not-for profit sectors.

Conflict of Interest

Authors declares that there is no conflict of interests.

Author Contributions

Design of the study: D. Olgun Erdikmen, O. Gundemir and S. Duro. Preparation of the study and data collection: D. Olgun Erdikmen, H. Hartoka, M. O. Dayan. Article writing, data analysis and editing: D. Olgun Erdikmen, W. Pérez, O. Gundemir, C. Parkan Yaramis, G. Pazvant.

References

1. Bidmos MA, Asala SA: Discriminant function sexing of the calcaneus of the South African whites. *J Forensic Sci,* 48 (6): 1213-1218, 2003. DOI: 10.1520/JFS2003104

2. Sakaue K: Sex assessment from the talus and calcaneus of Japanese. *Bull Natl Mus Nat Sci,* Ser D, 37, 35-48, 2011.

3. Kim DI, Kim YS, Lee UY, Han SH: Sex determination from calcaneus in Korean using discriminant analysis. *Forensic Sci Int,* 228 (1-3): 177.e1-177.e7, 2013. DOI: 10.1016/j.forsciint.2013.03.012

4. Uzuner MB, Geneci F, Ocak M, Bayram P, Sancak İT, Dolgun A, Sargon MF: Sex determination from the radiographic measurements of calcaneus. *Anatomy,* 10 (3): 200-204, 2016. DOI: 10.2399/ana.16.039

5. Kadic LIM, Rodgerson DH, Newsom LE, Spirito MA: Description of a rare osteochondrosis lesion of the medial aspect of the distal intermediate ridge of the tibia in seven Thoroughbred horses (2008-2018). *Vet Radiol Ultrasound,* 61 (3): 285-290, 2020. DOI: 10.1111/vru.12843

6. Jeffcott LB, Buckingham SHW, McCarthy RN, Cleeland JC, Scotti E, McCartney RN: Non-invasive measurement of bone: A review of clinical and research applications in the horse. *Equine Vet J*, 20, 71-79, 1988. DOI: 10.1111/j.2042-3306.1988.tb04651.x

7. Gonçalves LM, Pozzobon R, dos Anjos BL, Pellegrini DC, Azevedo MS, Dau SL, Klaus R: Radiological evaluation of juvenile osteochondral conditions in Brazilian warmblood horse. *J Equine Vet Sci,* 85:102844, 2020. DOI: 10.1016/j.jevs.2019.102844

8. Dorner C, Fueyo P, Olave R: Relationship between the distal phalanx angle and radiographic changes in the navicular bone of horses: A radiological study. *Glob J Med Res,* 17 (2): 7-13, 2017.

9. Zakaria MS, Mohammed AH, Habib SR, Hanna MM, Fahiem AL: Calcaneus radiograph as a diagnostic tool for sexual dimorphism in Egyptians. *J Forensic Leg Med*, 17 (7): 378-382, 2010. DOI: 10.1016/j.jflm.2010.05.009

10. Šimunović M, Nizić D, Pervan M, Radoš M, Jelić M, Kovačević B: The physiological range of the Böhler's angle in the adult Croatian population. *Foot Ankle Surg,* 25 (2): 174-179, 2019. DOI: 10.1016/j.fas.2017.10.008

11. Gündemir O, Olğun Erdikmen D, Ateşpare ZD, Avanus K: Examining stance phases with the help of infrared optical sensors in horses. *Turk J Vet Anim Sci,* 43 (5): 636-641, 2019. DOI: 10.3906/vet-1902-43

12. Vosugh D, Nazem MN, Hooshmand AR: Radiological anatomy of distal phalanx of front foot in the pure Iranian Arabian horse. *Folia Morphol, 76* (4): 702-708, 2017. DOI: 10.5603/FM.a2017.0028

13. Fürst A, Meier D, Michel S, Schmidlin A, Held L, Laib A: Effect of age on bone mineral density and micro architecture in the radius and tibia of horses: An Xtreme computed tomographic study. *BMC Vet Res,* 4:3, 2008. DOI: 10.1186/1746-6148-4-3

14. Cruz CD, Thomason JJ, Faramarzi B, Bignell WW, Sears W, Dobson H, Konyer NB: Changes in shape of the Standardbred distal phalanx and hoof capsule in response to exercise. *Equine Comp Exerc Physiol,* 3 (4): 199-208, 2006. DOI: 10.1017/S1478061506617258

15. Dingemanse W, Müller-Gerbl M, Jonkers I, Vander Sloten J, van Bree H, Gielen I: A prospective follow up of age related changes in the subchondral bone density of the talus of healthy Labrador Retrievers. *BMC Vet Res,* 13:57, 2017. DOI: 10.1186/s12917-017-0974-y

Kafkas Universitesi Veteriner Fakultesi Dergisi
ISSN: 1300-6045 e-ISSN: 1309-2251
Journal Home-Page: http://vetdergikafkas.org

Kafkas Univ Vet Fak Derg
27 (6): 803-809, 2021
DOI: 10.9775/kvfd.2021.26373

RESEARCH ARTICLE

Bioinformatic Analysis of Differentially Expressed Genes in Porcine Intestinal Epithelial Cells Infected with Transmissible Gastroenteritis Virus

Xu-xuan ZHANG [1,a] Guo-wei LAN [2,b] Zhe WANG [1,c] Chen-hao JIANG [1,d]
Jing XI [3,e] Yao LI [1,f] Jun QIAO [3,g (*)] Yan REN [1,h (*)]

[1] First Affiliated Hospital of School of Medicine, Shihezi University, Shihezi 832000, CHINA
[2] School of Chemistry and Chemical Engineering, Shihezi University, Xinjiang, 832003, CHINA
[3] School of Animal Science and Technology, Shihezi University, Shihezi 832000, CHINA
ORCIDs: [a] 0000-0003-3359-3917; [b] 0000-0002-2956-0090; [c] 0000-0003-3704-4966; [d] 0000-0002-8033-1066; [e] 0000-0002-6361-8882
[f] 0000-0002-3819-0083; [g] 0000-0001-5210-4379; [h] 0000-0002-4034-9376

Article ID: KVFD-2021-26373 Received: 09.08.2021 Accepted: 11.11.2021 Published Online: 15.11.2021

Abstract

Transmissible Gastroenteritis Virus (TGEV) infection is one of the leading causes of diarrhea in piglets. Intestinal immune system plays an important role in maintaining the intestinal mucosa's integrity and resisting infection by pathogens. However, the relationship between the immune response induced by TGEV infection and disease progression is unclear. Using the microarray data set GSE41756 from the Gene Expression Omnibus database, we analyzed porcine small intestinal epithelial cells at 6 and 12 h of TGEV infection. Differentially expressed genes (DEGs) were detected using the 'limma' R package. Gene Ontology, Kyoto Encyclopedia of Genes and Genomes pathway enrichment, and the protein-protein interaction network analyses were performed with the detected DEGs. We found 56 DEGs (47 up-regulated and 9 down-regulated) after the intersection. Pathway enrichment analysis revealed that the DEGs were mainly associated with immune response, extracellular space, cytokine activity, and positive regulation of nuclear factor-κB import into the nucleus. This revealed the strong relationships among DEGs in the tumor necrosis factor signaling pathway, inflammatory bowel disease, and influenza A. Interleukin 6 *(IL6), IL8, IL18,* tumor necrosis factor, and toll-like receptor hub genes may play important roles during TGEV infection.

Keywords: *DEGs, Immune response, TGEV, TNF, TLR2*

Bulaşıcı Gastroenterit Virüsü İle Enfekte Domuz Bağırsak Epitel Hücrelerinde Diferansiyel Gen Ekspresyonlarının Biyoinformatik Analizi

Öz

Bulaşıcı Gastroenterit Virüs (TGEV) enfeksiyonu, domuz yavrularında ishalin önde gelen nedenlerinden birisidir. Bağırsaklardaki bağışıklık sistemi, mukozal bütünlüğün korunması ve patojenlerin neden olduğu enfeksiyonlara karşı koymada önemli bir rol oynar. Ancak, TGEV enfeksiyonunun neden olduğu bağışıklık yanıt ile hastalığın ilerlemesi arasındaki ilişki açık değildir. Gene Expression Omnibus veri tabanından GSE41756 mikroarray veri setini kullanarak, 6 ve 12 saatlik TGEV enfeksiyonunda domuz ince bağırsak epitel hücrelerini analiz ettik. Diferansiyel gen ekspresyonları (DEGs), 'limma' R paketi kullanılarak tespit edildi. Tespit edilen DEG'lerin, Gen Ontology, Kyoto Genler ve Genomlar Ansiklopedisi yolak zenginleştirme ve protein-protein etkileşim ağı ile analizleri gerçekleştirildi. Kesişim noktasından sonra 56 DEG (ekspresyonu artmış 47 gen ve ekspresyonu azalmış 9 gen) saptadık. Yolak zenginleştirme analizi, DEG'lerin esasen immun yanıt, ekstraselüler boşluk, sitokin aktivitesi ve çekirdeğe nükleer faktör-κB girişinin pozitif yönde düzenlenmesi ile ilişkili olduğunu ortaya koydu. Bu, tümör nekrozis faktör sinyal yolu, inflamatuar bağırsak hastalığı ve influenza A'daki DEG'ler arasındaki güçlü ilişkileri ortaya çıkardı. İnterlökin 6 *(IL6), IL8, IL18,* tümör nekrozis faktör ve toll-like reseptör asıl genleri, TGEV enfeksiyonu sırasında önemli roller oynayabilir.

Anahtar sözcükler: *DEGs, İmmün yanıt, TGEV, TNF, TLR2e*

INTRODUCTION

Transmissible Gastroenteritis Virus (TGEV) is a contagious porcine enteropathogenic virus belonging to the alpha-coronavirus family. TGEV infects intestinal epithelial cells, resulting in severe and frequently fatal diarrhea with mortality rates reaching 100% in piglets less than 2 weeks old [1]. However, piglets that live for more than six to eight days after infection may recover, although they may have stunted growth [2] and can spread TGEV to uninfected swine

How to cite this article?

Zhang XX, Lan GW, Wang Z, Jiang CH, Xi J, Li Y, Qiao J, Ren Y: Bioinformatic analysis of differentially expressed genes in porcine intestinal epithelial cells infected with transmissible gastroenteritis virus. *Kafkas Univ Vet Fak Derg,* 27 (6): 803-809, 2021.
DOI: 10.9775/kvfd.2021.26373

(*) Corresponding Author

Tel: +9 15809935356 (J. Qiao) +9 15309914118 (R. Yan)
E-mail: qj710625@shzu.edu.cn (J. Qiao) rycb1225@163.com (R. Yan)

for several weeks. The intestinal tract is a site of digestion and nutrient absorption and acts as a barrier for harmful pathogens and toxins [3]. TGEV infection damages the small intestines and promotes secondary infection by other pathogens; thus, damaging immune function and increasing the pathogenic bacterial load. The intestinal immune system plays an essential role in maintaining intestinal mucosal homeostasis and protecting against pathogen invasion. Chronic inflammation is the cause of many diseases [4].

Genome-wide molecular profiling reveals molecular changes in the adsorption and invasion of viral infection and is an efficient approach for identifying essential genes. We performed a genome-wide molecular profiling analysis to identify essential genes and pathways associated with TGEV infection by integrating a bioinformatic analysis based on the gene expression omnibus (GEO) datasets. The data obtained indicate that some genes may continue to participate in TGEV infection.

Material and Methods

Data Sources

The GSE41756 gene expression data [5] were obtained from the Gene Expression Omnibus database (GEO; *http://www.ncbi.nlm.nih.gov/geo)*. Expression profiling arrays were generated using the GPL3533 platform. In addition, 9 porcine cells in the database, including 3 uninfected cells, 3 cells at 6 h of infection, and 3 cells at 12 h of infection were collected for further analysis.

DEG Identification

The transcripts per million approach was used for background correction and normalization. DEGs between infected and uninfected cells were processed using packages in R Software. The screening criteria for DEGs were adjusted P-value <0.05 and log2 fold change (log2FC).

GO and KEGG Pathway Enrichment Analysis of DEGs

Gene Ontology (GO) was used to annotate genes from various ontologies. The Kyoto Encyclopedia of Genes and Genomes (KEGG) *(http://www.kegg.jp/* or *http://www.genome.jp/kegg/)* data resource was used for genes and genomes with assigned corresponding functional significances. The database for annotation visualization and integrated discovery (DAVID) *(https://david.ncifcrf.gov)* was applied for GO annotation and KEGG pathway analysis with a statistically significant P-value <0.05.

PPI Network Analyses

The protein-protein interaction (PPI) network identified functional links between proteins, using a search tool to retrieve interacting genes/proteins software (version 11.0, *http://www.string-db.org)*. A composite score of >0.4 was considered a statistically significant interaction.

Module Analysis and Selection of Hub Genes

The PPI network analysis results were loaded into Cytoscape (version 3.6.1) [6] software for visual adjustment. The hub genes were identified using the CytoHubba plug-in of the Cytoscape software. CytoHubba ranks nodes based on their qualities in the network. In this study, the top five genes ranked by the MCC (Mathew correlation coefficient) method were defined as hub genes.

Results

Identification of DEGs

We analyzed DEGs at 6 and 12 h after TGEV infection. The results showed 52 up-regulated and 12 down-regulated genes at 6 h (adj P<0.05, | log (FC) | >1) *(Fig. 1)* and 75 up-regulated and 0 down-regulated genes at 12 h (adj P<0.05, | log (FC) | >1) *(Fig. 2)*. We found 47 up-regulated and 9 down-regulated genes (adj P<0.05, | log (FC) | >1) *(Table 1, Fig. 3)* by taking the intersections. The cluster heat-map plot and volcano plot of the DEGs are shown in *Fig. 1* and *Fig. 2*, respectively.

GO and KEGG Pathway Enrichment Analysis of DEGs

GO analysis consists of biological processes (BP), cellular components (CC), and molecular function (MF) terms. The main DEG biological process changes were collected in the immune response, extracellular space, cytokine activity, and positive regulation of nuclear factor-κB (NF-κB) were imported into the nucleus. Cell component changes were predominantly observed in the plasma membrane's extracellular region and external side (P<0.05, *Table 2)*. The KEGG pathway analysis results revealed the potent relationships among DEGs in the tumor necrosis factor (TNF) signaling pathway with inflammatory bowel disease (IBD) and influenza A (P<0.05, *Table 3)*.

PPI Network Formation

The PPI network analysis aimed to provide an understanding of the biological properties of DEG. The network comprises 49 nodes and 221 edges *(Fig. 4)*. Next, Cytoscape was used to identify the densely connected regions of PPIs for DEGs and the most significant modules selected, including the interleukin 6 *(IL6),* interleukin 8 *(IL8),* interleukin 18 *(IL18),* TNF, and toll-like receptors (TLR2) as shown in *Fig. 5*.

Discussion

This study performed gene expression profiles integration analysis from cells with or without TGEV infection to identify the DEGs, related key signaling pathways, and hub genes. Data obtained at 6 and 12 h of infection were included in the analysis. Furthermore, 56 DEGs, comprising 47 up-regulated and 9 down-regulated genes, were identified

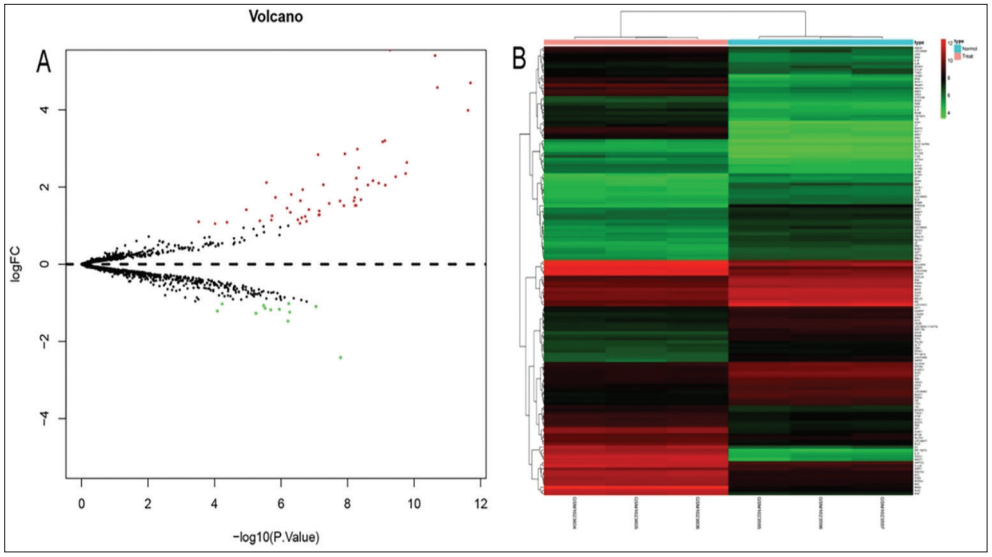

Fig 1. A. Gene expression data are presented using volcano plots. Cells were infected with TGEV for 6 h. Red points represent the up-regulated genes (n=52); green points, the down-regulated genes (n=12); and gray points, non-differentially expressed genes, **B.** Heat-map results of DEGs at 6 h

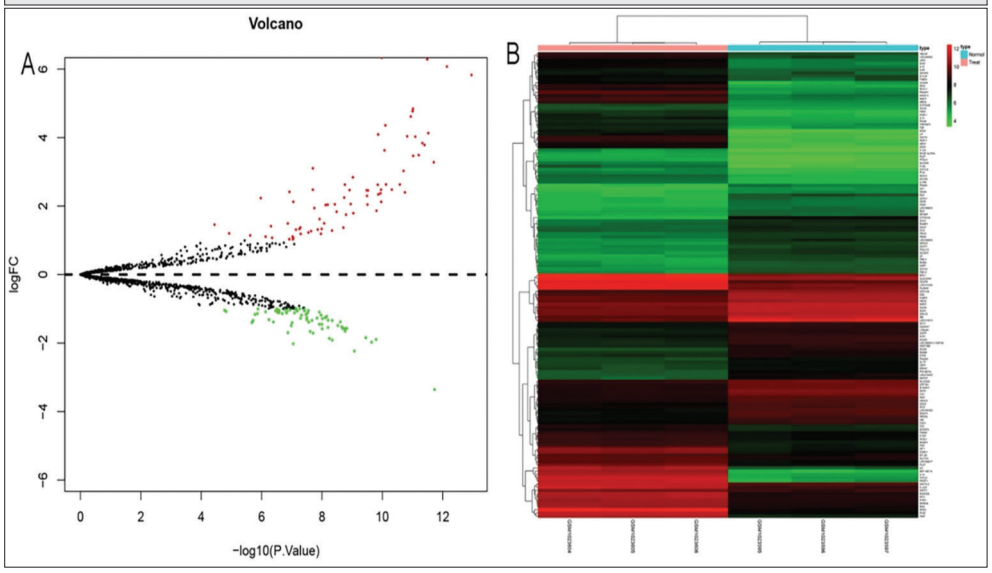

Fig 2. A. Gene expression data are presented using volcano plots. Cells were infected with TGEV for 12 h. Red points represent the up-regulated genes (n=75); green points, the down-regulated genes (n=70); and gray points, non-differentially expressed genes, **B.** Heat-map results of DEGs at 12 h

Table 1. *Screening upregulated and downregulated DEGs.expressed genes*

DEGs	Gene Symbol
Upregulated (47)	RHIV-1|PMAIP1|NFKBIA|TEC|EDN1| |YP3A46|MT-2B|IFRD1|RND3 LOC414396|MCL1|VCAM1|TNFRSF5|PLANH1|PLET|SLC5A |MMP7 IL6|OAS1|ARG1|TLR2|MCP-1|TNF|PLAT|AMCF-I|CXCL2|RANTES CEBPB|LOC396677|PIAP|IL1A|IRF1|MYC|MIP-1BETA|IL18|ACSL1 AMCF-II|IL1RN|C-JUN|PGAR|FBN1|LIF|IRG6|PLK |IL15|LOC448984|ICAM-1
Downregulated (9)	PTHR |CNN1|SLC5A1|LOC396603|UCHL1|EGF|LOC396850|UF|CYP2C33

from the GSE95368 database. The GO enrichment analysis showed that these DEGs associated with TGEV infection were mainly enriched in the immune response, extracellular space, cytokine activity, and positive regulation of NF-κB import into the nucleus. The KEGG pathway enrichment analysis found that the DEGs were mainly concentrated in the TNF signaling pathway and cytokine-cytokine receptor interaction. The *IL6*, *IL18*, *IL8*, *TLR2*, and *TNF* genes were considered hub genes for TGEV infection by the construction and module analysis of the PPI network.

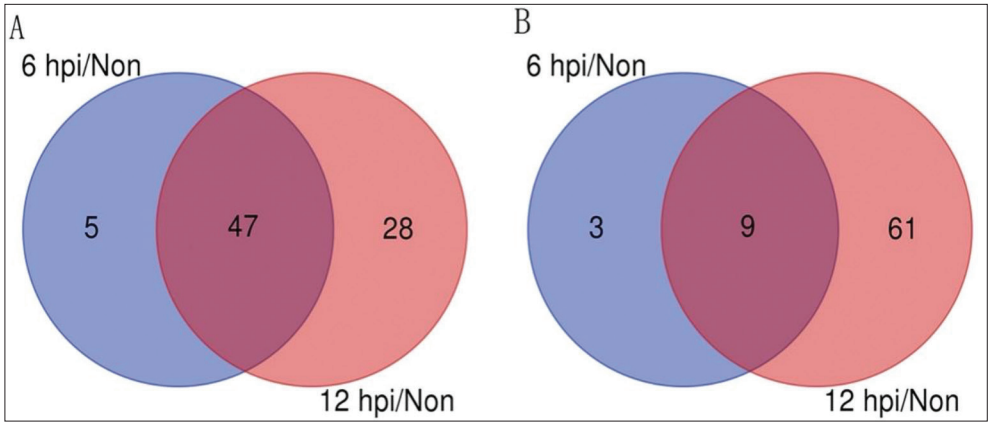

Fig 3. Differentially expressed genes

Table 2. *Go enrichment analysis of differentially expressed genes*

Term	Description	Count	P Value
GO:0006955	Immune response	8	1.95E-06
GO:0005615	Extracellular space	12	6.19E-06
GO:0005125	Cytokine activity	6	2.77E-05
GO:0042346	Positive regulation of NF-kappaB import into nucleus	3	4.98E-04
GO:0031663	Lipopolysaccharide-mediated signaling pathway	3	0.00136604
GO:0032755	Positive regulation of interleukin-6 production	3	0.001864123
GO:0006006	Glucose metabolic process	3	0.002857244
GO:0042127	Regulation of cell proliferation	4	0.00573518
GO:0045944	Positive regulation of transcription from RNA polymerase II promoter	6	0.010185653
GO:0008284	Positive regulation of cell proliferation	4	0.019487934
GO:0006954	Inflammatory response	4	0.019487934
GO:0032496	Response to lipopolysaccharide	3	0.02110949
GO:0005576	Extracellular region	5	0.028858636
GO:0009897	External side of plasma membrane	3	0.046693492

Table 3. *KEGG pathway analysis of DEGs*

Pathway	ID	Count	P Value	Genes
TNF signaling pathway	ssc04668	10	5.37E-10	LIF|VCAM1|IL6|TNF|CEBPB|EDN1| CXCL2|NFKBIA|IL15
Rheumatoid arthritis	ssc05323	7	1.66E-06	AMCF-II|IL6|TNF|IL18|TLR2|IL15| IL1A
Legionellosis	ssc05134	6	6.58E-06	IL6|TNF|IL18|CXCL2|TLR2|NFKBIA
Malaria	ssc05144	5	7.34E-05	VCAM1|IL6|TNF|IL18|TLR2
Tuberculosis	ssc05152	7	9.50E-05	IL6|TNF|CEBPB|IL18|TLR2|IL1A
Inflammatory bowel disease (IBD)	ssc05321	5	1.38E-04	IL6|TNF|IL18|TLR2|IL1A
Pertussis	ssc05133	5	2.77E-04	AMCF-II|IL6|TNF|IRF1|IL1A
African trypanosomiasis	ssc05143	4	4.29E-04	VCAM1|IL6|TNF|IL18
Influenza A	ssc05164	6	7.48E-04	IL6|TNF|IL18|NFKBIA|OAS1|IL1A
Herpes simplex infection	ssc05168	6	0.001102297	IL6|TNF|TLR2|NFKBIA|OAS1|IL15
NOD-like receptor signaling pathway	ssc04621	4	0.001261979	IL6|TNF|IL18|NFKBIA
Cytokine-cytokine receptor interaction	ssc04060	6	0.001715922	LIF|IL6|TNF|IL18|IL15|IL1A
Hepatitis C	ssc05160	5	0.002223641	TNF|IRF1| NFKBIA|OAS1|EGF
Leishmaniasis	ssc05140	4	0.002491745	TNF|TLR2|NFKBIA|IL1A
Measles	ssc05162	5	0.002559994	IL6|TLR2|NFKBIA|OAS1|IL1A

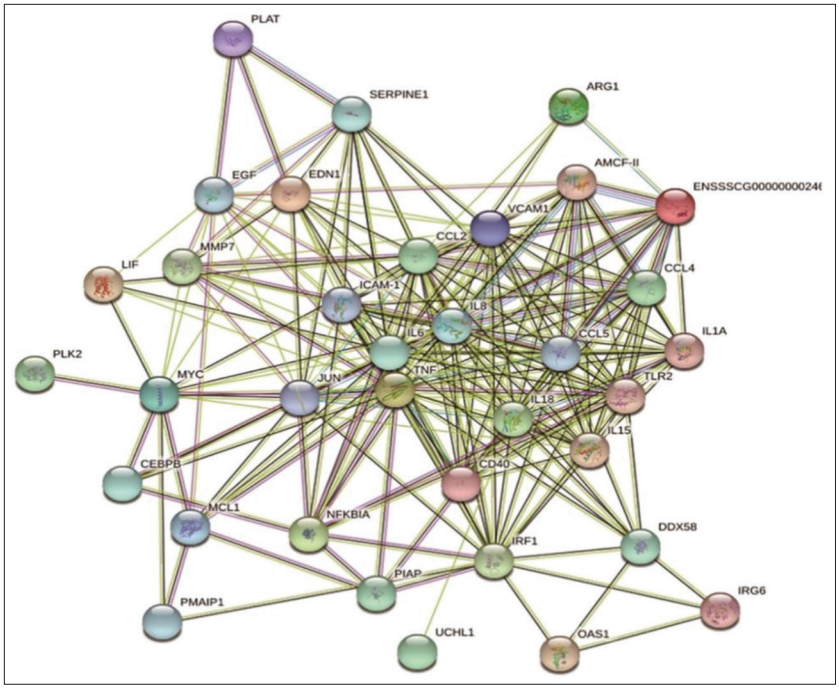

Fig 4. Results of PPI network analysis of DEGs

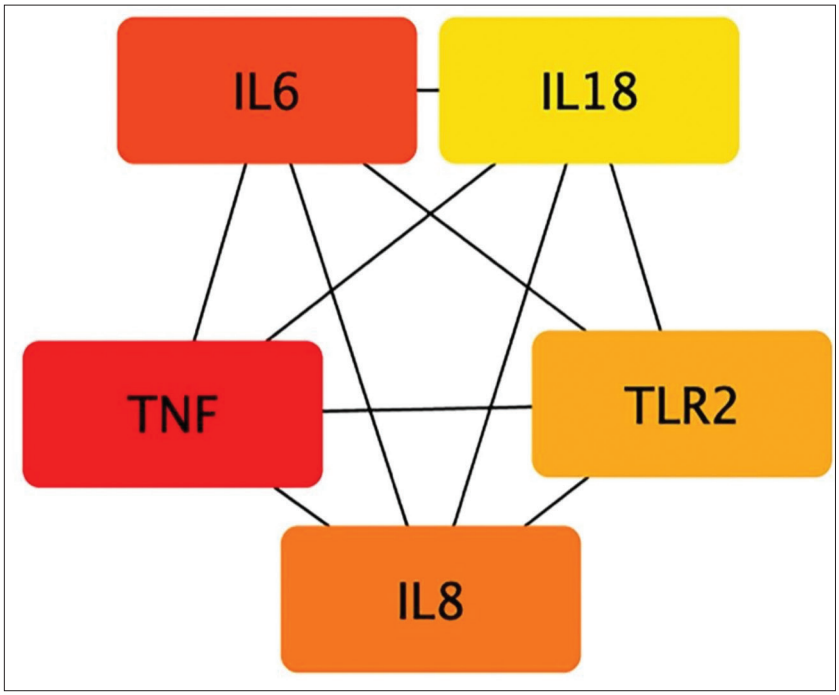

Fig 5. PPI network of the module

The invasion of viruses causes an inflammatory response, a key mediator of host responses to microbial pathogens [7]. In addition, the inflammatory factors produced promote a strong immune response. TGEV infection enhances the expression levels of *IL18, IL6, IL8,* and *TNF-α,* which are essential factors in chronic inflammation. Severe gastroenteritis is an important clinical sign of TGEV infection, and NF-κB is a key regulator of inflammation because it induces the transcription of proinflammatory genes such as *TNF-α*, *IL1β*, *IL6*, and *IL8* [8]. *IL8* is a prototypic human chemokine factor that plays an essential role in promoting cell survival and antagonizes interferon's antiviral activities [9]. Studies have shown that TGEV nucleocapsid protein up-regulates *IL8* expression in host cells by inducing endoplasmic reticulum stress and NF-κB expression [10].

Although excessive inflammation can lead to tissue damage, proinflammatory cytokines are essential for pathogen clearance. They are essential factors in chronic inflammatory responses that promote epithelial-mesenchymal transition (EMT), suggesting that persistent TGEV infection may promote EMT *in vivo* [11]. EMT is a process in which epithelial cells lose polarity and are transformed into mesenchymal cells with migration ability after cytoskeletal remodeling [12]. Inflammatory conditions induced by pathogen infections promote EMT due to the sustained activation of the NF-κB and mitogen-activated protein kinase (MAPK) modules, controlling the expression of mesenchymal markers [13]. After EMT, porcine intestinal epithelial cells were more prone to adhere to other bacteria such as enterotoxigenic *Escherichia coli* (ETEC) K88. ETEC is a common cause of enteric colibacillosis in neonatal and early-weaned pigs.

TNF-α can synergize with TGF-β and other inflammatory factors to induce EMT and control the expression of multiple other cytokines [14]. For example, TGF-β, IFN-α, and TNF-α together can induce EMT-like changes in human cancer cell lines *in vitro* [15]. In addition, in human colorectal cancer cell lines, TNF-α and TGF-β induce EMT-like changes in a NOD-like receptor family pyrin domain containing 3, Snail1 axis-dependent manner, or via an increase in expression of claudin-1 [16]. In the latter case, claudin-1 is delocalized from the membrane and activates the steroid receptor co-activator and ERK1/2 MAP kinase pathways.

The TLR family transfers extracellular antigen recognition information to intracellular antigens by recognizing their respective pathogen-related molecular patterns to initiate immune responses and induces the expression of intracellular immune-related factors [17]. TLR2 plays a role in acute and chronic infections caused by a variety of microorganisms. Studies have shown that TLR2 and TLR4 are less expressed in intestinal epithelial cells in healthy intestines [18]. However, as inflammation progresses, the expression of TLR2 and TLR4 increases, worsening the inflammation. The small intestine of pigs expresses different TLRs such as TLR1, TLR2, TLR3, TLR4, TLR6, TLR8, TLR9, and TLR10 [19]. TLR2 and TLR4 recognize viral proteins. Various TLRs exhibit different expression patterns. TLR2 is expressed abundantly in peripheral blood leukocytes and mediates host immune responses to Gram-positive bacteria and yeast via NF-κB stimulation [20]. TLR2 is expressed mainly in the lamina propria mononuclear cells and intestinal epithelial cells at low levels in normal intestines.

This study identified essential genes and related pathways by analyzing TGEV-infected porcine small intestine epithelial cells. However, the conclusions drawn in this study need to be verified in clinical trials. In addition, there is a need to research new methods on the underlying mechanism of TGEV infection from the perspective of inflammatory changes. Provide research direction and basis for further research on diarrhea caused by TGEV infection.

Availability of Data and Materials

The datasets during and/or analyzed during the current study available from the corresponding author on reasonable request.

Acknowledgments

The authors wish to thank Professor Jun Qiao (School of Animal Science and Technology, Shihezi University) for his careful modification of the manuscript. The authors would also like to thank Associate Professor Yan Ren (First Affiliated Hospital of School of Medicine, Shihezi University) for his serious guidance, for providing the facilities to carry out the experiments.

Funding Information

Funding (This work was supported by grands from the National Natural Science Foundation of China (Grant No: 81760386).

Ethics Approval

Not applicable.

Competing Interests

This manuscript has not been submitted for publication elsewhere and has been approved by all co-authors. The authors declare no conflict of interest.

Authors' Contributions

ZXX analyzed the samples and statistical data and wrote the manuscript. LGW and WZ analyzed and discussed the data. JCH and XJ revised the manuscript. QJ and RY are the corresponding authors, who designed the study and supervised the entire program. All authors have read and approved the final draft of the manuscript.

References

1. Pritchard GC, Paton DJ, Wibberley G, Ibata G: Transmissible gastroenteritis and porcine epidemic diarrhoea in Britain. *Vet Rec,* 144 (22): 616-618, 1999. DOI: 10.1136/vr.144.22.616

2. Weingartl HM, Derbyshire JB: Binding of porcine transmissible gastroenteritis virus by enterocytes from newborn and weaned piglets. *Vet Microbiol,* 35 (1-2): 23-32, 1993. DOI: 10.1016/0378-1135(93)90113-I

3. Peck BCE, Shanahan MT, Singh AP, Sethupathy P: Gut microbial influences on the mammalian intestinal stem cell niche. *Stem Cells Int,* 2017:5604727, 2017. DOI: 10.1155/2017/5604727

4. Xia L, Dai L, Yu Q, Yang Q: Persistent transmissible gastroenteritis virus infection enhances enterotoxigenic *Escherichia coli* K88 adhesion by promoting epithelial-mesenchymal transition in intestinal epithelial cells. *J Virol,* 91 (21): e01256-17, 2017 DOI: 10.1128/JVI.01256-17

5. Cruz JLG, Becares M, Sola I, Oliveros JC, Enjuanes L, Zúñiga S: Alphacoronavirus protein 7 modulates host innate immune response. *J Virol,* 87 (17): 9754-9767, 2013. DOI: 10.1128/JVI.01032-13

6. Cui LJ, Bai T, Zhi LP, Liu ZH, Liu T, Xue H, Yang HH, Yang XH, Zhang M, Niu YR, Liu YF, Zhang Y: Analysis of long noncoding RNA-associated

competing endogenous RNA network in glucagon-like peptide-1 receptor agonist-mediated protection in β cells. *World J Diabetes,* 11 (9): 374-390, 2020. DOI: 10.4239/wjd.v11.i9.374

7. Qian S, Gao Z, Cao R, Yang K, Cui Y, Li S, Meng X, He Q, Li Z: Transmissible gastroenteritis virus infection up-regulates FcRn expression via nucleocapsid protein and secretion of TGF-β in porcine intestinal epithelial cells. *Front Microbiol,* 10:3085, 2020. DOI: 10.3389/fmicb.2019.03085

8. Underdahl NR, Mebus CA, Torres-Medina A: Recovery of transmissible gastroenteritis virus from chronically infected experimental pigs. *Am J Vet Res*, 36 (10): 1473-1476, 1975.

9. Jung C, Hugot JP, Barreau F: Peyer's patches: The immune sensors of the intestine. *Int J Inflam,* 2010:823710, 2010. DOI: 10.4061/2010/823710

10. Sanchez CM, Pascual-Iglesias A, Sola I, Zuñiga S, Enjuanes L: Minimum determinants of transmissible gastroenteritis virus enteric tropism are located in the n-terminus of spike protein. *Pathogens,* 9 (1):2, 2019. DOI: 10.3390/pathogens9010002

11.Bekiaris V, Persson EK, Agace WW: Intestinal dendritic cells in the regulation of mucosal immunity. *Immunol Rev,* 260 (1): 86-101, 2014. DOI: 10.1111/imr.12194

12. Hu M, Guo W, Liao Y, Xu D, Sun B, Song H, Wang T, Kuang Y, Jing B, Li K, Ling J, Yao F, Deng J: Dysregulated ENPP1 increases the malignancy of human lung cancer by inducing epithelial-mesenchymal transition phenotypes and stem cell features. *Am J Cancer Res,* 9 (1): 134-144, 2019.

13. Garidou L, Heydari S, Gossa S, McGavern DB: Therapeutic blockade of transforming growth factor beta fails to promote clearance of a persistent viral infection. *J Virol,* 86 (13): 7060-7071, 2012. DOI: 10.1128/JVI.00164-12

14. Huss DJ, Winger RC, Peng H, Yang Y, Racke MK, Lovett-Racke AE: TGF-beta enhances effector Th1 cell activation but promotes self-regulation via IL-10. *J Immunol,* 184 (10): 5628-5636, 2010. DOI: 10.4049/jimmunol.1000288

15. Pang MF, Georgoudaki AM, Lambut L, Johansson J, Tabor V, Hagikura K, Jin Y, Jansson M, Alexander JS, Nelson CM, Jakobsson L, Betsholtz C, Sund M, Karlsson MC, Fuxe J: TGF-β1-induced EMT promotes targeted migration of breast cancer cells through the lymphatic system by the activation of CCR7/CCL21-mediated chemotaxis. *Oncogene,* 35 (6): 748-760, 2016. DOI: 10.1038/onc.2015.133

16. Ricciardi M, Zanotto M, Malpeli G, Bassi G, Perbellini O, Chilosi M, Bifari F, Krampera M: Epithelial-to-mesenchymal transition (EMT) induced by inflammatory priming elicits mesenchymal stromal cell-like immune-modulatory properties in cancer cells. *Br J Cancer,* 112 (6) :1067-1075, 2015. DOI: 10.1038/bjc.2015.29

17. Park GB, Chung YH, Kim D: Induction of galectin-1 by TLR-dependent PI3K activation enhances epithelial-mesenchymal transition of metastatic ovarian cancer cells. *Oncol Rep,* 37 (5): 3137-3145, 2017. DOI: 10.3892/or.2017.5533

18. Kim J, Durai P, Jeon D, Jung ID, Lee SJ, Park YM, Kim Y: Phloretin as a potent natural TLR2/1 inhibitor suppresses TLR2-induced inflammation. *Nutrients,* 10 (7): 868, 2018. DOI: 10.3390/nu10070868

19. Pasternak JA, Aiyer VIA, Hamonic G, Beaulieu AD, Columbus DA, Wilson HL: Molecular and physiological effects on the small intestine of weaner pigs following feeding with deoxynivalenol-contaminated feed. *Toxins (Basel),* 10 (1): 40, 2018. DOI: 10.3390/toxins10010040

20. Ma SQ, Wei HL, Zhang X: TLR2 regulates allergic airway inflammation through NF-κB and MAPK signaling pathways in asthmatic mice. *Eur Rev Med Pharmacol Sci,* 22 (10): 3138-3146, 2018. DOI: 10.26355/eurrev_201805_15073

Kafkas Universitesi Veteriner Fakultesi Dergisi
ISSN: 1300-6045 e-ISSN: 1309-2251
Journal Home-Page: http://vetdergikafkas.org

Kafkas Univ Vet Fak Derg
27 (6): 811-814, 2021
DOI: 10.9775/kvfd.2021.26330

CASE REPORT

Subcutaneous Cavernous Cervicofacial Lymphangioma and It's Surgical Treatment in a Calf

Yesari ERÖKSÜZ [1,a (*)] Emine ÜNSALDI [2,b] Murat TANRISEVER [2,c]
Canan AKDENİZ İNCİLİ [1,d] Hatice ERÖKSÜZ [1,e]

[1] Department of Pathology, Faculty of Veterinary Medicine, Firat University, TR-23119 Elazig - TURKEY
[2] Department of Surgery, Faculty of Veterinary Medicine, Firat University, TR-23119 Elazig - TURKEY
ORCIDs: [a] 0000-0001-5962-8810; [b] 0000-0003-1320-0709; [c] 0000-0003-3815-8543; [d] 0000-0003-1893-7531; [e] 0000-0002-8407-5792

Article ID: KVFD-2021-26330 Received: 26.07.2021 Accepted: 04.11.2021 Published Online: 04.11.2021

Abstract

A 20-day-old, Simmental male calf showed a subcutan mass locating left side of chin, buccal and neck regions. The mass covering the 70% of left side of the face consisted of cystic structures under the skin. It was surgically excised and no recurrence occurred three months after the excision. The cut surfaces of mass were measured by 20×15×8 cm in size. Histologically, the mass was diagnosed as cavernous lymphangioma which composed of thin-walled cystically dilated spaces which were lined with one or rarely more layers of flat endothelial cells. Mitotic figures were not present. The channels did not contain red blood cells in contrast to, endothelial cells lining adjacent blood vessels. The endothelial cells of cystic dilated spaces gave positive cytoplasmic immunoreaction forpodoplanin. In conclusion, this report presents clinical, pathological, immunohistochemical features and surgical treatment of cervicofacial lymphangioma in a calf.

Keywords: *Bovine, Calf, Lymphangioma, Pathology, Immunohistochemistry, Surgical treatment*

Bir Buzağıda Subkutan Kavernöz Servikofasiyal Lenfangiom ve Cerrahi Tedavisi

Öz

Yirmi günlük Simental erkek bir buzağının çene, yanak ve boyun bölgesinin sol tarafında düzensiz şekilli bir kitle mevcut olup, yüzün %70'ini kaplayan kitle, cilt altında kistik yapılardan oluşuyordu. Cerrahi olarak eksize edilen kitlenin postoperatif olarak üç ay sonrasında nüks etmediği saptandı. Kitlenin kesit yüzeeri 20×15×8 cm boyutlarında ölçüldü. Histolojik olarak kitleye bir veya nadiren daha fazla düz endotelyal hücre tabakasıyla döşeli olduğu, ince duvarlı, kistik genişlemiş boşluklardan oluştuğu saptandı ve kavernöz lenfangiom tanısı konuldu. Mitotik figürler mevcut değildi. Kanallar, bitişik kan damarlarını kaplayan endotel hücrelerinin aksine eritrositleri içermiyordu. Kistik boşlukları döşeyen endotel hücreleri podoplaninle pozitif sitoplazmik immünoreaksiyon gösterdi. Sonuç olarak, bu raporda bir buzağıda servikofasiyal lenfangiomun klinik, patolojik, immünohistokimyasal özellikleri ve cerrahi tedavisi sunulmaktadır.

Anahtar sözcükler: *Sığır, Buzağı, Lenfangjom, Patoloji, İmmünohistokimya, Cerrahi tedavi*

INTRODUCTION

Lymphangiomas are rare benign congenital cystic lesions originating from the lymphatics. In human pathology, it is enigmatic whether these cysts are hamartomas or tumors of lymphatic system [1]. However, World Health Organization favors this lesion in animals as a congenital malformation (hamartoma) which appears most commonly in newborn animals [2]. Few authors stressed that controversy of this dilemma is impractical because of the benign nature of the lesion [1]. Four theories are supposed to elucidate the origin of lymphangioma. The first one suggested the failure of the connection between lymphatic system-venous system, the second theory directed attention to abnormal budding from the vein to form lymphatics, the third one is the lymphatic obstructions caused by trauma, infections, and chronic inflammations [1], the last theory is that lymphangiomas originate from single lymphatic

How to cite this article?

Eröksüz Y, Ünsaldı E, Tanrısever M, Akdeniz İncili C, Eröksüz H: Subcutaneous cavernous cervicofacial lymphangioma and it's surgical treatment in a calf. *Kafkas Univ Vet Fak Derg,* 27 (6): 811-814, 2021.
DOI: 10.9775/kvfd.2021.26330

(*) Corresponding Author

Tel: +90 424 237 0000-4045 Fax: +90 424 238 8173
E-mail: yeroksuz@firat.edu.tr (Y. Eröksüz)

with a neoplastic proliferative behavior [3]. Based on the depth and the size of these abnormal lymph vessels, the lymphangiomas are classified into three subtypes including microcystic (capillary lymphangiomas), macrocystic (cavernous lymphangiomas) and cystic hygromas [1]. The cavernous or macrocystic form occurs on surfaces of the body where the lesion can expand freely such as the areas containing loose connective tissue and the anatomical areas where do not pressure on the cyst [4].

Incidence rate of lymphangioma in man is 1.2-2.8 per 100.000, and more than 50% and 90% are diagnosed at birth and 2-year-old children, respectively [4]. However, in animal species, this malformation is substantially less evaluated with reference to incidence, morphological features and treatment [5-9].

The aim of this report is to emphasize the infrequency of lymphangioma in cattle and to characterize the clinical, pathological and immunohistochemical findings in subcutaneous lymphangioma in head and neck in a calf.

Case History

A 10-day-old Simmental male calf was referred to our clinic with an irregular swelling beneath the skin of left chin, buccal and neck regions *(Fig.1-A)*. According to the history, the mass was present at birth, however it increased in size gradually over the past 20 days and caused the distortion. The main clinical signs were difficulty in breathing and sucking due to the mass lesion. Clinical examination did not show any abnormality in the organ system. Covering the face of 70% of the left side of, the mass consisted of vesicular structures under the skin *(Fig. 1-B)*. It was spongy like in appearance and elevated in 15 cm with no peduncle. The cut surfaces had lobular structure measured 20×15×8 cm in size. The owner of the calf was informed about the surgical procedures to be performed and an informed consent letter was signed by the owner.

To excise totally the mass, the calf was sedated by intramuscular solution of xylazine hydrochloride (Rompun, Bayer,

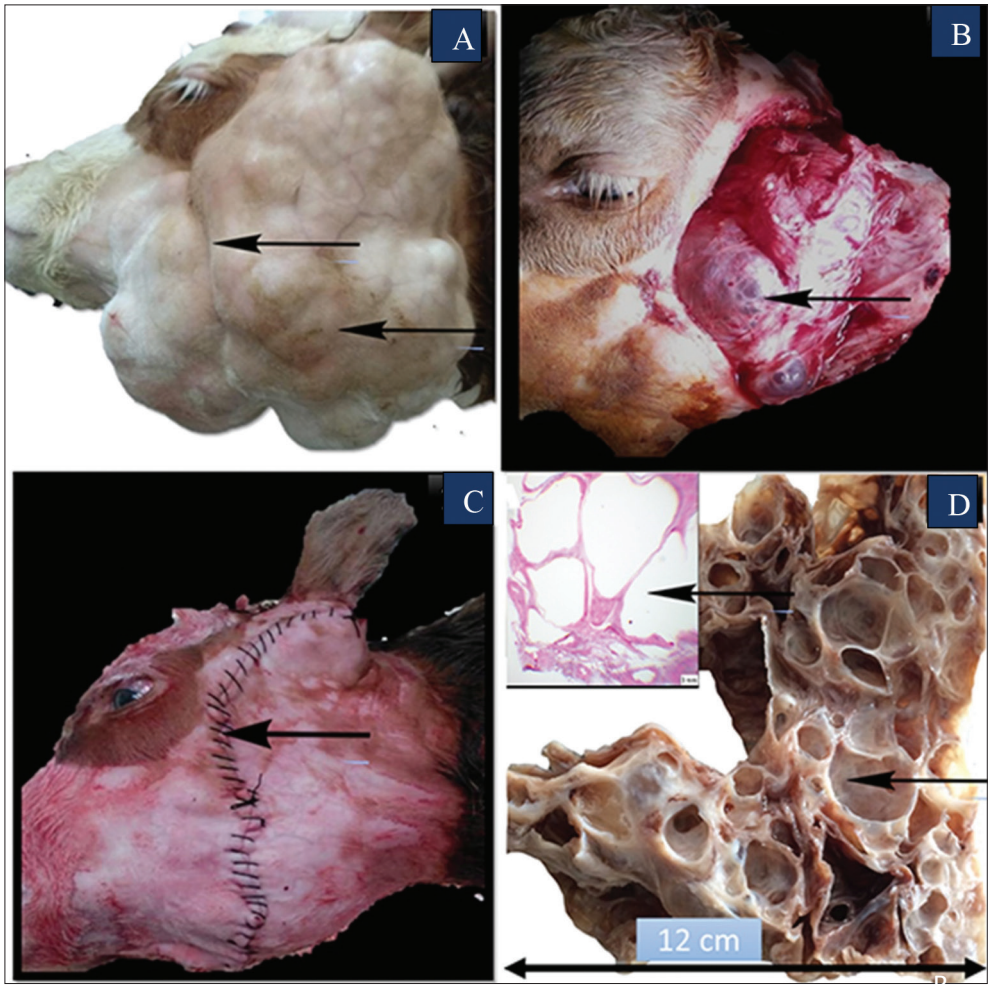

Fig 1. A: Grossly, the limits of tumor started under the ear in the left facial region and extended downwards from the edge of the mandible and extended back to the neck area covering approximately 70% of the left face, the tumor contained blisters *(arrows)* on the outer surface, **B:** Intraoperative gross appearance of tumor containing vesicular cystic spaces *(arrow)*, **C:** Postoperatively, the calf with the surgical sutures in operation line *(arrow)*, **D:** Subgross (inset) and gross appearance of empty cystic spaces *(arrows)* thin interstitial tissue

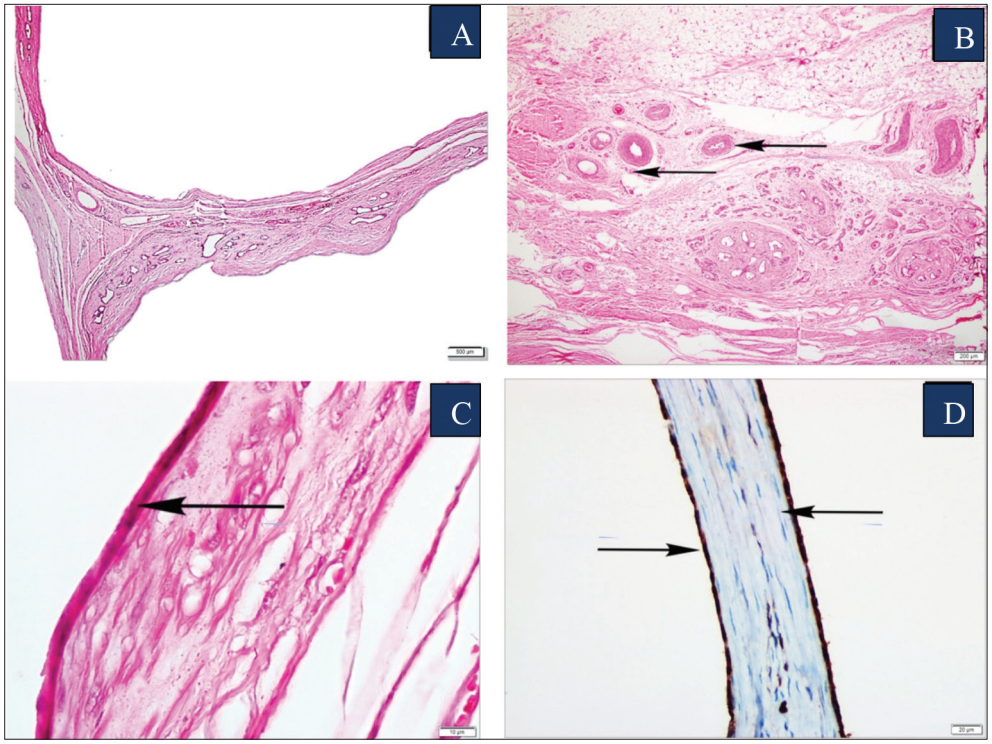

Fig 2. A: Histologically, the mass composed of dilated empty lymphatic spaces, (H&E), **B:** Stromal tissue containing vascular structures, fibrous connective tissue and subcutaneous fat tissue, (H&E), **C:** Single layer of flat endothelial cells lined the lymphatic channels *(arrow),* (H&E), **D:** Positive staining of endothelial cells with podoplanin *(arrows)*

Turkey) in the dose of 0.1 mg/kg and operated under local anesthesia with lidocaine HCl (Vilcain, Vilsan, Turkey). Under aseptic conditions, it was exposed through medial incision and totally extirpated by passing the skin and subcutaneous connective tissue *(Fig. 1-B)*. After the total extirpation, the skin was closed with simple sutures *(Fig. 1-C)*. Although the mass was not encapsulated and attached the underlying tissue, special attention was taken to completely clean the mass from the subcutaneous tissues and not to leave any residual tissue mass behind. No involvement in trachea and esophagus was present.

Postoperatively, intramuscular procaine penicillin G + dihydrostreptomycin (Sanovel, Turkey) was administered in the dose of 3 mL/100 kg/day for 7 days and sub-cutaneous analgesic/anti-inflammatory meloxicam (Meloxicam, Bavet, Turkey) in the dose of 0.2 mg/kg/day. The operation line was cleaned with antiseptic solution (0.1% lugol solution) for 1 week. In phone interviews with the owner, no local recurrence was observed within 3 months postoperatively.

Gross Findings

Macroscopically; the mass composed of multiple cystic-cavernous spaces measuring 1 to 5 cm *(Fig. 1-D)*. These vesicles contain serous fluid and look like frog eggs.

Histopathological and Immunohistochemical Studies

Tissue samples were fixed in a 10% solution of phosphate-buffered formalin before being routinely processed and stained with hematoxylin and eosin (H&E) for light microscopic examination. Selected sections were stained with Masson's trichrome stain and immuno-histochemical stain for podoplanin, desmin and smooth muscle actin. Immunohistochemical staining was performed using Ventana NexES system.

The mass was sharply circumscribed, but not encapsulated. It composed of thin-walled cystically dilated spaces *(Fig. 2-A)*. They were lined with one or rarely more layers of flat endothelial cells which were elongated or flat in appearance. Their cytoplasms contained elongate to irregular hyperchromatic nuclei and had scant, pale basophilic cytoplasm. The cell borders were indistinct showing minimal anisocytosis and anisokaryosis. Mitotic figures were not present. Moderate number of lymphocytes and plasma cells often form small discrete aggregates around blood vessels. Scant interstitial tissue contained blood vessels, connective tissue, muscular arteries and focal lymphocytic infiltrates *(Fig. 2-B)*. The endothelial cells of cystic spaces were elongated or flat in appearance *(Fig. 2-C)*, and they gave positive cytoplasmic immunoreaction for podoplanin *(Fig. 2-D)*. The channels did not contain red blood cells in contrast to endothelial cells lining adjacent blood vessels.

Discussion

This report highlights the clinical, pathological and immuno-

histochemical findings of cervicofacial lymphangioma in a calf. This lesion may occur anywhere on the skin, subcutaneous tissue or mucous membranes [1]. Cervicofacial lymphangioma is most commonly reported in children (70% to 80%). At this anatomic site; primordial lymphatics or also known as the lymph sacs are formed embryologically [1,4]. Therefore, the development of lymphangiomas is closely related to the genesis of lymph vessels [1].

Differential list for lymphangiomas includes lymphangiomatosis, lymphangiosarcoma, branchial cleft cyst, thyroglossal duct cyst, tumors of salivary gland, hematoma, carotid body tumors, actinobacillosis, actinomycosis, soft tissue sarcomas and thyroid masses [1,5].

A number of treatment alternative methods in humans include surgical excision, sclerotherapy, electrocoagulation, liquid nitrogen therapy and carbon dioxide laser therapy. The recurrence of lymphangioma in man is at the rate of 10-15% unless completely excised surgically [10]. As the large volume of the mass is considered, the methods other than the surgical option was not feasible in the present case. In human medicine, various substances, such as sodium morrhuate, dextrose, tetracycline, doxycycline, ethanol, bleomycin, ethibloc and OK-432 were used as sclerotherapeutic agents. Apart from OK-432, the other agents cause perilesional fibrosis and complicate surgical excision. Doxycycline can cause neural damage and, OK-432 may be associated with sepsis, shock, myalgia, and bleomycin might be cause of pulmonary fibrosis. Ethanol is an effective sclerosant, however might cause a series of complications including the pain and nerve injury [4]. Although the operation was problematical in regard to large volume and anatomical location, the calf was delivered to the owner without complication.

In conclusion, this report presents clinical, pathological, immunohistohemical features and surgical treatment of cervicofacial lymphangioma in a calf. Lymphangioma might also be added to the differential diagnosis list for cystic lesions in the head and neck region in cattle.

Availability of Data and Materials

The datasets during and/or analyzed during the current study available from the corresponding author on reasonable request.

Funding Support

None

Competing Interests

Authors declared that there is no conflict of interest in this study

Authors' Contributions

Conceptualization, Y.E. and H.E.; methodology, E.Ü., M.T., and C.A.İ.; writing-original draft preparation, Y.E., H.E., and C.A.İ.; writing, review and editing, Y.E. and H.E.

References

1. Wiegand S, Eivazi B, Barth PJ, Rautenfeld DB, Folz BJ, Mandic R, Werner JA: Pathogenesis of lymphangiomas. *Virchows Arch*, 453, 1-8, 2008. DOI: 10.1007/s00428-008-0611-z

2. Hendrick MJ, Mahaffery EA, Moore FM, Vos JH, Walder EJ: Histological Classification of Mesenchymal Tumors of Skin and Soft Tissues of Domestic Animals. 2nd ed., 22-25, Washington D.C. Armed Forces Institute of Pathology, American Registry of Pathology, 1998.

3. Colangeli W, Facchini V, Kapitonov A, Zappalà M, Bozza F, Becelli R: Cystic lymphangioma in adult: A case report and a review of the literature. *J Surg Case Rep,* 7, 179, 2020. DOI: 10.1093/jscr/rjaa179

4. Zhou Q, Zheng JW, Mai HM, Luo QF, Fan XD, Su LX, Wang YA, Qin ZP: Treatment guidelines of lymphatic malformations of the head and neck. *Oral Oncol*, 47 (12): 1105-1109, 2011. DOI: 10.1016/j.oraloncology.2011.08.001

5. Ginn PE, Mansell JEKL, Rakich PM: Skin and appendages. **In**, Maxie MG (Ed): Jubb, Kennedy and Palmers Pathology of Domestic Animals. 5th ed., 768, Elsevier, Philadelphia, PA, 2007.

6. Lawler DF, Evans RH: Multiple hepatic cavernous lymphangioma in an aged male cat. *J Comp Pathol*, 109 (1): 83-87, 1993. DOI: 10.1016/s0021-9975(08)80242-3

7. Driessen F, Cushing T, Baines SJ: Retroperitoneal lymphatic malformation in a dog. *Acta Vet Scand*, 62:8, 2020. DOI: 10.1186/s13028-020-0506-9

8. Espinosa J, Ferreras MC, García D, Vallejo R, Pérez V: Case report: Multiple cavernous pericardial lymphangioma (pericardial lymphangiomatosis) in a captive peregrine falcon *(Falco peregrinus brookei). Front Vet Sci*, 8:662157, 2021. DOI: 10.3389/fvets.2021.662157

9. Junginger J, Rötting A, Staszyk C, Kramer K, Hewicker-Trautwein M: Identification of equine cutaneous lymphangioma by application of a lymphatic endothelial cell marker. *J Comp Pathol*, 143 (1): 57-60, 2010. DOI: 10.1016/j.jcpa.2009.11.005

10. Fliegelman LJ, Friedland D, Brandwein M, Rothschild M: Lymphatic malformation: Predictive factors for recurrence. *Otolaryngol Head Neck Surg*, 123, 706-710, 2000. DOI: 10.1067/mhn.2000.110963

AUTHOR INDEX - 2021

INSTRUCTION FOR AUTHORS

1- Kafkas Universitesi Veteriner Fakultesi Dergisi (abbreviated title: Kafkas Univ Vet Fak Derg), published bi-monthly (ISSN: 1300-6045 and e-ISSN: 1309-2251). We follow a double-blind peer-review process, and therefore the authors should remove their name and any acknowledgment from the manuscript before submission. Author names, affiliations, present/permanent address etc. should be given on the title page only.

The journal publishes full-length research papers, short communications, preliminary scientific reports, case reports, observations, letters to the editor, and reviews. The scope of the journal includes all aspects of veterinary medicine and animal science.

Kafkas Universitesi Veteriner Fakultesi Dergisi is an Open Access journal, which means that all content is freely available without charge to the user or his/her institution. Users are allowed to read, download, copy, distribute, print, search, or link to the full texts of the articles, or use them for any other lawful purpose, without asking prior permission from the publisher or the author. This is in accordance with the BOAI definition of Open Access.

The official language of our journal is **English**. Additionally, all the manuscripts must also have Turkish title, keywords, and abstract (translation will be provided by our journal office for foreign authors).

2- The manuscripts submitted for publication should be prepared in the format of Times New Roman style, font size 12, A4 paper size, 1.5 line spacing, and 2.5 cm margins of all edges. The legend or caption of all illustrations such as figure and table and their appropriate position should be indicated in the text. Refer to tables and figures in the main text by their numbers. Also figure legends explanations should be given at the end of the text.

The figures should be at least 300 dpi resolution.

The manuscript and supplementary files (figure etc.) should be submitted by using online manuscript submission system at the address of *http://vetdergi.kafkas.edu.tr/*

During the submission process, the authors should upload the figures of the manuscript to the online manuscript submission system. If the manuscript is accepted for publication, the **Copyright Transfer Agreement Form** signed by all the authors should be sent to the editorial office.

3- The authors should indicate the name of the institute approves the necessary ethical commission report and the serial number of the approval in the material and methods section. If necessary, the editorial board may also request the official document of the ethical commission report. In case reports, a sentence stating that "informed consent" was received from the owner should be added to the main document. If an ethical problem is detected (not reporting project information, lack of ethical committee information, conflict of interest, etc.), the editorial board may reject the manuscript at any stage of the evaluation process.

4- Authors should know and take into account the issues listed in the "**Ethical Principles and Publication Policy**" section regarding scientific research and authors.

5- Types of Manuscripts

Original (full-length) manuscripts are original and proper scientific papers based on sufficient scientific investigations, observations and experiments.

Manuscripts consist of the title, abstract and keywords, introduction, material and methods, results, discussion, and references and it should not exceed 12 pages including text. The number of references should not exceed 50. The page limit does not include tables and illustrations. Abstract should contain 200±20 words.

Short communication manuscripts contain recent information and findings in the related topics; however, they are written with insufficient length to be a full-length original article. They should be prepared in the format of full-length original article but the abstract should not exceed 100 words, the reference numbers should not exceed 15 and the length of the text should be no longer than 6 pages in total. The page limit does not include tables and illustrations. Additionally, they should not contain more than 4 figures or tables.

Preliminary scientific reports are a short description of partially completed original research findings at an interpretable level. These should be prepared in the format of full-length original articles. The length of the text should be no longer than 4 pages in total.

Case reports describe rare significant findings encountered in the application, clinic, and laboratory of related fields. The title and abstract of these articles should be written in the format of full-length original articles (but

the abstract should not exceed 100 words) and the remaining sections should be followed by the Introduction, Case History, Discussion and References. The reference numbers should not exceed 15 and the length of the text should be no longer than 4 pages in total. The page limit does not include tables and illustrations.

Letters to the editor are short and picture-documented presentations of subjects with scientific or practical benefits or interesting cases. The length of the text should be no longer than 3 pages in total. The page limit includes tables and illustrations.

Reviews are original manuscripts that gather the literature on the current and significant subject along with the commentary and findings of the author on a particular subject (It is essential that the author/s have international scientific publications on this subject). The title and summary of this manuscript should be prepared as described for the full-length original articles and the remaining sections should be followed by introduction, text (with appropriate titles), conclusion, and references. The length of the text should be no longer than 15 pages in total.

6- The necessary descriptive information (thesis, projects, financial supports, etc.) scripted as an italic font style should be explained below the manuscript title after placing a superscript mark at the end of the title.

7- At least 30% of the references of any submitted manuscript (for all article categories) should include references published in the last five years.

References should be listed with numerical order as they appear in the text and the reference number should be indicated inside the parentheses at the cited text place. References should have the order of surnames and initial letters of the authors, title of the article, title of the journal (original abbreviated title), volume and issue numbers, page numbers and the year of publication and the text formatting should be performed as shown in the example below.

Example: **Yang L, Liu B, Yan X, Zhang L, Gao F, Liu Z:** Expression of ISG15 in bone marrow during early pregnancy in ewes. *Kafkas Univ Vet Fak Derg,* 23 (5): 767-772, 2017. DOI: 10.9775/kvfd.2017.17726

If the reference is a book, it should follow surnames and initial letters of the authors, title of the book, edition number, page numbers, name and location of publisher and year of publication. If a chapter in a book with an editor and several authors is used, names of chapter authors, name of chapter, editors, name of the book, edition number, page numbers, name and location of publisher and year of publication and the formatting should be performed as shown in the example below.

Example: **Mcllwraith CW:** Disease of joints, tendons, ligaments, and related structures. **In,** Stashak TS (Ed): Adam's Lameness in Horses. 4th ed., 339-447, Lea and Febiger, Philadelphia, 1988.

DOI number should be added to the end of the reference.

In the references can be reached online only, the web address and connection date should be added at the end of the reference information. The generally accepted scientific writing instructions must comply with the other references. Abbreviations, such as "et al" and "and friends" should not be used in the list of the references.

Follow the link below for **EndNote Style of Kafkas Universitesi Veteriner Fakultesi Dergisi;**
https://researchsoftware.com/downloads/journal-faculty-veterinary-medicine-kafkas-university

8- Latin expression such as species names of bacteria, virus, parasite, and fungus and anatomical terms should be written in italic character, keeping their original forms.

9- The editorial board has the right to perform necessary modifications and a reduction in the manuscript submitted for publication and to express recommendations to the authors. The manuscripts sent to authors for correction should be returned to the editorial office within a month. After pre-evaluation and agreement of the submitted manuscripts by the editorial board, the article can only be published after the approval of the field editor and referee/s specialized in the particular field.

10- All responsibilities from published articles merely belong to the authors. According to the ethical policy of our journal, plagiarism/self-plagiarism will not be tolerated. All manuscripts received are checking by plagiarism checker software, which compares the content of the manuscript with a broad database of academic publications.

11- There is no copyright fee for the authors.

12- The authors are charged a fee on acceptance of the manuscript to cover printing costs and other expenses. This payment information can be found at *http://vetdergi.kafkas.edu.tr/*

SUBMISSION CHECKLIST

Please use below list to carry out a final check of your submission before you send it to the journal for review. Ensure that the following items are present in your submission:

- Cover letter

• Importance and acceptability of the submitted work for the journal have been discussed (Please avoid repeating information that is already present in the abstract and introduction).

• Other information has been added that should be known by the editorial board (e.g.; the manuscript or any part of it has not been published previously or is not under consideration for publication elsewhere.

- Title page

• Title, running title (should be a brief version of the title of your paper, no exceed 50 characters)

• The author's name, institutional affiliation, Open Researcher and Contributor ID **(ORCID)**

• Congress-symposium, project, thesis etc. information of the manuscript (if any)

• Corresponding author's address, phone, fax, and e-mail information

- Manuscript

• Title, abstract, keywords and main text

• All figures (include relevant captions)

• All tables (including titles, description, footnotes)

• Ensure all figure and table citations in the text match the files provided

• Indicate clearly if color should be used for any figures in print

- Availability of Data and Materials

- Acknowledgements

- Funding Support

- Competing Interests

- Authors' Contributions

Further considerations

• Journal policies detailed in this guide have been reviewed

• The manuscript has been "spell checked" and "grammar checked"

• Relevant declarations of interest have been made

• Statement of Author Contributions added to the text

• Acknowledgment and conflicts of interest statement provided